

STUDIES ON SELECTIVELY FLUORINATED CYCLOALKANES

Zeguo Fang

A Thesis Submitted for the Degree of PhD
at the
University of St Andrews



2020

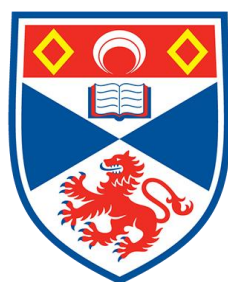
Full metadata for this item is available in
St Andrews Research Repository
at:
<http://research-repository.st-andrews.ac.uk/>

Please use this identifier to cite or link to this item:
<http://hdl.handle.net/10023/19999>

This item is protected by original copyright

Studies on selectively fluorinated cycloalkanes

Zeguo Fang



University of
St Andrews

This thesis is submitted in partial fulfilment for the degree of
Doctor of Philosophy (PhD)
at the University of St Andrews

February 2020

Candidate's declaration

I, Zeguo Fang, do hereby certify that this thesis, submitted for the degree of PhD, which is approximately 38,000 words in length, has been written by me, and that it is the record of work carried out by me, or principally by myself in collaboration with others as acknowledged, and that it has not been submitted in any previous application for any degree.

I was admitted as a research student at the University of St Andrews in September 2015.

I received funding from an organisation or institution and have acknowledged the funder(s) in the full text of my thesis.

Date

Signature of candidate

Supervisor's declaration

I hereby certify that the candidate has fulfilled the conditions of the Resolution and Regulations appropriate for the degree of PhD in the University of St Andrews and that the candidate is qualified to submit this thesis in application for that degree.

Date

Signature of supervisor

Permission for publication

In submitting this thesis to the University of St Andrews we understand that we are giving permission for it to be made available for use in accordance with the regulations of the University Library for the time being in force, subject to any copyright vested in the work not being affected thereby. We also understand, unless exempt by an award of an embargo as requested below, that the title and the abstract will be published, and that a copy of the work may be made and supplied to any bona fide library or research worker, that this thesis will be electronically accessible for personal or research use and that the library has the right to migrate this thesis into new electronic forms as required to ensure continued access to the thesis.

I, Zeguo Fang, confirm that my thesis does not contain any third-party material that requires copyright clearance.

The following is an agreed request by candidate and supervisor regarding the publication of this thesis:

Printed copy

No embargo on print copy.

Electronic copy

No embargo on electronic copy.

Date

Signature of candidate

Date

Signature of supervisor

Underpinning Research Data or Digital Outputs

Candidate's declaration

I, Zeguo Fang, hereby certify that no requirements to deposit original research data or digital outputs apply to this thesis and that, where appropriate, secondary data used have been referenced in the full text of my thesis.

Date

Signature of candidate

Acknowledgements

First of all, I would like to say thank you to my supervisor, Prof. David O'Hagan, from the bottom of my heart. Although it has already been over 4 years, I can still clearly remember the first dialogue between David and me. David said, "St Andrews is a very nice and ancient University, and it is a good place to live and study." Really thank you for giving me the opportunity to study in your group. Therefore, I have the chance to come to this beautiful and quiet town. I have covered every corner of St Andrews and already regarded it as my second home. More importantly, it is an absolutely great honour for me to work under your guidance. Without your constant encouragements and useful suggestions during my PhD career, I probably could not make any progress. At the same time, your keen interest to chemistry and rigorous research attitude deeply influenced me. I learnt those valuable characters from you and that is a treasure of my life.

I would like to express my sincere thanks to China Scholarship Council (CSC). Without your funding support, I couldn't study abroad and experience a different life. Thanks for all the staff in Education Section of the Embassy of the People's Republic of China in the United Kingdom of Great Britain and Northern Ireland for your contribute so that I can study here safely and peacefully. I do wish you all the best!

I have to express my hearty gratitude to my father and mother. I know I caused you a lot of troubles during my PhD career, but really thank you for your support, patience and understanding! I also want to express my thanks to Liyang Fan. Thank you for your accompany and I hope you can be happy in the coming days.

There is no doubt that my research work can not be finished without many excellent scientists. Thanks to Mrs. Melanja Smith, Dr. Tomas Lebl and Dr. Siobhan Smith for the NMR analysis. My thanks are extended as well to Prof. Alex Slawin and Dr. David Cordes for X-ray analysis. The whole O'Hagan group (present and past) helped me a lot especially when I firstly arrived here. It is so happy to work and be friends with you guys. Particularly, I would like to mention Dr. Nawaf Al-Maharik for your daily guidance and assistance in the lab. Sometimes, we have different opinions on something, but it proves that you are always right. Dr Neil Keddie for your general knowledge; Dr. Qingzhi Zhang for your help both inside and outside the lab. As a colleague, but mostly as a friend, I wish you all the best in the future.

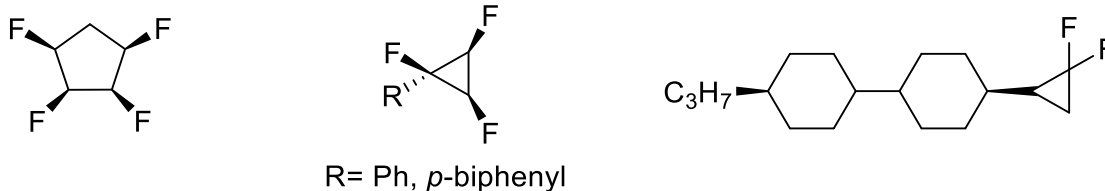
I would like to offer my thanks to all my Chinese friends in St Andrews, including Lutao Zhang, Teng Li, Xuan Feng, Cihang Yu, Rongtian Suo, Shuangbin Li, Peng Ma, Meng Zhang, Chengfei Li, Shitao Wu, Jianing Hui and others. Many thanks for your accompany.

Finally, I have to thank myself. Thank you for working hard and never giving up. It is not easy to get a PhD degree, but you successfully overcome all the obstacles during this journey. I do hope you can keep working hard and becoming a good person in the future!

I gratefully acknowledge the EPSRC for funding (GR: EP/R013799/1) and the China Scholarship Council for PhD studentship support.

Abstract

The thesis focuses on the synthesis of novel fluorinated cycloalkanes and their polar properties. Selected molecules are shown below:



Chapter 2 describes the synthesis of all *cis*-1,2,3,4-tetrafluorocyclopentane and its deuterated isotopomer. They were prepared from the dicyclopentadiene. The structure of *cis*-1,2,3,4-tetrafluorocyclopentane was characterised by NMR and X-ray crystallography. This structure proved to have high polarity and a calculated dipole moment is 4.9 Debye. The deuterated isotopomer was also characterised by NMR and it indicated that this molecule has highly polarized faces similar to all *cis*-1,2,3,4-tetrafluorocyclopentane. The polarity of the isotopomers were compared by GC-MS analysis and this gave an indication that per-deuterated isotopomer is more polar than the all *cis*-1,2,3,4-tetrafluorocyclopentane.

Chapter 3 describes the synthesis of a series of fluorinated cyclopropanes, with a particular focus on the preparation of the all *cis*-1,2,3-trifluorocyclopropane motif. The synthesis started from the fluorinated styrene, followed by bromofluorocarbene (:CFBr) addition and reductive debromination. This provided the first synthetic access to this motif. The lipophilicity (Log P) of a series of fluorinated cyclopropanes was investigated and the results demonstrated that the all *cis*-1,2,3-trifluorocyclopropane was the most polar compound among this series.

Chapter 4 describes unexpected results from the fluorination of benzo[*a,e*]cyclooctatetraene with NBS, HF·Py and AgF(I), which was anticipated to generate all-*cis*-5,6,11,12-tetrafluoro-5,6,11,12-tetrahydrodibenzo[*a,e*]cyclooctane. However, the reaction gave a mixture of products and the product outcomes strongly suggests that an extensive carbocation/phenonium rearrangements pathway occurred during the reaction. The origin of oxygen in the final ether products was shown by an ¹⁸O isotope labelling experiment with water and the result suggests a {Ag}O⁻ species is the most likely oxygen provider.

Chapter 5 describes the synthesis of a series of novel liquid crystals with fluorinated cyclopropane motifs at their terminus. The synthesis proved straightforward such that these novel liquid crystal candidates can be prepared on scale. Their thermodynamic and physical properties, such as birefringence (Δn), dielectric anisotropy ($\Delta\epsilon$) and rotational viscosity (γ) were analysed by Merck & Co. Although none of the liquid crystal candidates met all the criteria for Liquid Crystal Display (LCD) development, the study gives an insight into the potential for fluorinated cyclopropane motifs in liquid crystals.

Abbreviations

Ac	Acetyl group
AIBN	Azobisisobutyronitrile
amu	Atomic mass unit
Bu	Butyl group
BuLi	Butyllithium
b.p.	Boling point
bs	Broad singlet
COD	1,5-cyclooctadiene
CI	Chemical ionisation
D	Debye
d	Doublet
dd	Doublet of doublets
DAST	Diethylaminosulfur trifluoride
DBCOT	Dibenzo[a,e]cyclooctatraene
DCM	Dichloromethane
Deoxofluor	Bis(2-methoxyethyl)amonosulfur trifluoride
DFT	Density functional theory
DSC	Differential scanning calorimetry
E_n	Vibrational energy
e.e.	Enantiomeric excess

EI	Electron impact
equiv.	Equivalent
ESI	Electrospray ionization
Et	Ethyl group
Fluolead	4-Tertbutyl-2,6-dimethyl phenylsulfur trifluoride
GC	Gas chromatography
HRMS	High resolution mass spectrometry
IR	Infrared spectroscopy
<i>J</i>	Coupling constant
m	Multiplet
mCPBA	<i>meta</i> -Chloroperoxybenzoic acid
Me	Methyl group
MHz	Megahertz
MOF	Metal organic framework
m.p.	Melting point
MS	Mass spectrometry
Δn	Birefringence
NBS	N-Bromosuccinimide
NDHPI	<i>N,N</i> -Dihydroxypyromellitimide
NMR	Nuclear magnetic resonance
POM	Polarising optical microscope

ppm	Parts-per-million
PTFE	Poly(tetrafluoroethylene)
<i>p</i> TSA	<i>p</i> -Toluenesulfonic acid
r.t.	Room temperature
s	Singlet
SET	Single electron transfer
t	Triplet
TBAF	Tetrabutylammonium fluoride
Tf	Triflyl (Trifluoromethanesulfonyl)
TFA	Trifluoroacetic acid
THF	Tetrahydrofuran
TN	Twisted nematic
Ts	Tosyl (Toluenesulfonyl)
UV	Ultraviolet
VA	Vertical alignment
Xtalfluor	Aminodifluorosulfonium tetrafluoroborate salts
$\Delta\epsilon$	Dielectric anisotropy
Υ	Rotational viscosity

Table of Contents

Chapter 1. Introduction	1
1.1 Background of fluorine	1
1.2 The properties of fluorine	2
1.2.1 The physical properties of fluorine	2
1.2.2 The chemical properties of fluorine.....	10
1.3 Properties and effect of the C-F bond	11
1.3.1 Hyperconjugation and the ' <i>gauche</i> ' effect	11
1.3.2 Dipole–dipole interactions.....	12
1.3.3 Charge–dipole interactions.....	14
1.4 C-F Bond formation.....	15
1.4.1 Nucleophilic fluorination.....	15
1.4.2 Electrophilic fluorination.....	19
1.4.3 Radical fluorination	22
1.5 Organofluorine chemistry	28
1.5.1 Polymers.....	28
1.5.2 Pharmaceuticals and agrochemicals.....	29
1.5.3 Liquid Crystals	31
Summary	31
Reference.....	32
Chapter 2. All <i>cis</i>-1,2,3,4-tetrafluorocyclopentane	35
2.1 Multvicinal fluorinated alkanes.....	35
2.2 Vicinal fluorinated cyclohexanes	36
2.3 Fluorine substitution of cyclopentane	40
2.4 Aims and objectives	43
2.5 Results and discussions.....	44
2.6 All <i>cis</i> -1,2,3,4-[² H ₆]-tetrafluorocyclopentane.....	52
2.6.1 Introduction of deuterium	52
2.6.2 Kinetic Isotopic effect	52
2.6.3 Chemical-shift isotopic effect	54
2.6.4 Aims and objective.....	57

2.6.5 Results and discussions	57
2.7 Conclusion	64
Reference	65
Chapter 3. Fluorinated cyclopropanes	67
3.1 Introduction of cyclopropane	67
3.2 Preparation of Cyclopropanes	69
3.2.1 Simmons-Smith reaction	69
3.2.2 Cyclopropanation through diazo compounds	71
3.2.3 Free carbenes	74
3.3 Fluorinated cyclopropanes	76
3.3.1 Fluorocarbene addition to alkenes	77
3.3.2 Carbene addition to fluoroalkenes	81
3.3.3 Direct fluorination	84
3.4 All cis-1,2,3-trifluorocyclopropanes	86
3.4.1 Aims and objectives	88
3.4.2 Results and discussion	89
3.4.3 Measurement of Log P values	102
3.5 Conclusion	107
Reference	108
Chapter 4. Fluorination of dibenzo[a,e]cyclooctatetraene	112
4.1. Dibenzo[a,e]cyclooctatetraene	112
4.1.1 Synthesis of DBCOT	113
4.1.2 Selected applications of DBCOT	116
4.2. Aims and objectives	119
4.3. Results and discussions	120
4.4. Conclusions	141
Reference	142
Chapter 5. Liquid crystal containing fluorinated cyclopropanes	144
5.1. Introduction of liquid crystal	144
5.1.1 Background of liquid crystal	144
5.1.2 Classes of liquid crystals	145
5.1.3 The structure of liquid crystals	146

5.2 The properties of liquid crystals.....	147
5.2.1 Optical anisotropy of a liquid crystal	147
5.2.1 Dielectric anisotropy of a liquid crystal.....	148
5.3 Applications of liquid crystals	149
5.4 Negative dielectric anisotropic liquid crystals	150
5.4.1 Nitrile group in a perpendicular orientation.....	151
5.4.2 2,3-Disubstituted phenyl unit	152
5.4.3 Axially fluorinated cyclohexane unit.....	153
5.4.4 Tetrafluoroindane and tetrafluorocyclohexane liquid crystals	155
5.5 Aims and objectives	157
5.6 Results and discussion	158
5.7 Conclusions	164
Reference.....	166
Chapter 6. Experimental.....	167
6.1 General experimental	167
6.2 Compounds preparation for Chapter 2.....	171
6.2.1 <i>cis</i> 1,2,3,4-Diepoxy cyclopentane	171
6.2.2 All <i>cis</i> -1,2,3,4-tetrafluorocyclopentane	172
6.2.3 [² H ₆]-Cyclopentadiene.....	173
6.2.4 [² H ₆]- <i>cis</i> -1,2,3,4-diepoxy cyclopentane.....	174
6.2.5 All <i>cis</i> -1,2,3,4-[² H ₆]-tetrafluorocyclopentane.....	175
6.3 Compounds preparation for Chapter 3.....	176
6.3.1 (2-Bromo-1-fluoroethyl)benzene.....	176
6.3.2 4-(2-Bromo-1-fluoroethyl)-1,1'-biphenyl.....	176
6.3.3 (1-Fluorovinyl)benzene	177
6.3.4 4-(1-Fluorovinyl)-1,1'-biphenyl	177
6.3.5 (1-Azidovinyl)benzene.....	178
6.3.6 4-(1-Azidovinyl)-1,1'-biphenyl.....	178
6.3.7 2-Fluoroacetophenone	179
6.3.8 1-(Biphenyl-4-yl)-2-fluoroethanone.....	179
6.3.9 1-Phenyl-1,1,2-trifluoroethane	180
6.3.10 4-(1,1,2-Trifluoroethyl)-1,1'-biphenyl	180

6.3.11 <i>Cis</i> - α,β -Difluorostyrene	181
6.3.12 (<i>Z</i>)-4-(1,2-Difluorovinyl)-1,1'-biphenyl	182
6.3.13 Benzyl fluoride	183
6.3.14 Bromofluoromethylbenzene.....	183
6.3.15 (1 <i>R</i> *, 2 <i>R</i> *)-1,2-Difluoro-1,2-diphenylcyclopropane.....	184
6.3.16 2-Chloro-2-fluoro-1-phenylcyclopropane.....	187
6.3.17 <i>Trans</i> -2-Fluorocyclopropylbenzene	187
6.3.18 <i>Cis</i> -2-Fluorocyclopropylbenzene.....	188
6.3.19 2-Chloro-1,2-difluorophenylcyclopropane	188
6.3.20 <i>Cis</i> -1,2-Difluorocyclopropylbenzene.....	189
6.3.21 <i>Trans</i> -1,2-Difluorocyclopropylbenzene	189
6.3.22 4-(2-Chloro-1,2-difluorocyclopropyl)-1,1'-biphenyl	190
6.3.23 <i>Cis</i> -4-(1,2-Difluorocyclopropyl)-1,1'-biphenyl.....	191
6.3.24 <i>Trans</i> -4-(1,2-Difluorocyclopropyl)-1,1'-biphenyl	192
6.3.25 2-Chloro-1,2,3-trifluorocyclopropylbenzene	193
6.3.26 4-(2-Chloro-1,2,3-trifluorocyclopropyl)-1,1'-biphenyl.....	194
6.3.27 4-((1 <i>S</i> *,2 <i>S</i> *,3 <i>R</i> *)-1,2,3-Trifluoro-2-iodocyclopropyl)-1,1'-biphenyl	195
6.3.28 4-((1 <i>S</i> *,2 <i>R</i> *,3 <i>R</i> *)-1,2,3-Trifluoro-2-iodocyclopropyl)-1,1'-biphenyl	196
6.3.29 (<i>Z</i>)-1-([1,1'-Biphenyl]-4-yl)-2,3-difluoroprop-2-en-1-one	196
6.3.30 (2-Bromo-1,2,3-trifluorocyclopropyl)benzene.....	197
6.3.31 4-(2-Bromo-1,2,3-trifluorocyclopropyl)-1,1'-biphenyl.....	197
6.3.32 ((1 <i>S</i> ,2 <i>R</i> ,3 <i>S</i>)-1,2,3-Trifluorocyclopropyl)benzene	198
6.3.33 ((2 <i>S</i> *,3 <i>S</i> *)-1,2,3-Trifluorocyclopropyl)benzene	198
6.3.34 4-((1 <i>S</i> ,2 <i>R</i> ,3 <i>S</i>)-1,2,3-Trifluorocyclopropyl)-1,1'-biphenyl	199
6.3.35 4-((2 <i>S</i> *, 3 <i>S</i> *)-1,2,3-Trifluorocyclopropyl)-1,1'-biphenyl	199
6.3.36 1,2,2,3-Tetrafluorocyclopropylbenzene	200
6.3.37 4-(1,2,2,3-Tetrafluorocyclopropyl)-1,1'-biphenyl	201
6.4 Compounds preparation for Chapter 4.....	202
6.4.1 (1 <i>aR</i> *,5 <i>bS</i> *,6 <i>aR</i> *,10 <i>bS</i> *)-1 <i>a</i> ,5 <i>b</i> ,6 <i>a</i> ,10 <i>b</i> -Tetrahydrodibenzo[3,4:7,8]cycloocta[1,2- <i>b</i> :5,6- <i>b'</i>]bis(oxirene)	202
6.4.2 <i>trans</i> -11,13-Difluoro-9,10-dihydro-9,10-(methanooxymethano)anthracene	203
6.4.3 <i>cis</i> -11,13-Difluoro-9,10-dihydro-9,10-(methanooxymethano)anthracene	204
6.4.4 (<i>meso</i>)-5,6-Difluoro-5,6-dihydrodibenzo[<i>a,e</i>]cyclooctatetraene	204

6.4.5 (5R*,6R*,Z)-5,6-difluoro-5,6-dihydrodibenzo[a,e]cyclooctatetraene	205
6.4.6 5-(Difluoromethyl)-5 <i>H</i> -dibenzo[a,d]cycloheptatriene	205
6.4.7 (5R*,6R*,11R*,12R*)-5,6,11,12-Tetrafluoro-5,6,11,12-tetrahydrodibenzo[a,e]cyclooctatetraene.....	206
6.5 Compound preparation for Chapter 5	207
6.5.1 4-(2,2-Difluorocyclopropyl)-4'-propyl-1,1'-bicyclohexyl	207
6.5.2 4-(1-Fluorovinyl)-4'-propyl-1,1'-bi(cyclohexane)	208
6.5.3 4-Propyl-4'-(1,2,2-trifluorocyclopropyl)-1,1'-bi(cyclohexane)	209
6.5.4 4'-Propyl-[1,1'-bi(cyclohexane)]-4-ol	210
6.5.5 4-Propyl-4'-(vinyloxy)-1,1'-bi(cyclohexane)	211
6.5.6 4-(2,2-Difluorocyclopropoxy)-4'-propyl-1,1'-bi(cyclohexane)	212
6.5.7 4-Methylene-4'-propyl-1,1'-bi(cyclohexane)	213
6.5.8 1,1-Difluoro-6-(4-propylcyclohexyl)spiro[5.2]octane	214
References	215
Appendix-Crystallographic Data	216
Appendix-Publications	231

Chapter 1. Introduction

1.1 Background of fluorine

Fluorine is the 13th most abundant element in the Earth's crust and largely found in minerals in the form of CaF_2 .¹ It is widely used in almost every aspects of daily life in products derived from chemical processes, which originate from hydrogen fluoride to elemental fluorine. Because of its reactive nature, elemental fluorine has an interesting history in terms of its discovery. Calcium fluoride (also called Fluorspar) was originally reported by Georgius Agricola in 1529,² who gave the element its name. *Fluo* means "flow" in Latin because fluorspar becomes soft on heating. Since then, many scientists have investigated fluoride's properties and composition. In 1764, Andreas Sigismund Marggraf heated fluoride with concentrated sulfuric acid³⁻⁴ and characterized hydrofluoric acid (HF), for the first time. It was in 1810 that fluorine was proposed as an element by André-Marie Ampère although it was not characterized until much later.⁵ Fluorine still remains a challenge to isolate when prepared by electrolysis because of its corrosiveness. Several chemists have died or sustained injuries in their quest to isolate fluorine. However, French chemist Henri Moissan, after much trial and error, successfully isolated elemental fluorine in 1886 through electrolysis of anhydrous hydrogen fluoride with added potassium bifluoride.⁶ The key to his success is that he used very low temperature to decrease the reactivity of the fluorine and also used a cell, made of platinum and iridium, to resist the corrosiveness of the element. Because of this work, he received Nobel Prize for Chemistry in 1906. The apparatus is shown in **Figure 1**. It was not until the Second World War, during the Manhattan Project, that fluorine was

produced in large quantity. This involved the synthesis of uranium hexafluoride (UF_6) for isotope enrichment for the development of nuclear weapons, a process which also saw the beginning of the nuclear energy industry.⁷

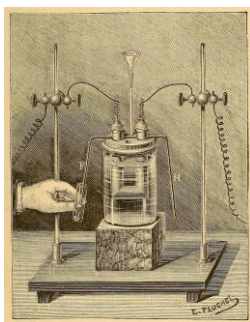


Figure 1. Moissan's fluorine apparatus.

1.2 The properties of fluorine

1.2.1 The physical properties of fluorine

1.2.1.1 Electronic effects

Fluorine has the highest electronegativity of all elements and Pauling assigned the maximum value of $\chi = 4.0$.⁸ When you look at the configuration of fluorine, it has nine electrons outside the nucleus, and owing to its high electronegativity, it is the most difficult of the Period II elements to remove one electron to generate F^+ , because the electrons are held most tightly by nucleus. Due to attraction of the nuclear charge for these electrons, fluorine has the smallest atomic radius of the Period II elements with an atomic radius which lies between hydrogen and oxygen.

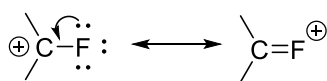
Table 1.0. The Van der Waals radii and electronegativity of selected elements.⁹

	H	C	N	O	F
Van der Waals radii/ Å	1.2	1.7	1.55	1.52	1.47
Electronegativity	2.1	2.5	3.0	3.5	4.0

High electronegativity influences electron distribution, e.g., the C-F bond is viewed as the strongest covalent bond in organic chemistry, because the electron density is concentrated around the fluorine, leading to significant ionic character to the bond ($C^{\delta+}-F^{\delta-}$).¹⁰

Despite its high electronegativity, fluorine just like oxygen and nitrogen can stabilise an α -cationic center by donating lone pair electrons into the empty p orbital of a carbocation,³ as illustrated in **Figure 2**. This stabilisation is the most modest of F, O and N. In the case of a carbocation at the β position, fluorine destabilises through its inductive effect.

Resonance effect (modestly stabilising)



Inductive effect (significantly destabilising)

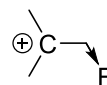
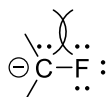


Figure 2. Fluorine stabilise an α -carbocation and destabilise a β -carbocation.³

In contrast, an α -anionic center is generally destabilised with fluorine by a charge repulsion, but an anion at the β position is stabilised by both inductive and hyperconjugation effects. Hyperconjugation arises due to electron donation into the deficient C-F anti-bonding orbital ($C-F^{\sigma*}$). Sometimes, an elimination reaction will occur as a result of this, as illustrated in the **Figure 3**.

Charge repulsion (destabilising)



Hyperconjugation and Inductive effect

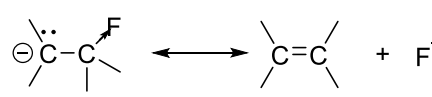
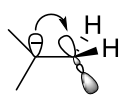


Figure 3. Fluorine stabilises β -anions and destabilises α -carbocations.³

1.2.1.2 Lipophilicity

Lipophilicity is an important molecular parameter in drug design.¹¹ Compounds of optimal lipophilicity typically obtain good biodistribution. Therefore, it is important to know how to control the lipophilicity of a compound. Fluorine has proven to be a useful tool to influence lipophilicity.¹²⁻¹⁴ But the effect of fluorination on lipophilicity is complex and unpredictable. As a general rule, a single aliphatic H/F change leads to a more lipophilic molecule, increasing Log D values roughly 0.25.¹³ The Log D is the logarithmic coefficient for distribution of a compound between octanol and water at pH 7.4 (Log P and Log D are identical for nonionisable solutes). Fluorination, e.g. F, CF₃ always increases the lipophilicity of aromatic compounds, however, terminal mono-, di- or even trifluorination of a saturated alkyl group decreases lipophilicity because of strong bond dipoles and the polarisation effect on neighbouring hydrogens. When hetero-substituents are present, the result is complex and unpredictable. Lipophilicity decreases only when the fluorination site is remote from the heteroatom. Some relevant details are shown in **Table 1.1** and **Table 1.2**. Two competing effects influence lipophilicity, namely changes in polarity (polar C-F bond) and the hydrophobic surface area.¹⁵ For a non-polar compound, it is the polarity that determines the lipophilicity, whereas for polar compounds, changes in hydrophobic surface area tend to dominate.

Table 1.1. Lipophilicity decreases with fluorination.¹²

	μ (D)	Log P (octanol-H ₂ O)
CH ₃ CH ₃	0	1.81
CH ₃ CHF ₂	2.27	0.75
CH ₃ (CH ₂) ₃ CH ₃	--	3.11
CH ₃ (CH ₂) ₃ CH ₂ F	--	2.33

Table 1.2. Lipophilicity of alcohols.¹²

	Log P	Δ Log P
CH ₃ CH ₂ OH	-0.32	
CF ₃ CH ₂ OH	0.36	0.68
CH ₃ (CH ₂) ₂ OH	0.34	
CF ₃ (CH ₂) ₂ OH	0.39	0.05
CH ₃ (CH ₂) ₄ OH	1.19	
CF ₃ (CH ₂) ₄ OH	1.14	-0.04

1.2.1.3 Acidity and basicity

Due to the significant inductive effect, the introduction of fluorine has a strong influence on the acidity or basicity of nearby functional groups. For example,^{16,17} sequential introduction of fluorine increases the acidity (pK_a) of acetic acid analogues (**Table 1.3**). Whereas, the basicity (pK_b) of ethylamine progressively decreases with the introduction of a β -fluorine (**Table 1.3**).

Table 1.3 pK_a and pK_b of organic compounds.^{16,17}

Acid	pK_a	Base	pK_b
CH ₃ COOH	4.76	CH ₃ CH ₂ NH ₂	10.7
CH ₂ FCOOH	2.59	CH ₂ FCH ₂ NH ₂	8.97
CHF ₂ COOH	1.24	CHF ₂ CH ₂ NH ₂	7.52
CF ₃ COOH	0.23	CF ₃ CH ₂ NH ₂	5.7

The change of the pK_a usually leads to a change in the pharmacokinetic properties and binding affinity of the compound in medicinal chemistry. For example, if a strong basic group is required for binding, it becomes protonated and may result in low bioavailability due to its limited ability to pass through membranes. Therefore, chemists have utilized fluorine to tune pK_a . The discovery of 5HT_{1D} receptor ligands is an example.¹⁸ The nonfluorinated indole **1** had a very low bioavailability with a $pK_a = 9.7$. However, the monofluorinated analogue **2** was found to have a lower pK_a and a better bioavailability. The difluoro analogue **3** had a lower binding affinity again compared to **1** and **2**, due to the lower pK_a value, as illustrated in **Figure 4**.

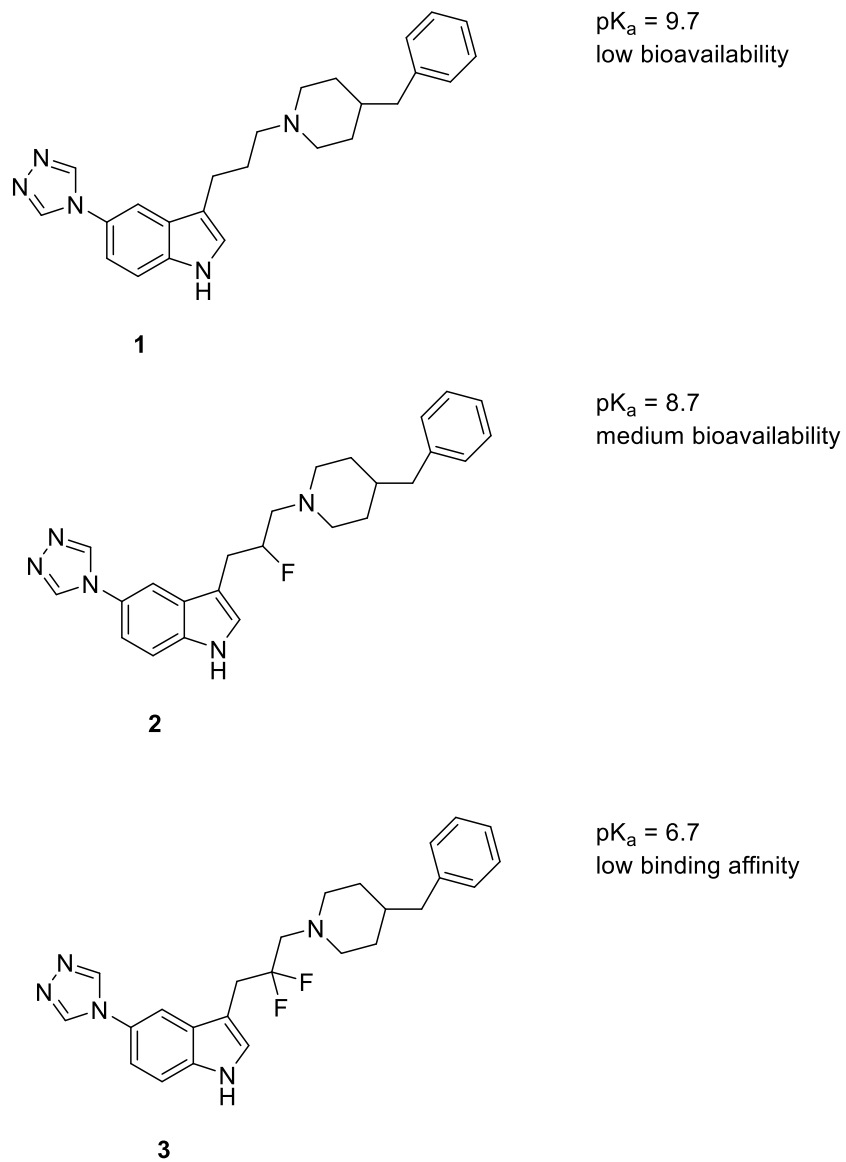


Figure 4. Effect of pK_a value on the bioavailability for a set of $5HT_{1D}$ agonist.¹⁸

1.2.1.4 Hydrogen bonding

It may be anticipated that the C-F bond would behave similarly to C-O and C-N and act as a good hydrogen bond acceptor. However, due to fluorine's lower polarizability and high electronegativity, fluorine emerges as a weak hydrogen bond acceptor. The strength of an optimal F...H interaction has been estimated to be between 2 to 3.2 Kcal/mol, approximately half

of that for an oxygen hydrogen bonding interaction.¹⁹ Hybridization in an optimal situation [C(sp³)-F...H-O in the gas phase], influences this interaction. The C(sp²)-F...H-O bond strength has been estimated to be 1.48 Kcal/mol, significantly lower than that of the C(sp³)-F...H-O (2.38 Kcal/mol), as illustrated in **Figure 5**. This weaker C(sp²)-F hydrogen bonding can be rationalised in that the fluorine lone pairs are involved in conjugation with the double bond and are less able to participate in the hydrogen bonding interaction and also that the sp² carbon is more electropositive than the sp³ carbon.



Figure 5. The hydrogen bond strength of C(sp³)-F and C(sp²)-F.¹⁹

Dalvit and Vulpetti had demonstrated that the fluorine of the RCH₂F moiety is a superior hydrogen-bond acceptor when compared to the RCHF₂ and RCF₃ in the context of the intermolecular hydrogen bonding by ¹⁹F NMR titration experiment.²⁰ Fluoromethyl benzene, difluoromethyl benzene and trifluoromethyl benzene were used to form intermolecular hydrogen bonds with *p*-fluorophenol as a donor. The ¹⁹F signal of *p*-fluorophenol is shifted upfield by a magnitude related to the strength of the hydrogen bond. After titration, by comparing the Δ(¹⁹F) values for fluoromethyl benzene, difluoromethyl benzene and trifluoromethyl benzene, they found fluoromethyl benzene had the strongest interaction with *p*-fluorophenol (Δ = 1.38 ppm), as illustrated in Table **1.4**.

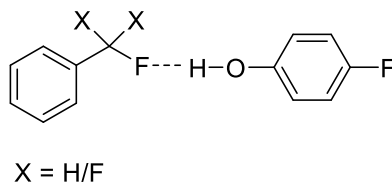


Table 1.4. The $\Delta\delta(^{19}\text{F})$ values for fluorinated molecules interacting with p-fluorophenol.²⁰

Molecule	$\Delta\delta(^{19}\text{F})$ [ppm] of p-fluorophenol
(fluoromethyl)benzene	1.38
(difluoromethyl)benzene	0.55
(trifluoromethyl)benzene	Too weak

The intramolecular hydrogen bond in a conformationally flexible system was explored by Linclau and co-workers through NMR and computation (Figure 6).²¹ A theory study found that the most stable conformer of *syn*-4-fluoropentan-2-ol, represented about 39 % of the conformer population at 25°C, which had an intramolecular hydrogen bond. When the temperature was decreased to -50°C, the population increases to 59 %. The ¹H NMR of the hydroxyl hydrogen (OH) showed a coupling constant (¹J_{OH··F} = 6.6 Hz at 25°C), which agreed well with the computed value (-7.9 Hz). At -50°C, a significant increase ¹J_{OH··F} (9.9 Hz) in the coupling constant was observed, which was attributed to a further increase in the population of that conformer.

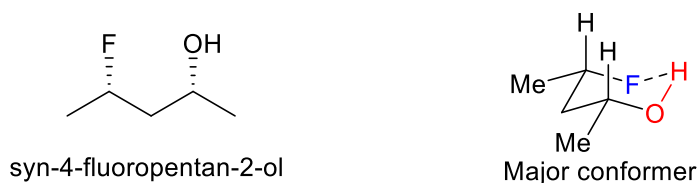


Figure 6. Intramolecular hydrogen bond in 4-fluoropentan-2-ol.²¹

1.2.2 The chemical properties of fluorine

Of all the elements, fluorine is the most reactive non-metal. Its high reactivity can be rationalized by a weak F-F bond (154.8 KJ/mol) and the corresponding strength of covalent bonds to carbon, e.g. the C-F bond (485 KJ/mol).²² The reactivity of the F-F bond can be understood by the small size of fluorine and its high electronegativity. When two fluorine atoms come together to complete the octet, there is a very strong charge repulsion across the short bond distance. This coupled with the high electronegativity makes it a very weak bond. An analogous but less energetic system is found in peroxide (R-O-O-R).

Fluorine gas is a powerful oxidizing agent, which can react with almost all organic and inorganic compounds. The extraordinary versatile and reactive chemistry of F₂ is illustrated in **Figure 7**.

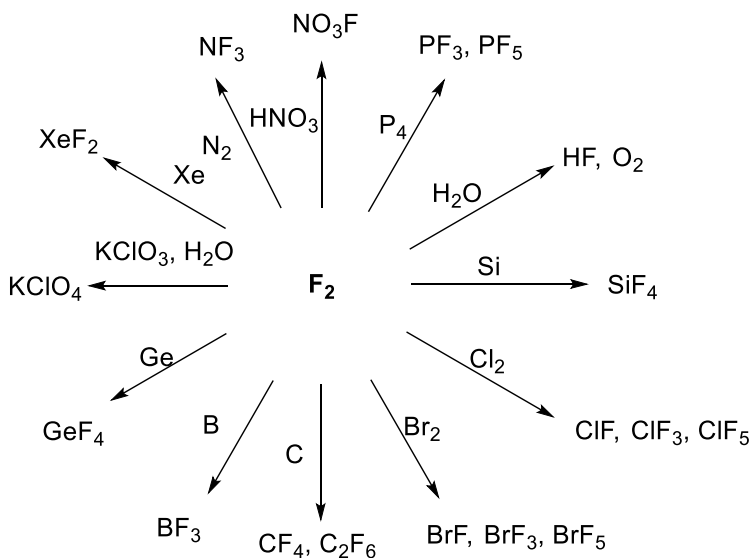


Figure 7. The selected reactions of F₂.

1.3 Properties and effect of the C-F bond

Fluorine substitution for hydrogen in organic compounds influences the conformation of a given molecule, and this can result in changing properties and behaviour. The most important interactions in this respect are dipole-dipole and charge-dipole interactions, although weaker stereo-electronic effect are also relevant in this discussion.

1.3.1 Hyperconjugation and the '*gauche*' effect

The most widely discussed stereo-electronic effect with fluorine in organic chemistry is the *gauche* effect. The *gauche* effect characterizes any X-C-C-X *gauche* conformer which is more stable than the *anti* conformer. The effect was first described by Saul Wolfe in 1970.²³ A good example is represented with 1,2-difluoroethane (**Figure 8**). Experimental data and calculations, suggest that the *gauche* conformation is more stable by ~ 0.8 kcal/mol.⁹ This is unexpected, as there are two unfavourable interactions to overcome. One is the steric and electronic repulsion between the two larger fluorines relative to hydrogen. The other is the partial alignment of C-F bond dipoles generating a larger molecular dipole for the *gauche* conformer. However, hyperconjugation and the bent bond models have been used to rationalise the *gauche* effect, with hyperconjugation being the most widely discussed.

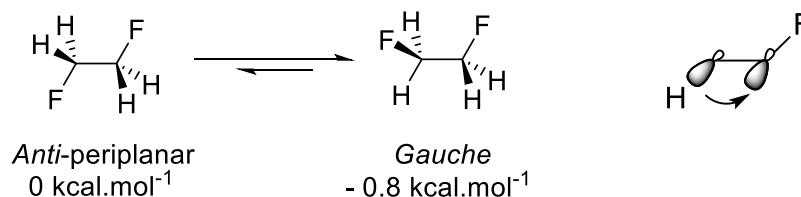


Figure 8. Hyperconjugation explanation of the "*gauche* effect."⁹

The hyperconjugation model was first proposed by Weinhold *et al.*²⁴ This hypothesis assumes that the σ^* anti-bonding orbital of the C-F bond can receive electron density from an electron rich σ bonding orbital of a C-H bond. During hyperconjugation, the C-F bond becomes longer and less covalent as the antibonding orbital is populated, however the conjugation lowers the energy of this conformation. This interaction can only occur when the C-H bond is *anti*-periplanar to the C-F bond as found only in the *gauche* conformation.

Wiberg attributed the lower energy of *gauche* conformer to a bent bond analysis.²⁵ The precise definition of the bond is the path of the maximum charge density between the pair of bonded atoms. In the *trans* form of 1,2-difluoroethane, the C-C bond is distorted in different directions, leading to reduced overlap and a weaker C-C bond, whereas in the case of *gauche* conformer, the electron density of C-C bond is actually bent in the same direction resulting in improved overlap, as is shown in **Figure 9**.



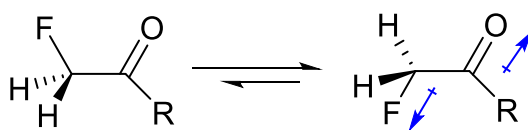
Figure 9. The bent bond model of 1,2-difluoroethane (dash line --- the direction of electron density).

1.3.2 Dipole–dipole interactions

Dipole-dipole interactions can be either intermolecular or intramolecular. Intermolecular interactions are very important in medicinal chemistry, since the C-F bonds of fluorinated drugs will orient towards receptors of the target proteins by aligning compensating dipoles.¹⁰ However, intermolecular interactions are generally much weaker in comparison to intramolecular

interactions. Specific examples of intramolecular interactions are found in α -fluorocarbonyls^{26,27} and 1,3-difluoro repulsions.²⁸

α -Fluorocarbonyl compounds prefer a conformation where the C-F bond sits *anti*-periplanar to the carbonyl group (**Figure 10**).^{26,27} This is because the dipole of the C-F bond opposes the carbonyl dipole, and this reduces the overall molecular dipole. This effect is strongest when the carbonyl is an amide, because amide bonds have the largest dipole of the carbonyl series, certainly when compared to esters, ketones and aldehydes. In the amide case, the *anti* over the *syn* preference has been calculated to be very significant at ~ 7.5 kcal/mol.⁹



R	E/kcal.mol ⁻¹
NH ₂	-7.5
OMe	-4.5
Me	-2.2
H	-1.7

Figure 10. Energy difference between “ α -fluorocarbonyl” conformers.⁹

1,3-Difluoro repulsion occurs when C-F bonds are placed 1,3 to each other. In those cases, they tend to favor conformations where the C-F bonds are orthogonal. This effect can be seen in 1,3-difluoropropane (**Figure 11**). Here, the lowest energy is GG, where the C-F bonds do not align. The least preferred conformation is GG' because it maximizes 1,3-difluoro repulsion. The calculated energy difference between these two conformations is 3.3 kcal/mol.²⁸ The main factor in this interaction is an unfavourable dipole-dipole interaction between two aligned C-F bonds.

AA and GA are less preferred conformations. GA has one hyperconjugation (*gauche*) interaction whereas AA does not, so AA has a higher energy compared to GA.⁹

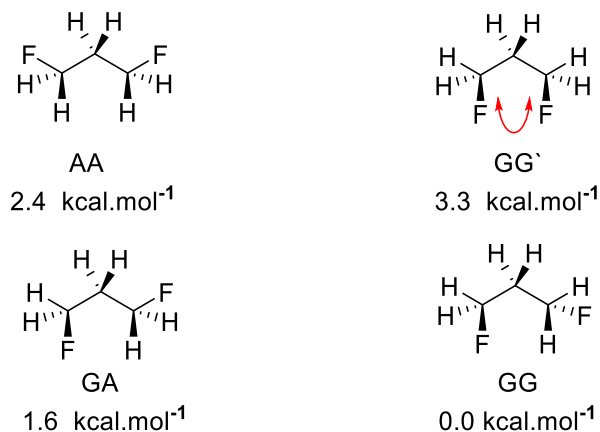


Figure 11. Relative energies of the conformers of 1,3-difluoropropane (G = *gauche* and A = *anti*).⁹

1.3.3 Charge–dipole interactions

Intramolecular charge-dipole interactions are observed clearly in N-fluoroethylpyridinium systems (**Figure 12**).^{9,29} Similarly when amines become protonated, the C-F bond will adopt conformations of close alignment. This was first highlighted for 2-fluoropiperidinium ring systems.²⁹ The preferred conformation places the negative end of the dipole closer to the positive charge of the ammonium group and so there is a significant electrostatic attraction as well as through bond stereoelectronic effects, so stabilisation is significantly greater than that found in the more classical *gauche* effect. A dipole-dipole interaction is also observed here due to the *anti* alignment of the N^{δ-}-H^{δ+} and C^{δ+}-F^{δ-} bonds.

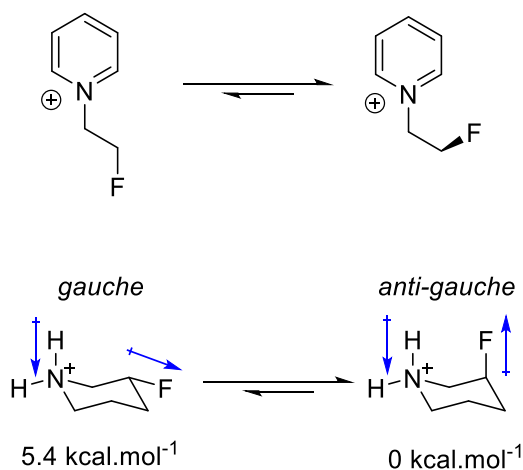


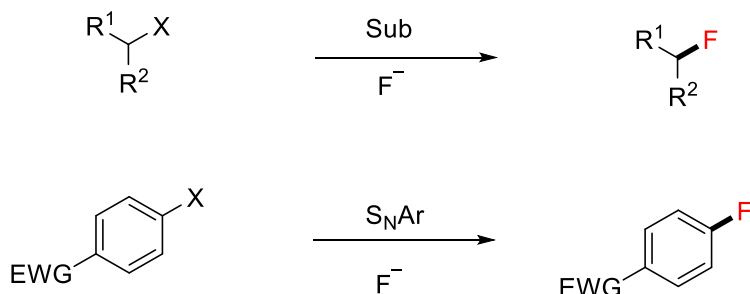
Figure 12. The charge-dipole interaction. The dipoles are shown in blue.^{9,29}

1.4 C-F Bond formation

There are a variety of chemical methods which have been developed to create a C-F bond and they can generally be organised into three groups depending on which form the fluorine atom originates: these can be classified as nucleophilic, electrophilic, and radical fluorinations.

1.4.1 Nucleophilic fluorination

For nucleophilic fluorination, fluoride ion is the nucleophile. For simple cases (**Scheme 1**), the substrate bearing a leaving group (usually halides or sulfonates) reacts with a fluoride source. However, the challenge in nucleophilic fluorination is that the high electronegativity of fluorine, leads to a high kinetic barrier for fluoride to form a C-F bond. The ability of fluoride ion to form strong hydrogen bonds also decreases nucleophilicity when hydrogen bond donors are present. Therefore, polar aprotic solvents are the best solvents for nucleophilic fluorination.³⁰ Also the basicity of the fluoride ion often leads to HF elimination side products, when hydrogen bond donors are absent.



Scheme 1. Schematic of nucleophilic fluorinations.

A wide range of effective fluorination reagents have been developed over the past decades including alkali metal fluorides (e.g., KF, AgF), HF-based reagents (e.g., HF/pyridine, Et₃N·3HF) and tetraalkylammonium fluorides (e.g., tetrabutylammonium fluoride, abbreviated TBAF). Selected examples of traditional reagents used for nucleophilic fluorination are shown in **Figure 13**.

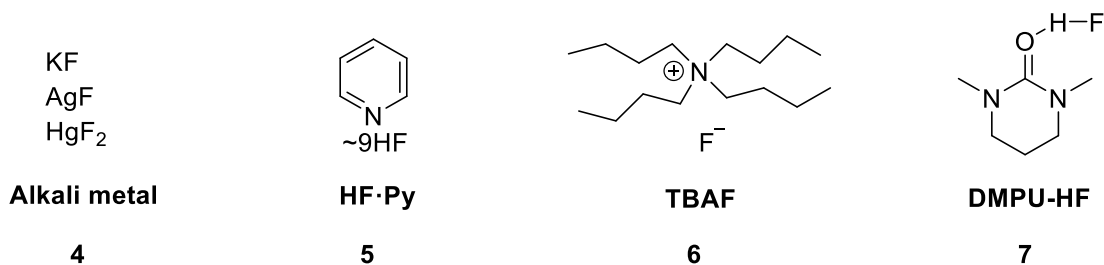
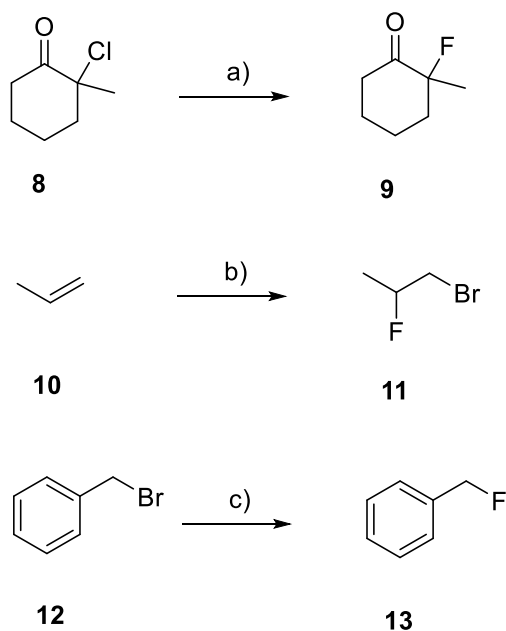


Figure 13. Examples of nucleophilic fluorination reagents.³¹⁻³⁷

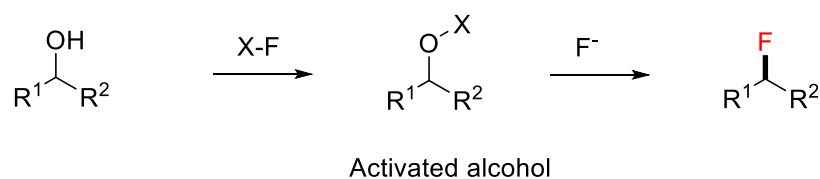
The strong lattice energy of alkali metals renders them a weak nucleophile and poorly soluble in organic solvents. Crown ethers can be used in combination with the metal fluorides to increase solubility.³¹ Anhydrous hydrogen fluoride is a toxic and corrosive gas, but HF can be complexed to amines to form stable liquid reagents. The most commonly used reagents of this class are HF·Pyridine **5** (Olah's reagent) and triethylamine trihydrogen fluoride (Et₃N·3HF).³²⁻³⁴ HF·Pyridine

is more acidic and is not stable under high temperature whereas $\text{Et}_3\text{N}\cdot 3\text{HF}$ is more stable and is a more neutral reagent. For this reason, it cannot react directly with alkenes. These organic bases reduce the acidity of HF and the bases can interfere with metal catalysts. The recently introduced (2014) HF-based reagent DMPU-HF **7** was developed to overcome these drawbacks.³⁵ It is significantly more acidic than Olah's reagent and $\text{Et}_3\text{N}\cdot 3\text{HF}$. TBAF **6** is a good source of nucleophilic fluoride,³⁶ due to its good solubility in organic solvents. However, TBAF is partially hydrated, which in turn decreases the nucleophilicity of the fluoride ion and also side reactions can occur due to the remaining basic hydroxide (OH). Rigorously anhydrous TBAF was prepared by Di-Magno *et al.*³⁷ in 2005 and is a powerful fluorination reagent. Some reactions using these reagents are shown in **Scheme 2**.



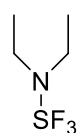
Scheme 2. Reactions using KF, HF·Py and TBAF. *Reagents and conditions:* a) KF, 18-crown-ether, CH_3CN , 31 %;³¹ b) HF·Py, NBS, 25°C, 40 %;³² c) TBAF, MeCN, 25°C, 95 %.³⁶

A very valuable and widely used approach in nucleophilic fluorination involves the deoxyfluorination reaction (Scheme 3). For such protocols, specialised fluorination reagents are required to firstly accomplish oxygen activation, then the leaving group is generally displaced by a SN₂ reaction involving fluoride, to generate the corresponding alkyl fluoride.

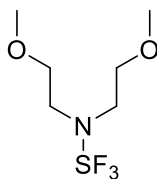


Scheme 3. Deoxyfluorination.

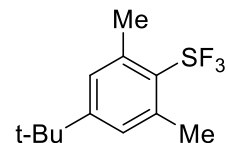
DAST **14** and Deoxofluor **15** are probably the most widely used S-F based nucleophilic reagents, as the nucleophilicity of fluoride greatly increases by pairing a soft Lewis acid with a hard Lewis base, F⁻. They are used to convert alcohols into alkylfluorides and carbonyls to geminal difluorides.^{38,39} Recently, some new deoxyfluorination reagents have been developed. For example, Umemoto⁴⁰ introduced Fluolead (4-tertbutyl-2,6-dimethyl phenylsulfur trifluoride) **16**, as a heat stable reagent for deoxyfluorination reactions. Xtalfluor reagents (aminodifluorosulfonium tetrafluoroborate salts) **17,18** were reported by Couturier and co-workers as bench stable and crystalline reagents.⁴¹ A low-cost and good chemoselective deoxyfluorination reagent, PyFluor **19** was later introduced by Doyle (Figure 14).⁴² Some typical reactions using these different reagents are shown in Scheme 4.



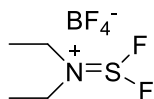
DAST
14



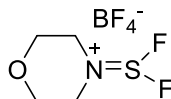
Deoxofluor
15



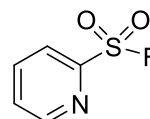
Fluolead
16



XtalFluor-E
17

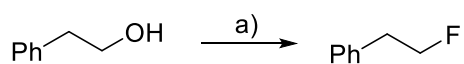


XtalFluor-M
18



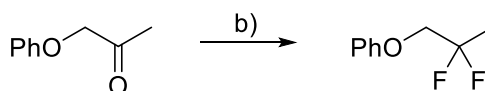
PyFluor
19

Figure 14. S-F based nucleophilic reagents.



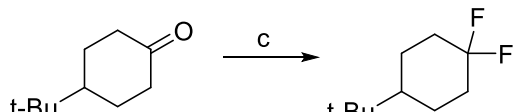
20

21



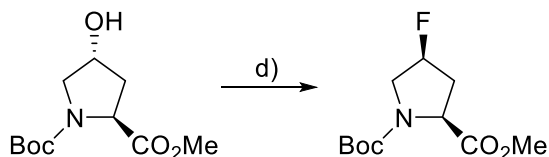
22

23



24

25



26

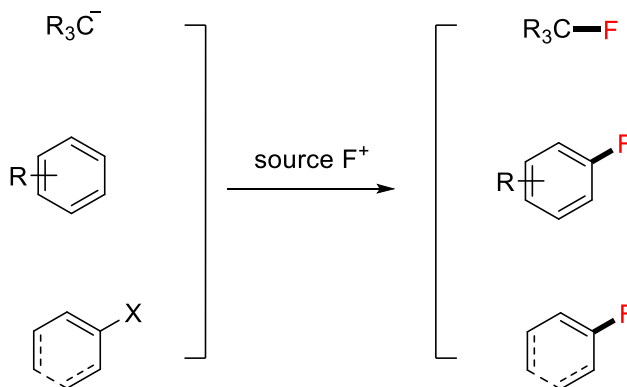
27

Scheme 4. Selected reactions. a) DAST, CH₂Cl₂, 40°C, 60%,³⁸ b) Deoxofluor, CH₂Cl₂, RT, HF·Py,³⁹ c) XtalFluor-M, 3HF·Et₃N, CH₂Cl₂, RT;⁴¹ d) PyFluor, DBU, Toluene⁴²

1.4.2 Electrophilic fluorination

For electrophilic fluorination, the substrate acts as the nucleophile while the reagent delivers a formal "F⁺". The nucleophile can be a carbanion, or electron rich unsaturated alkene or a

substrate bearing a nucleophilic, labile bond, e.g., C-Si, C-Sn, and C-B. This is illustrated in scheme 5.



Scheme 5. Schematic of electrophilic fluorinations.

Electrophilic fluorination reagents were first developed based on an O-F bond (e.g. CF_3OF , HOF), a Xe-F bond (e.g. XeF_2) or the F-F bond (elemental fluorine). However, the high reactivity, low selectivity and the hazardous preparation of these reagents limited their applications. The most practical reagents of this class have a N-F bond. The lower electronegativity of nitrogen over oxygen, makes the N-F bond stronger and consequently the reagents are more stable to handle and most are bench stable. Some common examples are shown in **Figure 15**.

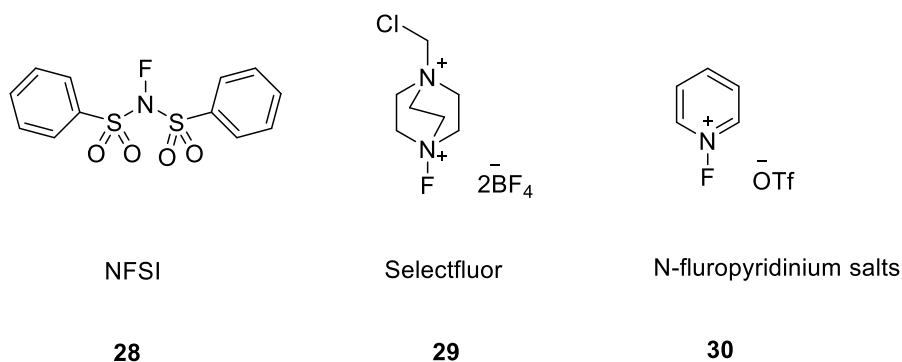
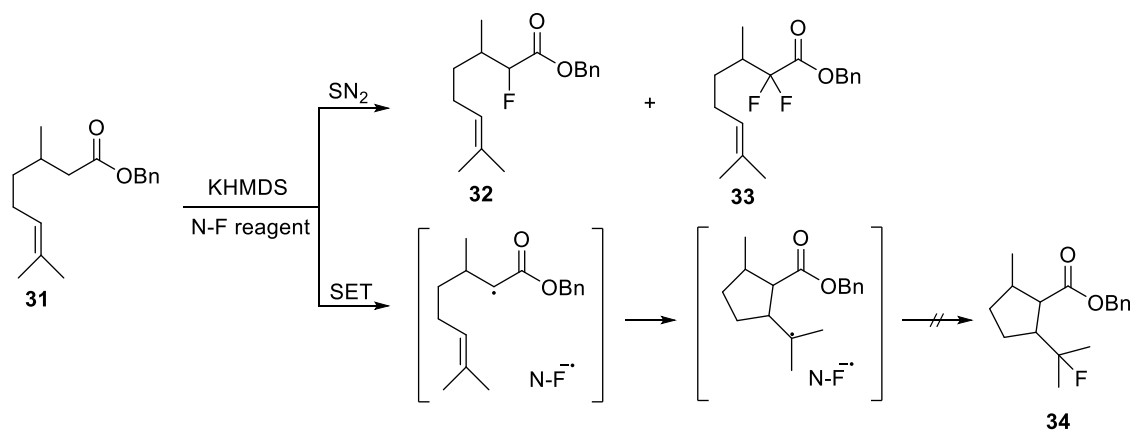


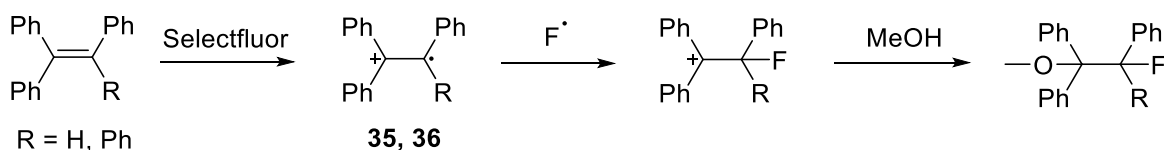
Figure 15. Commonly used electrophilic fluorination reagents.⁴³⁻⁴⁵

The symbol “F⁺” in electrophilic fluorination does not imply the generation of a fluoronium ion. It is used to indicate the transfer of fluorine. Since the introduction of N-F reagents, there has been a long discussion regarding the mechanism of the electrophilic fluorination, namely does it progress through a classical S_N2 process or a single electron transfer (SET) mechanism. In support of the S_N2 mechanism, the benzyl ester of citronellic acid **31** was chosen as a radical trap by Differding and co-workers.⁴⁶ An intermediate radical should cyclise to product **34** through the cyclopentylmethyl radical intermediate. However, the absence of any rearranged product suggested that fluorination occurs through S_N2 mechanism (Scheme 6).



Scheme 6. Fluorination of a citronellic ester enolate.⁴⁶

On the contrary, electrospray ionization (ESI-MS and ESI-MS/MS) was used by Y. Guo and co-workers who concluded a SET mechanism⁴⁷ for fluorination of triphenylethylene and tetraphenylethylene with Selectfluor. They observed the key radical cation intermediates **35**, **36** as depicted in **Scheme 7**.



Scheme 7. Radical cation in the fluorination of aryl-substituted olefins by Selectfluor.⁴⁷

More recently, a theory investigation by Geng and co-workers explored the mechanism of fluorination of aromatic compounds with Selectfluor.⁴⁸ They found that the transition state for the SET pathway is always more stable than that of the S_N2 process by about 3 Kcal/mol and that the electron transfer and the fluorine radical transfer occur successively from the π complexes to σ complexes during the process.

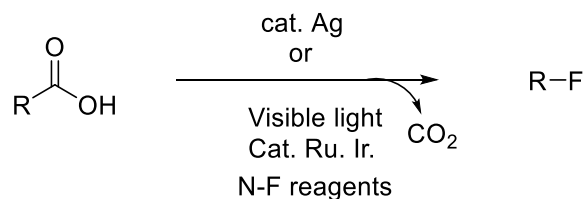
So there is conflicting evidence regarding the exact mechanism of electrophilic fluorination, however there is a greater consensus for a SET process.

1.4.3 Radical fluorination

Radical fluorination is complementary to nucleophilic and electrophilic fluorination. The C-F bond is formed by a reaction between a carbon-centered radical and an atomic fluorine source. Methods for radical fluorination has been limited due to the difficulty in handling fluorine gas, hypofluorite and xenon fluoride. Recently, radical fluorination has regained significant interest since the traditional N-F bond electrophilic fluorination reagents were found to act as fluorine sources. Numerous methodologies have been developed to form the C-F bond by radical process as shown below.

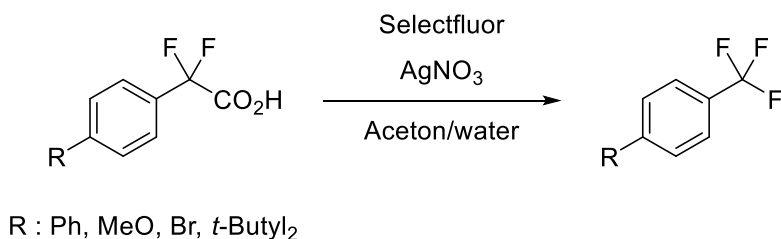
Decarboxylative fluorination

Carboxylic acids can be used to generate radicals under certain conditions (Scheme 8).



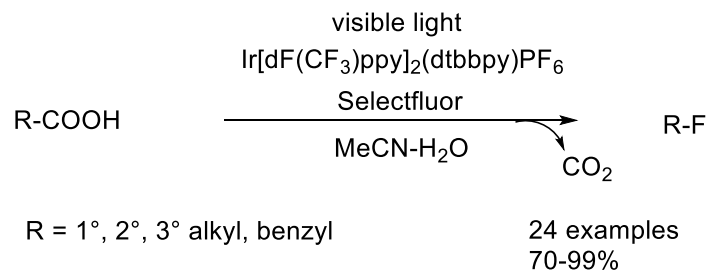
Scheme 8. Radical fluorination.

Silver nitrate was firstly used as a catalyst for the decarboxylative fluorination for aliphatic carboxylic acids by Li *et al.*⁴⁹ Methods were then reported that used silver nitrate to generate a series of fluorinated compounds, including di and tri-fluoromethyl arenes (Scheme 9).⁵⁰

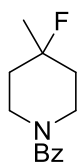


Scheme 9. Decarboxylative fluorination using AgNO₃.⁵⁰

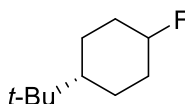
Recently, some photoredox catalysis were found to induce fluorodecarboxylation. For example, Macmillan *et al.* used an iridium photocatalyst to access a variety of fluorinated compounds.⁵¹ This method greatly expands the scope of the reaction extending across primary, secondary, tertiary and benzylic fluorides in excellent yields (Scheme 10).



Selected examples

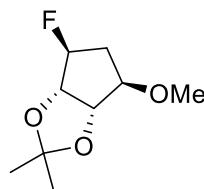


76%



70%

trans/cis 2.5 : 1

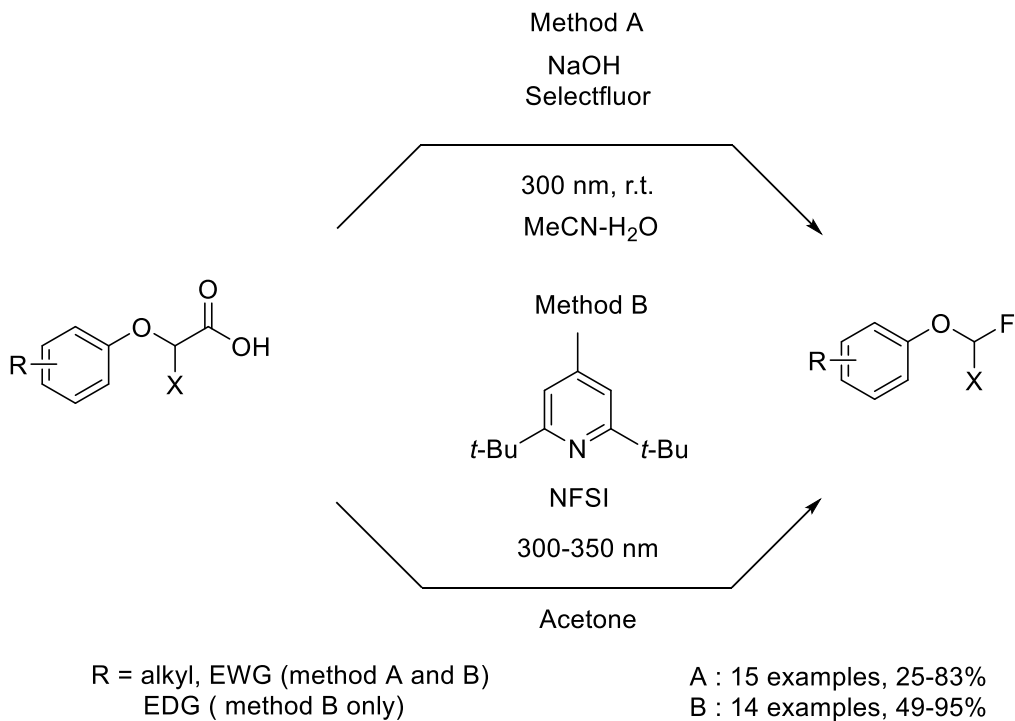


92%

trans/cis 2.5 : 1

Scheme 10. Ir-catalyzed decarboxylative fluorination.⁵¹

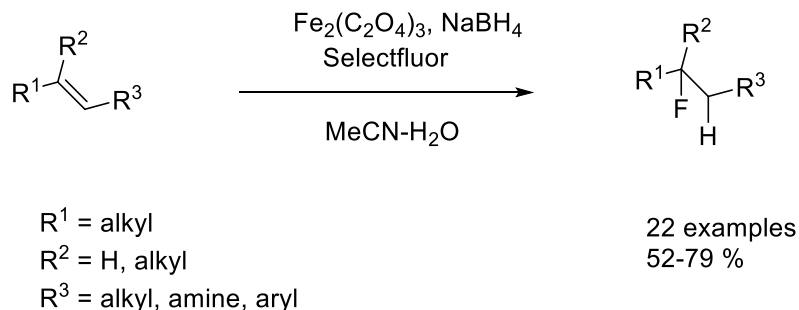
More specifically, with the help of UV-light irradiation or using a photosensitizer, phenoxyacetic acid derivatives can undergo fluorodecarboxylation, as reported by Sammis, Paquin *et al* (Scheme 11).⁵²



Scheme 11. Photofluorodecarboxylation of aryloxy acids.⁵²

Radical Fluorination of alkenes

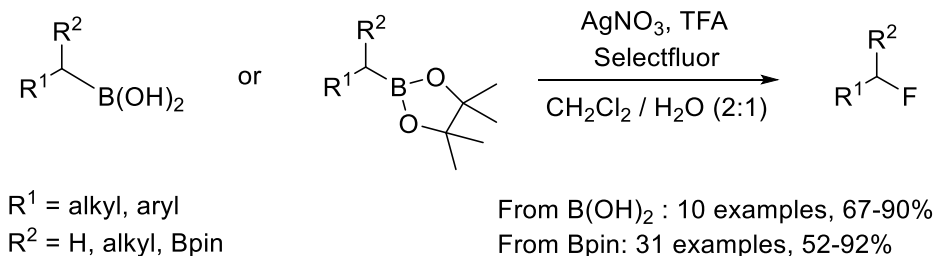
Boger *et al.* firstly reported a radical fluorination of alkenes using Selectfluor.⁵³ Fe(III) oxalate [Fe₂(C₂O₄)₃] and NaBH₄ were used as a hydride source in the reaction. A wide range of unactivated alkenes were converted into alkyl fluorides with exclusive Markovnikov regioselectivity (Scheme 12). Since the reaction time is short and substrate compatibility is wide, the introduction of the isotope ¹⁸F for PET imaging applications proved possible.



Scheme 12. Radical fluorination of unactivated alkene.⁵³

Fluorination using boronic acid substrates

Li *et al.* reported the first example of radical fluorination of alkyl boronic acid derivatives (Scheme 13). This used AgNO_3 as the catalyst.⁵⁴ A broad substrate scope and wide functional group compatibility was observed. The intermediate radical is believed to be generated by oxidation of alkylboronate by AgNO_3 .



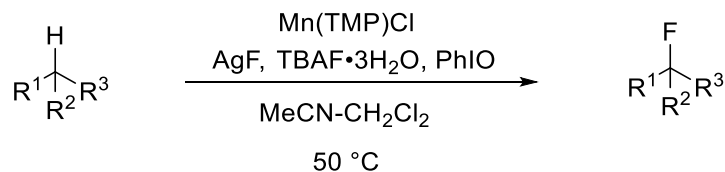
Scheme 13. Fluorination of alkyl boronates.⁵⁴

Ritter *et al.* also reported the fluorination of aryl trifluoroborates using a palladium catalyst.⁵⁵

C(sp³)-H Fluorination

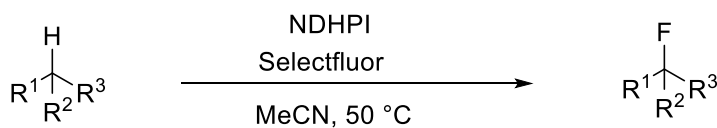
Direct C(sp³)-H fluorination has been extensively studied in the past few years. A number of metal catalysed, metal-free and photocatalysed methods have been developed. Examples are shown below.

Groves *et al.* reported manganese catalysed C(sp³)-H bond fluorination in 2012 (Scheme 14).⁵⁶ In this paper, a variety of aliphatic compounds were selectively fluorinated in good yields.



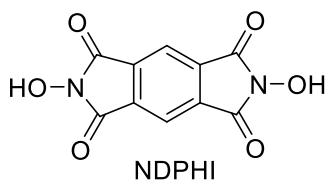
Scheme 14. Manganese catalysed C(sp³)-H fluorination.⁵⁶

C(sp³)-H fluorination is also possible without a metal. Inoue *et al.* reported the use of *N,N*-dihydroxypyromellitimide (NDHPI) for the fluorination of benzylic and aliphatic C-H bonds (Scheme 15).⁵⁷ A mechanistic study revealed that NDHPI was oxidized by Selectfluor *in situ* to generate a N-oxy radical, which abstracted the C(sp³)-H hydrogen to form a carbon centred radical, this radical then takes fluorine from Selectfluor.



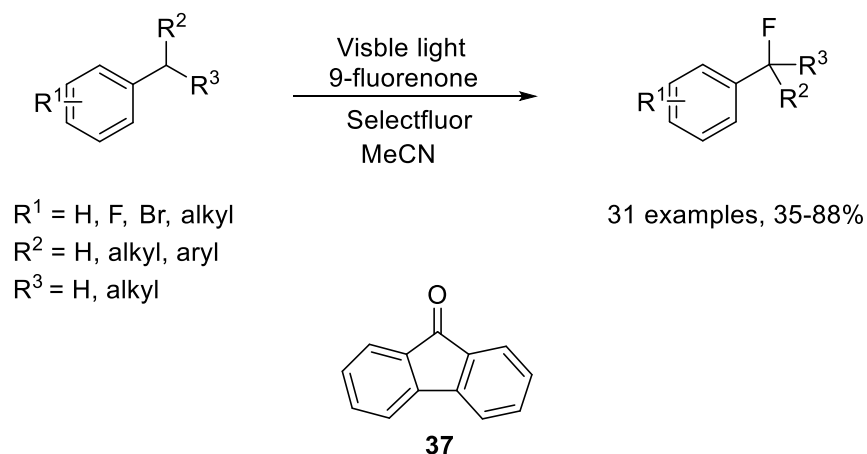
R¹, R², R³ = H, alkyl, aryl

26 examples, 28-86%



Scheme 15. N-Oxyl radical mediated C(sp³)-H fluorination.⁵⁷

An alternative method for C(sp³)-H fluorination uses photocatalysts. Chen *et al.* reported the use of 9-fluorenone **37** in combination with Selectfluor to catalyse the fluorination of benzylic hydrogens (scheme 16).⁵⁸ A number of electron-deficient benzyl fluorides were synthesized using this method.



Scheme 16. 9-Fluorenone **37** catalyses benzylic fluorination.⁵⁸

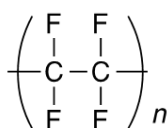
1.5 Organofluorine chemistry

As a consequence of interesting properties of fluorine, organofluorine chemistry has found a wide range of applications in the development of performance compounds in industry. Fluorine containing compounds are widely represented in the pharmaceutical, polymer, agrochemical and liquid crystal display sectors.

1.5.1 Polymers

One of the most important examples of industrial fluoropolymers is poly(tetrafluoroethylene) (PTFE) **38**, also known as Teflon. Teflon was accidentally discovered by Roy Plunkett while he was working for DuPont. It is prepared by free-radical polymerization of tetrafluoroethylene.⁵⁹ This

polymer is a thermoplastic material with a very high density ($\sim 2200 \text{ kg/m}^3$). In fact, it can withstand temperatures up to $260 \text{ }^\circ\text{C}$ and still retain the chemical properties observed at room temperature. It has a very low coefficient of friction⁵⁹ and substances seldom permanently adhere to Teflon coatings, so it is mainly used as a non-stick coating in cookware.⁶⁰ Teflon gains its attractive properties due to the strength of the carbon-fluorine bonds and the very low polarizability of fluorine and therefore it does not form hydrogen bond. Also it does not interact with hydrocarbons or water through van der Waal's interactions.



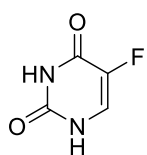
38

Figure 16. Teflon **38**.

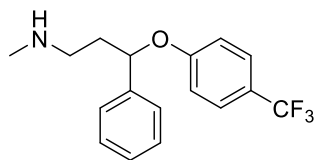
1.5.2 Pharmaceuticals and agrochemicals

Organofluorine compounds are used widely in pharmaceutical and agrochemical products as a consequence of a number of factors. Organofluorine compounds are rare in nature and the metabolism of fluorometabolites is hardly encountered. Also, the fluorine atom is sterically most similar to a hydrogen atom, which means that it can be integrated into a bioactive to modify the physical properties without a significant change in the overall steric profile. To date, around 30 % of agrochemicals and 20 % of pharmaceuticals contain a fluorine atom.⁶¹ Some well-known examples are depicted in **Figure 17**. Fluorouracil **39** is a medication which is used in the treatment of cancer. It irreversibly inhibits the DNA biosynthesis enzyme, thymidylate synthase. Fluoxetine **40**, also known as Prozac, is well known as an antidepressant. It is a selective serotonin reuptake

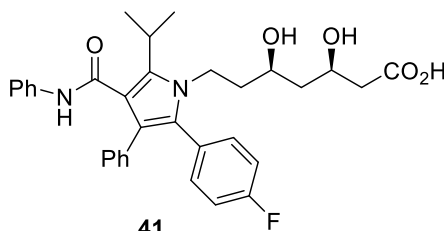
inhibitor (SSRI) and is used for treatment of major depressive disorders, such as bulimia nervosa, obsessive-compulsive, panic disorders and premenstrual dysphoric disorder.^{62,63} Lipitor **41** is another important fluorine containing drug. It was developed by Pfizer, as a medication for lowering cholesterol levels in blood. It operates as an inhibitor of the cholesterol biosynthesis enzyme, HMG-CoA reductase.⁶⁴ Over its active patent lifetime, it grossed sales of \$150 billion dollars. Sofosbuvir **42**, the current top-selling fluorine containing drug (\$ 16 billion sales alone in 2018), was developed by Pharmasset and is used for the treatment of hepatitis C.⁶⁵ Diflubenzuron **43** is a fluorinated insecticide most commonly used in forest management and on field crops to control insects and pests.⁶⁶



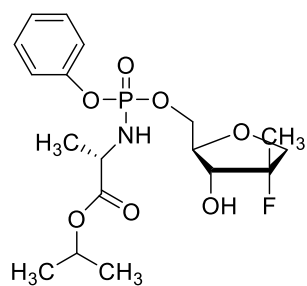
39
Fluorouracil



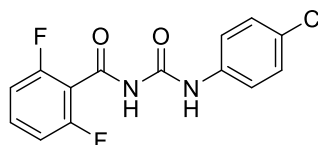
40
Fluoxetine



41
Lipitor



42
Sofosbuvir



43
Diflubenzuron

Figure 17. Blockbuster drugs and agrochemicals containing fluorine.⁶²⁻⁶⁶

1.5.3 Liquid Crystals

Many compounds nowadays used in liquid crystal displays are fluorinated, despite the extra cost and often complex synthesis. The incorporation of fluorine imparts both polarity and low viscosity, ideal characteristics for liquid crystalline materials which have to respond rapidly to switching electric fields. Some examples of fluorinated liquid crystals currently used in commercial devices are shown in Figure 18, with a permanent dipole orientated either along or perpendicular to the molecular axis.³ More details of fluorinated liquid crystals will be discussed in Chapter 5.

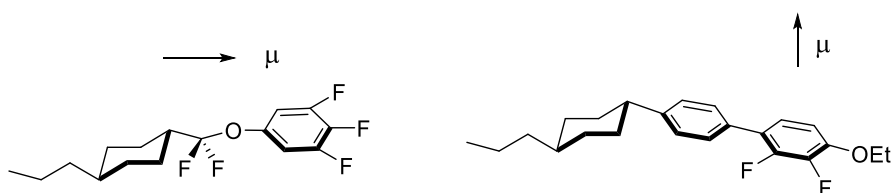


Figure 18. Fluorinated liquid crystalline compounds.

Summary

This introduction aims to highlight some of the most important roles of organofluorine compounds, including their properties and methods of synthesis. It has emphasised that a large number of bioactives and materials owe their unique properties due to fluorine, which makes the study of fluorine such a fascinating field. The rest of thesis describes my research, using fluorine to prepare novel polar aliphatics and liquid crystals.

Reference.

1. A. H. Neilson, *Organofluorines*, 2002, Springer-Verlag, p.122.
2. A. Greenwood, N. N. Earnshaw, *Chemistry of the Elements*, Pergamon Press 1984, 920-921.
3. P. Kirsch, *Modern fluoroorganic chemistry.*, Wiley-VCH, 2004, 3.
4. A. S. Marggraf, *Mémoires de l' Académie royale des sciences et belles-lettres*, 1770, 1-11.
5. A. Tressaud, *Angew. Chem., Int. Ed.*, 2006, **45**, 6792-6796.
6. H. Moissan, J. Dewar, *Proc. Chem. Soc.*, 1897, **183**, 175-186.
7. J. Prystupa, *Toxicol. Mech. Method.*, 2011, **21**, 103-170.
8. L. Pauling, *The Nature of the Chemical Bond and the Structure of Molecules and Crystals: An Introduction to Modern Structural Chemistry*, Cornell University Press, Ithaca, NY, 1939.
9. D. O'Hagan, *Chem. Soc. Rev.*, 2008, **37**, 308-319.
10. P. Beier, A. M. Z. Slawin, D. O'Hagan, *Tetrahedron: Asymmetry.*, 2003, **15**, 2447-2449.
11. M. J. Waring, *Expert. Opin. Drug. Discov.*, 2010, **5**, 235-248.
12. B. E. Smart, *J. Fluorine. Chem.*, 2001, **109**, 3-11.
13. H. J. Bohm, D. Banner, S. Bendels, M. Kansy, B. Kuhn, K. Müller, U. Obst-Sander, M. Stahl, *ChemBioChem.*, 2004, **5**, 637-643.
14. K. Mueller, C. Faeh, F. Diederich, *Science.*, 2007, **317**, 1881-1886.
15. Q. A. Huchet, B. Kuhn, B. Wagner, H. Fischer, M. Kansy, D. Zimmerli, E. Carreira, K. Müller, *J. Fluorine. Chem.*, 2013, **152**, 119-128.
16. C. Swain, N. M. J. Rupniak, *Ann. Rep. Med. Chem.*, 1999, **34**, 51-60.
17. MedChem Database, Biobyte Corporation and Pomona College, 2002.
18. M. V. Niel, I. Collins, M. Beer, H. Broughton, S. Cheng, S. Goodacre, A. Heald, K. Locker, A. MacLeod, D. Morrison, C. Moyes, D. O'Connor, A. Pike, M. Rowley, M. Russell, B. Sohal, J. Stanton, S. Thomas, H. Verrier, A. Watt, J. Castro, *J. Med. Chem.*, 1999, **42**, 2087-2104.
19. J. A. K. Howard, V. J. Hoy, D. O'Hagan, G. T. Smith, *Tetrahedron.*, 1996, **52**, 12613-12622.
20. C. Dalvit, C. Invernizzi, A. Vulpetti. *Chem. Eur. J.*, 2014, **20**, 11058-11068.

21. B. Linclau, F. Peron, E. Bogdan, N. Well, Z. Wang, G. Compain, C. Fontenelle, N. Galland, J. Questel, J. Fraton, *Chem. Eur. J.*, 2015, **21**, 17808-17816.
22. J. E. Huheey, *Inorganic Chemistry*, Harper Collins, New York, 1983.
23. S. Wolfe, *Acc. Chem. Res.*, 1972, **5**, 102-111.
24. T. K. Brunck, F. Weinhold, *J. Am. Chem. Soc.*, 1979, **101**, 1700-1709.
25. K. B. Wiberg, *Acc. Chem. Res.*, 1996, **29**, 229-234.
26. J. Banks, A. Batsanov, J. K. Howard, D. O'Hagan, H. Rzepa, S. Martin-Santamaria, *J. Chem. Soc., Perkin Trans. 2.*, 1999, 2409-2411.
27. R. Abraham, A. Jones, M. Warne, R. Ritter, C. Tormena, *J. Chem. Soc., Perkin Trans. 2.*, 1996, 533-539.
28. D. Wu, A. Tian, H. Sun, *J. Phys. Chem. A.*, 1998, **102**, 9901-9905.
29. A. M. Sum, D. C. Lankin, K. Hardcastle, J. P. Snyder, *Chem-Eur. J.*, 2005, **11**, 1579-1591.
30. D. W. Kim, C. E. Song, D. Y. Chi, *J. Am. Chem. Soc.*, 2002, **124**, 10278-10279.
31. C. L. Liotta, H. P. Harris, *J. Am. Chem. Soc.*, 1974, **96**, 2250-2252.
32. G. A. Olah, J. T. Welch, Y. D. Vankar, M. Nojima, I. Kerekes, J. A. Olah, *J. Org. Chem.*, 1979, **44**, 3872-3881.
33. M. A. McClinton, *Aldrichimica Acta.*, 1995, **28**, 31-35.
34. G. Haufe, *J. Prakt. Chem.*, 1996, **338**, 99-113.
35. O. E. Okoromoba, J. Han, G. B. Hammond, B. Xu, *J. Am. Chem. Soc.*, 2014, **136**, 14381.
36. A. Domenico, L. Dario, P. Michele, *J. Org. Chem.*, 1998, **63**, 9587-9589.
37. H. Sun, S. G. DiMugno, *J. Am. Chem. Soc.*, 2005, **127**, 2050-2051.
38. M. J. Tozer, T. F. Herpin, *Tetrahedron*, 1996, **52**, 8619-8683.
39. G. S. Lal, G. P. Pez, R. G. Syvret, *Chem. Rev.*, 1996, **96**, 1737-1756.
40. T. Umemoto, R. P. Singh, Y. Xu, N. Satio, *J. Am. Chem. Soc.*, 2010, **132**, 18199-18205.
41. F. Beaulieu, L. P. Beauregard, G. Courchesne, M. Couturier, F. LaFlammer, A. L'Heureux, *Org. Lett.*, 2009, **11**, 5050-5053.
42. M. K. Nielsen, C. R. Ugaz, W. Li, A. G. Doyle, *J. Am. Chem. Soc.*, 2015, **137**, 9571-9574.
43. T. Umemoto, K. Tomita, *Tetrahedron Lett.*, 1986, **27**, 3271-3274.
44. D. Edmond, O. Hans, *Synlett.*, 1991, **3**, 187-189.

45. R. E. Banks, S. N. Mohialdin-Khaffaf, G. Sanker Lal, I. Sharif, R. G. Syvret, *J. Chem. Soc., Chem. Commun.*, 1992, **8**, 595-596.
46. E. Differding, G. M. Ruegg, *Tetrahedron Lett.*, 1991, **32**, 3815-3818.
47. X. Zhang, Y. Liao, R. Qian, H. Wang, Y. Guo, *Org. Lett.*, 2005, **7**, 3877-3880.
48. C. Geng, L. Du, F. Liu, R. Zhu, C. Liu, *RSC Adv.*, 2015, **5**, 33385.
49. F. Yin, Z. Wang, Z. Li, C. Li, *J. Am. Chem. Soc.*, 2012, **134**, 10401-10404.
50. S. Mizuta, I.S.R. Stenhagen, M. O'Duill, J. Wolstenhulme, A. K. Kirjavainen, S. J. Forsback, M. Tredwell, G. Sanford, P. R. Moore, M. Huiban, S. K. Luthra, J. Passchier, O. Solin, V. Gouverneur, *Org. Lett.*, 2013, **15**, 2648-2651.
51. S. Ventre, F.R. Petronijevic, D.W.C. MacMillan, *J. Am. Chem. Soc.*, 2015, **137**, 5654-5657.
52. J. C. T. Leung, C. Chatalova-Sazepin, J. G. West, M. Rueda-Bacerril, J. F. Paquin, G. M. Sammis, *Angew. Chem. Int. Ed.*, 2012, **51**, 10804.
53. T.J. Barker, D.L. Boger, *J. Am. Chem. Soc.*, 2012, **134**, 13588-13589.
54. Z. Li, Z. Wang, L. Zhu, X. Tan, C. Li, *J. Am. Chem. Soc.*, 2014, **136**, 16439-16443.
55. A. R. Mazzotti, M.G. Campbell, P. Tang, J. M. Murphy, T. Ritter, *J. Am. Chem. Soc.*, 2013, **135**, 14012-14015.
56. W. Liu, X. Huang, M. J. Cheng, R. J. Nielsen, W. A. Goddard, J. T. Groves, *Science.*, 2012, **337**, 1322-1325.
57. Y. Amaoka, M. Nagatomo, M. Inoue, *Org. Lett.*, 2013, **15**, 2160-2163.
58. J. B. Xia, C. Zhu, C. Chen, *J. Am. Chem. Soc.*, 2013, **135**, 17494-17500.
59. T. Okazoe, *Proc. Jpn. Acad. Ser. B.*, 2009, **85**, 276-289.
60. S. K. Biswas, K. Vijayan, *Wear.*, 1992, **158**, 193-211.
61. D. O'Hagan, *J. Fluor. Chem.*, 2010, **11**, 1071-1081.
62. S. Purser, P. R. Moore, S. Swallow, V. Gouverneur, *Chem. Soc. Rev.*, 2008, **37**, 320-330.
63. D. T. Wong, J. S. Horng, F. P. Bymaster, K. L. Hauser, B. B. Molloy, *Life Sci.*, 1974, **15**, 471-479.
64. K. Muller, C. Faeh, F. Diederich, *Science.*, 2007, **317**, 1881-1886.
65. R. S. Koff, *Aliment Pharmacol Ther.*, 2014, **39**, 478-487.
66. G. W. Ivie, J. E. Wright, *J. Agric. Food Chem.*, 1978, **26**, 90-94.

Chapter 2. All *cis*-1,2,3,4-tetrafluorocyclopentane

2.1 Multivincinal fluorinated alkanes

In previous research at St Andrews, alkanes carrying multiple vicinal fluorine motifs ($[\text{CHF}]_{n=3,4,5,6}$) were explored and prepared as single stereoisomers in order to assess the preferred conformations of the vicinal C-F bonds.¹⁻⁴ For example, two stereoisomers of the multivincinal hexafluoro alkane motif **1** and **2** were synthesised.⁴ X-Ray crystallography (Figure 1) and NMR both indicated that the all-*syn*-isomer **1** adopts a helical arrangement of C-F bonds along the carbon chain, where each adjacent C-F bond is rotated by about 60 degrees to the next and the carbon chain is irregular. The *syn-anti-syn-anti-syn*-isomer **2** shows a more classical *zig-zag* conformation for the carbon chain. The vicinal C-F bonds orient *gauche* but more significantly 1,3 dipolar repulsions of the the C-F bonds dictate the overall conformation.

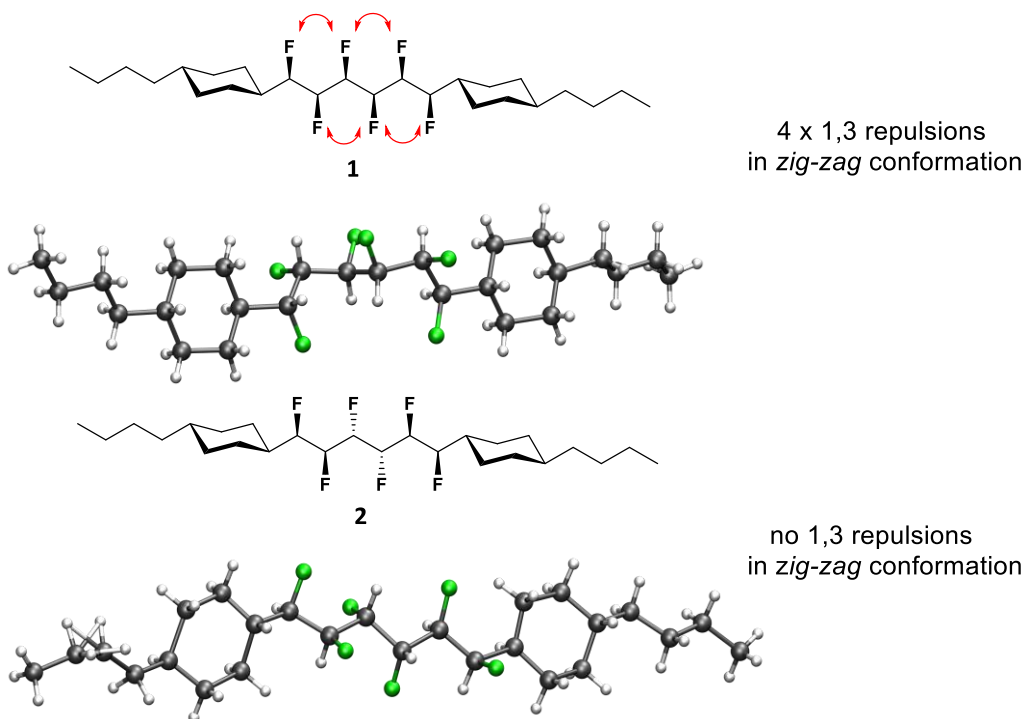


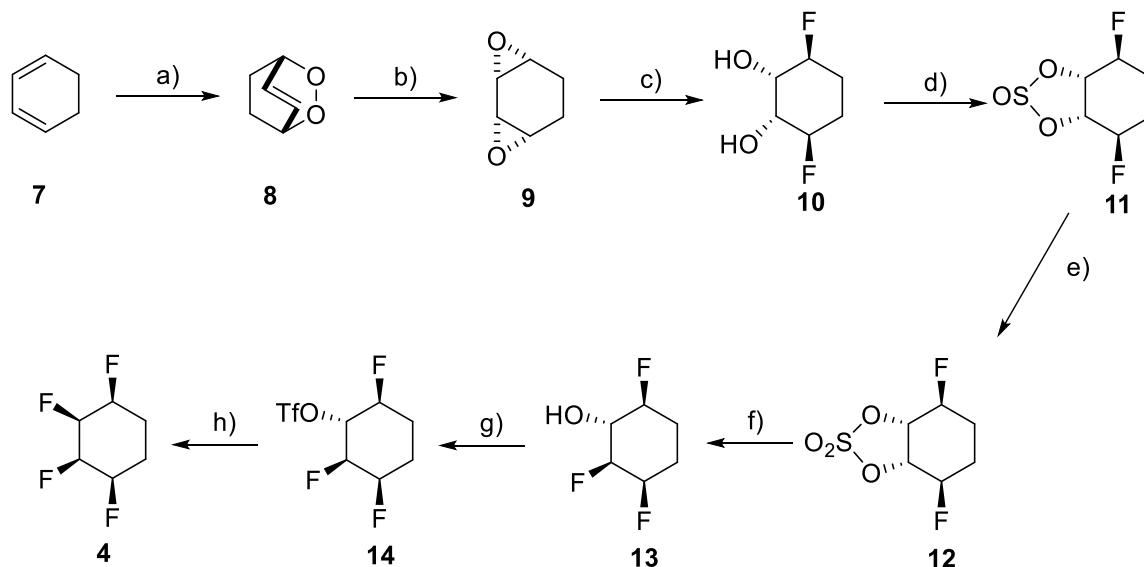
Figure 1. Stereoisomers of hexafluoro alkanes **1** and **2** and their corresponding crystal structures.⁴

In these flexible acyclic chains, the *syn*-vicinal isomer **1** adopts the helical structure to avoid 1,3 C-F bond repulsion and this reduces the overall polarity of the molecule. Therefore, to make this type polar molecules, it proved necessary to prepare a conformational constrained rigid ring system to overcome 1,3 C-F bond repulsion. In the end, cyclohexanes were explored.

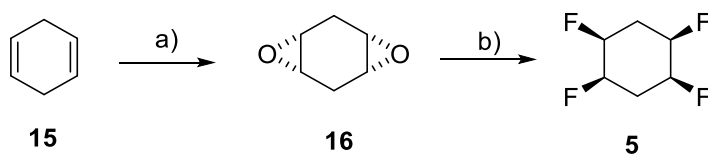
2.2 Vicinal fluorinated cyclohexanes

A range of cyclohexanes containing four or six fluorine atoms with only one fluorine on each carbon (CHF), and a stereochemistry where all fluorines are 'up', have been prepared in St Andrews.⁵⁻⁷ The idea was to make use of the polar C-F bond and force 1,3 diaxial C-F bonds, to induce high polarity. If all of the fluorines are incorporated onto the same face of the cyclohexane, it was anticipated that the cyclohexane motif will have some unusual properties, as the face

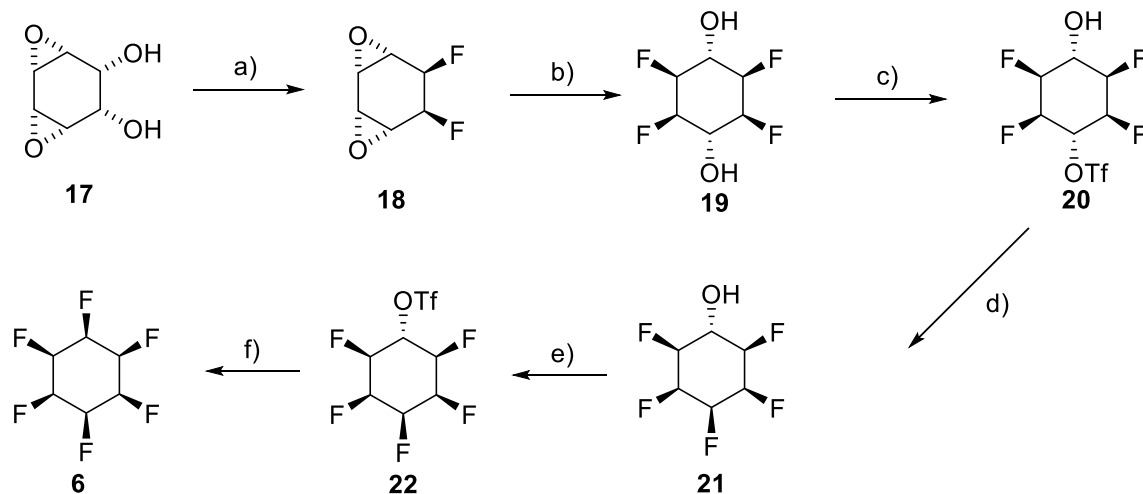
becomes polarized. The synthetic routes to the vicinal fluorinated cyclohexanes **4**, **5** and **6** are summarised in Schemes **1**, **-3** respectively.



Scheme 1. The synthesis of **4**.⁵ *Reagents and conditions:* a) P(OPh)_3 , O_3 , CH_2Cl_2 , -78°C ; b) $\text{Ru(PPh}_3)_3\text{Cl}_2$, CH_2Cl_2 , 0°C ; 47%; c) $\text{Et}_3\text{N} \cdot 3\text{HF}$, 90°C ; d) SOCl_2 , pyridine, CH_2Cl_2 , 0°C ; e) $\text{RuCl}_3 \cdot x\text{H}_2\text{O}$, NaIO_4 , MeCN , H_2O , 0°C ; f) $\text{Et}_3\text{N} \cdot 3\text{HF}$, 120°C , 70%; g) Tf_2O , pyridine, 0°C ; h) $\text{Et}_3\text{N} \cdot 3\text{HF}$, 120°C , 35%

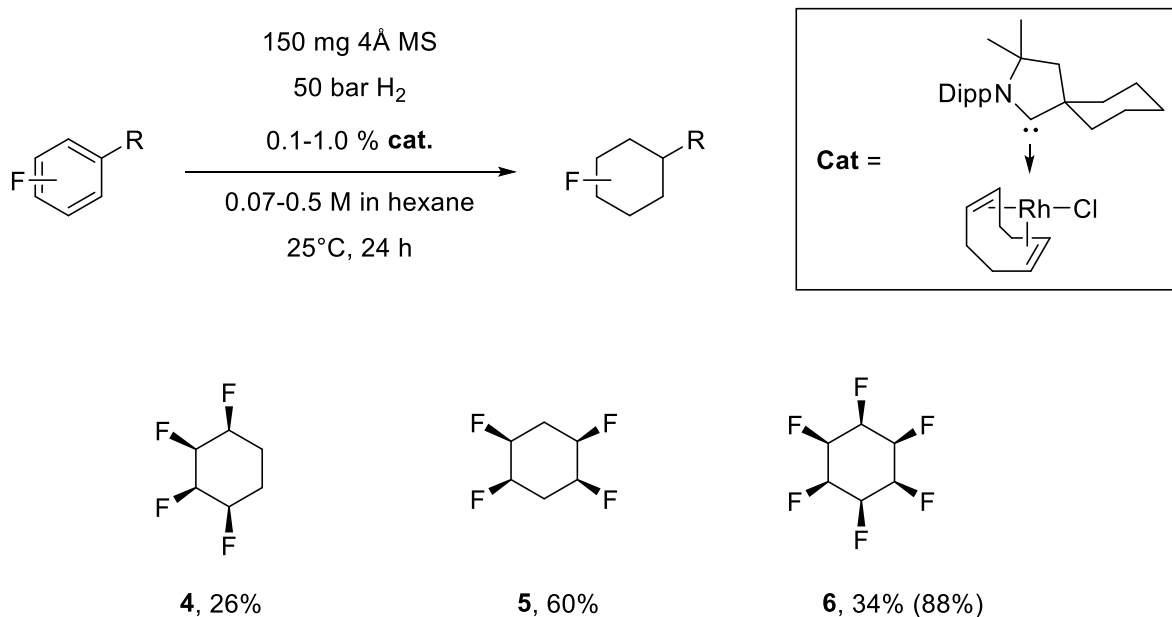


Scheme 2. The synthesis of **5**.⁶ *Reagents and conditions:* a) $m\text{CPBA}$, CH_2Cl_2 , -15°C , 52%; b) DAST, 70°C , 24%;



Scheme 3. The synthesis of *cis*-1,2,3,4,5,6-hexafluorocyclohexane.⁷ *Reagents and conditions:* a) Deoxofluor, THF, 60-100°C, microwave, 94%; b) Et₃N • 3HF, 180°C, microwave, 71%; c) Tf₂O, pyridine, CH₂Cl₂, 0°C, 71%; d) Et₃N • 3HF, 120°C, microwave, 40%; e) Tf₂O, pyridine, CH₂Cl₂, 0°C, 71%; f) Et₃N • 3HF, 180°C, microwave, 10%;

The synthesis of **4** and **5** proved quite straightforward and these cyclohexanes can be prepared in reasonable amounts. However, the synthesis of hexafluorocyclohexane **6** consists of 12 steps. The last fluorination step, owing to its low yield (10 %), renders this synthetic route inefficient. Although this route was used to prepare this compound for the first time, it is not appropriate for large production. Recently, a one-step direct hydrogenation method using a rhodium catalyst was reported by Glorius *et al.*^{8,9} and they were able to prepare multifluorinated cyclohexanes as well as fluorinated aliphatic heterocycles from their aromatic precursors. This method is much more efficient and generates **4**, **5** and **6** in one step in 24 %, 60 % and 84 % yield respectively, as illustrated in Scheme 4.



Scheme 4. Hydrogenation of fluorobenzenes to cyclohexanes.^{8,9}

The St Andrews group demonstrated that these all-*cis* fluorocyclohexane compounds are solid materials at RT and they have strong molecular dipole moments. For examples, *cis*-1,2,3,4-tetrafluorocyclohexane **4** has a melting point of 82 °C and a dipole moment of 4.9 D, and *cis*-1,2,4,5-tetrafluorocyclohexane **5**, has a melting point of 107 °C and a dipole moment of 5.2 D. The high melting points and high polarity arise because of forced 1,3 diaxial C-F bond orientations in the chair conformation of the cyclohexane ring and when the ring flips, the 1,3 interaction are retained. In the case of all *cis*-1,2,3,4,5,6-hexafluorocyclohexane **6**, there are three axial C-F bonds in the chair conformation. This molecule has an extraordinary high melting point of 206 °C and a dipole moment of 6.2 D, which is the most polar aliphatic compound described. The crystal structures are shown in Figure 2.

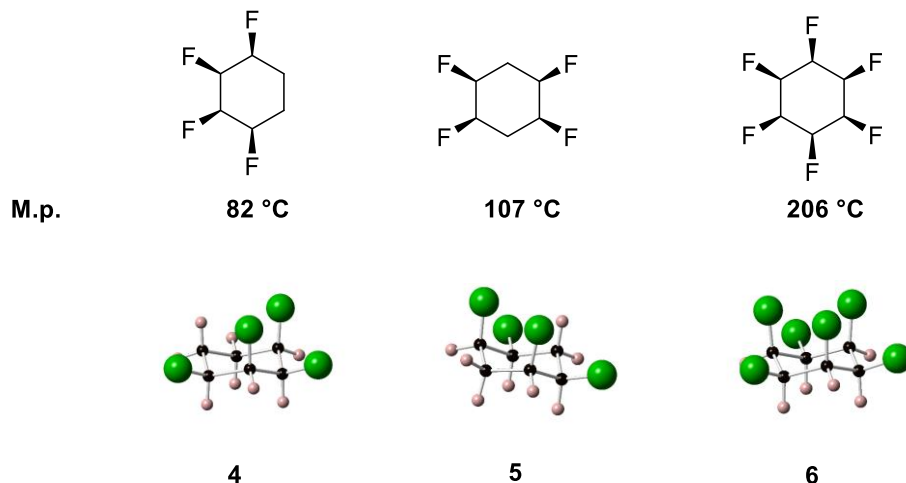


Figure 2. Crystal structures of vicinal fluorinated cyclohexanes.⁵⁻⁷

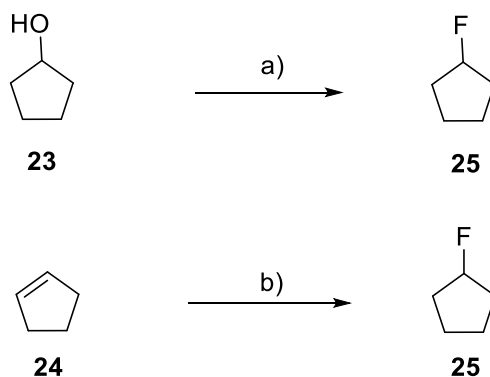
Due to their unique properties, these all-*cis* fluorinated cyclohexane molecules have been referred to as Janus face molecules,¹⁰ given the different polarisation of the faces of the ring. One interesting property of this type of molecule is their ability to bind cations to the electronegative fluorine face and anions to the electropositive hydrogen face.¹¹ This opens up prospects in supramolecular and metal organic framework (MOF) design.

2.3 Fluorine substitution of cyclopentane

The cyclohexane and cyclopentane rings are central motifs in organic chemistry. As has been discussed above, all-*cis* multivincinal fluorinated cyclohexane rings have facial polarity and a high molecular dipole. As an extension of the work on cyclohexane, it became an object to explore new motifs but with fewer carbon atoms and thus, the cyclopentane ring became the next focus of this research.

2.3.1 Mono- and di-substitution of cyclopentane

Monofluorocyclopentane is well known^{12,13} and has been synthesised in a number of ways. The most straightforward method involved deoxyfluorination of cyclopentanol using DAST. In another approach Olah's reagent was used to convert cyclopentene into monofluorocyclopentane (Scheme 5).

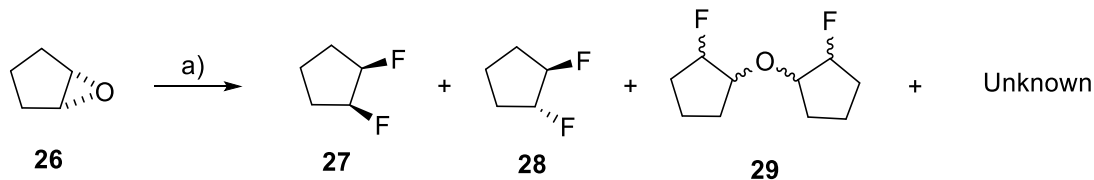


Scheme 5. Synthese of fluorocyclopentane. *Reagents and conditions:* a) DAST, DCM, 25°C;¹² b) HF·Py, DCM.¹³

1,1-Difluorocyclopentane was previously prepared by Strobach.¹⁴ In that case cyclopentanone was treated with SF₄ in the presence of HF to give the product.

The syntheses of both the *cis*- and *trans*-1,2-difluorocyclopentanes were reported by M. Hudlicky *et al.* in 1987 (Scheme 6) by treating cyclopentene oxide with DAST.¹⁵ Four different compounds were formed. The major compound was identified through ¹⁹F NMR as the *cis*-1,2-difluorocyclopentane **27** (88 %). The minor compound was not unambiguously identified but authors assumed it to be the *trans* 1,2-difluorocyclopentane **28**, the yield of which is not

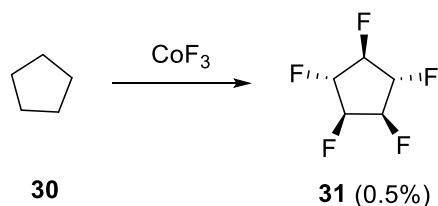
mentioned in the paper. The least volatile component was isolated from the product mixture and proved to be bis(2-fluorocyclopentyl) ether **29**. The fourth compound (0.3 %) was not identified.



Scheme 6. The synthesis of 1,2-difluorocyclopentane. *Reagents and conditions:* a) DAST, 55-60°C.¹⁵

2.3.2 Tri-, tetra- and penta-substitution of cyclopentane

There are no reports in the literature of tri- or tetra- fluorocyclopentanes, except compounds containing a CF₂ motif. However, there is a report¹⁶ from 1966 of the preparation and characterisation of a single stereoisomer of 1,2,3,4,5-pentafluorocyclopentane **30** (Scheme 7). It was prepared by direct fluorination of cyclopentane with cobalt trifluoride (CoF₃) and this gave **31** in a low yield (0.5%). The object of the study was to make perfluorocyclopentane, however this was a minor product of a large scale reaction. The stereochemistry, as assigned by NMR indicated the *trans, trans, cis, trans, cis* isomer, a stereochemistry where polarity is compromised, because there are fluorines on both sides of the ring.



Scheme 7. Direct fluorination of cyclopentane.¹⁶

2.4 Aims and objectives

It became an objective to make all-*cis*-1,2,3,4-tetrafluorocyclopentane **32** (Figure 3).

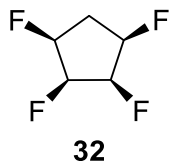
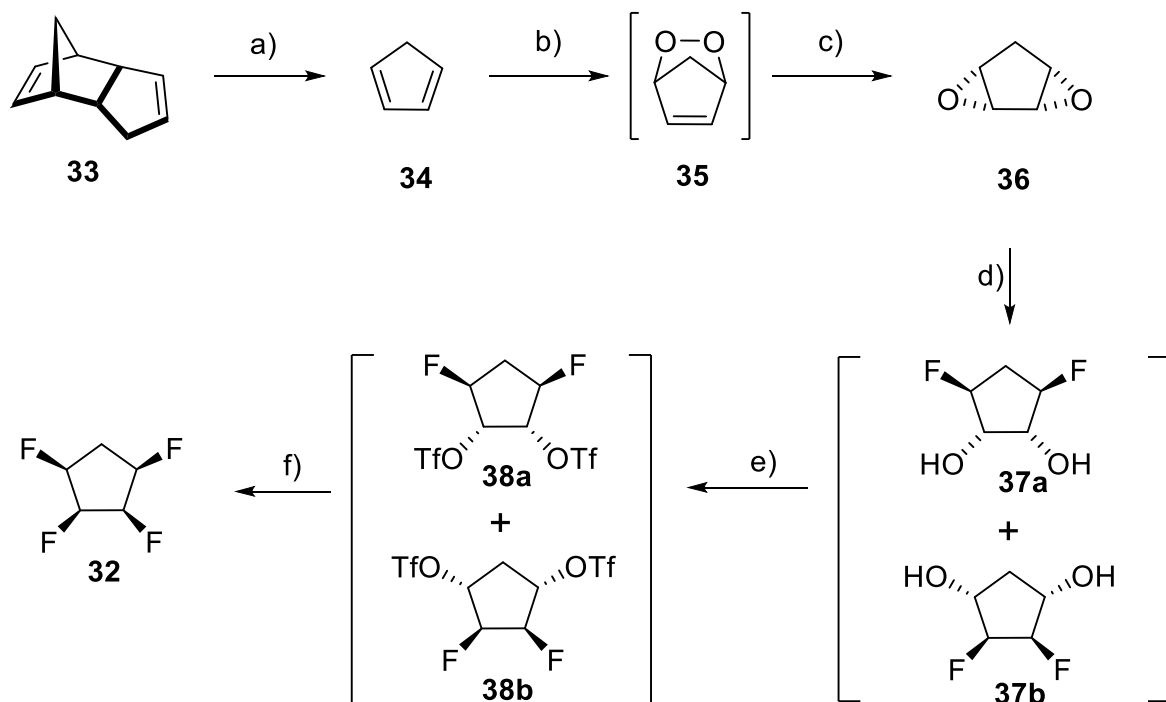


Figure 3. All-*cis*-1,2,3,4-tetrafluorocyclopentane **32**.

As discussed above, there is no literature on this molecule, and if prepared, it was anticipated to be polar and should have facial polarity similar to the all-*cis* fluorocyclohexanes. Cyclopentanes are conformationally more flexible than cyclohexanes, and it would be of interest to determine how ordered such a system would be in both the solution and solid state.

2.5 Results and discussions



Scheme 8. Synthesis of tetrafluorocyclopentane **32**. *Reagents and conditions:* a) heat, 78%; b) O_3 , $P(OPh)_3$, CH_2Cl_2 , $-78 \rightarrow -30^\circ C$; c) $Ru(PPh_3)_3Cl_2$, CH_2Cl_2 , $-78^\circ C$, 1h; $-40^\circ C$, 0.5 h; $-25^\circ C$, 1h, 38%; d) $Et_3N \cdot 3HF$, $120^\circ C$, 24h; e) Tf_2O , pyridine, RT, 24h; f) $Et_3N \cdot 3HF$, $100^\circ C$, 48h, 9% over steps (d) –(f).

The synthetic route taken in this work to tetrafluorocyclopentane **32** is shown in Scheme 8. It started from dicyclopentadiene **33**, a commercially available material. To obtain the cyclopentadiene monomer **34**, dicyclopentadiene **33** was cracked by heating. The pure cyclopentadiene was obtained after distillation in a 78% yield.

Cyclopentadiene **34** reacts in a Diels-Alder reaction with singlet oxygen, to give the *endo*-peroxide **35**.¹⁷ The conversion of *endo*-peroxide **35** to *cis*-diepoxy **36** by metal catalyst has been reported.¹⁸ Therefore, the preparation of *endo*-peroxide **36** was carried out as described by Murray *et al.*¹⁷ Treatment of a solution of triphenyl phosphite in CH_2Cl_2 with ozone at $-78^\circ C$

formed intermediate triphenyl phosphite ozonide, which is stable at temperatures below -35°C. When the reaction is warmed to -30°C, the triphenyl phosphite ozonide decomposes to form singlet oxygen. At this moment, cyclopentadiene **34** was added quickly to the reaction. The singlet oxygen then reacts with diene **34** in the Diels-Alder reaction to generate *endo*-peroxide **35**. This product is extremely unstable at temperatures above -30°C and therefore, it was carried on to the next step without isolation.

Endo-peroxide **35** was subject to isomerisation to *cis*-diepoxide **36** using a ruthenium catalyst following a protocol of Noyori.¹⁸ This reaction was successful and diepoxide **36** was purified by chromatography and isolated in a 38% yield from diene **34**.

Ring opening of the epoxide **36** was accomplished using Et₃N·3HF at 120°C, to generate a mixture of regioisomers of **37**. No starting material signals were observed by ¹H NMR and the conversion was judged to be high. Two major singlets appeared in the ¹⁹F {¹H} NMR spectrum in a ratio of 2:1 ($\delta_F = -182$ and -180 ppm), suggesting the presence of two regioisomers **37a** and **37b**. Due to the very close elution of these compounds by TLC, it was decided to convert them together to their corresponding ditriflates **38a** and **38b** without any purification.

Triflates **38** were formed using Tf₂O and pyridine at RT. This reaction proved relatively efficient and the resulting triflates were stable to aqueous work up. The products were washed with sat. aq. copper sulfate, dried and the solvent removed. At this stage, it still proved difficult to separate the isomers by chromatography, therefore, the residue was used directly for the final fluorination reactions, without further purification.

Finally, fluorination of the triflate isomers **38a** and **38b** using Et₃N·3HF at 100°C gave a single fluorinated product, the tetrafluorocyclopentane **32**. It took 2 days for the reaction to go to completion as followed by ¹⁹F {¹H} NMR. Analysis of the crude product by ¹⁹F {¹H} NMR showed that, there were two doublets in the region of -196 ppm and -219 ppm. There were other minor peaks which may have arose as elimination products, but there were no peaks in the region of -73 ppm, characteristic of residual triflate. Tetrafluorocyclopentane **32** proved to be rather volatile and subject to sublimation, however in the end a sample was isolated after purification by chromatography in a 9% overall yield from diepoxide **36**. This material was a crystalline solid (M.p. 39°C), and due to its tendency to sublime at RT, care had to be taken when the solvent was removed on the rotary evaporator, to achieve a good recovery.

All-*cis*-1,2,3,4-tetrafluorocyclopentane **32** was subject to X-ray structure analysis. Some perspectives of the resultant structure are shown in Figure 4.

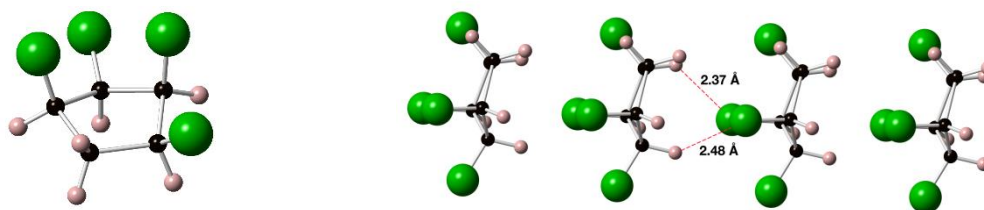


Figure 4. X-Ray structure of **32** (Prof A.M.Z. Slawin)

The crystal structure confirms the anticipated molecular structure and the all-*cis* stereochemistry. The left-hand image in Figure 4 shows an envelope structure with CHF at the tip of envelope. The right-hand image in Figure 4 shows a stacking structure indicative of facial polarity. Four molecules are shown stacked with each other and with the fluorine faces pointing to the hydrogen faces. The distances highlighted in Figure 4 are the shortest intermolecular CF...HC

contacts in the structure, 2.37 Å and 2.48 Å, respectively, indicating a strong electrostatic attraction between the different faces of the rings.

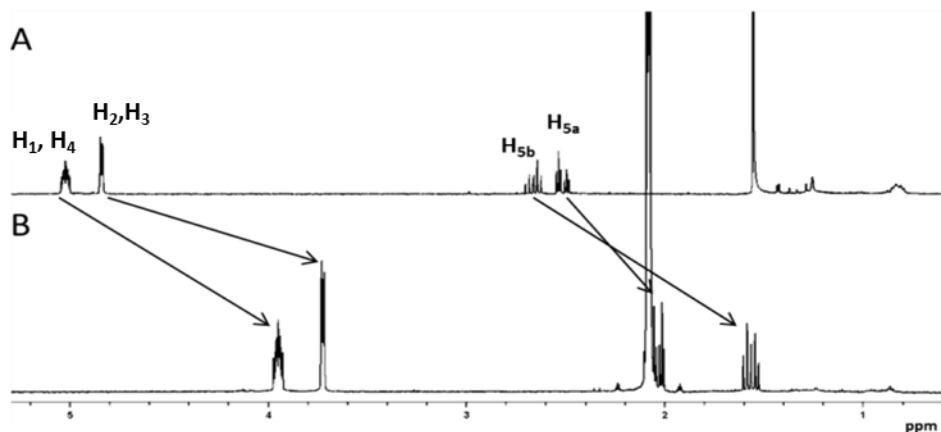


Figure 5. A) The ^1H $\{^{19}\text{F}\}$ NMR spectrum of **32** in CDCl_3 , and B) The ^1H $\{^{19}\text{F}\}$ NMR spectrum of **32** in $[\text{D}_8]$ toluene.

Table 1. Difference in chemical shift

Proton signal	δ CDCl_3 (ppm)	δ $[\text{D}_8]$ -Toluene (ppm)	$\Delta\delta$ (ppm)
H_{5a}	2.51	2.03	+0.48
H_{5b}	2.66	1.56	+1.10
H_2, H_3	4.84	3.77	+1.12
H_1, H_4	5.02	3.95	+1.10

In order to illustrate the polar aspect of this ring system, comparative ^1H NMR experiments were conducted in two solvents. When the ^1H NMR spectrum was carried out in d_8 -toluene, all protons experience a significant upfield shift, compared with the ^1H NMR spectrum run in CDCl_3 (Figure 5 and Table 1). These upfield shifts are most likely caused by the anisotropic field associated with

the aromatic ring and by the dipole- π interaction between the aromatic ring of toluene and the electropositive face (hydrogen) of the cyclopentane (Figure 6). Most of the protons shift upfield by over 1 ppm, however, the least shifted proton (+0.48 ppm) is H_{5a} located on the upper fluorine face (H_{5a} proton on the CH₂ methylene group). This smaller shift is consistent with its location in the more electronegative fluorine face of the cyclopentane ring, whereas the other protons in the more electropositive face are shielded to a larger extent by the toluene.

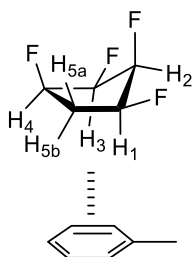


Figure 6. Representation of the interaction between toluene and all-*cis*-1,2,3,4-tetrafluorocyclopentane **32**.

It is well known that cyclopentane and its derivatives are conformationally more flexible than cyclohexanes. In order to explore the energies of the various conformations of **32**, density functional theory (DFT) optimisations at the B3LYP-D3/6-311+G (d,p) level were performed by Prof Michael Büehl.

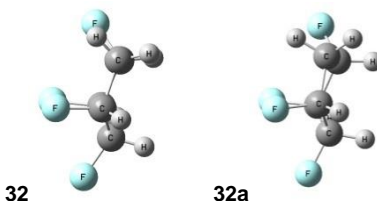


Figure 7. Calculated structures of **32** (B3LYP-D3/6-311+G (d,p) level of theory); at the left the X-ray structure, **32a** is the sole minimum in different orientations.

After optimisations, **32a** (Figure 7) emerged as the minimum energy structure. This structure is slightly twisted from the structure in the solid state **32**. As a consequence, this twist affords another envelope conformer, where the fluorine at the apex of the envelope is in an axial position, rather than in an equatorial position (compare the two structures of Figure 7). This small distortion occurs irrespective of the level of theory (other DFT functionals, MP2 level) or the environment (gas phase, a second molecule stacked on top or a polarisable continuum model).

In order to estimate the energy between the two structures **32** and **32a**, a partial optimisation, freezing the conformation of **32** (by fixing the C-C-C-C dihedral angles) and relaxing all other structural parameters, was performed. The solid state structure **32** derived from X-ray analysis is 2.2 kcal/mol higher in energy than the fully optimised minimum structure **32a**. Since this energy difference is small, it is almost certainly the packing forces in the crystal that cause the slightly higher energy conformer **32** in the solid state. A single molecule carved out of the crystal has a higher computed dipole moment (5.8 D) than that predicted for the gas phase minimum **32a** (4.9 D).

There are two alternative envelope forms (with a CH₂ group at the envelope tip) that can occur. These two forms are essentially isoenergetic, but they were not found to be minimum energy structures. They were transition states, involved in the rearrangement of **32a** with its mirror image, **32a'**. One of these transition states, **32b**, is depicted at the middle of Figure 8. The computed barrier for this pseudorotation-type rearrangement is $\Delta H^\ddagger = 2.5$ kcal/mol at room temperature. Consistent with this low energy barrier, VT ¹⁹F{¹H} NMR experiments in CDCl₃ failed to detect any line broadening even at temperatures as low as -80 °C (Figure 9).

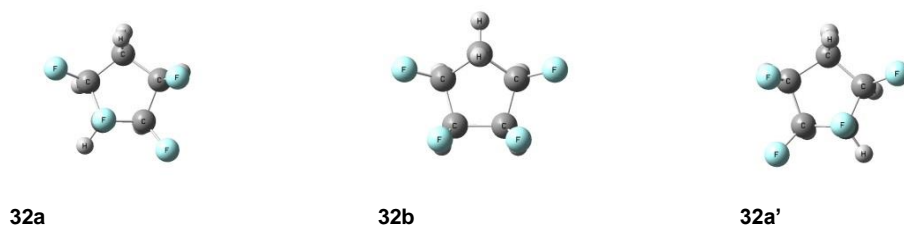


Figure 8. The transition state **32b**.

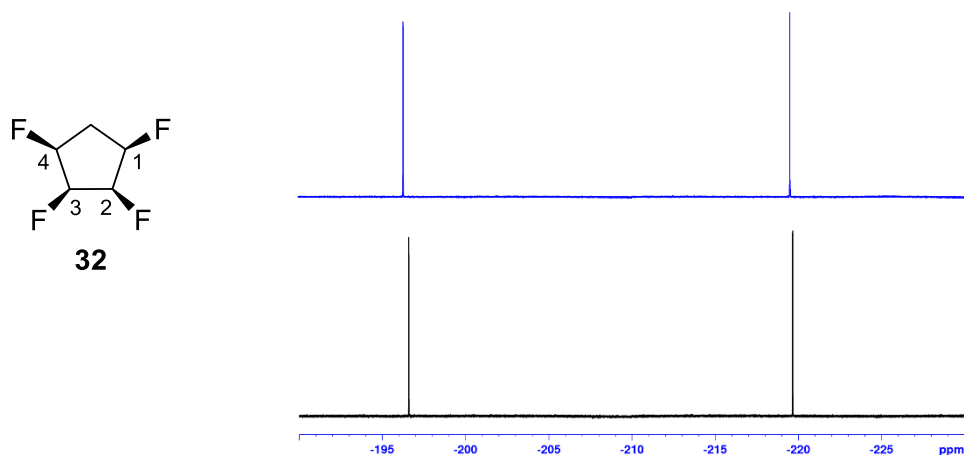
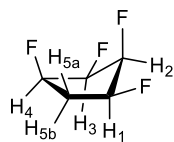


Figure 9. $^{19}\text{F} \{^1\text{H}\}$ NMR in CD_2Cl_2 of tetrafluorocyclopentane **32**. Blue line -80°C , black, 25°C .

Indirect spin-spin coupling constants involving the CH_2 group were computed at the BHandH/6-311+G (2d,p) level. The results are collated in Table 2 and clearly show quite reasonably that the solution structure cannot arise from the computed transition state structure **32b**, because there are large deviations between the observed and computed $J_{(\text{H}, \text{H})}$ values. Much better agreements are obtained for both the fully and partially optimised structures, and the values computed for the fully optimised minimum conformation of **32a** fit slightly better with experiment than those for **32** (see rightmost column in Table 2). These data support the interpretation that the dominant conformation in solution is closer to the pristine minimum **32a** than to the X-ray structure found in the solid state.



	$J_{H_{5a}-H_{5b}}$	$J_{H_{5a}-H_{1,4}^a}$	$J_{H_{5a}-H_{1,4}^b}$	Deviation ^b
NMR 32	16.3	4.3	7.4	n.a.
Calc. 32a	15.1	4.5	7.6	0.5
Calc. 32	15.8	1.8	7.6	1.1
Calc. 32b	10.9	10.8	5.6	5.5

Table 2: $J_{(H-H)}$ coupling constants (in Hz), BHandH/6-311+G (2d,p)//B3LYP-D3/6-311+G (d,p) level. ^aMean value of couplings to H₁ and H₄ ^bMean absolute deviation from experiment [absolute values used for $J_{(H_{5a}-H_{5b})}$]. ^cExperimental data (this work, CDCl₃).

An electron density map was calculated for **32a**. This calculation confirms that there is significant polarisation of the cyclopentane ring. It is clear that the fluorine face is electronegative and the protic face is electropositive.

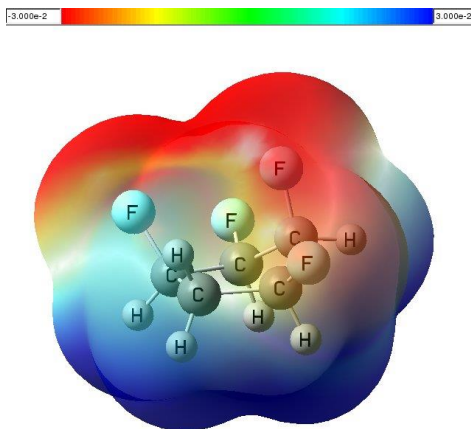


Figure 9. Electrostatic surface potential map for **32a** calculated at the (B3LYP-D3/6-311+G (d,p) level).

2.6 All *cis*-1,2,3,4-[²H₆]-tetrafluorocyclopentane

2.6.1 Introduction of deuterium

Deuterium (symbol D or ²H) is one of the two isotopes of hydrogen. It contains one proton and one neutron, so its atomic weight (2.014) is approximately twice that of hydrogen, and as a consequence deuterium is termed heavy hydrogen. The natural abundance of deuterium (²H) is low and accounts for only 0.0156% of hydrogen (¹H).

In 1932, Urey and his co-workers firstly reported spectroscopic evidence for heavy hydrogen.¹⁹ Later, Urey and Washburn reported the enrichment of heavy hydrogen in water upon electrolysis.²⁰ Very quickly, a small amount of pure heavy water was successfully isolated by Gilbert Lewis and his co-workers in 1933.²¹ After the isolation of heavy water, Polanyi and Eyring correctly postulated that protonated and deuterated compounds should react at different rates because of differences in zero point energies.²² Because of this isotopic effect, deuterium has been of value for the study of reaction mechanism. In 1934 alone, around 200 papers related to deuterium were published. Due to Urey's contribution to the discovery of deuterium, he was awarded the Noble Prize in 1934.

2.6.2 Kinetic Isotopic effect

The kinetic isotopic effect describes the change in a reaction rate as a consequence of an isotopic substitution of a molecule. Basically, isotopic substitution does not change the surface energy, it only effects the vibrational frequency of a bond (e.g. C-H to C-D), which results in a change in the reaction rate if that bond is broken. In principle, the vibrational energy (E_n) is dependent on the

frequency of the bond stretch (ν), which in turn depends on the reduced mass of the two connected atoms. Three important equations are showed below.²²

$$\nu = \frac{1}{2\pi c} \sqrt{\frac{k}{\mu}}$$

$$\mu = \frac{m_1 \times m_2}{m_1 + m_2}$$

$$E_n = (n + 1)h\nu$$

Where $n = 0, 1, 2, \text{ etc...}$

k = force constant

From the equations we can see that the magnitude of the isotope effect will depend on the difference in the mass after isotopic substitution. Proton and deuterium exchange has been widely used because there is a 100 % increase in mass compared to the $^{13}\text{C}/^{12}\text{C}$ (13 versus 12), where the mass increase is only 8.3%. As a consequence, the deuterium isotopic effect has become one of the most important tools in the elucidation of reaction mechanisms.

The Morse curve (Figure 10)²³ of C-H and C-D bonds are essentially identical. The lowest energy at the ground state is called the zero-point energy, which corresponds to the vibrational energy of the bonds of a molecule at absolute zero. At a given moment around 99% of the bonds are in the ground state since room temperature is close enough to absolute zero. Due to the mass difference, the length of the C-D bond is shorter than the C-H bond and the stretching frequency of the C-D bond is lower, so the zero-point energy of C-D is lower.

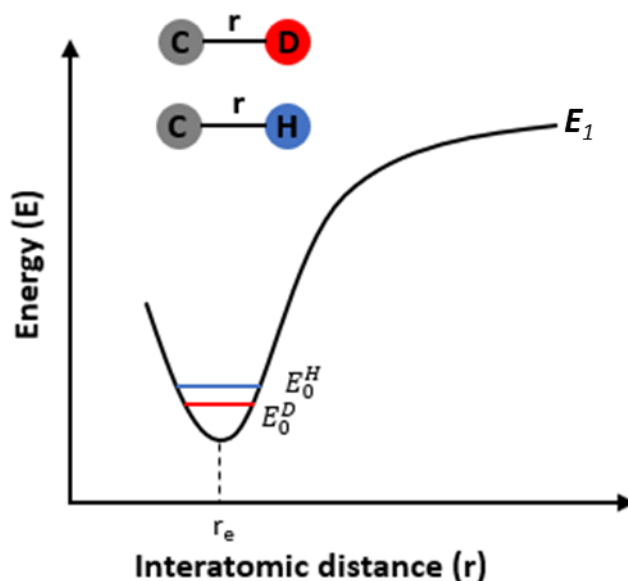


Figure 10. Morse curve.²³

The dissociation energy of a compound is the difference between E_1 and E_0 in Figure 10. Since the deuterium compound has the lower zero-point energy, it means that a greater energy input is needed and because the C-D bond is stronger than the C-H bond, if the rate determining step of a reaction involves C-H bond cleaving, the process will be slower than with C-D.

2.6.3 Chemical-shift isotopic effect

In NMR, the heavier isotopic substitution generally leads to an increased nuclei shielding for the atom bonded to deuterium. This results in a heavy atom upfield shift.²⁴ The magnitude of the isotope shift depends on the isotope and the position in the molecule. Deuterium usually causes relatively large changes compared to any other heavy-atom isotopes because of the larger change in mass on going from hydrogen to deuterium.²⁵ In physics, the upfield shift arises because of the lower zero-point energy of deuterium, while chemists attribute the chemical changes to increased electron density due to a shorter bond on the nuclei.

Geminal and vicinal isotopic effect have been investigated in ^{19}F NMR.²⁶ A series of fluorocyclohexane isotopomers **39** were prepared stereospecifically, and the geminal isotopic effect was measured by comparison with undeuterated cyclohexane ax-39 , eq-39 and $\text{trans-[2-}^2\text{H]-ax-39}$, $\text{trans-[2-}^2\text{H]-eq-39}$. The vicinal isotopic effect was evaluated similarly (Figure 11). In order to measure the chemical shift of the axial and equatorial conformers, low temperature (-85°C) ^{19}F NMR experiments were recorded to slow down the ring inversion, with CF_3CCl_3 as an internal reference. From these experiments, all ^{19}F NMR shifts were recorded to higher field. The observed three-bond isotope shifts are quite large, with the largest shift (0.35 ppm) observed in $\text{trans-[2-}^2\text{H]-ax-39}$ when C-F and C-D are *anti*-periplanar to each other, while the smallest shift, in $\text{cis-[2-}^2\text{H]-ax-39}$, was 0.13 ppm. The geminal effects are consistently larger than the vicinal effects. The geminal shift in $[\text{1-}^2\text{H]-39}$ is usually larger than 0.5 ppm. The vicinal effect appears to be additive. The shift induced by the four deuteriums in fluorocyclohexane $[\text{1,1,3,3-}^2\text{H}_4]\text{-ax-39}$ (1.06 ± 0.03) agrees with the sum of two axial-axial shift in $\text{trans-[2-}^2\text{H]-ax-39}$ and two axial-equatorial shift in $\text{cis-[2-}^2\text{H]-ax-39}$ (1.06 ± 0.1). While the shift of the conformer $[\text{1,1,3,3-}^2\text{H}_4]\text{-eq-39}$ (0.60 ± 0.03) is close to the sum of the shift of $\text{trans-[2-}^2\text{H]-eq-39}$ and $\text{cis-[2-}^2\text{H]-eq-39}$ (0.58 ± 0.08).

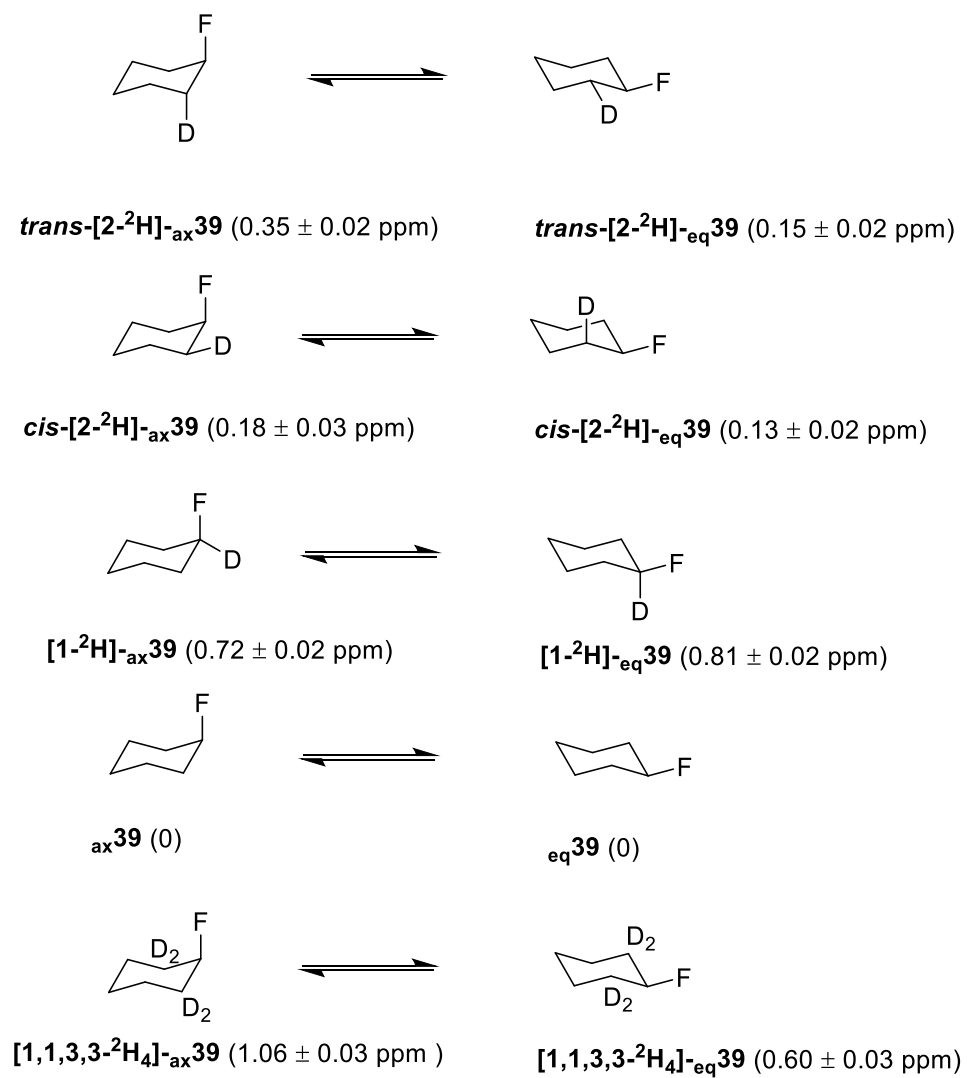


Figure 11. The isotopic shift of deuterated fluorocyclohexane.²⁶

2.6.4 Aims and objective

With a synthesis of tetrafluorocyclopentane **32** in place, it became attractive to prepare the perdeuterated all *cis*-1,2,3,4- $^{2}\text{H}_6$ -tetrafluorocyclopentane **32a**.

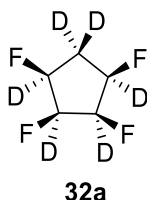
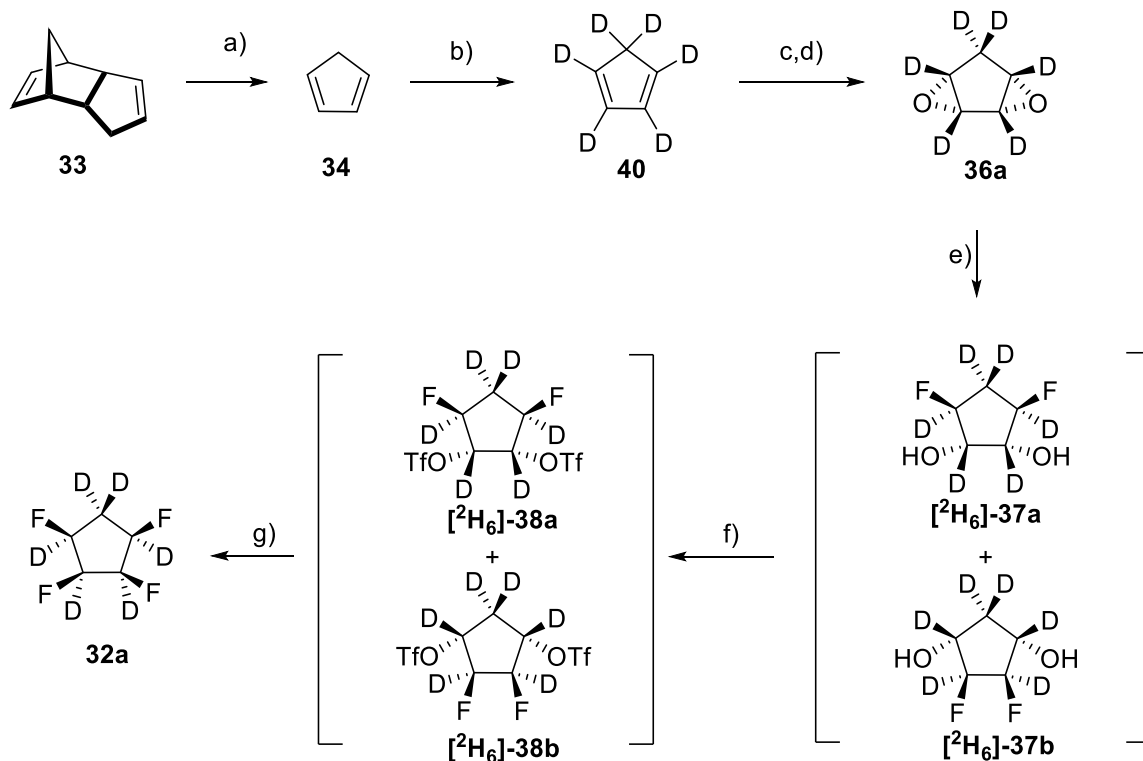


Figure 12. All *cis*- $^{2}\text{H}_6$ -tetrafluorocyclopentane **32a**.

This emerged to be of interest because the structure was anticipated to have a higher dipole moment than that of the protic molecule. This is because the polarity of this compound is caused by its molecular dipole moment. The C-D bond is shorter than that of C-H bond as discussed above, so when hydrogen is replaced by deuterium, the charge separation between the electropositive and electronegative faces should decrease and the polarity should increase.

2.6.5 Results and discussions

A synthesis of $^{2}\text{H}_6$ -tetrafluorocyclopentane **32a** was developed following that of the unlabelled tetrafluorocyclopentane **32**, as illustrated in Scheme 12.



Scheme 12. Synthesis of $[^2\text{H}_6]$ -tetrafluorocyclopentane **32a**. *Reagents and conditions:* a) heating, 78%; b) NaOD, D_2O , Me_2SO , 0°C , 44% (c) O_3 , $\text{P}(\text{OPh})_3$, CH_2Cl_2 , $-78 \rightarrow -30^\circ\text{C}$ (d) $\text{Ru}(\text{PPh}_3)_3\text{Cl}_2$, CH_2Cl_2 , -78°C , 1h; -40°C , 0.5 h; -25°C , 1h; (e) $\text{Et}_3\text{N}\cdot 3\text{HF}$, 120°C , 24h; (f) Tf_2O , pyridine, RT, 24h; (g) $\text{Et}_3\text{N}\cdot 3\text{HF}$, 100°C , 48h

The synthesis started again with dicyclopentadiene **33**, followed by distillation to acquire pure cyclopentadiene **34**.

The perdeuterated isotopmer of cyclopentadiene **40** has been reported by Lambert.²⁷ In that synthesis the product was recovered in 67% yield with 99% isotope exchange. The preparation of $[^2\text{H}_6]$ -cyclopentadiene **40** was therefore carried out as previously described.²⁷ Sodium was added to D_2O to generate the solution of NaOD/ D_2O . A cyclopentadiene solution in DMSO was then added and the reaction was stirred for 1 h at 0°C . The top layer (cyclopentadiene) was syringed into another flask containing NaOD/ D_2O and DMSO and was stirred for a further 1h. Complete reaction required the exchange at all six hydrogens by deuterium. The progress of the

exchange towards [$^2\text{H}_6$]-cyclopentadiene **40** (yield 47%) was followed by ^1H NMR spectroscopy until there were no proton signals, indicating that a fully deuterated cyclopentadiene **40** was formed.

The perdeuterated diepoxide [$^2\text{H}_6$]-**36a** was obtained using the previous protocol for **36**, although the yield in this case was only 13%. It proved difficult to follow the chemistry by ^1H -NMR, therefore it was decided to proceed through the fluorination, triflation and fluorination reactions without intermediate purifications. This proved successful and a sample of [$^2\text{H}_6$]-tetracyclopentane **32a** was prepared after a final purification by chromatography (yield 6.7 % through three steps reaction).

[$^2\text{H}_6$]-Tetrafluorocyclopentane **32a** was isolated as a white crystalline solid and it was subjected to X-ray crystal structure analysis. In the event, the X-ray analysis provided an indistinguishable structure to unlabelled **32** and there was no difference between C-C bond lengths or intermolecular distance C \cdots C, and there was no obvious suggestion of a more compact molecule.

The ^1H NMR of [$^2\text{H}_6$]-**32a** did not show any significant peaks indicating that all protons were replaced by deuterium. ^2H NMR was used to explore the extent of deuteration of compound **32a**. There were two broad peaks in the ^2H NMR spectrum at 4.86 and 2.37 ppm respectively, with a ratio 2 : 1 in the spectrum as illustrated in Figure 13. This is consistent with the structure and these two signals can be assigned to the four deuteriums from CDF and two deuteriums from CD_2 group.

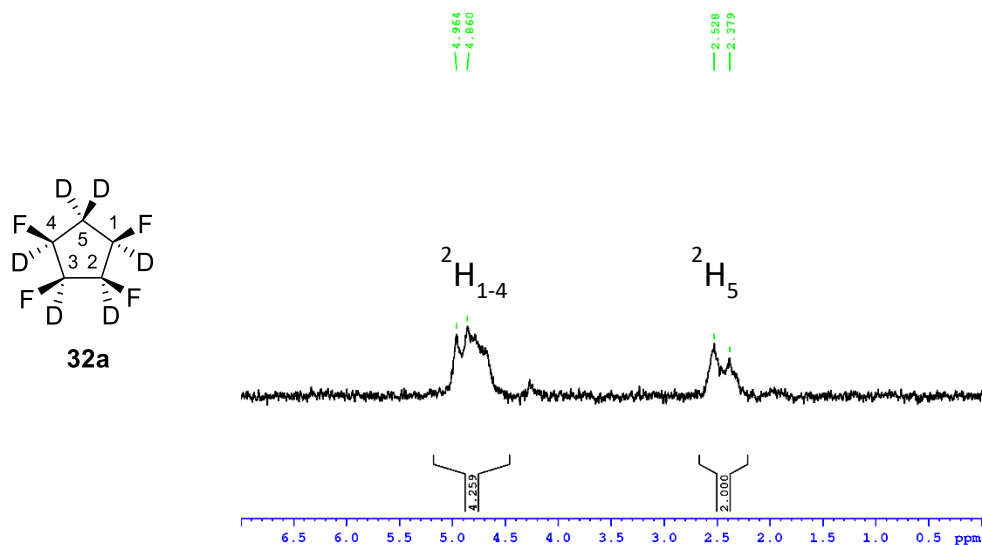


Figure 13. ^2H NMR of $[\text{}^2\text{H}_6]\text{-32a}$.

Analysis of the final product by ^{19}F $\{^1\text{H}\}$ NMR showed that, there were two broad peaks in the region of -197 ppm and -220 ppm, which is entirely consistent with expectation for $[\text{}^2\text{H}_6]\text{-32a}$. Due to the induced heavy atom isotope shift, the two fluorine peaks are shifted upfield by around 1.5 ppm and 1.1 ppm, respectively, as illustrated in Figure **14**, the blue traces are the $[\text{}^2\text{H}_6]$ **32a**, while the black traces are the unlabelled **32**.

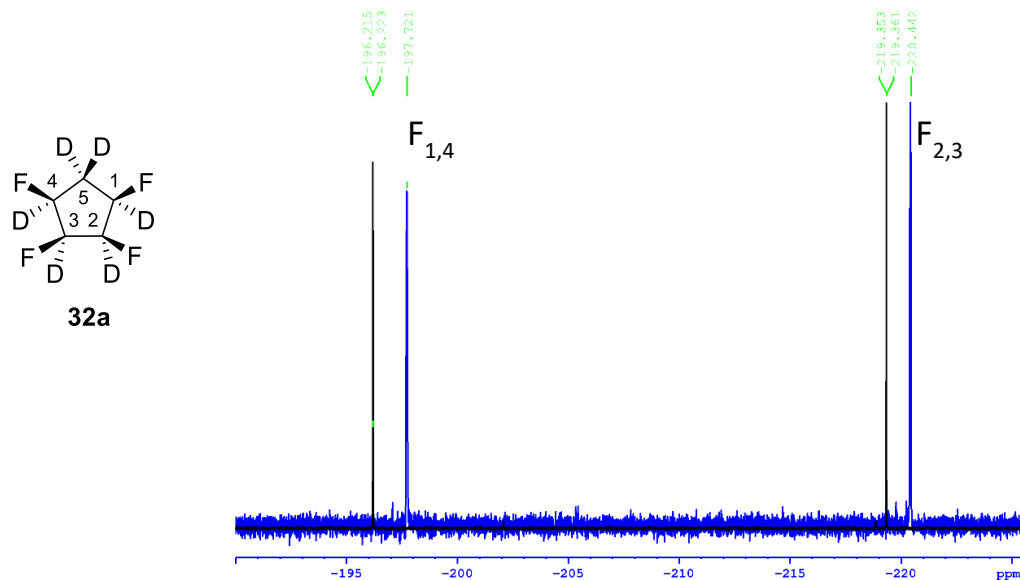


Figure 14. ^{19}F $\{^1\text{H}\}$ NMR of compound **32** and $[\text{}^2\text{H}_6]$ **32a**.

Again, in order to explore the polar aspect of this ring system, similar comparative ^2H NMR experiments were conducted in two solvents. When the ^2H NMR was carried out in toluene, all of the deuterium signals experience a significant upfield shift, compared with the ^2H NMR spectrum recorded in chloroform (Figure 15). However, the least shifted deuterium (D_a), as discussed above, is assigned to that of the upper face deuterium, from the CD_2 methylene group in the ring.

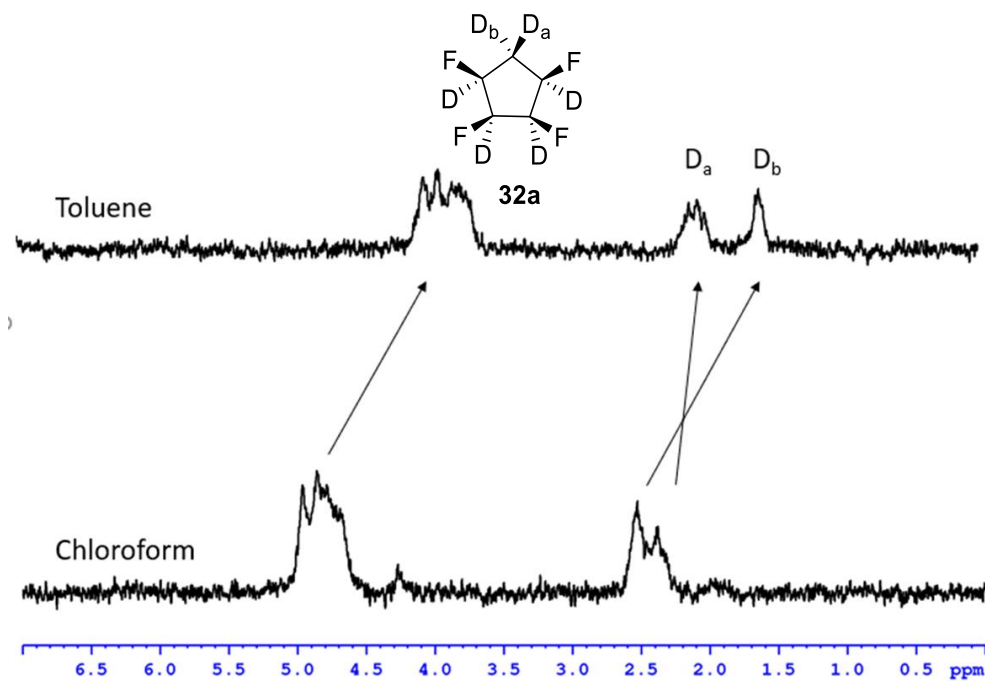


Figure 15. ^2H NMR of compound [$^2\text{H}_6$] **32a** in toluene and chloroform at RT.

Finally, GC-MS was used to measure the retention time of the two isotopmers. A reverse phase column was used to access separation of the two compounds. The more polar compound is anticipated to have a shorter retention time with reverse phase. Both compounds were mixed together and the mixture was injected into the GC machine. A clear peak for the mixture was recorded (Figure 16).

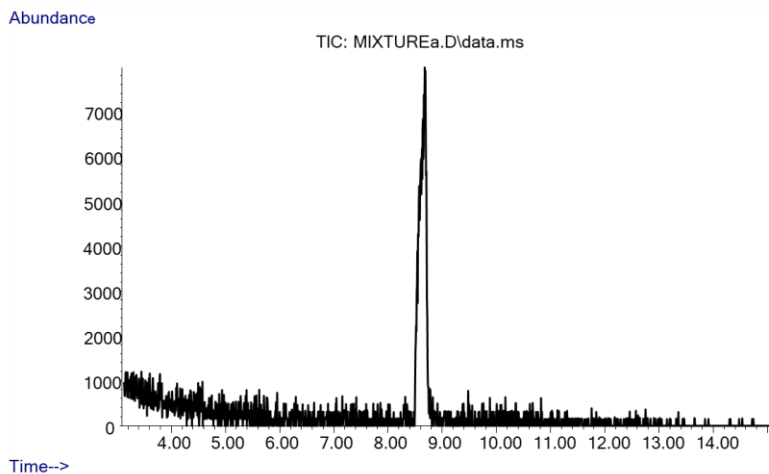


Figure 16. The GC-MS peak of the mixture of isotopmers **32** and [$^2\text{H}_6$] **32a**.

Analysis of this peak indicates many fragment peaks as illustrated in Figure 17. Among these fragments, the two most abundant peaks, with recorded masses of 77 amu and 80 amu, correspond to ions of $C_3F_2H_3^+$ and $C_3F_2D_3^+$, respectively. Compound **32** and **32a** behaved in a similar manner by GC-MS and both are cleaved into these two fragments.

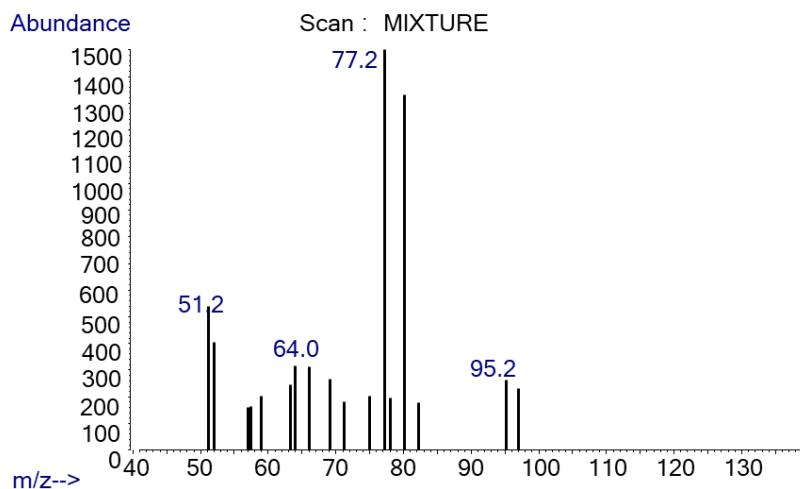


Figure 17. Fragment peaks.

Finally, the relative retention times were determined by GC-MS by monitoring the molecular ions at 77 and 80 amu (Figure 18). From the data it can be seen that, even though the difference of peak 77 and 80 is very small, the deuterated fragment elutes before the protic fragment. This observation supports the idea that perdeuteration increases molecular polarity, although the increase in polarity is small.

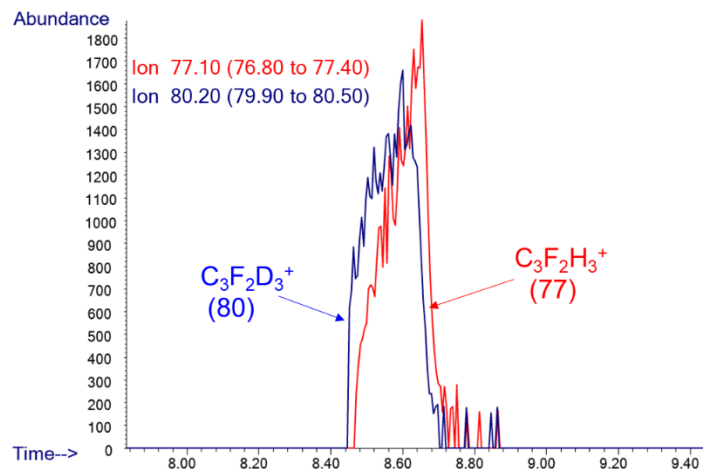


Figure 18. The retention time of molecular ions 77 aum and 80 aum.

2.7 Conclusion

Chapter 2 describes the successful synthesis of the all *cis*-1,2,3,4-tetrafluorocyclopentane **32** and its deuterated isotopomer **32a**. The studies were compared experimentally by X-ray analysis in the solid state, NMR studies in solution and computational studies. NMR data indicated that this molecule has highly polarized faces. GC-MS analysis gave some indication that per-deuterated isotopomer is more polar than the unlabelled cyclopentane.

Reference.

1. M. Nicoletti, D. O'Hagan, A. M. Z. Slawin, *J. Am. Chem. Soc.*, 2005, **127**, 482-483.
2. L. Hunter, D. O'Hagan, A. M. Z. Slawin, *J. Am. Chem. Soc.*, 2006, **128**, 16422.
3. D. Farran, A. M. Z. Slawin, P. Kirsch, D. O'Hagan, *J. Org. Chem.*, 2009, **74**, 7168-7171.
4. L. Hunter, P. Kirsch, A. M. Z. Slawin, D. O'Hagan, *Angew. Chem. Int. Ed.*, 2009, **48**, 5457-5460.
5. A. J. Durie, A. M. Z. Slawin, T. Lebl, P. Kirsch, D. O'Hagan, *Chem. Commun.*, 2011, **47**, 8265-8267.
6. A. J. Durie, A. M. Z. Slawin, T. Lebl, P. Kirsch, D. O'Hagan, *Chem. Commun.*, 2012, **48**, 9643-9645.
7. N. S. Keddie, A. M. Z. Slawin, T. Lebl, D. Philp, D. O'Hagan, *Nat. Chem.*, 2015, **7**, 483-488.
8. M. P. Wiesenfeldt, Z. Nairoukh, W. Li, F. Glorius, *Science*, 2017, **357**, 908-912.
9. M. P. Wiesenfeldt, T. Knecht, C. Schlepphorst, F. Glorius, *Angew. Chem. Int. Ed.*, 2018, **57**, 8297-8230.
10. N. Santschi, R. Gilmour, *Nat. Chem.*, 2015, **7**, 467-468.
11. B. E. Ziegler, M. Lecours, R. A. Marta, J. Featherstone, E. Fillion, W. Hopkins, V. Steinmetz, N. Keddie, D. O'Hagan, T. B. McMahon, *J. Am. Chem. Soc.*, 2016, **138**, 7460-7463.
12. V. A. Petrov, S. Swearingen, W. Hong, W. C. Petersen, *J. Fluorine Chem.*, 2001, **109**, 25-31.
13. G. A. Olah, J. T. Welch, Y. D. Vankar, M. Nojima, I. Kerekes, J. A. Olah, *J. Org. Chem.*, 1979, **44**, 3872-3881.
14. D. R. Strobach, G. A. Boswell, *J. Org. Chem.*, 1971, **36**, 818.
15. M. Hudlicky, *J. Fluorine Chem.*, 1987, **36**, 373-384.
16. A. Bergomi, J. Burdon, T. M. Hodgins, R. Stephens, J. C. Tatlow, *Tetrahedron*, 1966, **22**, 43-51.
17. R. W. Murray, M.L. Kaplan, *J. Am. Chem. Soc.*, 1969, **91**, 5358.
18. M. Suzuki, H. Ohtake, Y. Kameya, N. Hamanaka, R. Noyori, *J. Org. Chem.*, 1989, **54**, 5292.
19. H. C. Urey, F. G. Brickwedde, G. M. Murphy, *Phys. Rev.*, 1932, **39**, 164.
20. E. W. Washburn, H. C. Urey, *PNAS.*, 1932, **18**, 496-498.

21. G. N. Lewis, R. T. MacDonald, *J. Chem. Phys.*, 1933, **1**, 341.
22. K. B. Wiberg, *Chem. Rev.*, 1955, **55**, 713.
23. F. H. Westheimer, *Chem. Rev.*, 1961, **61**, 295.
24. H. Batiz-Hernandez, R. A. Bernheim, *Progr. Nucl. Magn. Resonance Spectroscopy*. 1967, **3**, 63.
25. J. B. Lambert, L. G. Greifenstein, *J. Am. Chem. Soc.*, 1974, **96**, 5120-5124.
26. J. B. Lambert, L. G. Greifenstein, *J. Am. Chem. Soc.*, 1973, **95**, 6150-6152.
27. J. B. Lambert, R. B. Finzel, *J. Am. Chem. Soc.*, 1983, **105**, 1954-1958.

Chapter 3. Fluorinated cyclopropanes

3.1 Introduction of cyclopropane

The cyclopropane ring was first prepared by the Austrian chemist August Freund in 1881.¹ This was achieved through an intramolecular Wurtz reaction using sodium and 1,3-dibromopropane, as illustrated in Scheme 1. The yield of this reaction was later improved by Gustavson using zinc instead of sodium.² Cyclopropane was used as an early anaesthetic as developed by Henderson and Lucas.³ However, since cyclopropane and oxygen mixtures are explosive, it never developed as a practical anaesthetic.



Scheme 1. The first synthesis of cyclopropane.¹

Unlike cyclohexane and cyclopentane, cyclopropane has a rigid conformation with a planar triangular structure. All of the C-C-C bond angles are 60°. Because these bond angles are significantly narrower than the standard sp³ hybridised tetrahedral angle of 109°, a significant angular strain is generated. In addition, torsion strain also occurs in cyclopropanes because all of the C-H bonds eclipse each other, adding to the ring strain.

The C-C bonding in cyclopropane is often called a bent bond,⁴⁻⁵ following the Coulson-Moffitt model (Figure 1). In this model, the carbon-carbon bonds are bent by about 22° outward from the imaginary line connecting the nuclei, which results in approximately 20 % less effective overlap relative to the normal sp³ hybridized orbitals. Another explanation of Coulson-Moffitt

model is that the C-C-C bond angle is about 104° ($60^\circ + 2 \times 22^\circ$), therefore the C-C bonds have greater p character than normal, which is frequently invoked to rationalize that cyclopropane often reacts like an alkene.

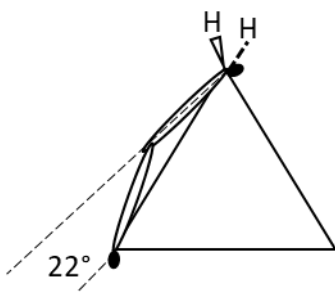


Figure 1. The Colson Moffitt model.

However, the strain energy of cyclopropane (27.6 kcal/mol),⁶ which is only slightly larger than that of cyclobutane (26.5 kcal/mol)⁶ has been attributed to σ aromaticity, by Dewar.⁷ The three C-C bonds delocalize their six electrons, and thus by invoking the $4n+2$ rule, cyclopropane has some aromaticity. It follows that cyclobutane with 8 electrons, is anti-aromatic. Based on this analysis, some other properties of cyclopropanes can be rationalized. For example, in ^1H NMR, the proton chemical shift (ppm) of cyclopropane is shifted significantly upfield (around 0.2 ppm) compared to a standard aliphatic CH_2 (around 1.3 ppm), consistent with ring current effects (Figure 2).

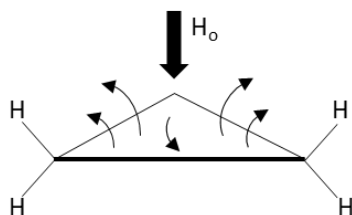
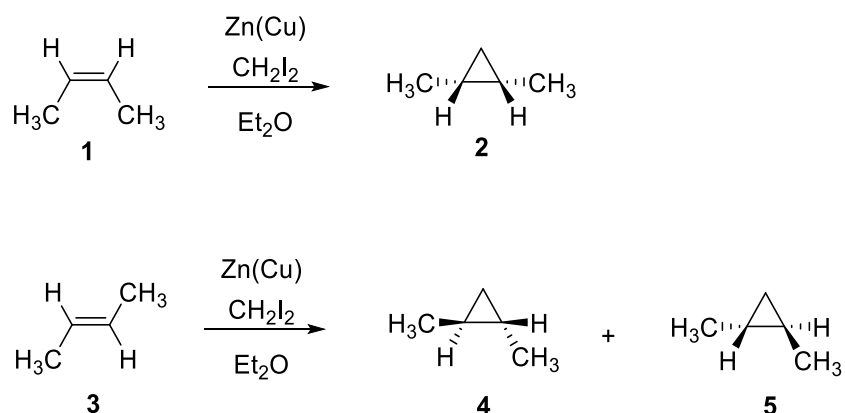


Figure 2. Ring current effects in cyclopropane in a magnetic field (H_0).

3.2 Preparation of Cyclopropanes

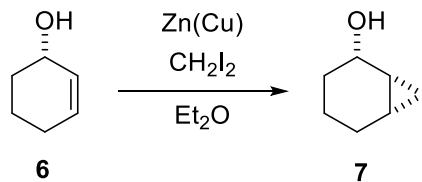
3.2.1 Simmons-Smith reaction

The most widely used method for the synthesis of cyclopropanes is *via* the Simmons-Smith reaction, named after H. E. Simmons and R. D. Smith. In 1958, they reported the addition of methylene carbene to various olefins using diiodomethane and zinc-copper couple.^{8,9} During the reaction, the olefin reacts with a carbene in a concerted manner, so the reaction is stereospecific where the stereochemical information of the original (*E/Z*) olefins is transferred to the (*syn/anti*) product (Scheme 2).



Scheme 2. Simmons-Smith reaction.

In addition, diastereocontrol is largely governed by steric or co-ordination effects in the Simmons-Smith reaction. An example is shown in Scheme 3.¹⁰ The hydroxyl group coordinates the zinc and directs a *syn* cycloaddition to the hydroxy group, resulting in only one single diastereoisomer.



Scheme 3. Cycloaddition of 2-cyclohexen-1-ol.¹⁰

Despite the convenience of the Simmons-Smith reaction, the high cost of diiodomethane and a lack of reproducibility lead to many modifications of this reaction. Wittig reported diazomethane and zinc iodide as an alternative to diiodomethane in 1959.¹¹ Furthermore, Furukawa and co-workers found when diethylzinc was used to replace the zinc-copper couple, the resulting carbene was usually more reactive than that of the original conditions.¹² Under these conditions, electron rich olefins react well, such as styrenes, enol ethers and enamines. However, for unfunctionalized olefins, the reaction proved challenging. In order to increase the reactivity of the zinc carbenoid, a significant improvement was made by Shi and co-workers.¹³ They described a series of novel (iodomethyl) zinc species generated from Brønsted acids, such as alcohols and carboxylic acids, and they found increase acidity led to increased reactivity. With trifluoroacetic acid, the reaction rate increased dramatically. Carbenoid (CF₃COO)ZnCH₂I is one of the most reactive reagents currently used for cyclopropanation. A new family of zinc carbenoids generated from phosphoric acid also has high reactivity,¹⁴ and these zinc reagents are illustrated in Figure 3.

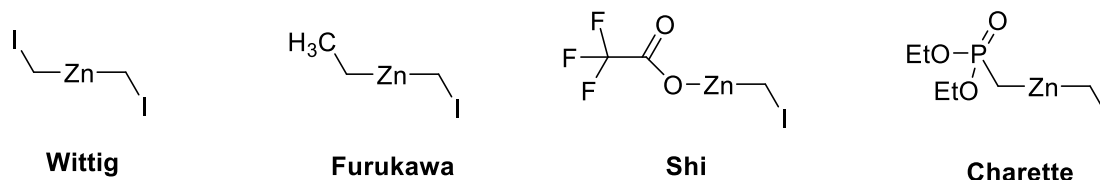
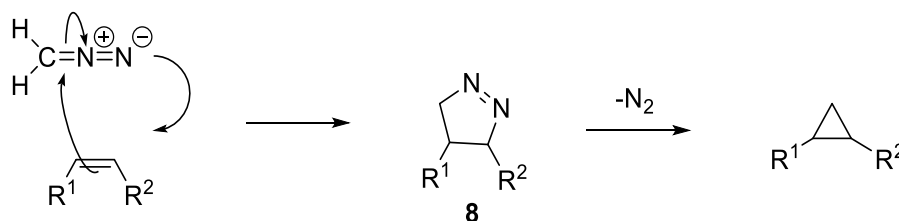


Figure 3. Typical zinc reagents for cyclopropanation.¹¹⁻¹⁴

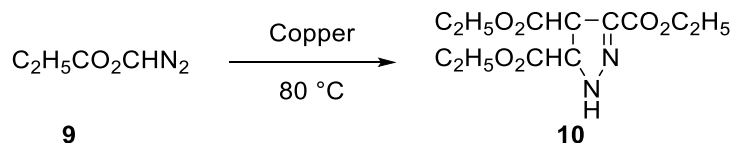
3.2.2 Cyclopropanation through diazo compounds

Cyclopropanes can be formed from diazo compounds with or without transition metal activation. For example, diazomethane can react directly with an olefin to generate the cyclopropane with N_2 as a by-product. In the first step, the reaction undergoes 1,3-dipolar cycloaddition to generate a pyrazoline **8**, which then eliminates nitrogen (Scheme 4). Because this reaction does not involve a transition metal, it can be considered to be superior to metal catalysed methods in terms of green chemistry. However, special care needs to be taken when using diazomethane due to its reactivity.



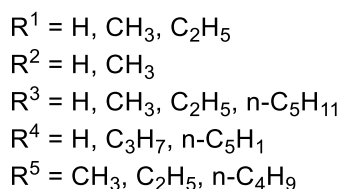
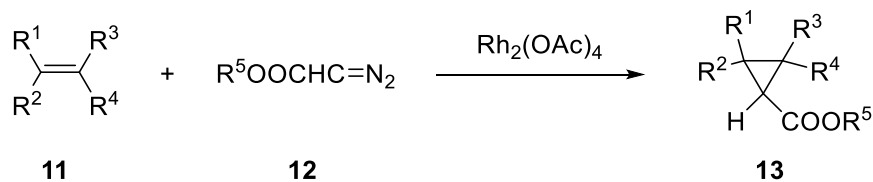
Scheme 4. Cycloaddition of olefin using diazomethane.

The Metal-catalysed decomposition of diazo compounds was first reported by Silberrad and Roy in 1906.¹⁵ They found that copper dust can decompose diazoacetate at temperatures above 80°C to form ethyl 4,5-dihydropyrazole-3,4,5-tricarboxylate **10** (Scheme 5).



Scheme 5. Decomposition of ethyl diazoacetate **8**.¹⁵

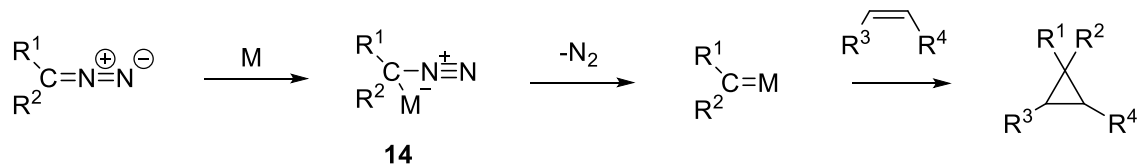
Since then, a significant focus has been placed on this area. Copper complexes, such as (i-PrO₃)PCuCl,¹⁶ have been used to catalyse carbene addition to olefins. Another significant improvement was made by Teyssie and co-workers,¹⁷⁻¹⁹ who found that palladium and rhodium complexes are suitable alternatives to copper. Nowadays, rhodium carboxylate complexes, such as dirhodium tetraacetate, are most commonly used to catalyse cyclopropanation and the reaction scope is quite broad (Scheme 6).



Scheme 6. Intermolecular cyclopropanation using dirhodium tetraacetate.¹⁹

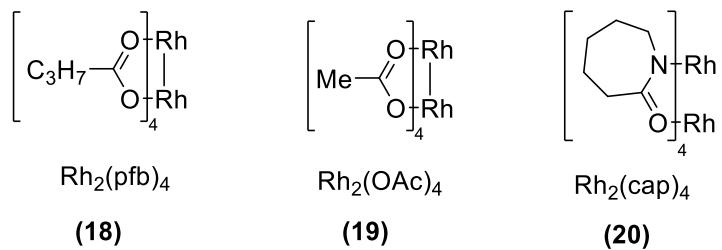
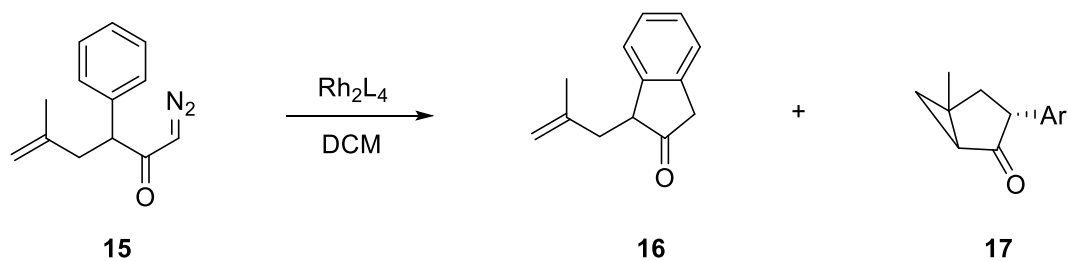
The mechanism of the rhodium catalysed cyclopropanation remains unclear, but can be rationalized as illustrated in Scheme 7. The diazo compounds react with the metals to form a zwitterionic metal alkyl complex **14**, which expels nitrogen (N₂) to afford a metal carbene

intermediate, which adds to the olefin. When R_1 and R_2 are different, the reaction usually generates a mixture of diastereoisomers.



Scheme 7. Metal catalysed carbenoid cyclopropanation.

Several issues need to be taken into account when considering metal catalysed carbenoid cyclopropanation. Firstly, the carbenoid is normally generated *in situ* due to the poor stability of the diazo substrates. Also, carbene dimerization competes with cyclopropanation and thus slow addition of the diazo species to an excess of olefin is generally required for success. Chemoselectivity is another issue since a C-H insertion pathway is also possible. In this respect, Padwa and co-workers found that chemoselectivity is greatly influenced by the nature of the catalyst used.²⁰ In their study, for the diazoketone **15**, changing the dirhodium(II) ligand from perfluorobutyrate (pfb) **18** to acetate (OAc) **19** or caprolactam (cap) **20**, resulted in different product profiles, as illustrated in Scheme 8. When $Rh_2(OAc)_4$ was used as the catalyst, a 1:1 ratio of C-H insertion compound to cyclopropanation resulted, whereas $Rh_2(cap)_4$ only generated the cyclopropane product **17**. By contrast, the use of $Rh_2(pfb)_4$ resulted predominantly in C-H insertion, to give **16** as the major product.

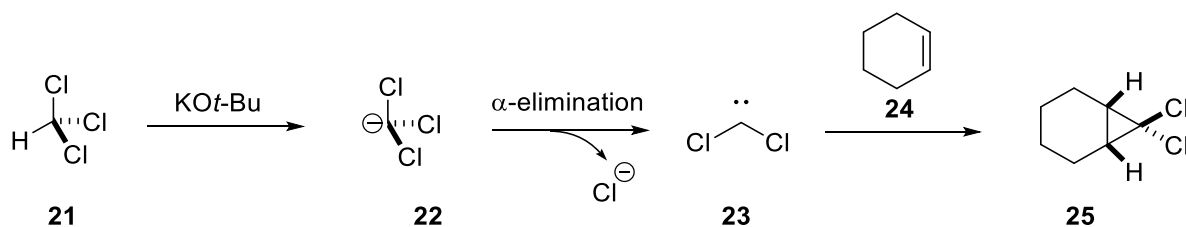


Compound 16:17	86:14	48:44	> 1:99
-----------------------	--------------	--------------	------------------

Scheme 8. Chemoselectivity between C-H insertion and cyclopropanation.²⁰

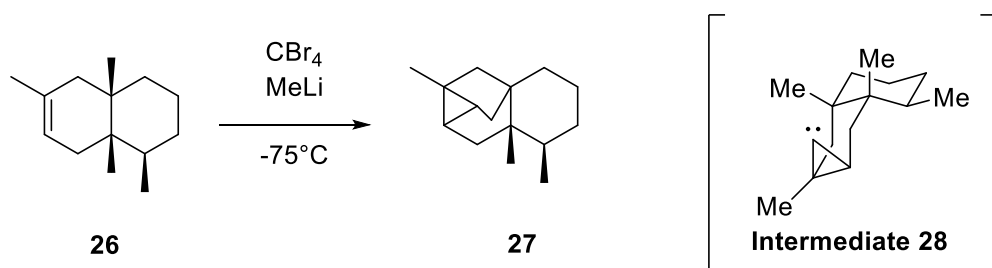
3.2.3 Free carbenes

Geuther²¹ in 1862 originally suggested that dichlorocarbene was generated after the treatment of chloroform with alkali. Significant effort was explored to clarify the involvement of a carbene. Almost 100 years later, Doering and Hoffmann presented the first structural evidence for the generation of dichlorocarbene from chloroform.²² They added potassium *t*-butoxide to a solution of cyclohexene and chloroform and demonstrated the formation of a product with the formula C₇H₁₀Cl₂. This was later proved to be the 7,7-dichlorobicyclo[4.1.0]-heptane **25** (Scheme 9).



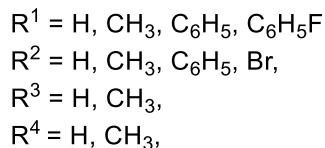
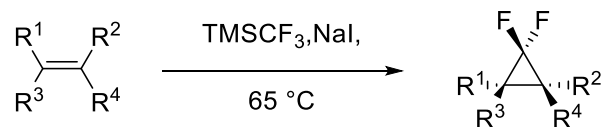
Scheme 9. The formation of 7,7-dichlorobicyclo[4.1.0]heptane *via* dichlorocarbene.²²

Free carbene (:CH₂) can be used for the cyclopropanation. However, due to the limitation of carbene precursors and the difficulty of producing carbene itself, most carbenes used in cyclopropanation reactions are dihalocarbenes. For dibromocarbene, tetrabromomethane and bromoform are the most convenient precursors.^{23,24} Cory and McLaren ingeniously used dibromocarbene during the total synthesis of ishwarane **27** as illustrated in Scheme 10. Dibromocarbene was generated by treating tetrabromomethane with an excess of methyllithium at -78 °C to generate dibromocyclopropane products, then lithium halogen exchange occurred and later participated in a C-H insertion reaction to yield ishwarane **27**.



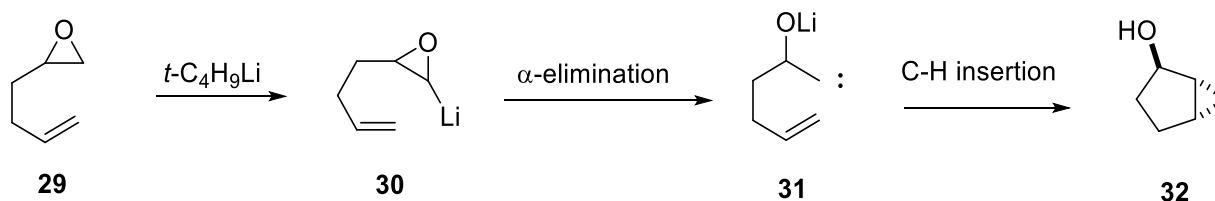
Scheme 10. Synthesis of ishwarane **27**.²³

For difluorocarbene, the Ruppert-Prakash reagent (TMSCF₃) is most widely used nowadays due to accessibility and bench stability. A variety of gem-difluorocyclopropane compounds have been made by using sodium iodide as the initiator to generate difluorocarbene (Scheme 11).²⁵



Scheme 11. Cycloaddition using TMSCF_3 .²⁴

In 1967, Crandall and Lin reported that lithiation of an epoxide led to carbene formation.²⁶ Accordingly, 5,6-epoxy-1-hexene was transformed into *trans*-2-bicyclo[3.1.0]hexanol **32** (yield 9 %) after treatment with *t*-butyllithium (**Scheme 12**).



Scheme 12. Lithiation and α -elimination of an epoxide.²⁶

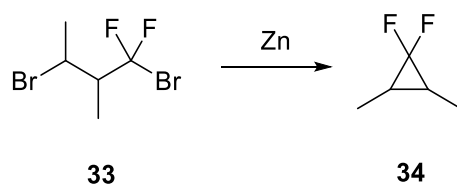
Given the low yield of **32** and a stereochemistry that is opposite to the Simmons-Smith outcome, Hodgson continued to optimise these reaction conditions and found that high yields (60-80 %) could be obtained by slowly adding LiTMP to the epoxide solution.²⁷

3.3 Fluorinated cyclopropanes

The cyclopropane ring is found in many natural and unnatural compounds. Some of these have interesting biological properties.^{28,29} The introduction of such a motif in medicinal chemistry has advantages in that it can modify chemical properties and the ring is conformationally rigid. In

addition, the incorporation of fluorine(s) onto the cyclopropane ring will lead to modified properties relative to cyclopropane itself due to fluorine's high electronegativity. For this purpose, there has been a significant interest in methods towards the preparation of fluorinated cyclopropanes.

The first example of a fluorinated cyclopropane was reported by Atkinson in 1952.³⁰ 1,1,2,2,3,3-Hexafluoro-cyclopropane was prepared in low yield by photosensitization of tetrafluoroethylene. However, the first purposely prepared fluorinated cyclopropane was described in 1955.³¹ Tarrant and co-workers prepared 1,1-difluoro-2,3-dimethylcyclopropane **34** after treating 1,3-dibromo-1,1-difluoro-2-methylbutane with Zn (Scheme 13), the yield of **34** is not mentioned in the paper.



Scheme 13. The first purposely prepared fluorinated cyclopropane.³¹

Since then, the most frequently used methods to generate fluorinated cyclopropanes involve the addition of either a fluorinated carbene to an alkene or a hydrocarbon carbene to a fluoroalkene. For monofluorinated cyclopropanes, direct fluorination has been successful under certain conditions.

3.3.1 Fluorocarbene addition to alkenes

Clearly when fluorine is directly attached to a carbene centre, it will decrease the stability of the carbene due to its strong electronegativity. However, fluorine is also π donating and thus the

effect is attenuated. For monofluoro carbene, the stabilising conjugation effect outweighs the destabilising inductive effect, so a single fluorine stabilises the singlet state,³² as is illustrated in **Figure 3**. This effect can also be seen when fluorine acts as an *ortho*, *para* directing group in electrophilic aromatic substitution reactions.

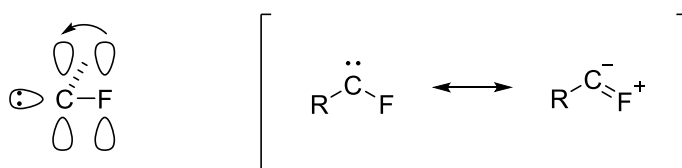
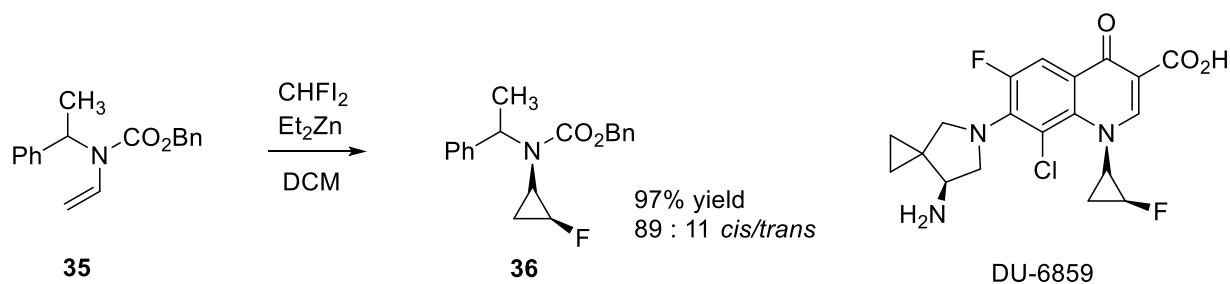


Figure 3. The resonance structure of fluorine carbene.

The most widely used fluorocarbene is difluorocarbene (:CF₂), used to generate gem-difluorocyclopropanes. However, because of the unreactive nature of this carbene, it remained a challenge to successfully generate, until it was realized that high temperature was necessary to overcome the energy barrier of addition. There are many convenient and excellent methods to generate :CF₂. For example, the pyrolysis of sodium chlorodifluoroacetate at 190 °C in diglyme or using the Seyferth's reagent, PhHgCF₃.^{33,34} Some drawbacks are also present here. For the former method, an excess of the reagent chlorodifluoroacetate is required. Seyferth's reagent, is toxic and its use is unacceptable. So the most effective current source of :CF₂ carbene is the Ruppert-Prakash reagent (TMSCF₃),³⁵ which decomposes in the presence of NaI in refluxing THF to form a reactive :CF₂ species.

Even though monofluorocarbene is more reactive than difluorocarbene, there are not many useful and convenient methods for generating monofluorocarbene (:CHF). This is perhaps because the most obvious precursors are CHFBr₂ and CHFI₂,^{36,37} which are quite inaccessible.

Monofluorocarbene can be generated *in situ* by treatment of CHFBr_2 or CHFCl_2 with diethylzinc under modified Furukawa Simmons-Smith conditions.¹² Tamura and co-workers applied this method to prepare a key intermediate **36** to quinolonecarboxylic acid, DU-6859 (**Scheme 14**).³⁷

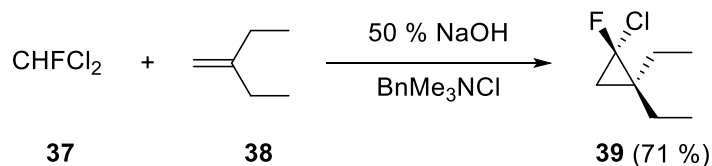


Scheme 14. Cyclopropanation of **35**.³⁷

Instead of using zinc, copper powder had been used by Kawataba and his co-workers to activate CHFCl_2 . However, finely granulated copper powder and longer reaction times are required.³⁸ Since these reactions are not widely used to directly prepare monofluorocyclopropanes, it has been most usual to proceed through the addition of either chlorofluorocarbene or bromofluorocarbene to an alkene, followed by reductive dehalogenation of the chlorine or bromine atoms.

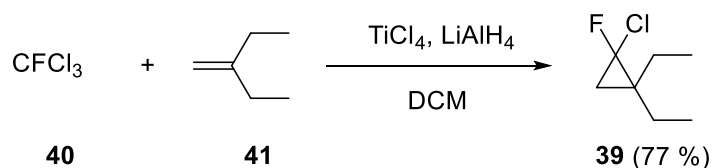
Chlorofluorocarbene has been the subject of a significant amount of research. This interest lies in the higher reactivity of chlorofluorocarbene relative to difluorocarbene, due to the less electronegative chlorine. There are three general methods to prepare chlorofluorocarbene. The earliest used the Seyferth's reagent (PhHgCFCl_2), however, this method is no longer recommended due to the toxicity of mercury. The other two methods involve using Freons (CHFCl_2 or CFCl_3) as the carbene precursor. Dehydrochlorination of CHFCl_2 can be effectively accomplished using base under phase transfer catalyst conditions (Scheme 15).³⁹ The presence

of a phase transfer catalyst minimises the reaction between carbene and base and therefore increases the yield of reaction.



Scheme 15. Cyclopropanation using a phase transfer catalyst.³⁹

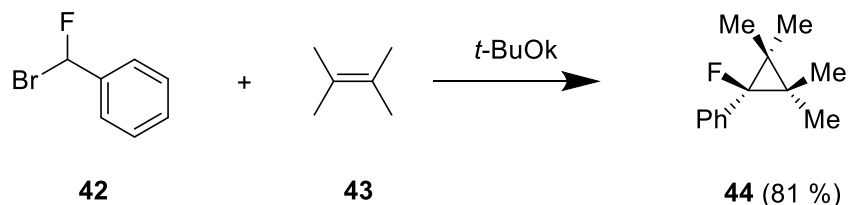
A useful and convenient approach was developed by Dolbier.⁴⁰ This involves the dechlorination of CFCl_3 using reduced titanium, in a cocktail of titanium tetrachloride and lithium aluminium hydride. A variety of chlorocyclopropanes were obtained in good to excellent yield using this method (Scheme 16).



Scheme 16. Cyclopropanation using CFCl_3 as precursor.⁴⁰

In comparison to the other fluorocarbenes, bromofluorocarbene and iodofluorocarbene have not received much attention, even though their reactivity is similar to that of chlorofluorocarbene. This is perhaps due to the inaccessibility of their precursors (CHFBr_2 and CHF_2). One universally useful method for the preparation of bromofluorocarbene and iodofluorocarbene is to use a two phase system. The reaction of CHFBr_2 (CHF_2) and sodium hydroxide with triethylbenzylammonium chloride (TEBAC) as a phase transfer agent to generate the respective carbene, has been reported.^{41,42}

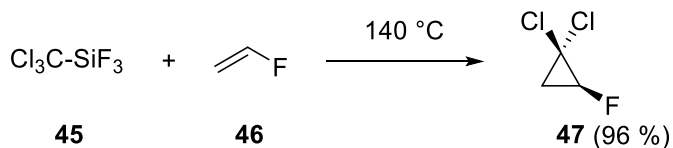
Phenylfluorocarbene has also been used in cyclopropanation reactions. Moss found that treatment of α -bromo- α -fluorotoluene with a slight excess of potassium *t*-butoxide in tetramethylethylene and butene led to 1-fluoro-1-phenylcyclopropanes **44** (Scheme 17).⁴³



Scheme 17. Phenylfluorocarbene addition of tetramethylethylene.⁴³

3.3.2 Carbene addition to fluoroalkenes

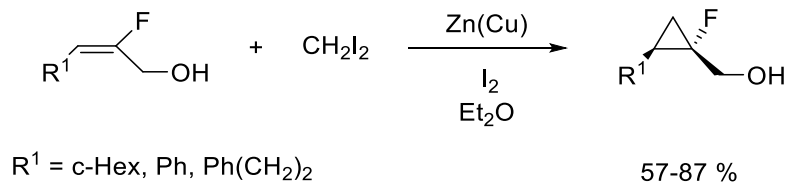
Access to fluorocyclopropane by the addition of a carbene to a fluorinated olefin has been explored, however this is a less common approach. The first example of this type of reaction was reported by Haszeldine.⁴⁴ 1,1-Dichloro-2-fluorocyclopropane **47** was synthesized by vapor-phase pyrolysis of trichloromethyltrifluorosilane in an excess of vinyl fluoride in high yield (Scheme 18).



Scheme 18. Cycloaddition of vinyl fluoride.⁴⁴

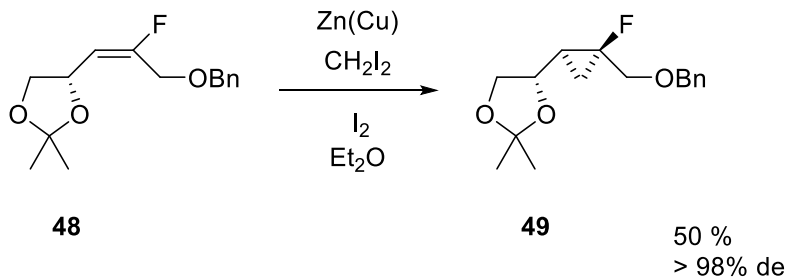
In recent years, such additions have become more common due to the contributions of Taguchi. Fluorinated olefins are usually considered to be deactivated substrates for the Simmons-Smith reaction. Therefore, Taguchi used vinyl fluorinated allylic alcohols to direct the carbene, as illustrated in Scheme 19. Moderate to good yields of fluorocyclopropane were generated and

with good diastereoselectivity to give either the *cis* or *trans* products, from starting materials with E or Z allylic alcohols, using the Simmons-Smith reaction.⁴⁵



Scheme 19. Cyclopropanation of a fluoroallyl alcohol.⁴⁵

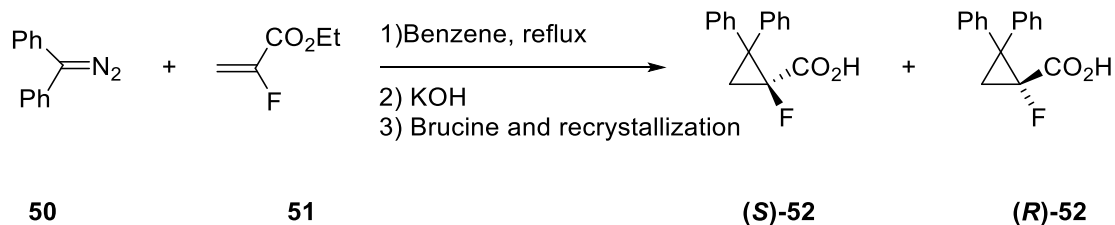
The study was extended to explore the asymmetric cyclopropanation of fluoroalkene derivatives. Highly diastereoselective cyclopropanation (*de* : up to 98%), was observed with substrate **48**, derived from (*R*)-glyceraldehyde acetonide (Scheme 20). This stereoselective reaction was attributed to the complexation of the zinc with the allylic oxygen of the dioxolane ring.



Scheme 20. Asymmetric cyclopropanation of **48**.⁴⁵

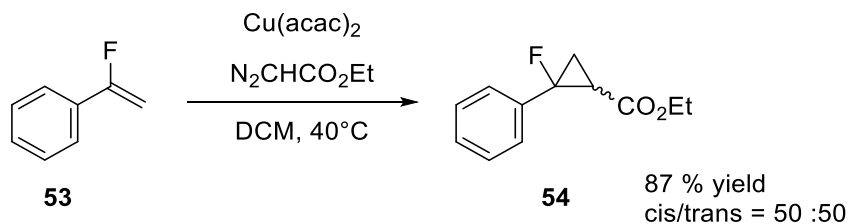
Diazo precursors also represent an important carbene source for addition to fluorinated alkenes. The first example was reported by Wolborsky.⁴⁶ Racemic 1-fluoro-2,2-diphenylcyclopropanecarboxylic acid **52**, was prepared after treatment of diazodiphenylmethane **50** with ethyl α -fluoroacrylate **51**. This was followed by ester hydrolysis. The final optically pure

enantiomers (*S*)-**52** and (*R*)-**52** carboxylic acids were obtained after resolution of the racemate, using salts of the brucine alkaloid and then recrystallization (Scheme 21).



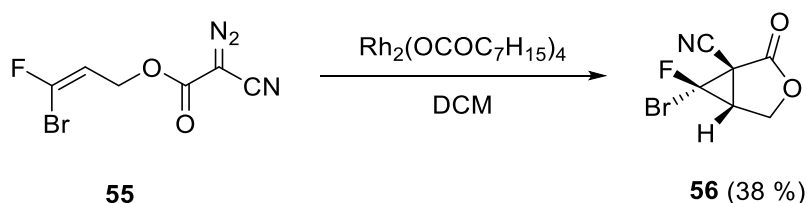
Scheme 21. The cyclopropanation of α -fluoroacrylate.⁴⁶

Transition-metal-catalyzed decomposition of diazo precursors for addition of a carbene to fluoroalkenes has also been developed and has played an important role in asymmetric cyclopropanation. Schlosser *et al.* found that the decomposition of diazoacetate derivatives under rhodium catalysis and with fluorodienes, afforded fluorovinylcyclopropanes.⁴⁷ The yield and stereoselectivity were however poor. Later, Häufe and co-workers reported copper catalysts for the cyclopropanation of fluorinated alkenes.⁴⁸ Better yields were achieved relative to the rhodium and palladium catalysts. Therefore, the cyclopropanation of α -fluorostyrene **53** with ethyl diazoacetate was carried out using copper acetate ($\text{Cu}[\text{acac}]_2$) in excellent yield (87 %) (Scheme 22).



Scheme 22. Cyclopropanation using copper acetate.⁴⁸

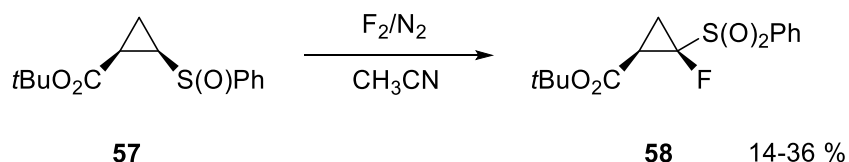
Intramolecular cyclization of diazoester **55** was accomplished using a transition-metal catalyst. Charette *et al.* used the rhodium(II) octanoate dimer to catalyze the cyclopropanation of **55** to **56**.⁴⁹ The single diastereoisomer was obtained as a consequence of the intramolecular nature of this reaction (Scheme 23).



Scheme 23. Intramolecular cyclopropanation.⁴⁹

3.3.3 Direct fluorination

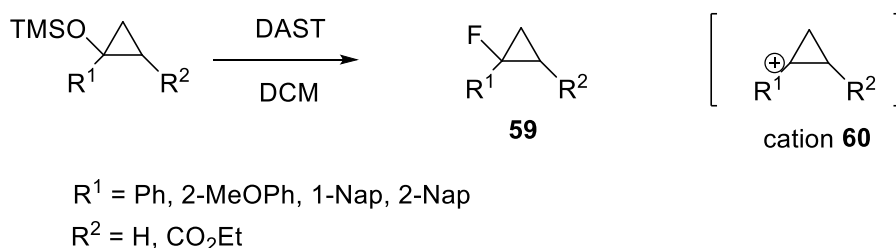
There are only a few examples of the preparation of fluorinated cyclopropanes, by direct fluorination. The diastereoselective synthesis of *t*-butyl *cis*-2-fluorocyclopropane-1-carboxylate **58** was reported by Toyota *et al.*⁵⁰ A Pummerer-like replacement of the α -hydrogen of phenylsulfinylcyclopropane **57** was achieved using dilute elemental fluorine, to give the product **58** in low yield (Scheme 24).



Scheme 24. Fluorination of the *tert*-butyl *cis*-2-phenylsulfinylcyclopropane-1-carboxylate.⁵⁰

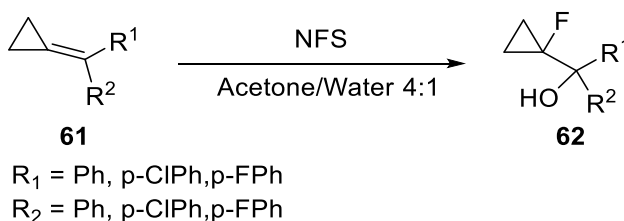
In 2003, Kiriara *et al.* reported the fluorination of tertiary cyclopropyl silyl ethers with diethylamino sulfur trifluoride (DAST).⁵¹ Reaction with DAST usually causes ring opening of cyclopropane to generate allylic fluorides, however, the authors demonstrated that

cyclopropane reactivity was highly dependent on the electronic properties of the ring substituents. If a strong electron-donating substituent is combined with a silyl ether at the same carbon (C1) or an electron-withdrawing substituent at C2, then a fluorinated cyclopropane is generated. The proposed mechanism suggested that an electron-withdrawing substituent at C2 carbon can destabilize allylic cation, therefore the cyclopropyl cation **60** survives long enough to react with fluoride ion (Scheme 25).



Scheme 25. Fluorination of the tertiary cyclopropyl silyl ethers.⁵¹

The inexpensive and easy to handle electrophilic fluorine reagent N-fluorosuccinimide (NFS), was reported by Liu *et al* for the preparation of fluorocyclopropylmethanol **62**.⁵² Halohydroxylation of methylenecyclopropanes generated these products in moderate yield (Scheme 26).

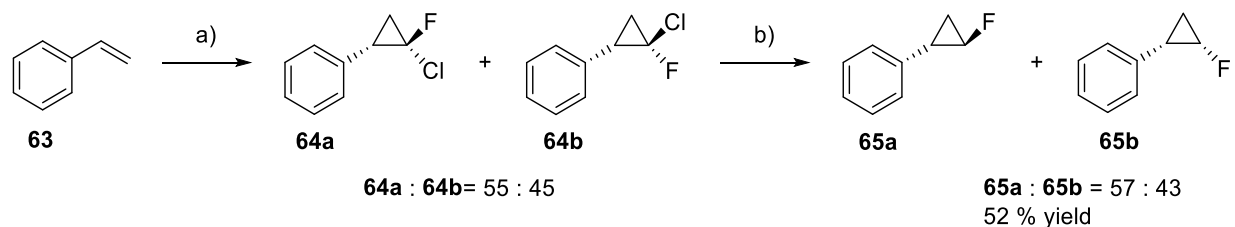


Scheme 26. Fluorination of methylenecyclopropanes.⁵²

3.4 All *cis*-1,2,3-trifluorocyclopropanes

Mono fluorinated phenyl cyclopropane

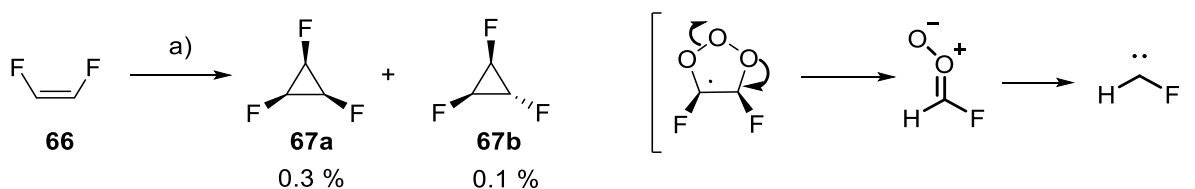
Mono fluorinated cyclopropanes are well known. The most straightforward and efficient method to their preparation involves :CFCl carbene addition to an olefin followed by dehalogenation as shown in Scheme 27.⁵³ Notably the direct :CHF carbene addition to styrene is not reported.



Scheme 27. Synthesis of fluorocyclopropane **65a** and **65b**.⁵³ *Reagents and conditions:* a) NaOH, $\text{CFCl}_2\text{COOCH}_3$, MeOH, 25°C; b). Bu_3SnH , AIBN, 90°C.

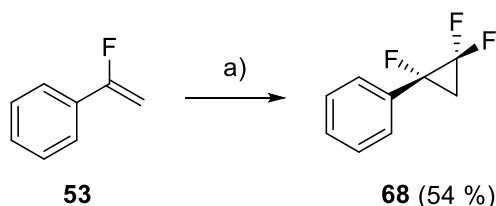
Di, tri fluorinated phenyl cyclopropane

There is very little in the literature describing the synthesis of vicinal difluorinated cyclopropanes, although geminal difluorinated cyclopropanes are well known. There are no examples of derivatives of all *cis*-trifluorocyclopropanes having been reported in the literature. The two stereoisomers, of unsubstituted 1,2,3-trifluorocyclopropane have been prepared, including the all-*cis* isomer **67a**. The isomers emerged as minor products of an ozonolysis reaction of *cis*-1,2-difluoroethene **66** (Scheme 28).⁵⁴ Milligram samples of each isomer were secured by preparative gas chromatography and their integrity and stereochemistry was assigned by vibrational and microwave spectroscopy.



Scheme 28. Ozonolysis of cis 1,2-difluoroethene **66**.⁵⁴ *Reagents and conditions:* a) O₃, CF₃Cl, -95°C

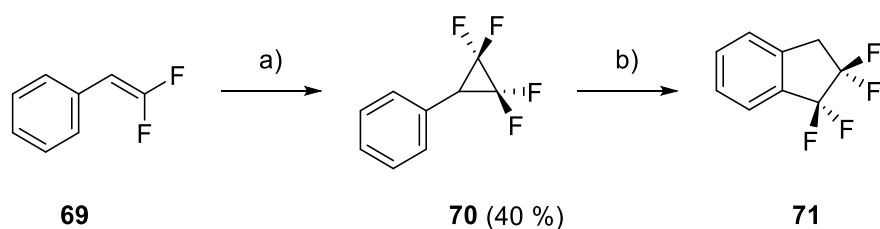
There is a recent paper from the St Andrews lab reporting the preparation of 1,1,2,2-trifluorocyclopropyl benzene **68**. The method involved :CF₂ carbene addition to α-fluorostyrene (Scheme 29).⁵⁵



Scheme 29. Cycloaddition of α-fluorostyrene **53**.⁵⁵ *Reagents and conditions:* a) TMSCF₃, NaI, THF, 65°C

1,1,2,2-Tetrafluoro-3-phenylcyclopropane

A reaction of 2,2-difluorostyrene **69** and sodium chlorodifluoroacetate generated the 1,1,2,2-tetrafluoro-3-phenylcyclopropane **70** as the primary product,⁵⁶ however, after prolonged reaction, the cyclopropane was transferred to 1,1,2,2-tetrafluoroindane **71** (Scheme 30). The driving force for this process was proposed to be that the C-C bonds of the cyclopropane ring is weakened due to the presence of multiple fluorine atoms.



Scheme 30. Cycloaddition of β, β -difluorostyrene **71**.⁵⁶ *Reagents and conditions:* a) $\text{CF}_2\text{ClCOONa}$, Diglyme, 180°C , 1h; b) $\text{CF}_2\text{ClCOONa}$, Diglyme, 180°C , 12h

3.4.1 Aims and objectives

The aim of this Chapter was to synthesise derivatives of all-*cis*-1,2,3-trifluorocyclopropane **67a**

(Figure 4).

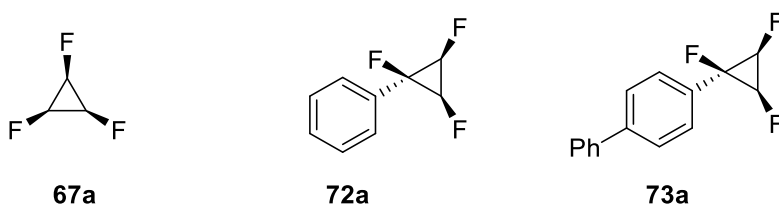


Figure 4 All-*cis*-1,2,3-trifluorocyclopropane.

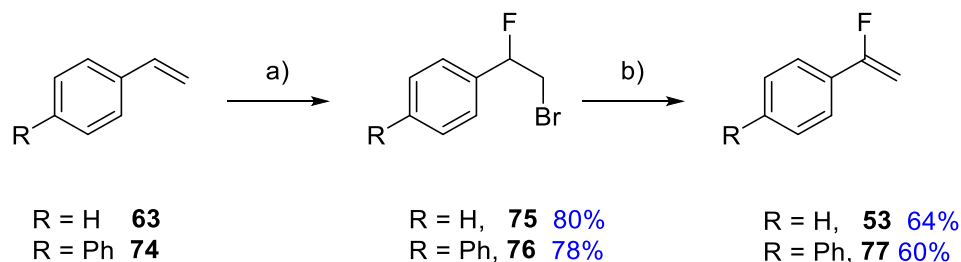
As discussed in the Chapter 2, all-*cis*-1,2,3,4,5,6 hexafluorocyclohexane, a molecule with a CHF group on each of the six carbons, and with a stereochemistry where all the fluorines are on one face of the ring, is a highly crystalline solid (M.p. $> 206^\circ\text{C}$) and among the most polar aliphatic motifs known. All-*cis*-1,2,3,4-tetrafluorocyclopentane, also has a high dipole moment. These rings show conformational flexibility and the cyclohexane and cyclopentane ring systems are rather large in terms of considering them as substituents in drug discovery. As a consequence, it became of interest to prepare all-*cis*-1,2,3-trifluorocyclopropane **67a**. This reduces the carbon count and the ring has a rigid conformation. Compound **67a** is also predicted to have polar

faces.⁵⁷ Therefore, it is necessary to get some compounds to test its properties. Given the volatility of unsubstituted cyclopropane **67a**, the aryl substituted derivatives **72a** and **73a** emerged as target compounds.

3.4.2 Results and discussion

Synthesis of fluorinated olefins **53**, **77**, **86** and **87**.

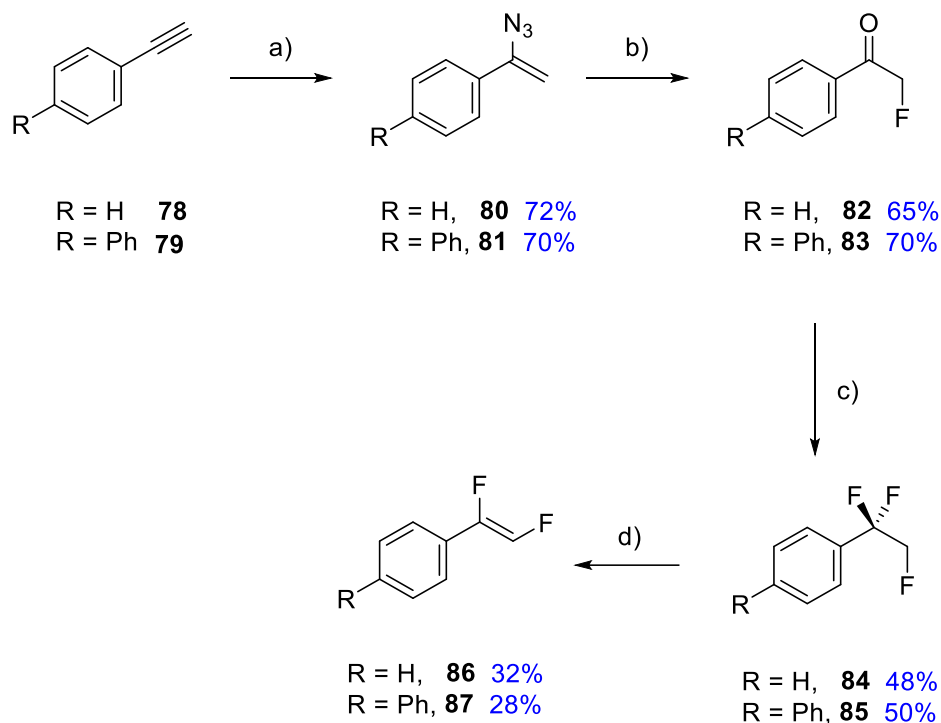
In order to make the desired cyclopropanes, fluorinated styrenes **53** and **77** were required as substrates. α -Fluorostyrene **53** and **77**, could be prepared by bromofluorination of styrene and 4-vinylbiphenyl to generate intermediates **75** and **76** then elimination of HBr, as illustrated in Scheme 31. Bromofluorination generated a single regioisomer of products **75** and **76** in both cases. An excess of potassium *t*-butoxide was then used to achieve dehydrobromination. This two-step approach to α -fluoro-olefins led to good isolated yields.



Scheme 31. Reagents and conditions: a) NBS, HF·Py, DCM, 0°C, 4h; b) *t*-BuOK, THF, RT.

The synthesis of the *cis*- α,β -difluorostyrene **86** and the corresponding *p*-biphenyl-*cis*- α,β -difluorostyrene **87** is shown in Scheme 32. Acetylenes **78** and **79** were used as starting materials. Hydroazidation of these acetylenes using a silver catalyst, generated vinyl azides **80** and **81**.⁵⁸ The next step followed recent methodology developed by Wu⁵⁹ to prepare α -fluoroketones **82** and **83**. This two-step reaction proved to be efficient and a full conversion was achieved within 2h. α -

Fluoroketones **82** and **83** were then treated with DAST to generate the trifluoroethyl aromatics **84** and **85**. Finally, a stereoselective elimination of hydrogen fluoride from **84** and **85** under base condition (*t*-BuOK) led to the *syn* difluorostyrenes **86** and **87**.⁶⁰



Scheme 32. Reagents and conditions: a) Ag₂CO₃, TMSN₃, H₂O, DMSO; b) Selectfluor, NaHCO₃, H₂O, CH₃CN; c) DAST; d) *t*-BuOK, *t*-BuOH.

Mechanism of elimination reaction

Even though the elimination of **85** to prepare *cis* difluorostyrene **87** had already been described, the exclusive *syn* outcome is intriguing, and we set out to explore the mechanism of the elimination reaction a little more. The elimination reaction was carried out in deuterated *tert*-butanol (*t*-BuOD) and the reaction process was monitored by ¹⁹F {¹H}NMR every hour, for four hours as illustrated in Figure 5.

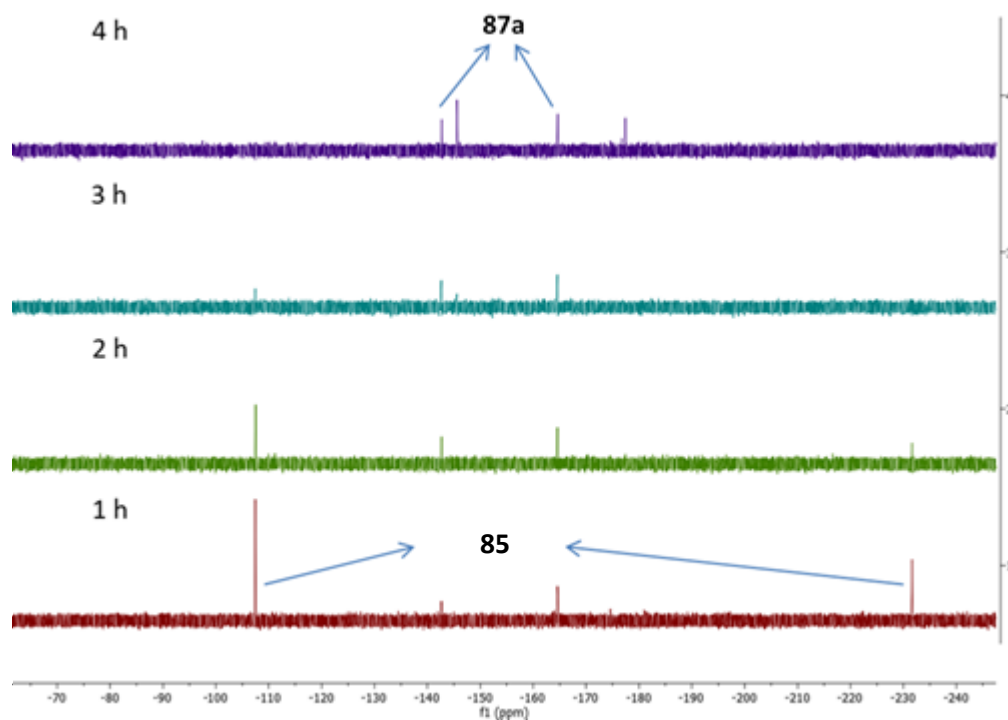
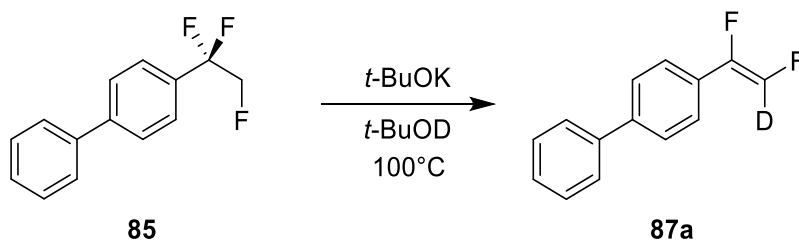
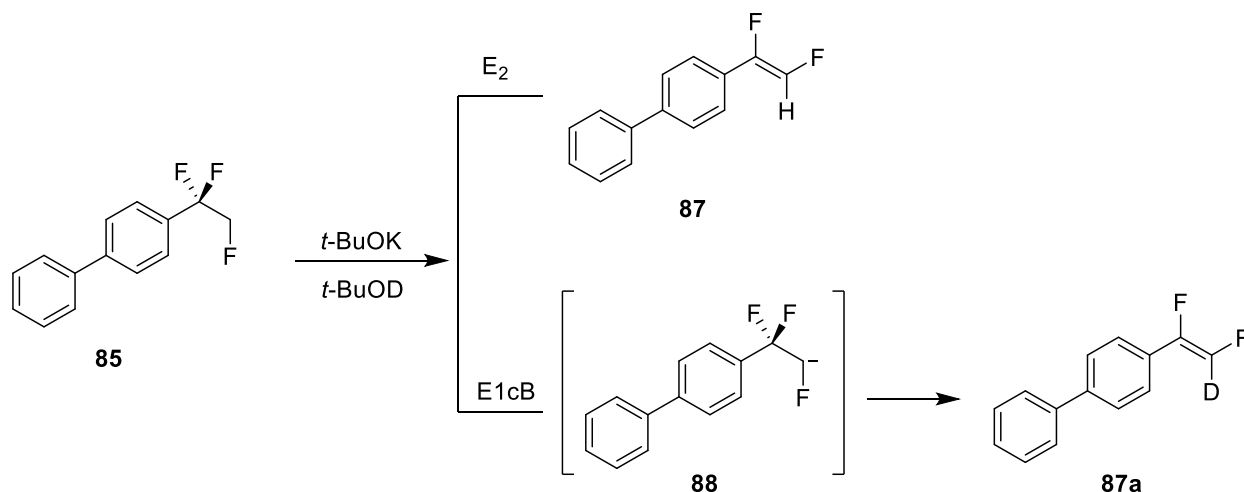


Figure 5. ^{19}F $\{^1\text{H}\}$ NMR of elimination reaction of **85** to **87a**.

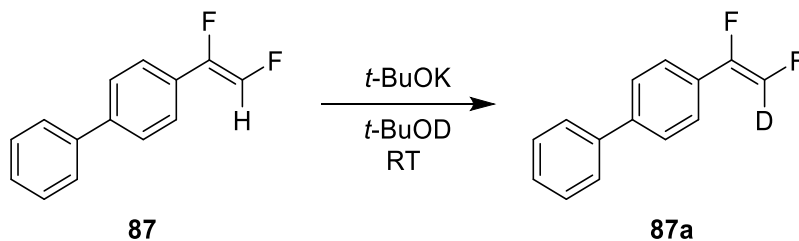
It is clear that the starting material **85** decreased as reaction time increased. After 4h, **85** had totally disappeared and at this time, the elimination product **87a** was isolated. The product emerged to be the deuterated styrene **87a**. This was unambiguously identified by two broad peaks in the ^{19}F $\{^1\text{H}\}$ NMR spectrum instead of two doublets for protic styrene **87**. This result initially suggested an E1cB process. If the reaction were an E₂ elimination, the only product should

be **87** due to the concerted nature of an E₂ reaction. By contrast, an E1cB process is consistent with deuterium exchange due to the formation of intermediate anion **88** (Scheme 33)



Scheme 33.

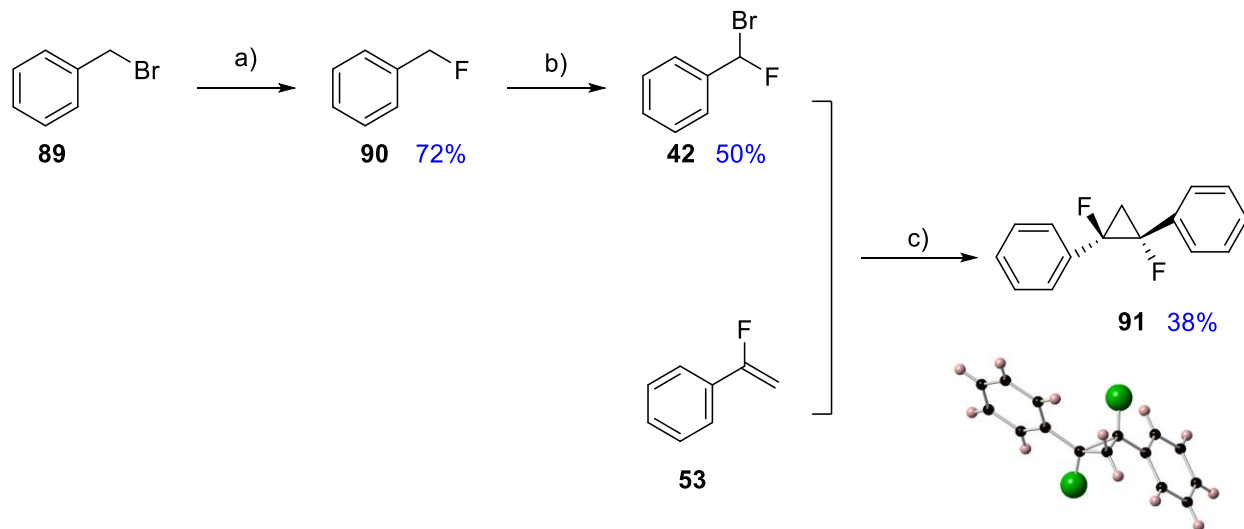
However, the stepwise nature of the E1cB process should generate some deuterated **85**. But in Figure 5, there was no evidence of exchange of deuterium into **85**. This is inconsistent with an E1cB process. Alternatively it suggests that the olefinic proton of **87** is probably sufficiently acidic, to be directly exchanged to **87a**. Thus a further reaction was conducted. Difluorostyrene **87** was treated with potassium *tert*-butoxide in deuterated *tert*-butanol (*t*-BuOD) at room temperature (Scheme 34). ¹H NMR analysis demonstrated that there was a rapid transformation of **87** to **87a**. This supported the direct exchange hypothesis. All in all, we conclude that the elimination is most probably an E₂ mechanism, but that olefinic proton of **87** is sufficiently labile to be exchanged by *t*-BuOD.



Scheme 34.

Synthesis of fluorinated cyclopropanes

With the fluorinated olefins **53**, **77**, **86** and **87** in hand, the synthesis of the all-*cis* 1,2,3-cyclopropane motif envisaged direct phenylfluorocarbene (:C(F)Ph) addition to α,β -difluorostyrene **86**. The reactivity was firstly explored with α -fluorostyrene **53** (Scheme 35). The necessary precursor to generate phenylfluorocarbene, α -bromo- α -fluorotoluene **42**, was obtained by direct fluorination of benzyl bromide **90**, using TBAF, then the photo-initiated action of N-bromosuccinimide on benzyl fluoride **91**. The addition of phenylfluorocarbene to vinyl fluoride **56** only leads to one stereoisomeric product **91**, where the fluorines are *trans* to each other on the cyclopropane ring. This was confirmed by obtaining a crystal structure of **91**. This product presumably arises due to the 1,2-difluoro repulsion as well as steric repulsion between the phenyl groups, favouring the *trans* product.



Scheme 35. The phenylfluorocarbene addition to the α -fluorostyrene **53**. *Reagents and conditions:* a) TBAF, CH_3CN ; b) NBS, CCl_4 , UV; c) *t*-BuOK, 50°C

In the ^1H NMR of **91** of the CH_2 group in the cyclopropane gave a second order signal. Because the two fluorines are chemically and magnetically equivalent, four different $^3J_{\text{HF}}$ coupling constants are obtained. In order to calculate accurate coupling constants, the DAISY software was used to simulate the ^1H NMR spectrum. As a result, the four coupling constants are $^2J_{\text{gemHH}} = 9.6$ Hz, $^3J_{\text{tranHF}} = 13.3$ Hz, $^3J_{\text{cisHF}} = 23.4$ Hz and $^3J_{\text{transFF}} = 6.9$ Hz, respectively. The $^{19}\text{F}\{^1\text{H}\}$ NMR spectrum of this product only had one fluorine peak at -173 ppm, as illustrated in Figure 6.

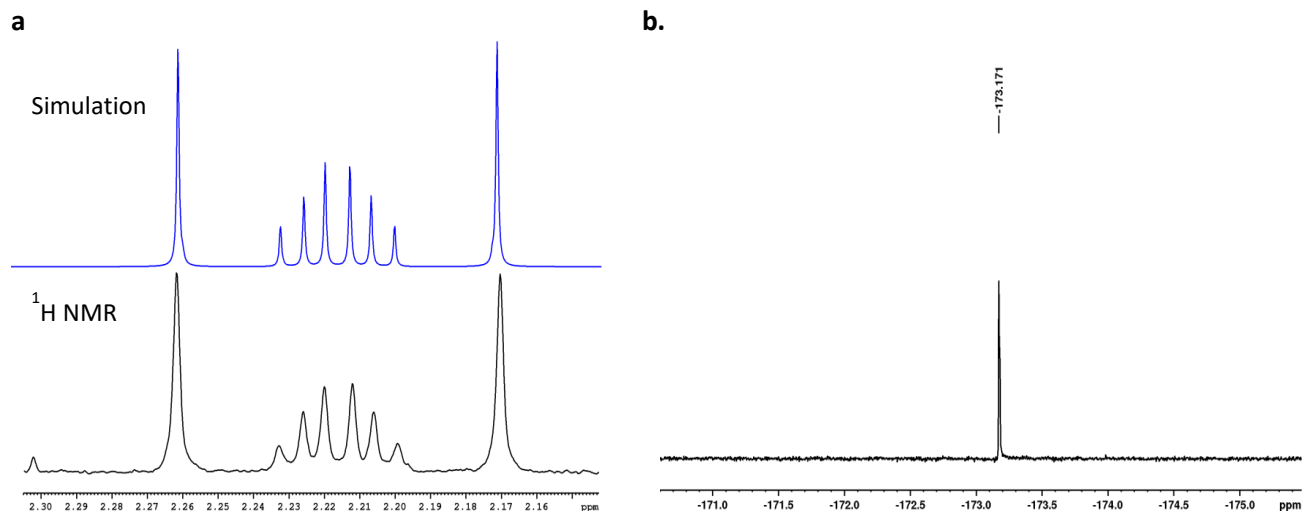
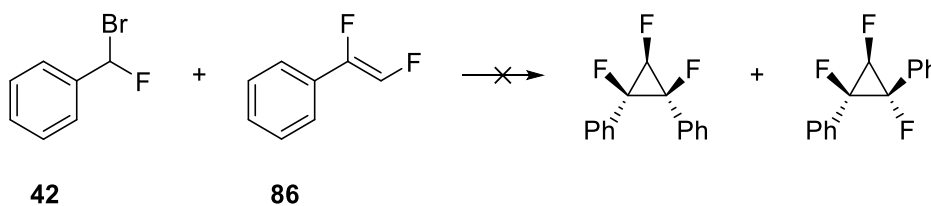


Figure 6. a) Simulation of ^1H NMR; b) $^{19}\text{F}\{^1\text{H}\}$ NMR of **91**.

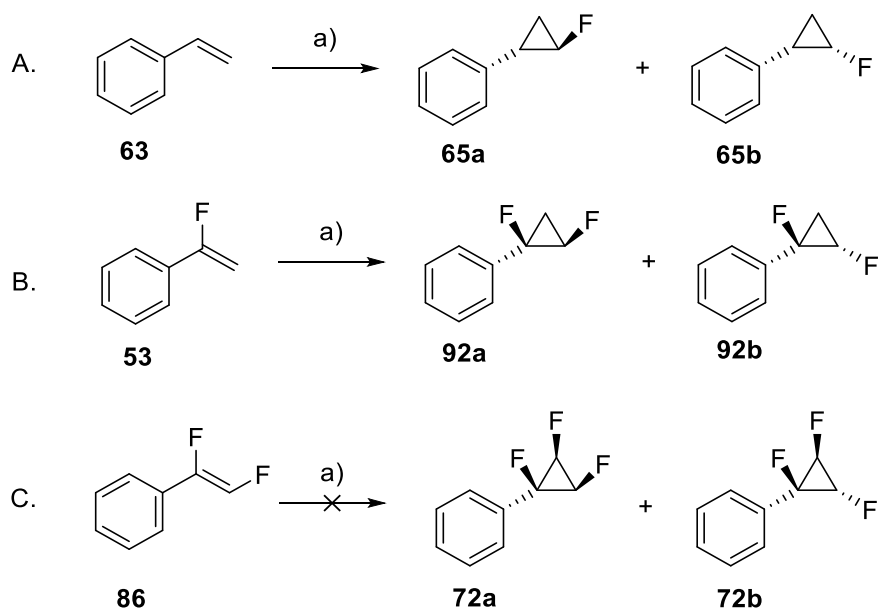
Phenylfluorocarbene **42** addition to α,β -difluorostyrene **86** was explored, however, there was no reaction at all (Scheme 36). This is presumably because the $:\text{PhCHF}$ carbene is not so reactive and the double bond of the difluorostyrene is also deactivated with two fluorines.



Scheme 36. Phenylfluorocarbene **42** addition to α,β -difluorostyrene **86**.

All-*cis* trifluorocyclopropane **67a** has been synthesised through an ozonolysis reaction of *cis*-1,2-difluoroethene (Scheme 28). The mechanism of that reaction involves the generation of $:\text{CHF}$ carbene from the decomposition of an ozonide intermediate, followed by carbene addition to generate product **67a**. Inspired by this, if a $:\text{CHF}$ carbene can be generated, then cyclopropanes **72a** and **73a** may be directly produced. Therefore the method for generating $:\text{CHF}$ carbene³⁷ was

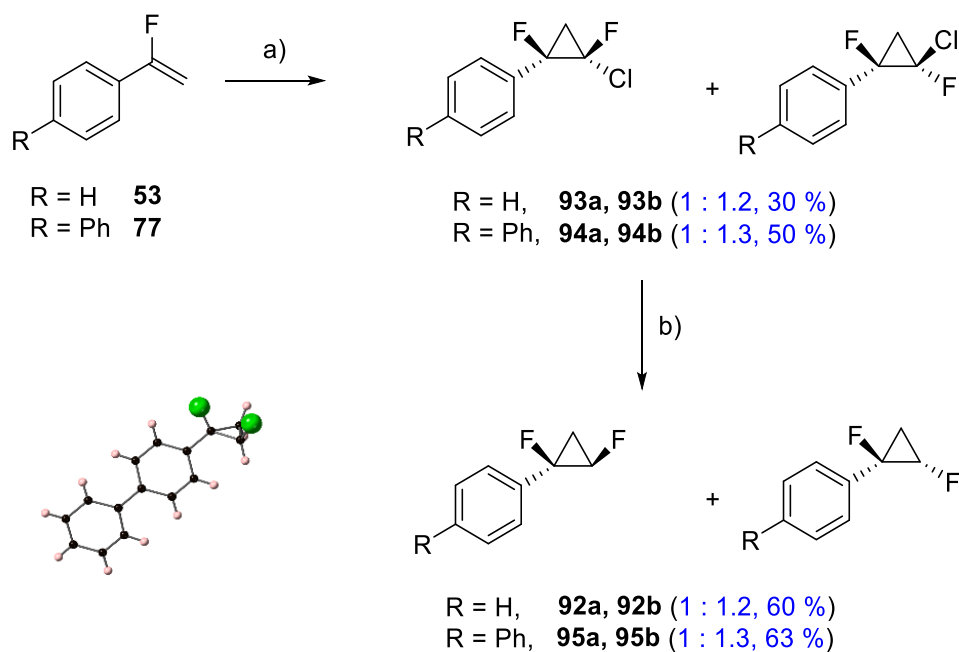
explored, for addition to styrene **63**, α -fluorostyrene **53** and α,β -difluorostyrene **86** (Scheme 37). The :CHF carbene, which was generated from CHF_2 , added relatively straightforwardly to styrene **63** itself, to give **65a/65b** (*trans* : *cis* = 2 : 1), but it gave less efficient conversions with α -fluorostyrene **53** to generate **92a/92b** (*cis* : *trans* = 1 : 1). However, the reactions of :CHF carbene with α,β -difluorostyrene **86** failed, presumably because the olefin is progressively less nucleophilic being deactivated by both fluorine atoms. Also when compared to *cis*-1,2-difluoroethene **68**, α,β -difluorostyrene **86** is less nucleophilic due to the conjugation of the double bond with the phenyl ring.



Scheme 37. The CHF: carbene addition to styrene **63**, α -fluorostyrene **53** and α,β -difluorostyrene **86**.
Reagents and conditions: a) CHF_2 , Et_2Zn , PE, 0°C .

In order to overcome this, the more electrophilic fluorohalocarbenes (:CXF, where X = F, Cl, Br and I) were then explored. Cyclopropanes **66** and **67** have already been synthesised by :CFCl carbene addition to styrene **63**, followed by reductive removal of chlorine (Scheme 27).⁵³

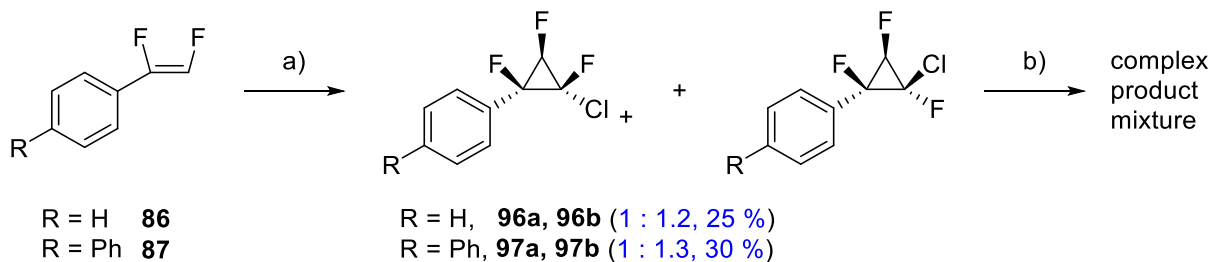
Therefore, in the first instance, :CFCl carbene addition to monofluorostyrene **52** and **77** was attempted. The required :CFCl carbene was generated from CFCl_3 using the method of Dolbier.⁶¹ After successful :CFCl carbene addition, a mixture of chlorofluorocyclopropane isomers **93-94** was generated. The individual isomers were not easily separated and the mixture was explored directly for dehalogenation ($\text{Bu}_3\text{SnH/AIBN}$). Dehalogenation resulted in the desired *cis* and *trans* difluorocyclopropanes **92a**, **92b** and **95a**, **95b**, but as a mixture. Careful chromatography allowed separation and the X-ray structure of **95a** was obtained which confirmed the structure and stereochemistry of this isomer (Scheme 38).



Scheme 38. Reagents and conditions: a) TiCl_4 , LiAlH_4 , CFCl_3 , THF, 0°C ; b) AIBN, Bu_3SnH , 90°C .

Chlorofluorocarbene (:CFCl) was next explored with α,β -difluorostyrenes **86** and **87**. This was also successful and efficiently generated the corresponding trifluorohalocyclopropanes **96-97**. However, in the event of reductive removal of the chlorine of trifluorohalocyclopropanes **96-97**,

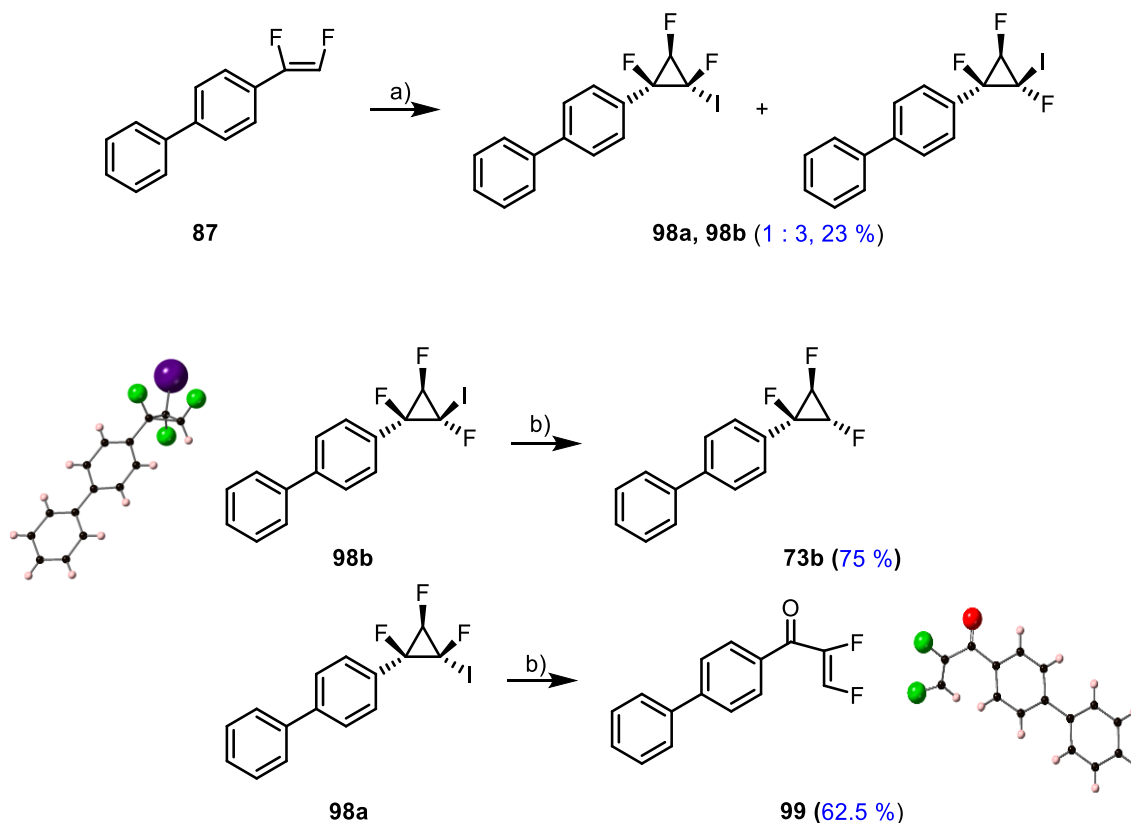
the reaction led to a complex product mixture. The desired products were present as minor components (as determined by ^{19}F -NMR) but there were significant levels of unidentifiable products (Scheme 39). Those unidentifiable products were generated maybe due to the cyclopropane ring opening at the necessary high reaction temperatures. Purification by chromatography, to isolate the desired products proved unsuccessful due to the low yield of the reaction. The dechlorination reaction was also explored at room temperature in order to minimise ring opening by-products, however, this reaction did not proceed and only starting trifluorohalocyclopropanes **96-97** remained there. The stability of the C-Cl bond is inconsistent with the low temperature.



Scheme 39. Reagents and conditions: a) TiCl_4 , LiAlH_4 , CCl_3 , THF, 0°C ; b) AIBN, Bu_3SnH , 90°C .

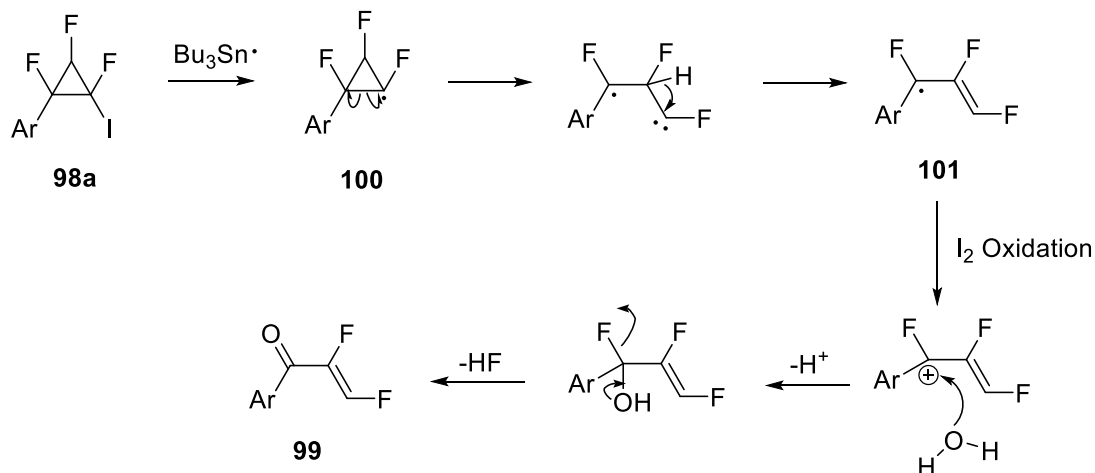
Due to the difficulty in achieving an efficient dechlorination, attention turned to iodine. Therefore, the synthesis of iodo cyclopropanes **98a** and **98b** was attempted by using Weyerstahl's methodology.⁴² Iodofluorocarbene ($:\text{CFI}$) was generated *in situ* using base, under phase transfer catalyst conditions, and then addition to difluoroolefin **87**. This successfully generated the resultant iodocyclopropanes **98a** and **98b** in a ratio of 1 : 3. Due to the excess of the *anti* isomer **98b**, this time, pure **98a** and **98b** were separated by column chromatography and then treated individually to achieve dehalogenation. Indeed, each could be reductively deiodinated at a lower

temperature than the corresponding chlorocyclopropanes. Treatment of the *anti* isomer **98b**, with AIBN/Bu₃SnH at room temperature, resulted in the production of *anti*-1,2,3-trifluorocyclopropane **73b**. NMR analysis indicated that deiodination had occurred with a retention of stereochemistry. However it was very frustrating that deiodination of the *syn*-isomer **98b** led to the formation of the unsaturated ketone **99**, in a good yield after a ring opening reaction. The structure of **99** was confirmed by X-ray structure analysis (Scheme 40).



Scheme 40. Reagents and conditions: a) CHF_2 , TEBAB, $\text{NaOH}\cdot\text{H}_2\text{O}$, DCM, 0°C ; b) AIBN, Bu_3SnH , RT.

The formation of compound **99** is intriguing as a ring-open pathway has occurred. The oxygen may come from moisture associated with Bu_3SnH . A possible mechanism for the formation of this product is showed in Scheme 41.

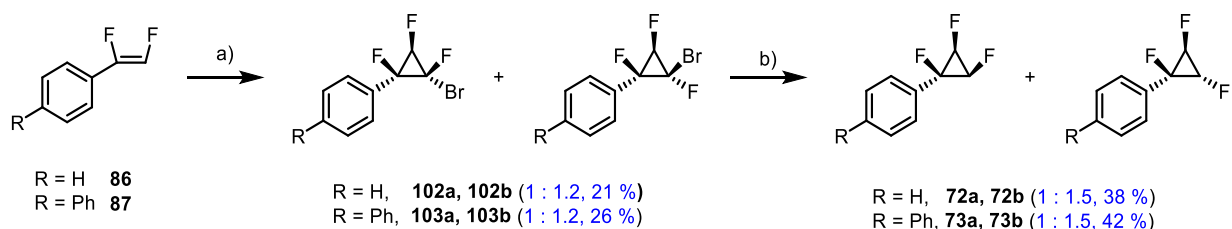


Scheme 41. Possible mechanism for formation of **99**.

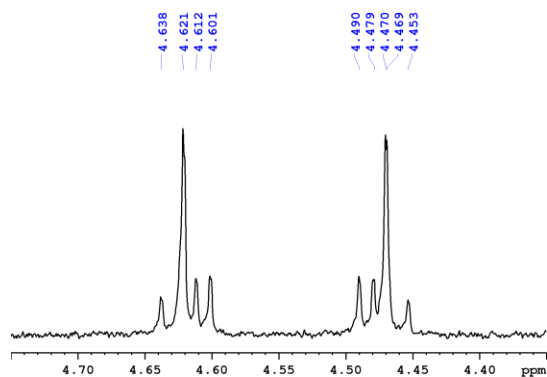
The reduction of *syn*-isomer **98a** immediately generated the radical **100**, instead of hydrogen abstraction from the organotin hydride, the cyclopropane ring rearranges to generate radical intermediate **101**, which is stabilised by both the phenyl ring and double bond. Oxidation can happen and then followed by substitution of hydroxide group from water and elimination, therefore compound **99** was formed.

Due to the inability to access *cis*-1,2,3-trifluorocyclopropane **72a** and **73a** by reductive dehalogenation of the chloro and iodo series, attention finally turned to the bromocyclopropanes **102** and **103**. Bromocyclopropanes **101**, **102** were synthesised by :CFBr carbene addition to difluoroolefins **86**, **87** using a similar method to that used to generate the :CFI carbene. Accordingly, dibromofluoromethane (CHFBr₂) was treated with base to generate the corresponding :CFBr carbene. Then carbene addition to the difluoroolefins **86**, **87** generated bromocyclopropanes **102**, **103**. The isomer mixture of products **102a**, **102b** and **103a**, **103b** were also subjected to reductive dehalogenation with AIBN/Bu₃SnH to generate the anticipated 1,2,3-trifluorocyclopropanes **72** and **73**. This time, the reductive removal of bromine worked reasonably

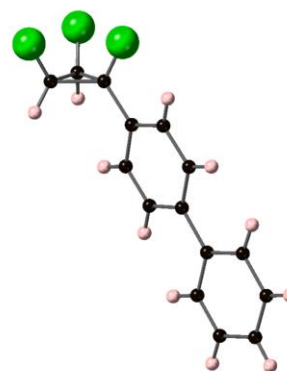
well and generated the desired trifluorocyclopropane products. The resultant *syn* and *anti* isomers could be easily separated by chromatography due to their difference in polarity. The all-*cis* isomer **72a** and **73a** had characteristic second order ^1H - and ^{19}F -NMR spectra associated with the symmetry of the nuclei on the cyclopropane ring. In the case of **73a**, a suitable crystal was selected for X-ray structure analysis as illustrated in Scheme 42. This confirmed the all-*syn* configuration of the three C-F bonds. This is the first preparation of such a derivatised cyclopropane.



^1H NMR of compound **72a**



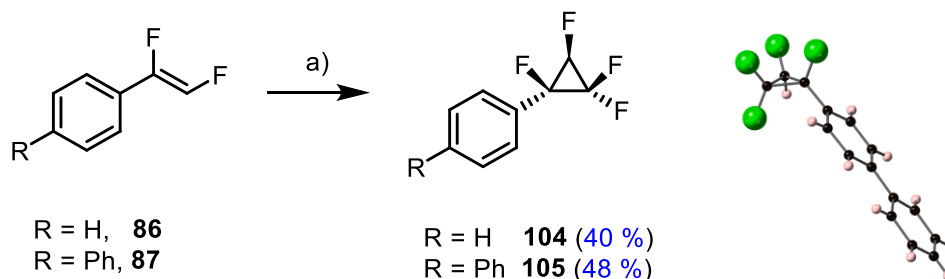
X-ray crystal structure of **73a**.



Scheme 42. Reagents and conditions: a) CHBrF_2 , TEAB, $\text{NaOH}\cdot\text{H}_2\text{O}$, DCM, RT; b) AIBN, Bu_3SnH , RT.

Finally, difluorocarbene was used to generate the tetrafluorocyclopropanes **104** and **105** from difluoroolefins **86**, **87** using the Ruppert-Prakash ($\text{TMS}\text{-CF}_3$) reagent (Scheme 43). This proved to be a straightforward reaction and the corresponding tetrafluorocyclopropanes **104** and **105** were

generated in good yields. The X-ray structure of **105** was also obtained to confirm its structure and stereochemistry.



Scheme 34. Reagents and conditions: a) TMSCF_3 , NaI, THF, reflux.

3.4.3 Measurement of Log P values

It was anticipated that the all-*cis* phenyl-1,2,3-trifluorocyclopropane **72a** will display significant polarity relative to cyclopropane and the other fluorinated analogues. To explore this, Log P values of the fluorine containing cyclopropanes **65a**, **65b**, **92a**, **92b**, **72a**, **72b** and **104** were evaluated experimentally by reverse phase HPLC.⁶² Each of these compounds (5-10 μL of 0.5 mg/mL in CH_3CN) was injected into HPLC using a Phenomenex Luna C_{18} 100A (250 mm X 4.60 mm) 5 μ column. The retention times of all of the compounds were measured using a 60:40 CH_3CN : Water as eluent, both supplemented with 0.05 % TFA. The addition of TFA tends to improve peak resolution. These compounds were selected because they differ only by the degree of fluorination on the cyclopropane ring. A series of reference compounds with known Log P literature values was also injected into the HPLC under the same conditions to establish their retention times (Table 1). Each measurement was repeated in triplicate to minimise errors. Here the “k” value means the capacity factor and can be calculated by the following equation:

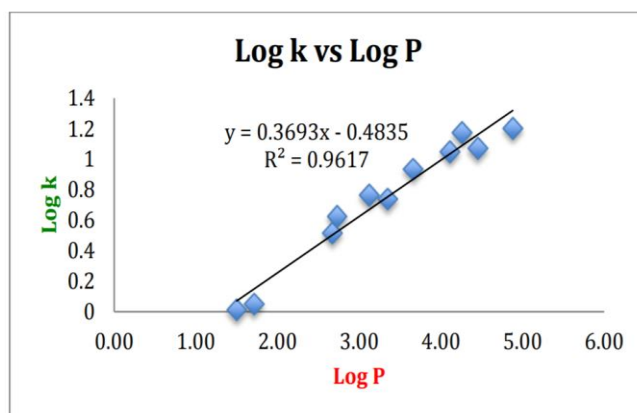
$$k = \frac{\text{Retention time} - \text{Dead time of column}}{\text{Dead time of column}}$$

The dead time of column was 1.97 min under the experiment conditions.

Table 1 Log P values, retention time and capacity factors of reference compounds⁶²

Reference	Log P	Rt 1(min)	Rt 2(min)	Rt 3(min)	Average Rt(min)	Capacity factor (k)	Log k
Phenol	1.50	4.300	4.300	4.259	4.298	1.187	0.075
2-Fluorophenol	1.71	4.201	4.208	4.495	4.301	1.189	0.075
Benzofuran	2.67	8.375	8.375	8.383	8.378	3.263	0.514
Toluene	2.73	10.256	10.274	10.253	10.261	4.222	0.626
<i>o</i> -Xylene	3.12	13.252	13.276	13.579	13.369	5.804	0.764
Naphthalene	3.35	12.733	12.734	12.758	12.742	5.484	0.739
Cumene	3.66	17.059	17.066	17.167	17.097	7.701	0.887
<i>t</i> -Butylbenzene	4.11	23.445	23.413	23.259	23.372	10.894	1.037
Butylbenzene	4.26	29.961	30.434	30.449	30.281	14.410	1.159
Anthracene	4.45	24.455	24.461	24.508	24.475	11.455	1.059
Pyrene	4.88	32.699	32.620	32.802	32.707	15.645	1.194

Finally, a linear regression equation, representing Log P against Log K, was obtained (Plot 1).



Plot 1. The linear regression equation.⁶²

The retention times of the cyclopropanes **65a**, **65b**, **92a**, **92b**, **72a**, **72b** and **104** were measured and then applied the equation shown in Plot 1 to obtain their Log P values. The results are shown in **Table 2**.

Table 2. Log P values of compounds **65a**, **65b**, **93a**, **93b**, **72a**, **72b** and **104**

Compound	Log P	Rt 1(min)	Rt 2(min)	Rt 3(min)	Average Rt(min)	Capacity factor (k)	Log k
72a	2.56	7.667	7.600	7.667	7.645	2.890	0.461
65a	2.97	10.003	9.995	10.001	10.000	4.089	0.612
65b	2.76	8.706	8.699	8.706	8.704	3.429	0.535
92a	2.73	8.560	8.551	8.569	8.560	3.356	0.526
92b	2.75	8.665	8.668	8.677	8.670	3.412	0.533
72b	2.74	8.613	8.805	8.613	8.610	3.382	0.529
104	2.94	9.841	9.671	10.000	9.828	4.002	0.602

For a more visual representation, structures are showed in decreasing lipophilicity in Figure 7.

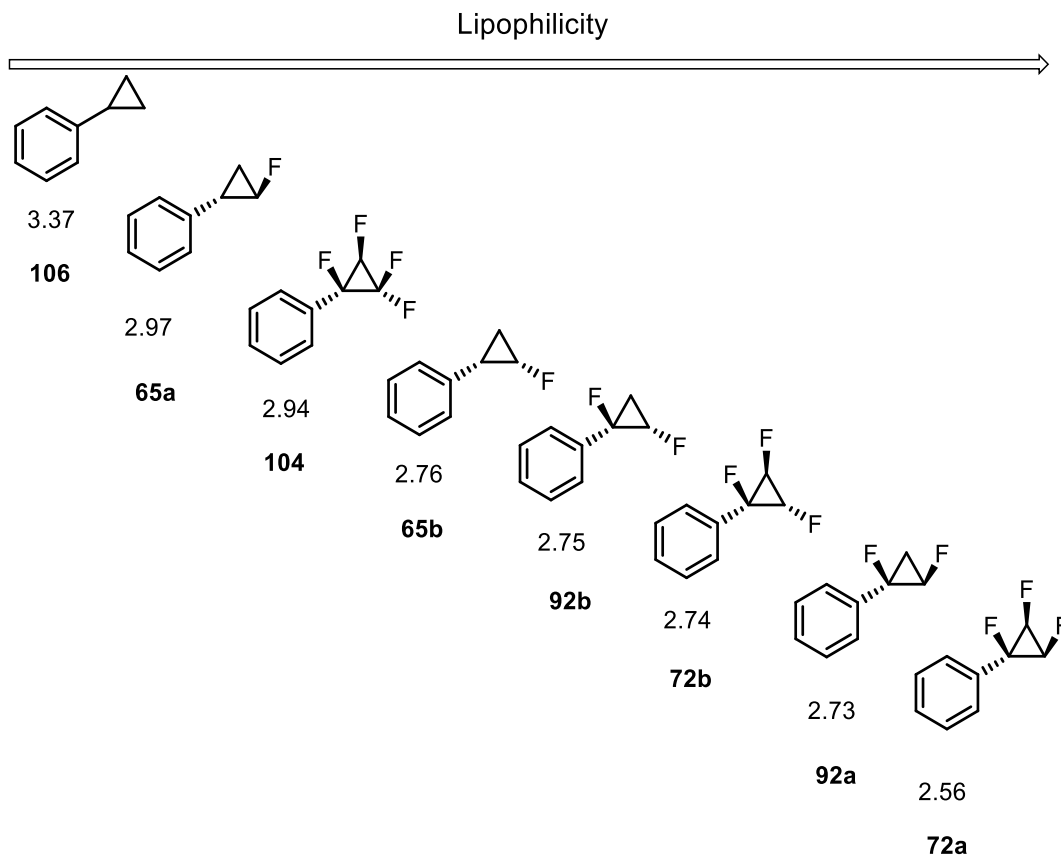


Figure 7. Comparison of Log P values of compounds **65a**, **65b**, **92a**, **92b**, **72a**, **72b**, **104** and **106**.

From this analysis, it is obvious that all of the partially fluorinated cyclopropanes are more polar than the phenylcyclopropane **106** itself, and it is clear that fluorination does affect the lipophilicity values, making the molecules progressively more polar. The lowest Log P value (2.56) is the all *cis*-1,2,3- trifluorocyclopropane **72a**, consistent with it being the most polar of the series. The reduced polarity of **72b** (Log P = 2.74) relative to **72a** is consistent with its lower molecular dipole. When comparing Log P values of compounds **65a**, **92a**, and **72a**, Log P values decrease as the dipole increases. Surprisingly, there is a significant difference in Log P values between compounds **65a** and **65b**, which may suggest that the phenyl ring together with fluorine plays a role in affecting lipophilicity.

Density functional theory (DFT) computational study optimisations at the B3LYP-D3/6-311+G (d,p) level was performed to calculate the dipole moment of all *cis*-trifluorocyclopropane **72a**. After optimisation, the calculated dipole moment of **72a** was 4.9 D. Additionally, the electrostatic surface potential map was also calculated for **72a**. This calculation confirms that the cyclopropane ring has two totally different faces, with a negative fluorine face and positive hydrogen face, as illustrated in Figure 8. This special character, combined with the high polarity makes this motif attractive to test its cation-anion electrostatic interactions.

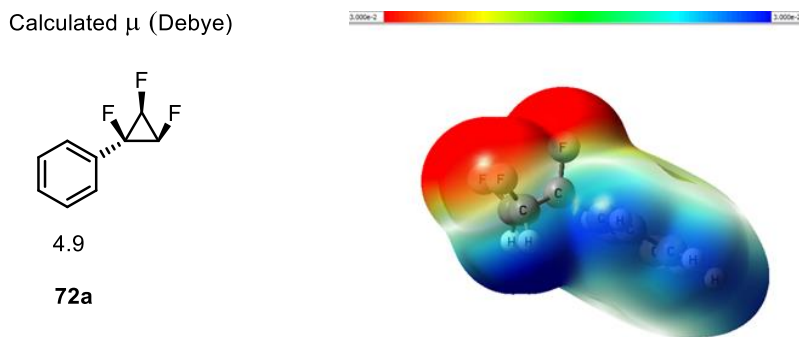


Figure 8. The calculated dipole moment and electrostatic potential map for **72a** at the B3LYP-D3/6-311+G (d,p) level.

3.5 Conclusion

In Chapter 3, a series of fluorinated cyclopropanes, with a particular focus on the preparation of the all *cis*-1,2,3-trifluorocyclopropane motif was synthesised. This was achieved through bromofluorocarbene addition to α,β -difluorostyrenes followed by selective reductive dehalogenation to remove the bromine. This provided the first synthetic access to this substituent. The lipophilicity (Log P) of these compounds was investigated and the results demonstrated that all have lower log P values (lower than 3) than the cyclopropane itself, making them potentially interesting motifs for drug discovery programmes. The all *cis*-1,2,3-trifluorocyclopropane was demonstrated to be the most polar among this series from its experimental Log P measurement. A theory study (DFT) was used to calculate the dipole moment of all *cis*-1,2,3-trifluorocyclopropane **72a**, and the calculated dipole moment of 4.9 D, is consistent with the Log P assessment.

Reference

1. A. Freund, *J. Prakt. Chem.*, 1882, **26**, 367-377.
2. G. Gustavson, *J. Prakt. Chem.*, 1887, **36**, 300-305.
3. G. H. W. Lucas, V. E. Henderson, *Can. Med. Assoc. J.*, 1929, **21**, 173-175.
4. C. A. Coulson, W. E. Moffitt, *J. Chem. Phys.*, 1947, **15**, 151.
5. C. A. Coulson, W. E. Moffitt, *Philos. Mag.*, 1949, **40**, 1-35.
6. J. D. Cox, G. Pilcher, *Thermochemistry of Organic and Organometallic Compounds*, Academic press: London, 1970.
7. M. J. S. Dewar, *J. Am. Chem. Soc.*, 1984, **106**, 669-682.
8. H. E. Simmons, R. D. Smith, *J. Am. Chem. Soc.*, 1958, **80**, 5323-5324.
9. H. E. Simmons, R. D. Smith, *J. Am. Chem. Soc.*, 1959, **81**, 4256-4264.
10. J. H. Chan, B. Rickborn, *J. Am. Chem. Soc.*, 1968, **90**, 6406-6411.
11. G. Wittig, K. Schwarzenbach, *Angew. Chem.*, 1959, **71**, 652.
12. J. Furukawa, N. Kawabata, J. Nishimura, *Tetrahedron Lett.*, 1966, **7**, 3353-3354.
13. Z. Yang, J. C. Lorenz, Y. Shi, *Tetrahedron Lett.*, 1998, **39**, 8621-8624.
14. M. C. Lacasse, C. Poulard, A. B. Charette, *J. Am. Chem. Soc.*, 2005, **127**, 12440-12441.
15. O. Silberrad, C. S. Roy, *J. Chem. Soc. Trans.*, 1906, **89**, 179-182.
16. W. R. Moser, *J. Am. Chem. Soc.*, 1969, **91**, 1141-1146.
17. R. Paulissen, P. Teyssie, A. J. Hubert, *Tetrahedron Lett.*, 1972, **13**, 1465-1466.
18. R. Paulissen, H. Reimlinger, E. Hayez, A. J. Hubery, Ph. Teyssié, *Tetrahedron Lett.*, 1973, **14**, 2233-2236.

19. A. J. Hubert, A. F. Noels, A. J. Anciaux, *Synthesis.*, 1976, **09**, 600-602.
20. A. Padwa, D. J. Austin, S. Hornbuckle, M. Semones, M. Doyle, M. Protopopova, *J. Am. Chem. Soc.*, 1992, **114**, 1874-1876.
21. A. Geuther, *Justus Liebigs Ann. Chem.*, 1862, **123**, 121-122.
22. W. V. Doering, A. K. Hoffmann, *J. Am. Chem. Soc.*, 1954, **76**, 6162-6165.
23. R. M. Cory, F. R. McLaren, *J. Chem. Soc., Chem. Commun.*, 1977, **17**, 587-588.
24. P. S. Skell, A. Y. Garner, *J. Am. Chem. Soc.*, 1956, **78**, 3409-3411.
25. F. Wang, T. Luo, J. Bo, Y. Wang, H. Krishnan, P. Jog, S. Ganesh, K. Prakash, G. Olah, *Angew. Chem. Int. Ed.*, 2011, **50**, 7153 –7157.
26. J. K. Crandall, L. H. C. Lin, *J. Am. Chem. Soc.*, 1967, **89**, 4526-4527.
27. D. M. Hodgson, Y. K. Chung, J. M. Paris, *J. Am. Chem. Soc.*, 2004, **126**, 8664-8665.
28. J. Salaün, M. S. Baird, *Curr. Med. Chem.*, 1995, **2**, 511-542.
29. A. Reichelt, S. F. Martin, *Acc. Chem. Res.*, 2006, **39**, 433-442.
30. B. Atkinson, *J. Chem. Soc.*, 1952, **0**, 2684-2694.
31. P. Tarrant, A. M. Lovelace, M. R. Lilyquist, *J. Am. Chem. Soc.*, 1955, **77**, 2783-2787.
32. D. A. Dixon, *J. Phys. Chem.*, 1986, **90**, 54-56.
33. J. M. Birchall, G. E. Cross, R. N. Haszeldine, *Proc. Chem. Soc.*, 1960, 81.
34. D. Seyferth, S. P. Hopper, *J. Org. Chem.*, 1972, **37**, 4070-4075.
35. I. Ruppert, K. Schlich, W. Volbach, *Tetrahedron Lett.*, 1984, **24**, 2195.
36. J. Nishimura, J. Furukawa, *Chem. Commun.*, 1971, **21**, 1375-1376.
37. O. Tamura, M. Hashimoto, Y. Kobayashi, T. Katoh, K. Nakatani, M. Kamada, I. Hayakawa, T. Akiba, S. Terashima, *Tetrahedron.*, 1994, **50**, 3889-3904.

38. N. Kawabata, M. Tanimoto, S. Fujiwara, *Tetrahedron*, 1979, **35**, 1919-1923.
39. L. V. Chau, M. Schlosser, *Synthesis*, 1973, **2**, 112.
40. W. R. Dolbier, Jr; H. Wojtowicz, C. R. Burkholder, *J. Org. Chem.*, 1990, **55**, 589-594.
41. P. Weyerstahl, G. Blume, C. Mueller, *Tetrahedron Lett.*, 1971, **42**, 3869-3872.
42. P. Weyerstahl, R. Mathias, G. Blume, *Tetrahedron Lett.*, 1973, **14**, 611-612.
43. R. A. Moss, *Tetrahedron Lett.*, 1968, **9**, 1961-1964.
44. R. Fields, R. N. Haszeldine, D. Peter, *J. Chem. Soc. C.*, 1969, **1**, 165-172.
45. T. Morikawa, H. Sasaki, K. Mori, M. Shiro, T. Taguchi, *Chem. Pharm. Bull.*, 1992, **40**, 3189-3193.
46. H. Walborski, L. Allen, H. Traenckner, E. Powers, *J. Org. Chem.*, 1971, **36**, 2937-2941.
47. S. Cottens, M. Schlosser, *Tetrahedron.*, 1988, **44**, 7127-7144.
48. O. G. J. Meyer, R. Fröhlich, G. Häufe, *Synthesis*, 2000, **10**, 1479-1490.
49. W. Lin, A. B. Charette, *Adv. Synth. Catal.*, 2005, **347**, 1547-1552.
50. A. Toyota, Y. Ono, C. Kaneko, I. Hayakawa, *Tetrahedron Lett.*, 1996, **37**, 8507-8510.
51. M. Kirihara, H. Kakuda, M. Tsunooka, A. Shimajiri, T. Takuwa, A. Hatano, *Tetrahedron Lett.*, 2003, **44**, 8513-8518.
52. Y. Yang, C. Su, X. Huang, Q. Liu, *Tetrahedron Lett.*, 2009, **50**, 5754-5756.
53. T. Ando, H. Yamanaka, F. Namigata, W. Funasaka, *J. Org. Chem.*, 1970, **35**, 33-38.
54. J. W. Agopovich, C. W. Gillies, *J. Am. Chem. Soc.*, 1982, **104**, 813-817.
55. C. J. Thomson, Q. Zhang, N. Al-Maharik, M. Bühl, D. Cordes, A. M. Z. Slawin, D. O'Hagan,

- Chem. Comm.*, 2018, **54**, 8415-8418.
56. C. Lee, S. Lin, S. Ke, *Tetrahedron*, 2007, **63**, 120-125.
57. S. A. C. McDowell, *Chem. Phys. Lett.*, 2016, **665**, 105-110.
58. Z. Liu, P. Liao, X. Bi, *Org. Lett.*, 2014, **16**, 3668–3671;
59. S-W. Wu, F. Liu, *Org. Lett.*, 2016, **18**, 3642-3645.
60. J. Leroy, *J. Org. Chem.*, 1981, **46**, 206-209.
61. W. R. Dolbier, C. R. Burkholder, *Tetrahedron. Lett.*, 1988, **29**, 6749-6752.
62. A. Rodil, S. Bosisio, M. Ayoub, L. Quinn, D. B. Cordes, A. M. Z. Slawin, C. Murphy, J. Michel, D. O'Hagan, *Chem.Sci.*, 2018, **9**, 3023-3028.

Chapter 4. Fluorination of dibenzo[a,e]cyclooctatetraene

4.1. Dibenzo[a,e]cyclooctatetraene

1,5-Cyclooctadiene (COD) is a fascinating molecule which has found wide applications, e.g., as a ligand for the preparation of the hydroboration reagent 9-BBN¹ and in the preparation of Crabtree's catalyst,² as shown in Figure 1.

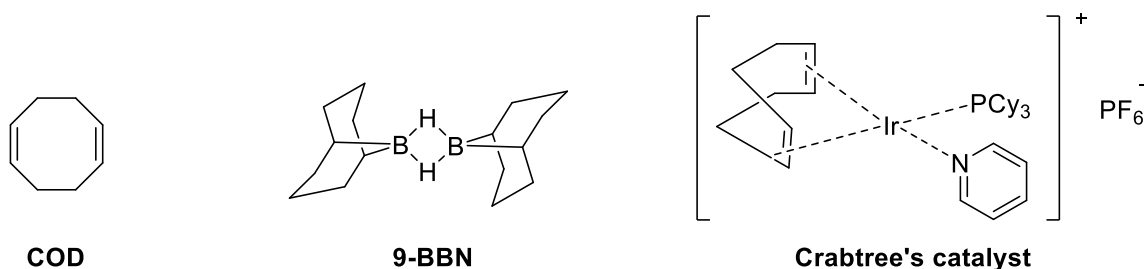


Figure 1. The applications of COD.^{1,2}

COD has played a significant role in transition metal chemistry where COD forms a variety of metal complexes due to its π acceptor properties. Dibenzo[a,e]cyclooctatetraene (DBCOT) **5**, which is a derivative of 1,5-cyclooctadiene (COD), has significantly different properties. It is found to have a stronger binding affinity to metals than COD,³ and as a consequence it emerges as the better ligand candidate than COD.

The X-ray structure of DBCOT **5** shows that it adopts a rigid boat conformation (Figure 2),⁴ consistent with its excellent ability to coordinate metals. Force-field calculations⁵ suggest that COD adopts a twist-boat conformation rather than the boat conformation preferred by DBCOT. This would account as to why DBCOT has the stronger binding ability. Another factor is the aryl

substituent. Aryl rings can be either electron withdrawing or electron donating depending on whether the σ framework or π framework is considered. Since the aryl rings are twisted relative to the C=C bond in the DBCOT structure, the π effect is decoupled and the electron acceptor ability of DBCOT increases substantially.³

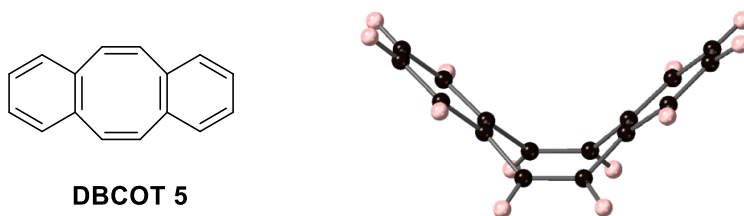
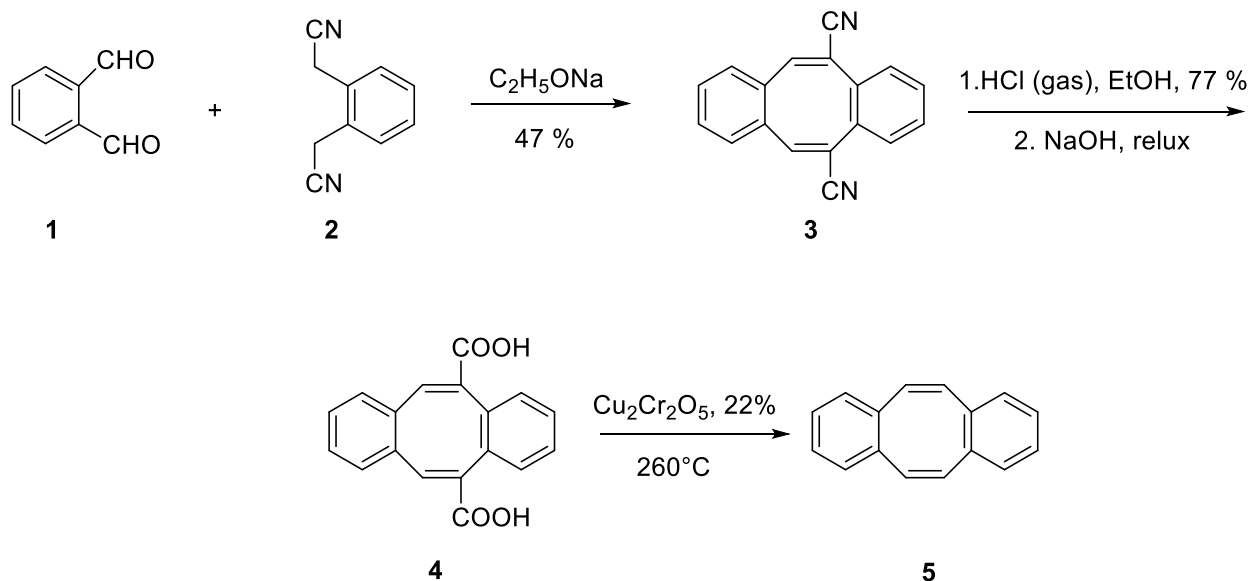


Figure 2. X-ray structure of DBCOT. ⁴

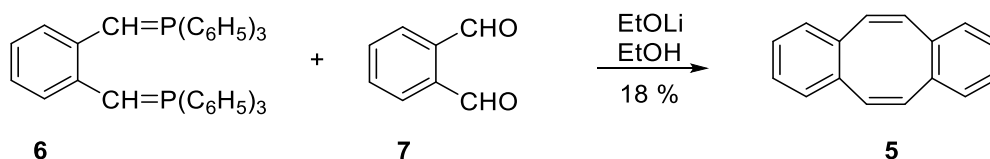
4.1.1 Synthesis of DBCOT

The first synthesis of DBCOT 5 dates back to 1946. Fieser and co-workers reported this compound which was prepared *via* the synthetic route shown in Scheme 1.⁶ Although the compound was prepared, the very poor yield of the decarboxylation reaction and the harsh reaction do not make this a very practical route.



Scheme 1. Original synthesis of DBCOT **5** by Fieser *et al.*⁶

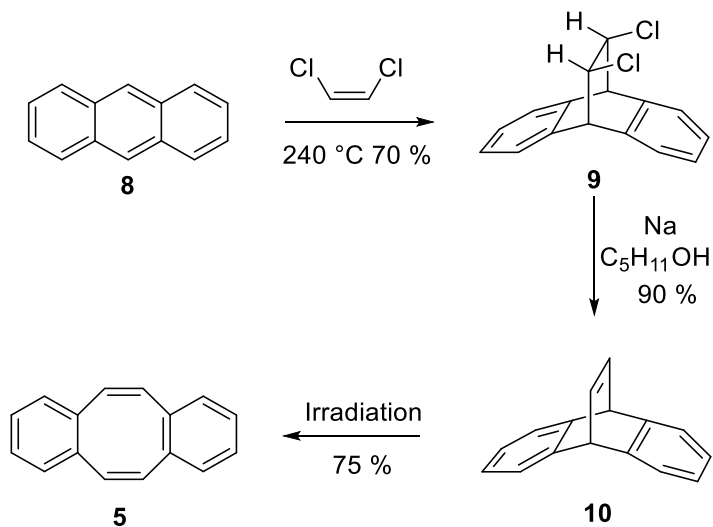
Subsequently in 1963, the Wittig reaction was applied to the synthesis of DBCOT as illustrated in Scheme 2.⁷ Although this appears to be a quite convenient one step reaction, the yield (18 %) is very poor. Wittig reactions favour the *trans* stereochemistry, whereas DBCOT is a highly rigid *cis* structure and this is not an optimal approach. In that case, polymer was also produced due to linear *trans* condensations and the poor propensity to cyclisation.



Scheme 2. Single step synthesis of DBCOT **5** through Wittig reaction.⁷

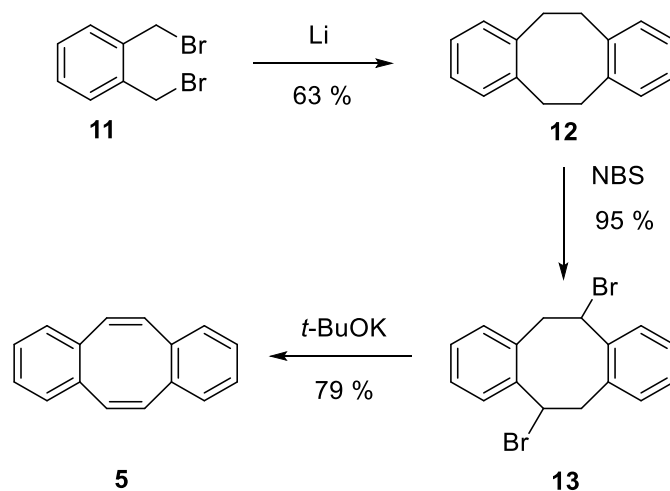
Other approaches to DBCOT involved a three-step route as shown in Scheme 3.⁸ In that case, anthracene was treated with *cis*-1,2-dichloroethylene to generate dichloride intermediate **9**. This was followed by a double dehalogenation to give the bridged olefin **10**. Irradiation of **10** resulted

in a photochemical rearrangement to generate DBCOT, in what was a remarkably efficient reaction. Again, very high temperature and long reaction times were needed.



Scheme 3. Synthesis of DBCOT **5** from anthracene.⁸

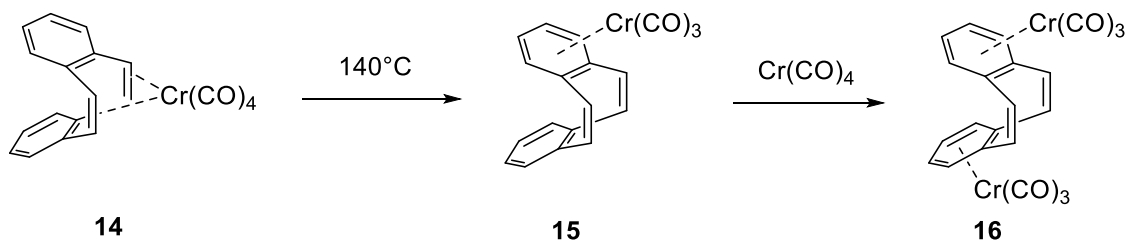
More recently, an improved synthesis of DBCOT **5** was reported by Sterling *et al.*, as illustrated in Scheme 4.⁹ In this case, lithium sand was used under sonication conditions to achieve a very efficient self-coupling reaction starting from the *bis*-benzylbromide **11**, then bromination of **11** followed by elimination gave DBCOT. This synthesis is amenable to scale up and can be carried out on a 50 g scale, but this needs special care due to the exothermic nature of the reaction.



Scheme 4. An improved synthesis of DBCOT **5**.⁹

4.1.2 Selected applications of DBCOT

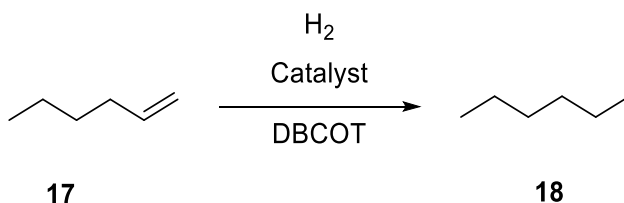
It is well established by X-ray and NMR analysis that DBCOT can coordinate a variety of transition-metals, to form remarkably stable complexes. A good example is its coordination with chromium, as illustrated in Scheme 5.¹⁰ It was observed that at temperatures above 140 °C, Cr(CO)₄ loses one CO and the bonding mode changes from ⁴η to ⁶η. Addition of a second equivalent of Cr(CO)₄ results in the formation of ⁶η bonding mode.



Scheme 5. The coordination of chromium to DBCOT **5**.¹⁰

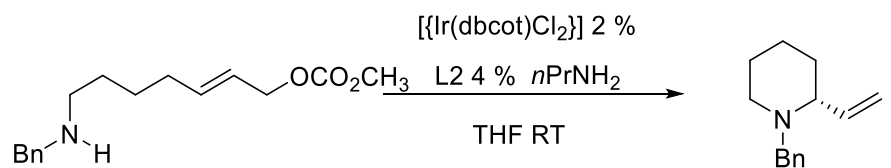
Since it displays a strong binding to platinum group metals, Crabtree reported that DBCOT can be used to determine whether catalyst formed from platinum group metal complexes is

homogeneous or heterogeneous.¹¹ If the catalyst is heterogeneous, the binding between metal and DBCOT would be weak, therefore there will be no decrease in efficiency of the catalyst during the reaction. It was observed that during the hydrogenation of 1-hexene (Scheme 6), with homogeneous catalysts, such as $[\text{Ir}(\text{cod})(\text{PMePh}_2)_2]\text{PF}_6$, $\text{RhCl}(\text{PPh}_3)_3$ or $\text{RuCl}(\text{PPh}_3)_3$, when DBCOT was added, inhibition was rapid. However, in the case of a heterogeneous catalyst, a Pd/C, hydrogenation was not inhibited even when an excess of DBCOT was added.

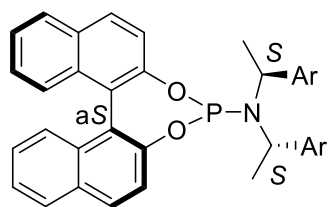


Scheme 6. Hydrogenation of 1-hexene.¹¹

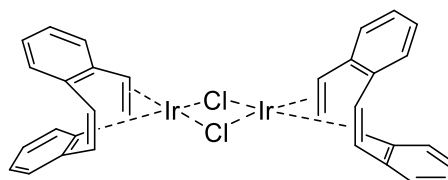
Based on the fact that DBCOT can coordinate transition metals, Günter and co-workers reported the use of an Ir complex of DBCOT to catalyze asymmetric allylic substitutions.¹² With a catalyst generated from 2 mol% of $[\text{Ir}(\text{dbcot})\text{Cl}]_2$ and 4 mol% of the phosphoramidite ligand (L2), the amination products were obtained under both air and argon, with yields up to 86 % (95 % *ee*, enantioselectivities), as illustrated in Scheme 7.



Ar: 86% ee (95%)
 Air: 85% ee (89%)



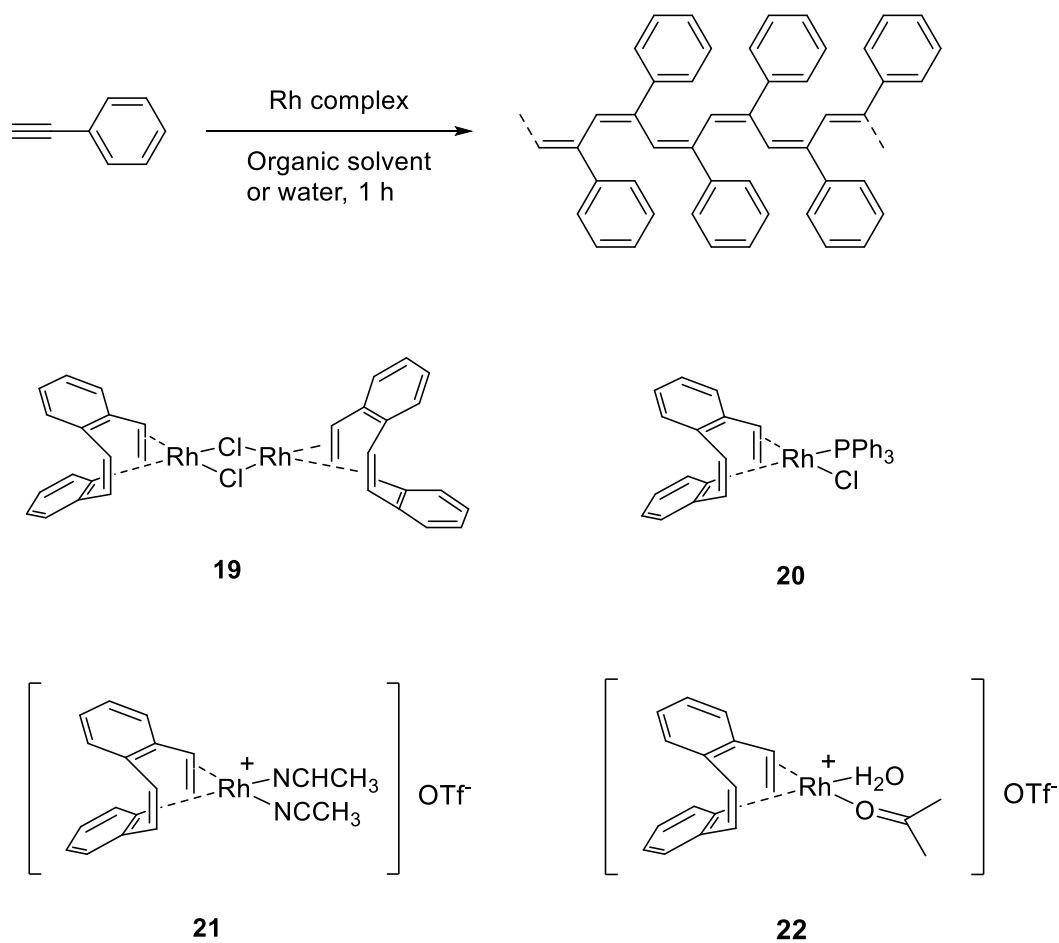
L2 Ar = *o*-(MeO)C₆H₄



Ir(III)(Cl)₂(dbcot)

Scheme 7. Intramolecular allylic amination.¹²

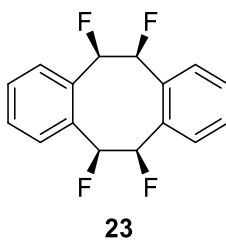
Similar work was carried out by Zhang and co-workers.¹³ They synthesised a series of Rh complexes bearing the DBCOT ligand and introduced catalysts for the polymerisation of phenylacetylene (Scheme 8). The DBCOT Rh complex proved to have higher catalytic activity than the corresponding COD-based Rh complex in both organic solvent and aqueous media. The resulting poly(phenylacetylene)PPA had good *cis*-content, moderate molecular weight and moderate to good polydispersity.



Scheme 8. Polymerization of phenylacetylene using DBCOT-Rh complexes.¹³

4.2. Aims and objectives

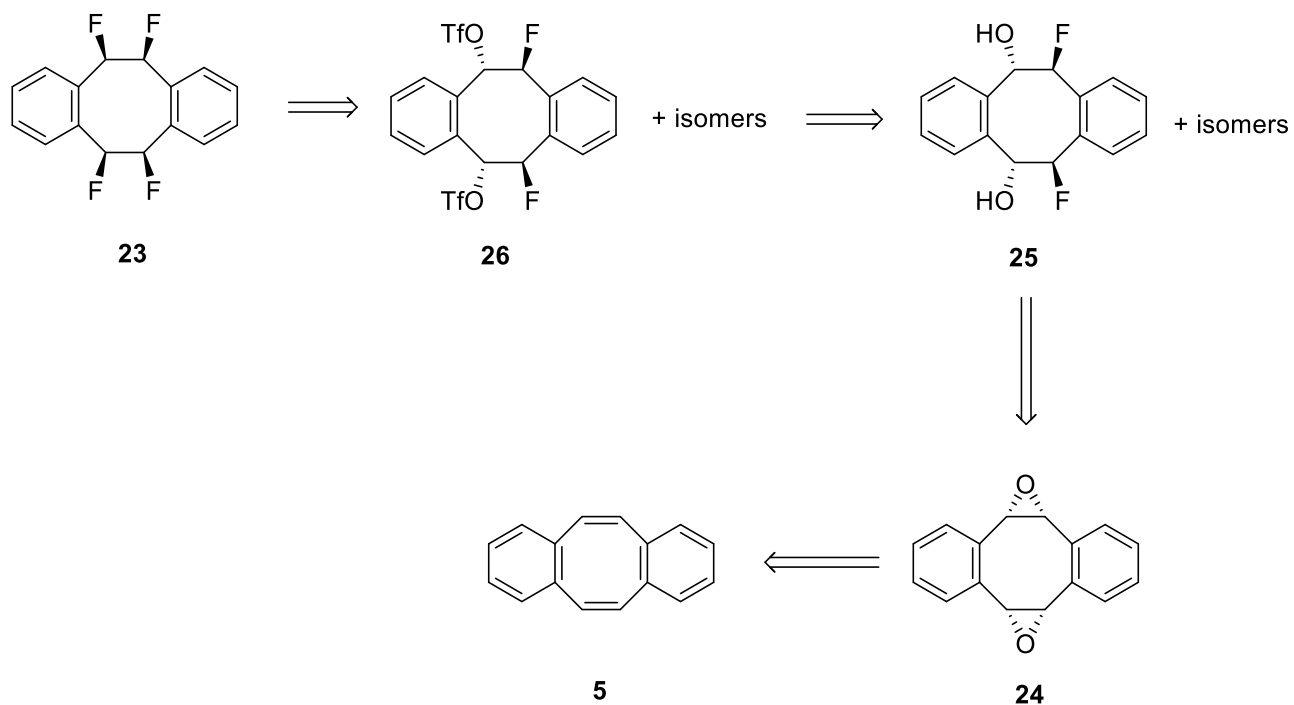
As an extension to the work in Chapters 2 and 3, the main object of this chapter was to try to synthesise all-*cis*-5,6,11,12-tetrafluoro-5,6,11,12-tetrahydrodibenzo[*a,e*]cyclooctatetrane **23**.



This molecule becomes of interest in the context of developing polar organic alicycles and our interest stemmed from the crystal structure of DBCOT **5**. In the solid state where it adopts a rigid boat conformation the four vinyl hydrogens are pointing almost in axial orientations. The idea was to explore if four fluorines in such a system would adopt co-axial orientations if this *tetra*-fluorinated motif could be synthesised. If so, this would generate a highly polarised molecule with a very concentrated area of negative electrostatic potential on the fluorine face. This would extend the family of facially polarised cycloalkanes. Of course, the four fluorines could also adopt equatorial positions due to repulsion between fluorines, and therefore the overall polarity of this conformation will be reduced. However, it was still interesting to prepare this compound to analyse its conformation and overall polarity and then to explore its interactions with electropositive systems. This project was initiated by a M. Chem. undergraduate student (Roscoe Z. Gillatt) who was under my supervision, and was developed by me after he had completed.

4.3. Results and discussions

The anticipated synthetic route to **23** is shown in a retrosynthesis in Scheme 9.



Scheme 9. Retrosynthesis to **23**.

Following from significant previous experience in St Andrews towards the preparation of *cis* vicinal fluorinated compounds, *cis*-diepoxide **24** emerged as a key intermediate. Diepoxide **24** could be generated by epoxidation of DBCOT **5**. This would be followed by hydrofluorination. The resultant fluorohydrins could then be activated by triflation and then fluorination to generate target **23**.

The treatment of DBCOT **5** with an excess of *m*CPBA generated three epoxidation products as illustrated in Figure 3. This was an efficient process and all of the starting material was consumed.

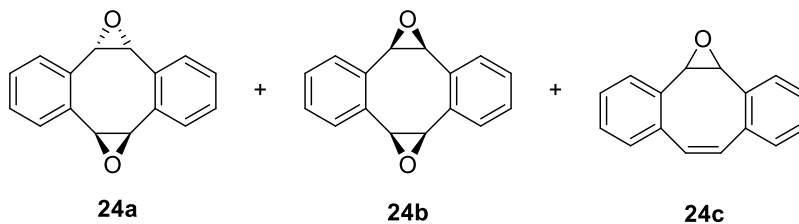


Figure 3.

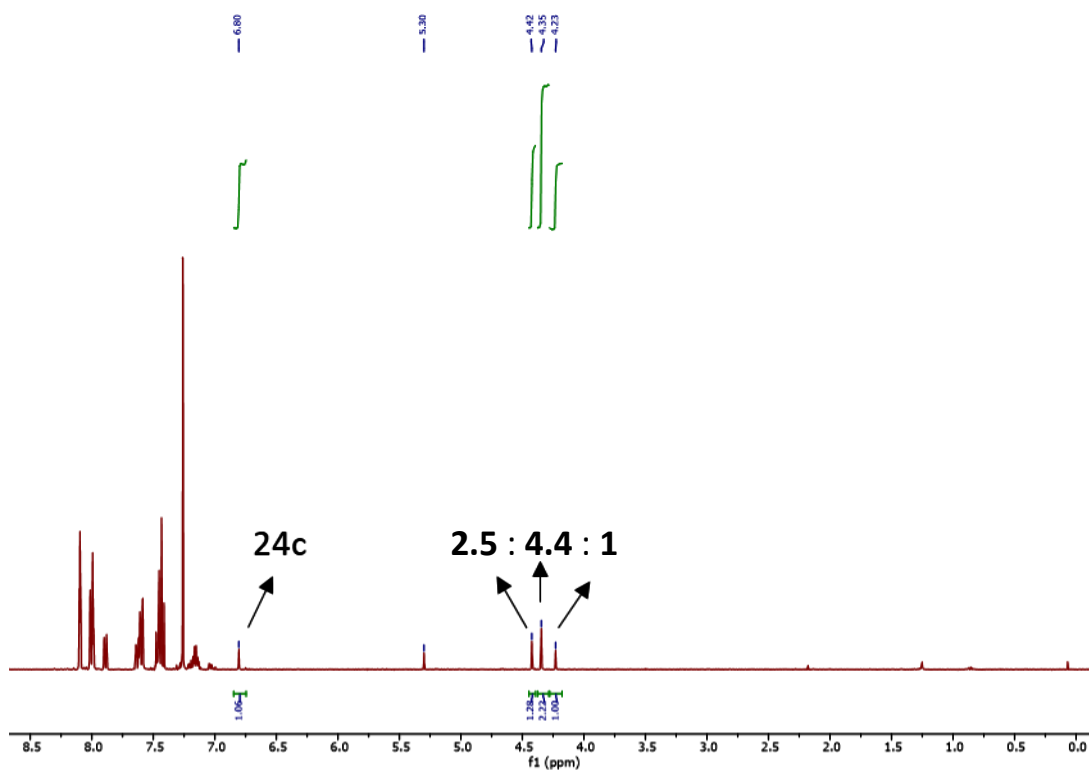


Figure 4. ^1H NMR of the crude mixture of **24**.

Analysis of the ^1H NMR spectrum indicates there are three products in a ratio of 2.5 : 4.4 : 1. The minor product turned out to be the mono-epoxide **24c**. It retained vinyl protons at 6.80 ppm, which has an equivalent integration to the epoxide hydrogens at 4.23 ppm. The diepoxy diastereoisomers were separated by chromatography and the stereochemistry of major product **24b**, with a proton chemical shift at 4.35 ppm, was confirmed by X-ray crystallography. The crystal

structure of **24b** shows that the central ring adopts a boat conformation with the two epoxide rings lying equatorial. The remaining product **24a**, probably has two epoxide rings one axial and one equatorial (^1H NMR singlet at 4.42 ppm), although an X-ray structure was not determined.

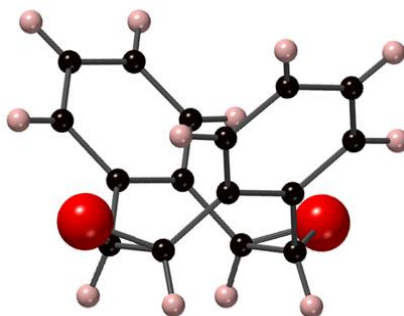


Figure 5. X-ray structure of **24b**.

With **24b** in hand, the next step involved using $\text{Et}_3\text{N}\cdot 3\text{HF}$ to catalyse ring-opening to generate a mixture of fluorohydrin-products. However, from **Table 1**, it can be seen that this reaction proved unsuccessful even at high temperature. There was no conversion even after extending reaction times to 72h. The diepoxide was stable and did not react. This result was somewhat unexpected due to the general success of this strategy with other diepoxide motifs. The reason why this reaction failed is not clear, however due to this disappointing result, an alternative synthetic route was explored.

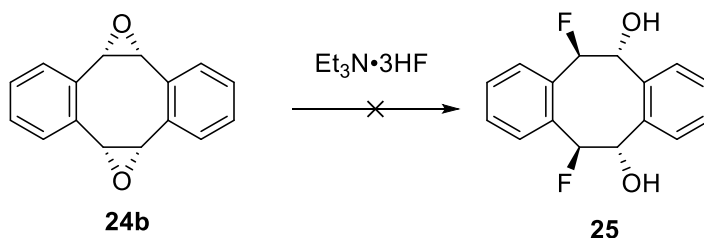
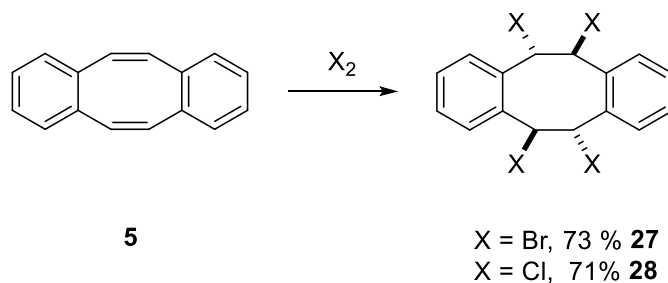


Table 1. Attempted ring-opening reactions using Et₃N·3HF

Entry	Eq. Et ₃ N·3HF	T / °C	Time (h)	Conversion (%)
1	excess.	100	72	<1
2	excess.	130	72	<1
3	excess.	180	24	<1
4	excess.	180	72	<1

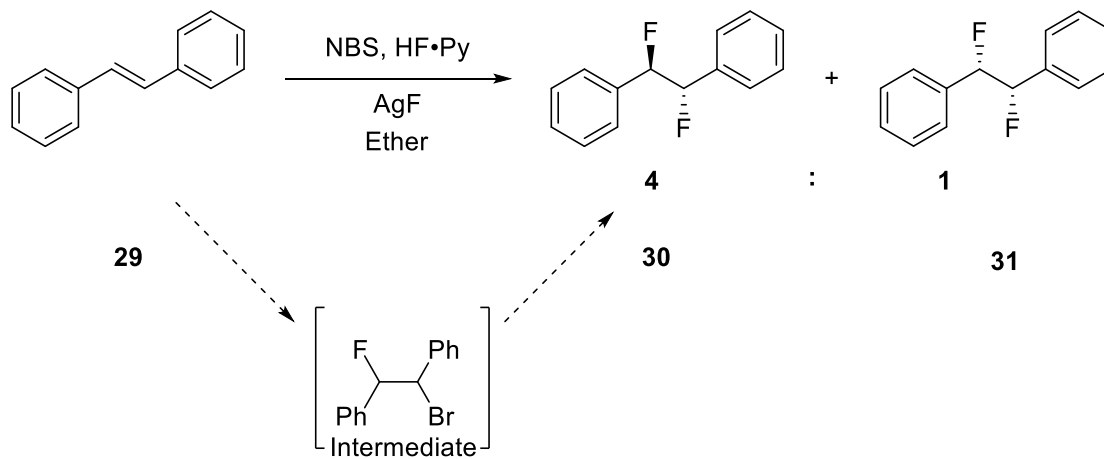
It is known that bromination or chlorination of DBCOT **5** using elemental bromine and chlorine results in the corresponding *tetra*-halogen isomers **27** and **28**. These reactions give good yields (Scheme 11).¹⁴ For the *tetra*-bromo product **27**, the stereochemistry was established by X-ray structure analysis where the vicinal bromines are arranged *anti* to each.^{15,16} In those reactions, both olefins are processed independently and there are no transannular products formed.



Scheme 11. Halogenation of DBCOT **5**.¹⁴

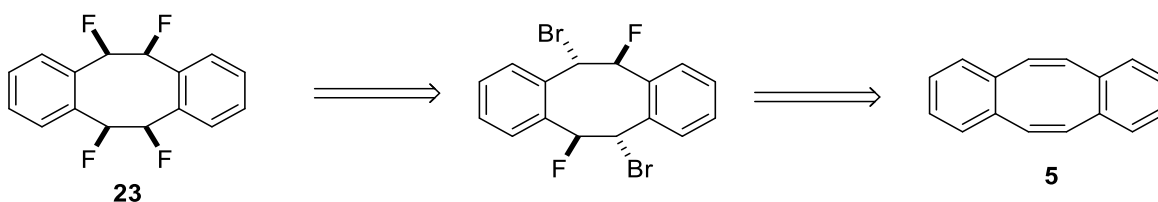
A previous group member, Martin Schöler, also reported a one-pot fluorination of stilbene (Scheme 12).¹⁷ In that reaction, N-bromosuccinimide was used as a source of bromine to generate a bromonium intermediate which readily reacted with fluoride from Olah's reagent (70 % HF·Py) to generate the vicinal bromo-fluoro intermediate. Direct substitution of the bromine

using silver fluoride *in situ* generated the vicinal difluoroproducts. The ratio of the *erythro*- to *threo*-stereoisomer was 4 : 1.



Scheme 12. One-pot fluorination of *trans*-stilbene **29**.¹⁷

Based on those results, a new synthetic route was designed, as illustrated in Scheme 13. The target molecule **23** seemed accessible from DBCOT **5** *via* a bromofluorination reaction of the central olefins, followed by direct fluorination. This was anticipated to give **23** with the desired *syn* arrangement of the fluorines.



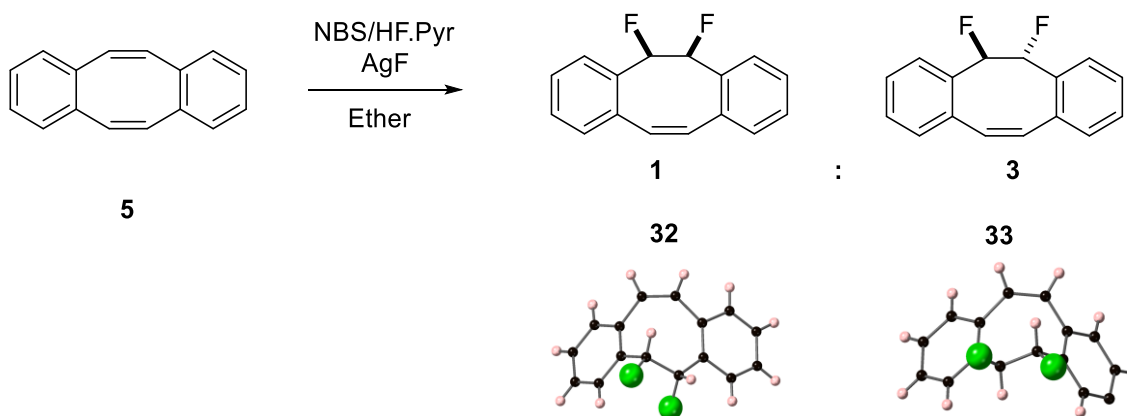
Scheme 13. A new approach to **23**.

With this background, a one-pot reaction was attempted, firstly using the Schüler's conditions. Subsequently a series of reaction conditions were investigated in order to maximise the yields of the products. The conditions are shown in Table 2.

Table 2. One-pot reaction conditions using ether as the solvent

Entry	Eq. NBS	Eq. HF/Py	Eq. AgF	T / °C	Conversion (%)
1	2	2	2	-78	>99
2	4	excess	4	-78	>99
3	4	excess	4	0	>99
4	4	excess	4	RT	>99

From the results, it can be seen that all of the conditions resulted in reactions that went to completion. For Entry 1, there appeared only 'one' major product with a strong fluorine singlet at -182 ppm in the ^{19}F {H} NMR spectrum, therefore this product was isolated first. In the event it turned out to be two compounds, which were characterized by NMR and their structures confirmed by X-ray analysis. These compounds are the *syn* and *anti* vicinal difluoro compounds **32** and **33**, formed in a ratio of around 1 : 3, as illustrated in Scheme 14.



Scheme 14. One pot reaction of **5** under literature condition.

In order to achieve further fluorination of the second double bond, more forcing conditions were attempted. This involved adding more equivalents of reactants or increasing the temperature

(Entries 2, 3, and 4), However, under those conditions, the results remained largely consistent, and still **32** and **33** emerged as the major products. In addition, fluorination of **32** or **33** using NBS, HF·Py and AgF was attempted separately. However, the consumption of the starting material was never significant, leaving the second double bond intact.

Given that only these difluoro compounds were obtained in ether, some other solvents (THF, DCM, acetonitrile, toluene) were explored. In THF, only *trans* isomer **33** was formed. However, a surprising result emerged when the reaction solvent was changed to DCM. Two major fluorine peaks emerged at -116 and -123 ppm in ^{19}F {H} NMR spectrum. The products were purified by chromatography and X-ray structure analysis revealed that these two compounds were isomers of the bridged α,α -difluoro ethers **34** and **35**. They were formed in about 1 : 1.2 ratio. A minor product was also recovered, and which was a crystalline solid. X-ray analysis revealed it was the all *trans* *tetra*-fluoro compound **36**, as shown in Figure 6.

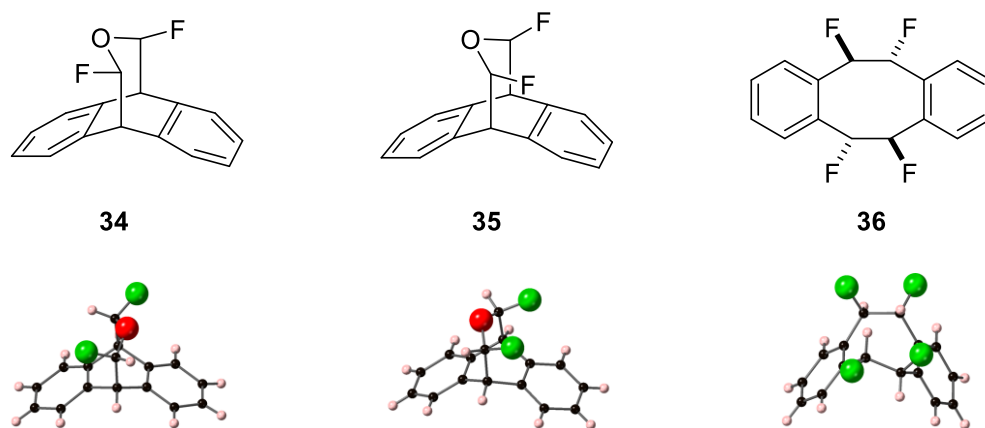


Figure 6. The products forming in the DCM.

When the reaction was conducted in the acetonitrile rather than DCM, there was a significant shift in the product profile towards *trans* difluoro isomer **33** as the major product. When toluene

was used as the solvent, the product containing a difluoromethyl group **37** emerged as a minor component. It was isolated after chromatography and its structure was also confirmed by X-ray crystallography, as illustrated in Figure 7. In addition, the large vicinal coupling constant $^3J_{\text{H-H}}$ value (8 Hz) is consistent with this its conformation.

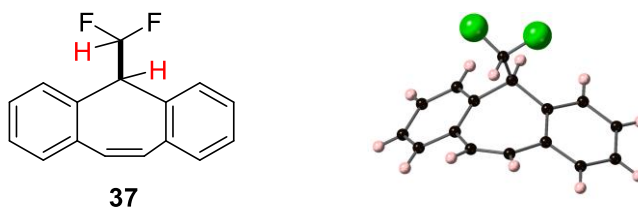
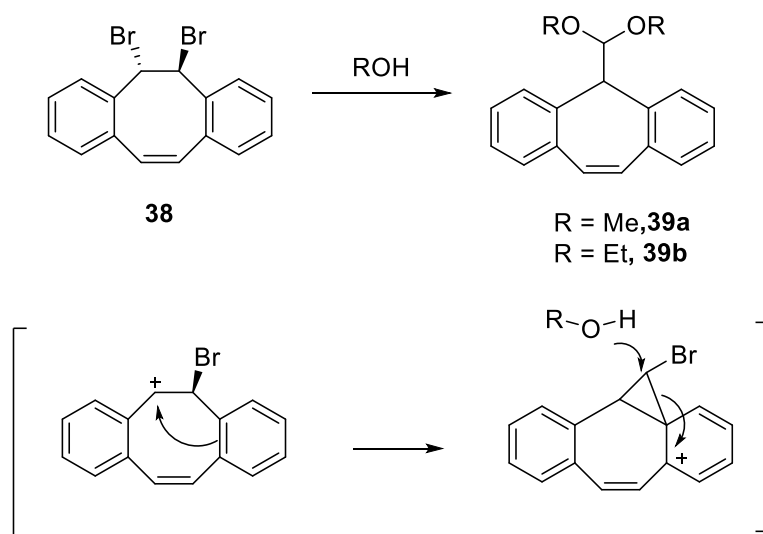


Figure 7. The X-ray structure of **37**.

It has been shown¹⁸ that solvolysis of dibromide **38** with methanol or ethanol generates ring contracted diacetals **39** with remarkable ease. This reaction occurs even under cool conditions. The outcome clearly indicates that a carbocation rearrangement happens during the reaction, as illustrated in Scheme 15. This provides some rationale for the formation of product **37**, which presumably progresses through a similar process, but with fluoride as a nucleophile.



Scheme 15. A mechanism for ring contraction **38** on solvolysis.¹⁸

Solvent proved to be important and influenced the product outcomes of these reactions as summarised in Table 3.

Table 3. Reaction outcomes treating **5** with HF·Py/NBS/AgF in different solvents^a.

Entry	Solvent	Product (Conv. %) ^b			
		34 and 35	37	32 and 33	36
1	DCM	95 (1 : 1.3)	0	5*	Trace
2	Acetonitrile	51 (1.2 : 1)	0	49 ⁺	0
3	Toluene	40 (1.6 : 1)	11	49 (1 : 7)	0
4	THF	12 (1.1 : 1)	0	88 ⁺	0
5	Et ₂ O	6 (1.1 : 1)	0	92 (1 : 3)	Trace

^a Unless otherwise noted, reactions were performed using NBS (2 equiv.), HF·Py (2 equiv.), AgF (2 equiv.) at RT. ^b Conversions were calculated by ¹H NMR of product mixtures prior to work up. * Isomer **32** only. ⁺ Isomer **33** only.

The formation of the ether diastereoisomers **34** and **35** immediately raised a question of a mechanism and where the oxygen atom had originated from. Control reactions were conducted in dry solvents under an argon atmosphere. Under those conditions, compounds **34** and **35** were still efficiently formed. Therefore, a source from molecular oxygen (air) or any moisture in the solvent was excluded. A possible source of the oxygen from moisture in the added HF·Py was also discounted. When the reaction was carried out with NBS and AgF in DCM and without adding

HF·Py, it continued to efficiently form compounds **34** and **35**, indicating that HF·Py is not essential and is not a source of moisture.

Another one possible source of oxygen was the NBS. Succinimide is not generally considered to be a nucleophile in organic reactions, but it is well established that silver and succinimide will form a 2:1 anion N-Ag succinimide complex **40** (Figure 8).^{19,20} The complex has been explored structurally both by IR and NMR. In the IR spectrum, the vibration of the C=O bond stretches are shifted to 1700 and 1570-1615 cm^{-1} and in ^{13}C NMR, the carbonyl signal underwent a low-field shift of around 10 ppm, both indicating a significant carbonyl delocalisation, with electron density on oxygen. This could increase its nucleophilicity.

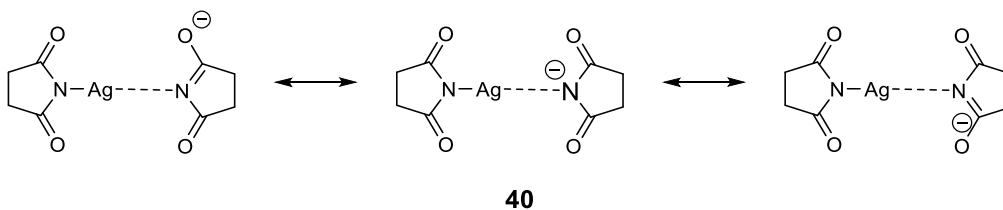
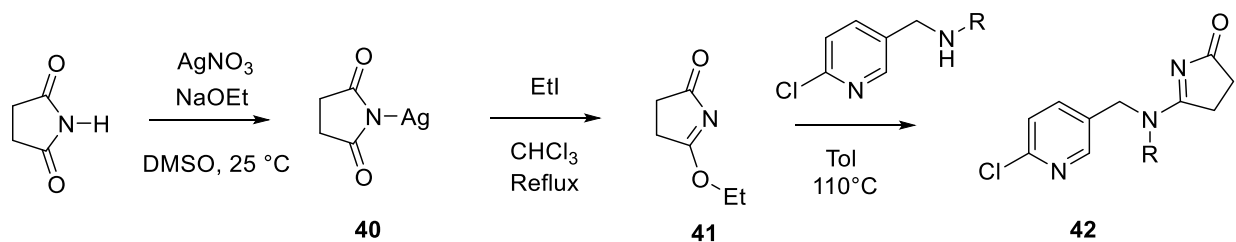


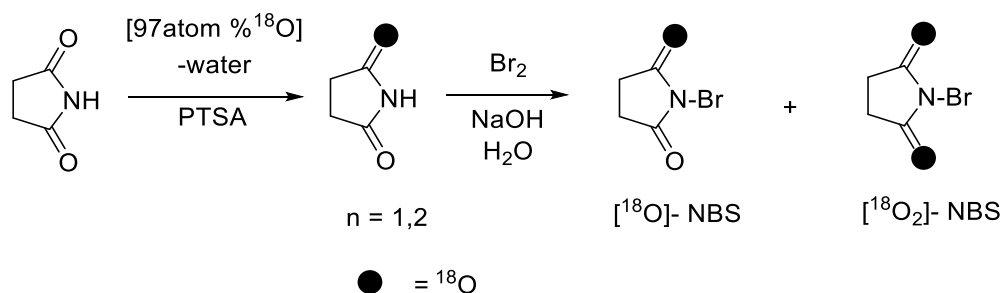
Figure 8. A representation of N-silver succinimide complex.^{19,20}

One good example showing the nucleophilicity of N-silver succinimide complex was in the synthesis of the analogue of the neonicotinoid insecticide,²¹ as illustrated in Scheme **16**. Succinimide and silver nitrate first produced the silver complex **40**, followed by attack of iodoethane, generated 2-ethoxypyrrolin-5-one **41**, which in turn reacted with the second amine to generate the desired product **42**.



Scheme 16. Synthesis of **42**.²¹

In order to explore if the oxygen of ethers **34** and **35** comes from NBS, oxygen-18 labelled [¹⁸O]-NBS was prepared as the substrate. There were no preparations of [¹⁸O]-NBS in the literature, therefore we set about to make it for the first time in our lab. Treatment of succinimide with *p*-toluenesulfonic acid monohydrate (pTSA) in [97%-atom-¹⁸O]-water at 60°C for 12 hours resulted in an exchange reaction and the accumulation of the [¹⁸O]-succinimide. The resultant [¹⁸O]-succinimide was then dissolved in sodium hydroxide solution and treated with elemental bromine to generate [¹⁸O]-NBS, as illustrated in the Scheme 17. The [¹⁸O]-NBS was purified by column chromatography.



Scheme 17. Preparation of ¹⁸O labelled NBS.

In order to determine the populations of the ¹⁸O incorporation in the NBS, the isolated [¹⁸O]-NBS was subject to mass analysis and the resultant spectrum is shown in Figure 9.

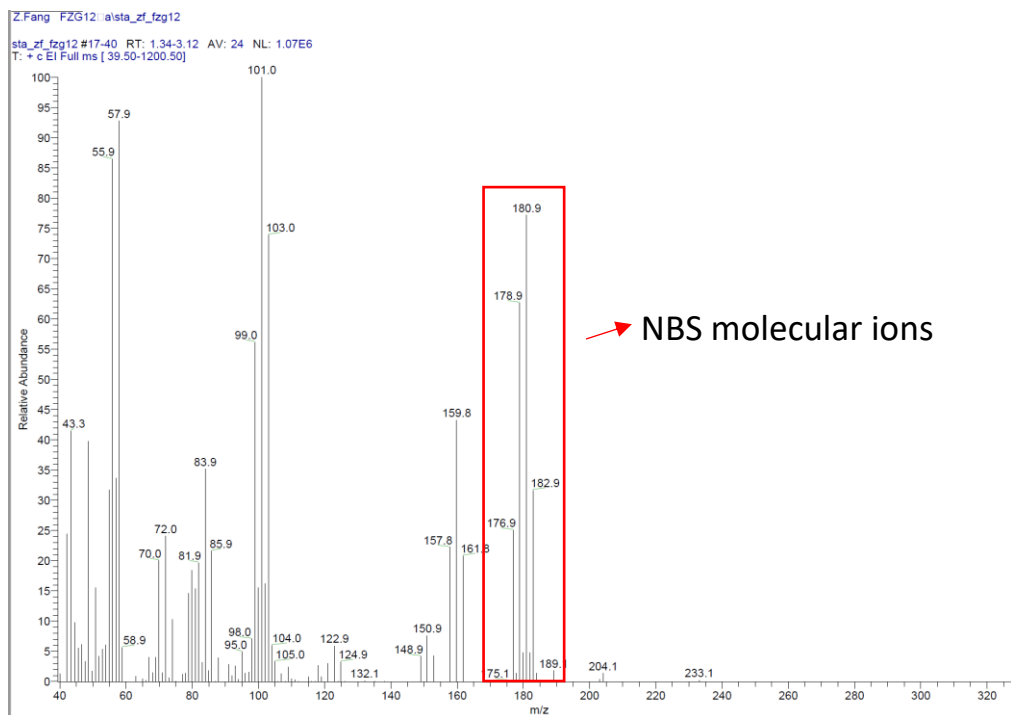
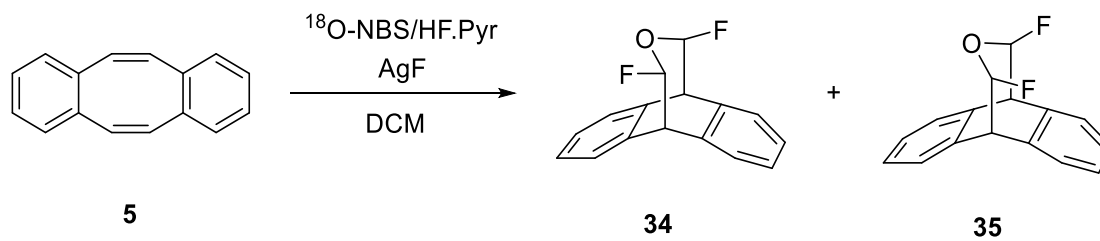


Figure 9. MS result for ^{18}O labelled NBS

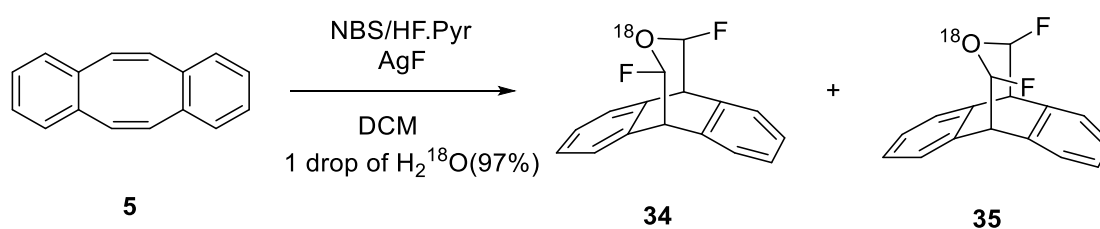
The molecular weight for unlabelled NBS is 176.9 ($\text{C}_4\text{H}_4\text{O}_2^{79}\text{Br}$) and 178.9 ($\text{C}_4\text{H}_4\text{O}_2^{81}\text{Br}$). From the result, it is quite clear that NBS has populations of both one and two ^{18}O atoms, because there are intensities at the 180.9 [M+2] and 182.9 [M+4] in the mass ion spectrum. Among them, the intensity of 182.9 ($\text{C}_4\text{H}_4^{18}\text{O}_2^{81}\text{Br}$) peak is around 31 %, which indicates, by difference that the intensity of $\text{C}_4\text{H}_4^{18}\text{O}^{81}\text{Br}$ (180.9) is around 56%. The overall intensity of the peak at 180.9 is around 77% in the MS spectrum, so the remaining intensity (21%) accounts for the $\text{C}_4\text{H}_4^{18}\text{O}_2^{79}\text{Br}$. It follows that the intensity of unlabelled NBS 176.9 ($\text{C}_4\text{H}_4\text{O}_2^{79}\text{Br}$) and 178.9 ($\text{C}_4\text{H}_4\text{O}_2^{81}\text{Br}$) are both approximately 25%. Again, the overall intensity of the peak at 178.9 is 62 %, so the intensity of $\text{C}_4\text{H}_4^{18}\text{O}^{79}\text{Br}$ is 37 %. All in all, the unlabelled NBS accounts for around 14.8 %, the monolabelled NBS 54.7% and the dilabelled NBS 30.5 % of the total population.

With the ^{18}O labelled NBS in hand, the reaction was conducted in DCM (Scheme 18). This gave ether products **34** and **35** in the usual way. After purification, isotope incorporation into **34** and **35** was estimated by mass analysis. However, there was no indication of isotope content. Also analysis of $^{19}\text{F}\{^1\text{H}\}$ -NMR did not reveal any upfield shifts caused by the heavy isotope.



Scheme 18. Reaction of **5** using [^{18}O] labelled NBS.

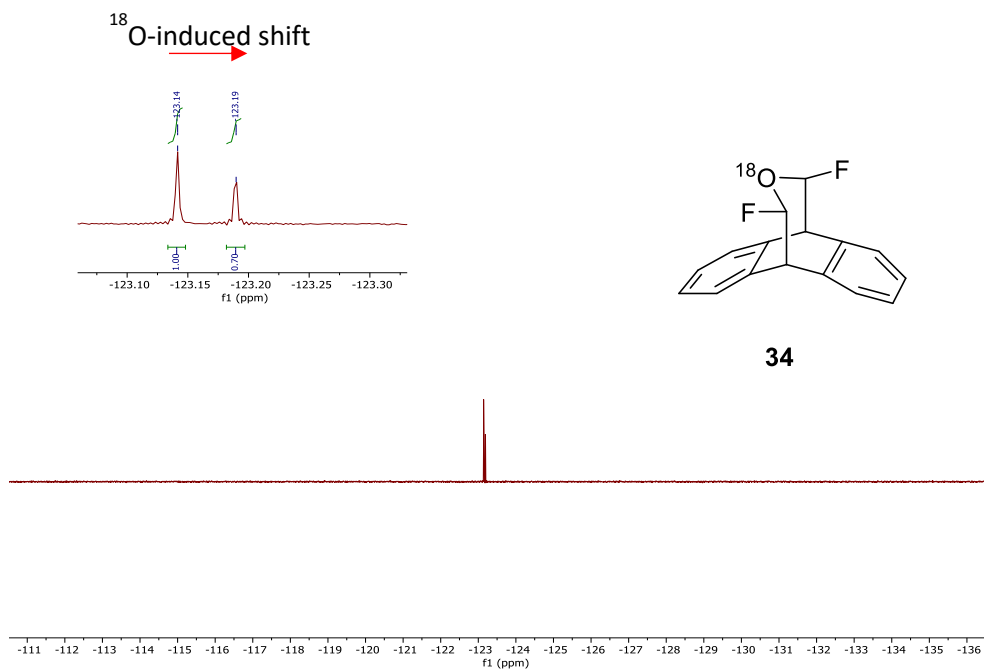
Based on these outcomes, it is clear that NBS is not the source of the ether oxygen. Having discounted oxygen, moisture from the solvents and NBS as a source of the ether oxygen, another possible source of the ether oxygen is a possible contamination of Ag_2O in the AgF . It should be noted that the source of AgF stated that it was analytically pure. But Ag(I)F is quite moisture sensitive and water will transfer AgF to Ag_2O . Therefore a reaction was carried out, adding [97%-atom- ^{18}O]-water in DCM to the reaction, as shown in Scheme 19.



Scheme 19. Reaction of **5** by adding 1 drop of H_2^{18}O .

The conversion to compounds **34** and **35** was suppressed under these conditions, but after workup **34** and **35** were isolated. This time the incorporation of ^{18}O into compounds **34** and **35** was observed both by mass spectrometry and $^{19}\text{F}\{^1\text{H}\}$ -NMR. In the MS spectrum, an isotope peak [M+2] appeared in both isomers **34** and **35**. In the $^{19}\text{F}\{^1\text{H}\}$ -NMR, an additional peak was apparent in the spectrum for both isomers. This peak was upper field shifted by the heavy atom (^{18}O), $\Delta = 0.05$ ppm for **34** and $\Delta = 0.04$ ppm for **35**. Integration of $^{19}\text{F}\{^1\text{H}\}$ -NMR spectrum indicated around 70 % ^{18}O and 56 % ^{18}O incorporation into ethers **34** and **35**, respectively. The results are shown in Figures 10 and 11.

(a)



(b)

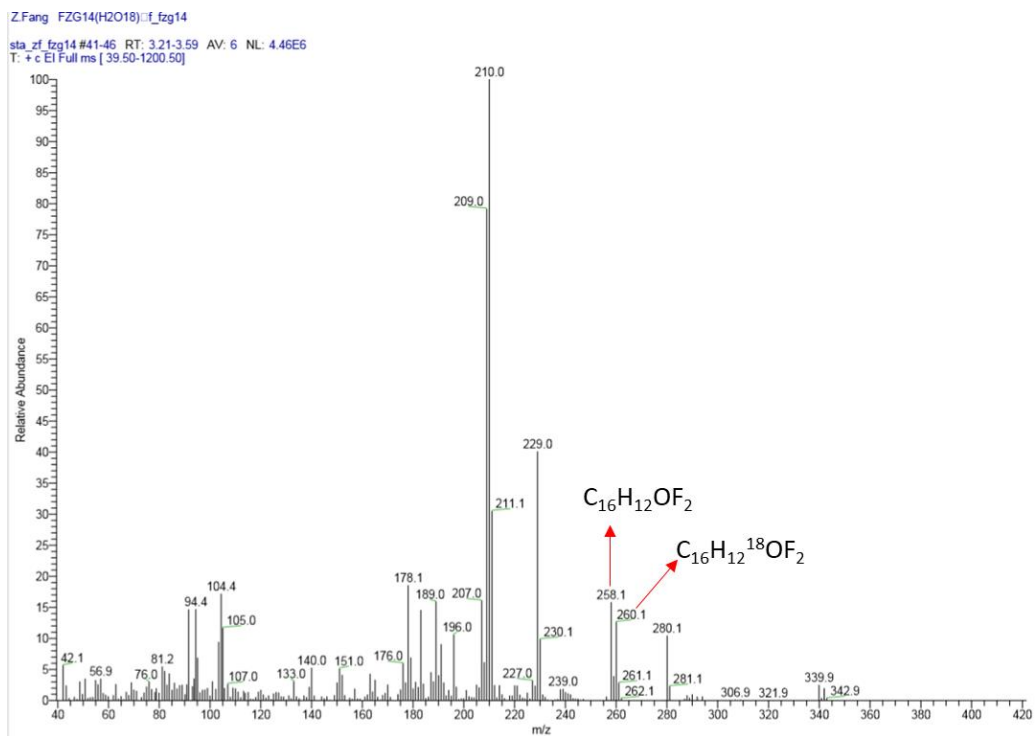
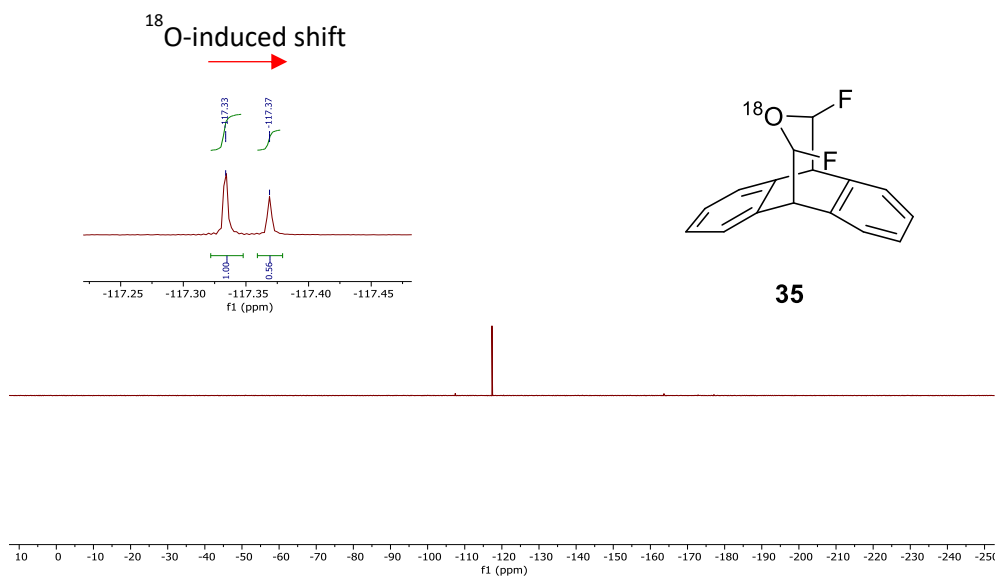


Figure 10. a). ¹⁹F {¹H} NMR of **34**; b). MS result for **34**.

(a)



(b)

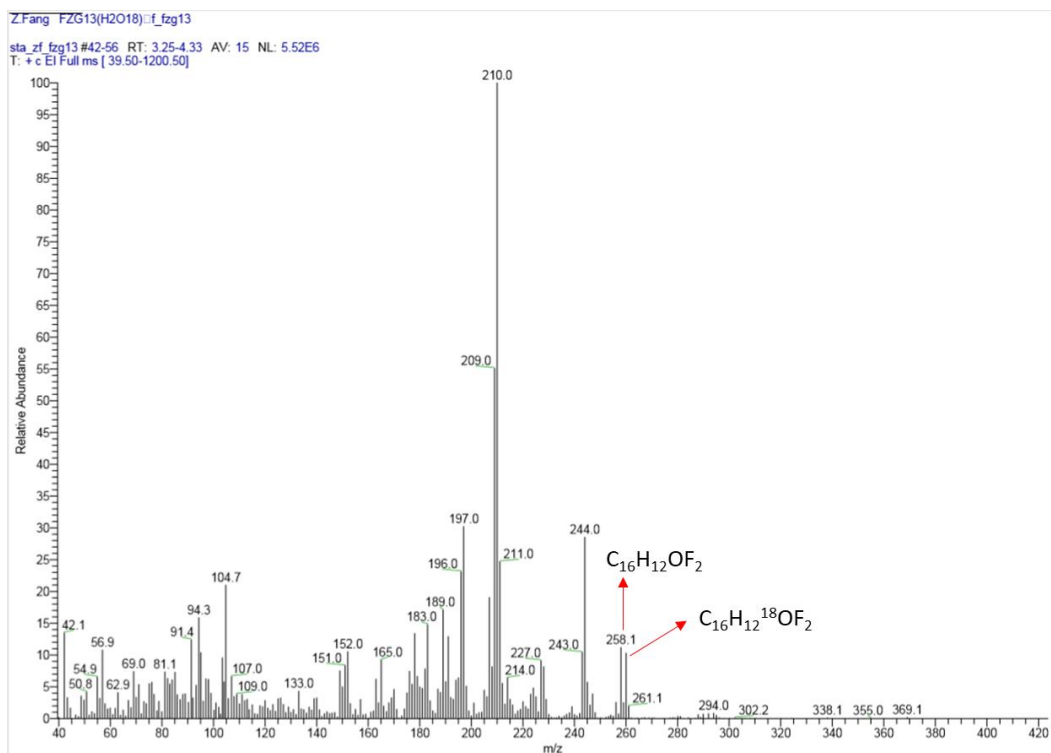


Figure 11. a). ¹⁹F {¹H} NMR of **35**; b). MS result for **35**.

The same reaction was conducted under the same conditions for the second time to prove its reproducibility. The reaction generated ^{18}O incorporated ethers **34** and **35** again, but incorporation level decreased (10 % for **34** and 14 % for **35** by integration of $^{19}\text{F}\{^1\text{H}\}$ -NMR). Additionally, the reaction was carried out by adding 1 drop of 10%-atom- ^{18}O -water into the reaction instead of 97%-atom- ^{18}O -water, ether compounds **34** and **35** still formed but with no isotope incorporation. The reduced level of the incorporation of ^{18}O from water indicates that water may not be the direct nucleophile. This result led to checking the purity of commercially supplied Ag(I)F. Infrared (IR) analysis of the Ag(I)F showed a very strong broad OH peak in O-H stretching frequency range, suggesting the presence of either water or an AgOH equivalent, as illustrated in Figure 12.

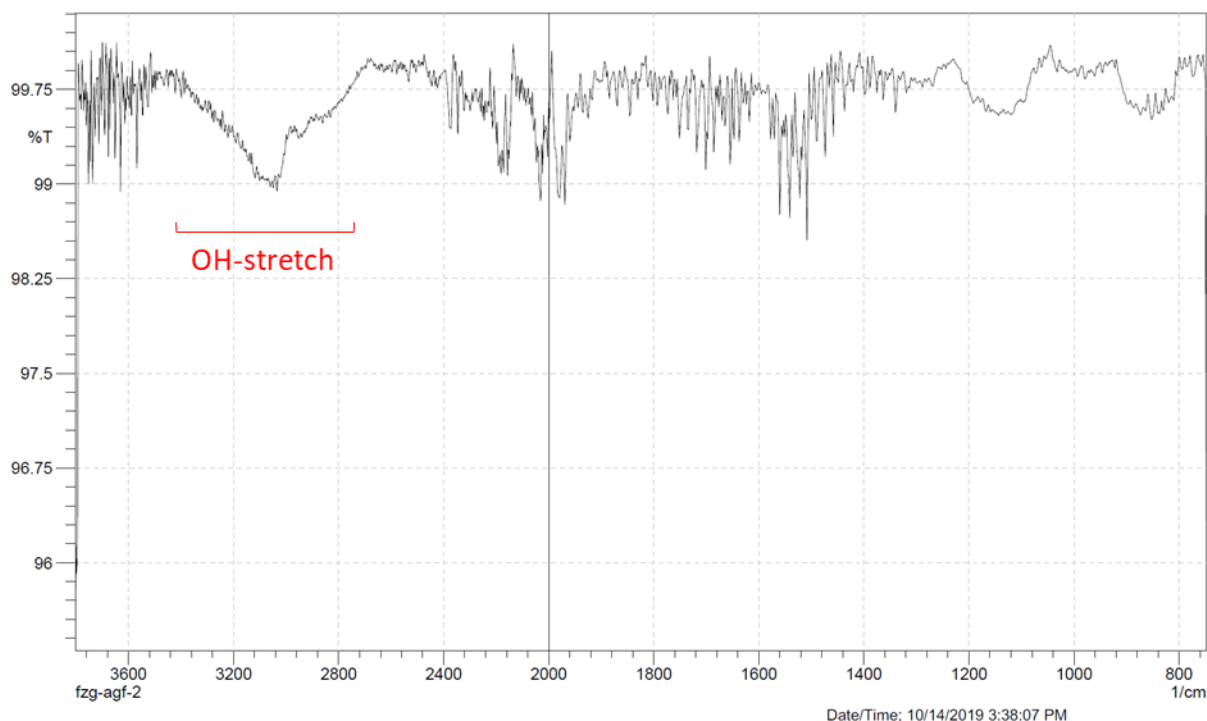
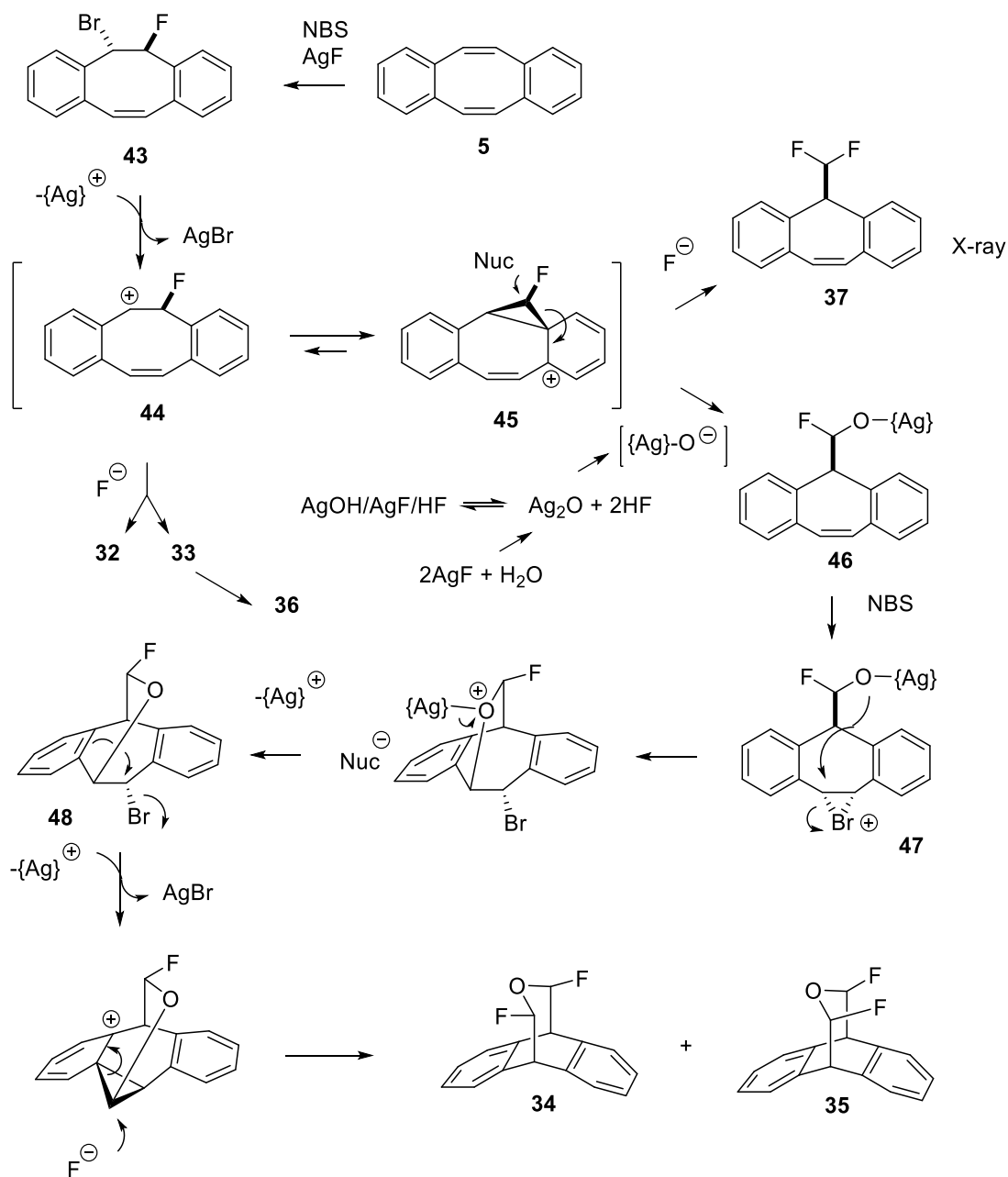


Figure 12. IR spectrum of AgF.

Water may convert AgF to AgOH and HF, and may even progress further to Ag₂O and HF. In another experiment, Ag₂O was added to the reaction in place of Ag(I)F, with HF.Pyr, and this had no adverse effect on the efficiency, both ethers were formed. Under these conditions Ag₂O will be converted to AgF. Therefore a mechanistic rationale, based on the observed products is illustrated in Scheme 20.



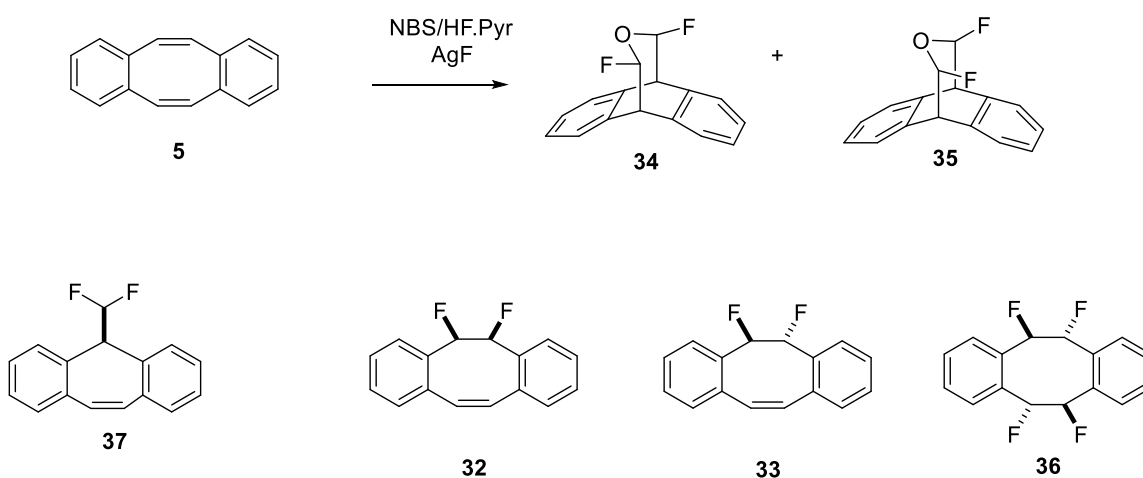
Scheme 20. A proposed mechanism for various products from treatment of **5** with NBS/HF-Py /AgF.

Bromofluorination of the starting material **5** first generates compound **43**, followed by dissociation of the bromide to generate carbocation **44**, which can be trapped by fluoride to give **32** and **33**/or **36**. However this carbocation can rearrange to a more favoured cation **45**, by delocalisation through the phenyl ring, which if attacked by fluoride will generate **37**. The present

water in Ag(I)F would probably form various equilibria between Ag₂O, AgF equivalents and HF. Therefore, the resultant surface bound nucleophilic {Ag}O⁻ equivalent will allow the introduction of oxygen to generate an intermediate generalised as **46**. The transannular reaction is then initiated by the bridging oxygen attacking the second bromine ion, with release of Ag(I) to generate **48**. Finally, a carbocation rearrangement results in the ethers **34** and **35**, respectively.

4.4. Conclusions

The main objective of this chapter was to synthesis all-*cis* tetrafluoro compound **23**. However, the first attempt from the *syn*-diepoxide **24a** proved unsuccessful due to its unusual stability. Another synthetic route from the treatment of benzo[*a,e*]cyclooctatetraene **5** with NBS , HF·Py and AgF generated unexpected results. Solvent influenced the product outcomes of this reaction and a mixture of new compounds were formed (Scheme 21).



Scheme 21. Reaction products.

The formation of products **34**, **35** and **37** clearly indicates that an extensive carbocation/phenonium rearrangements pathway occurred during the reaction, which is significantly different from direct chlorination and bromination. An isotope labelling experiment was conducted by adding [97 atom-%¹⁸O] water into reaction and this generated the ¹⁸O labelled **34** and **35**. This observation is consistent with the Ag(I)F hydrolysis to a {Ag}O- species, as the most likely nucleophile to provide the oxygen atoms to ethers **34** and **35**.

Reference

1. J. A. Soderquist, *J. Org. Chem.*, 1981, **46**, 4599-4600.
2. R. Crabtree, *Acc. Chem. Res.*, 1979, **12**, 331-337.
3. D. R. Anton, R. H. Crabtree, *Organometallics.*, 1983, **2**, 621-627.
4. H. Irngartinger, W.R.K. Reibel, *Acta Crystallogr., Sect. B.*, 1981, **B37**, 1724-1728.
5. N. L. Allinger, J. T. Sprague, *Tetrahedron.*, 1975, **31**, 21-24.
6. L. F. Fieser, M. M. Pechet, *J. Am. Chem. Soc.*, 1946, **68**, 2577-2580.
7. C. E. Griffin, J. A. Peters, *J. Org. Chem.*, 1963, **28**, 1715-1716.
8. T. C. W. Mak, H. N. C. Wong, K. H. Sze, L. Book, *J. Organomet. Chem.*, 1983, **255**, 123-134.
9. S. Chaffins, M. Brettreich, F. Wudl, *Synthesis*, 2002., **9**, 1191-1194.
10. M. Brown, J. D. Zubkowski, E.J. Valente, G. Yang, W. P. Henry, *J. Organomet. Chem.*, 2000, **613**, 111-118.
11. D. R. Anton, R. H. Crabtree, *Organometallics.*, 1983, **2**, 855-859.
12. S. Spiess, C. Welter, G. Frank, J. Taquet, G. Helmchen, *Angew. Chem. Int. Ed.*, 2008, **47**, 7652-7655.
13. P. Zhang, H. Wang, X. Shi, X. Yan, X. Wu, S. Zhang, B. Yao, X. Feng, J. Zhi, X. Li, B. Tong, J. Shi, L. Wang, Y. Dong, *J. Polym. Sci. Pol. Chem.*, 2017, **55**, 716-725.
14. M. Avram, I. G. Dinulescu, D. Dinu, *Tetrahedron*, 1963, **19**, 309-317.
15. T. R. Nauman, M. L. McLaughlin, F. R. Fronczek, S. F. Watkins, *J. Chem., Cryst.*, 1996, **26**, 107-110.
16. H. N. C. Wong, P. J. Garratt, F. Sondheimer, *J. Am. Chem. Soc.*, 1973, **96**, 5604-5605.

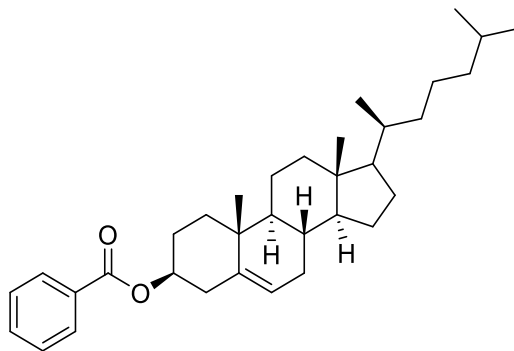
17. M. Schüler, D. O'Hagan, A. M. Z. Slawin, *Chem. Commun.*, 2005, 4324-4326.
18. M. P. Cava, R. Pohlke, B. W. Erickson, J. C. Rose, G. Fraenkel, *Tetrahedron*, 1962, **18**, 1005-1011.
19. J. Perron, A. L. Beauchamp, *Inorg. Chem.*, 1984, **23**, 2853-2869.
20. X. Tao, Y. Li, H. N. Wang, F. Du, Y. Shen, *Polyhedron.*, 2009, **28**, 1191-1195.
21. W. Zhang, J. D. Barry, D. Cordova, S. F. McCann, E. A. Benner, K. A. Hughes, *Bioorg. Med. Chem. Lett.*, 2014, **24**, 2188-2192.

Chapter 5. Liquid crystal containing fluorinated cyclopropanes

5.1. Introduction of liquid crystal

5.1.1 Background of liquid crystal

In 1888, the Austrian chemist Friedrich Reinitze was conducting experiments on cholesteryl benzoate (Figure 1) and trying to establish the correct formula and molecular weight.¹ He noticed that the compound had two melting points. At 145.5°C, the solid crystal melts into a cloudy liquid, and at 178.5°C it melts again and becomes a clear transparent liquid. The phenomenon was reversible. Initially, Reinitze thought this may due to an impurity, but further purification did not change the behaviour.



Cr 145.5 °C N* 178.5 °C I

Figure 1. Cholesterol benzoate.

Unable to explain this strange phenomenon of “double melting”, Reinitze asked help from German physicist Otto Lehmann, who was an expert in crystal optics. Otto Lehmann found that the intermediate cloudy fluid had a unique kind of order, while the transparent liquid had the

disordered state of all common liquids. The new "liquid crystal" state was coined, indicating that it was something between a liquid and a solid, and that it shared important properties of both. ²

5.1.2 Classes of liquid crystals

There are two types of liquid crystal: thermotropic and lyotropic. Lyotropic liquid crystals are the substances which form the liquid-crystal phase when dissolving them in water or other solvents. They are usually made of amphiphilic molecules, where one end of the molecule is hydrophilic, whereas the other end is hydrophobic. A good example is a fatty acid salt such as sodium heptadecanoate shown in Figure 2. ³

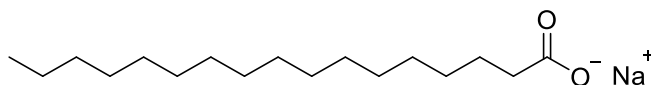


Figure 2. Sodium heptadecanoate.

Thermotropic liquid crystals are substances whose transition phases are determined by temperature. In this case, there are three transition phases: solid, liquid crystal and isotropic liquid. The temperature of the solid–liquid transition is called the melting temperature (T_m) and the temperature of the liquid crystal–isotropic transition is called the elucidation temperature (T_e). According to the structure of the liquid crystalline phase, liquid crystals can be divided into smectic, nematic or cholesteric (Figure 3).³ The smectic phase has the highest level of order, as the molecules have orientational order and partial positional order. There are many different smectic phases, all characterized by different types and degrees of positional and orientational order. The nematic phase is the least ordered phase, as there is no positional order, but there is orientational order, hence it is the most fluid and the least viscous phase. Therefore, it is the

nematic phase that is employed in the vast majority of liquid crystal display formats. Cholesteric liquid crystals are formed from chiral molecules extending from the original cholesterol benzoate observation. Therefore, the cholesteric phase exhibits chirality. In this phase, the molecules are ordered into layers and within each layer they are ordered in the same direction. Each layer is rotated by a defined angle relative to the adjacent layers, resulting in a helical assembly. These liquid-crystalline phases are usually identified using a polarising optical microscope (POM) in conjunction with differential scanning calorimetry (DSC).

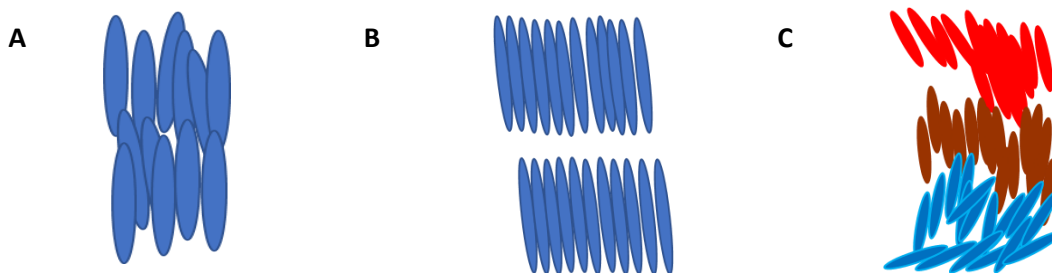


Figure 3. Liquid crystal phases. **A.** Nematic, **B.** Smectic and **C.** Cholesteric.

5.1.3 The structure of liquid crystals

The most common type of thermotropic liquid crystals are calamitic liquid crystals.⁴ Its typical rod-like structure with a high length to breadth ratio is illustrated in Figure 4.

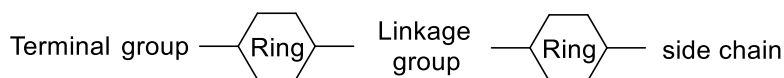


Figure 4. The template for calamitic liquid crystals.

The presence of rings provides the backbone of the liquid crystal and also affects its properties. Usually at least two rings are needed to generate the liquid crystal phase. Some typical ring structures are 1,4-disubstituted benzene rings, *trans* 1,4-disubstituted cyclohexane, 2,6-

disubstituted naphthalene and so on. The chemical stability of liquid crystals, their resistance to e.g. moisture or ultraviolet radiation, depends strongly on the central linkage. Some typical linkages are C=C, CF₂O-, COO- and so on. The side chain is usually a long linear hydrocarbon chain, since it can strongly influence the viscosity and the transition temperature of the liquid crystal phases. The terminal group is mostly used to determine the dielectric constant and its anisotropy. Some typical terminal groups are CN, F, and NCS, as illustrated in Figure 5.

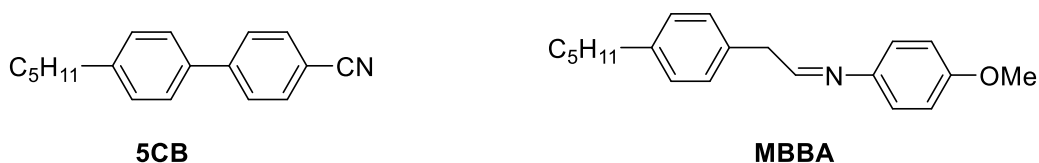


Figure 5. Examples of calamitic liquid crystals.

5.2 The properties of liquid crystals

5.2.1 Optical anisotropy of a liquid crystal

Like many other uniaxial crystals, liquid crystals are birefringent. They have two principal refractive indices, n_e and n_o . The ordinary refractive index (n_o) is for light where the electric vector is perpendicular to the optical axis, and the extraordinary refractive index (n_e) is for light where the electric vector is parallel to the optical axis. Therefore the birefringence is given by:

$$\Delta n = n_e - n_o$$

If $n_e > n_o$, the liquid is said to have a positive birefringence, if $n_e < n_o$, then it has a negative birefringence. Usually, most liquid crystals have positive birefringence ranging from 0.05-0.45.⁴ Materials containing aryl rings usually give higher Δn value than materials containing saturated alicyclic rings (Figure 6) due to their polarizability.



Figure 6. Liquid crystals with different birefringence.

5.2.1 Dielectric anisotropy of a liquid crystal

Because a liquid crystal is uniaxial, it will have different dielectric constants when an external electric field is applied. The dielectric anisotropy is defined as:

$$\Delta\epsilon = \epsilon_{//} - \epsilon_{\perp}$$

When an external electric field is applied parallel to the long axis of the liquid crystal, the dielectric constant is termed $\epsilon_{//}$. On the contrary, ϵ_{\perp} is when the electric field is perpendicular to the long molecular axis. Therefore, liquid crystals can be divided into two types; positive dielectric anisotropy and negative dielectric anisotropy liquid crystals. The positive dielectric anisotropy liquid crystal molecule will orient itself parallel to the electric field. In other words, the dipole moment is parallel to the long axis of the liquid crystal. Whereas the negative dielectric anisotropy liquid crystal will orient itself vertically to the electric field (Figure 7).

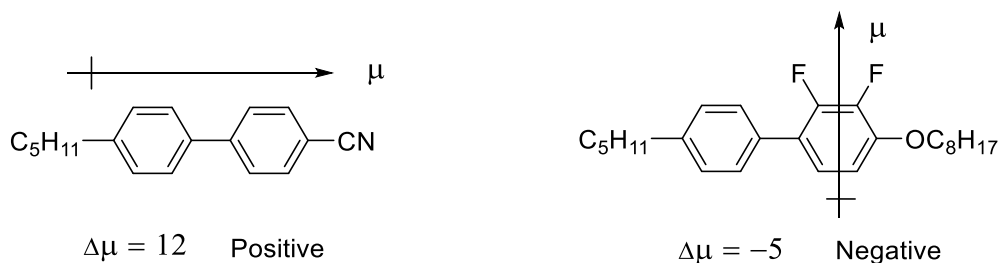


Figure 7. Positive and negative dielectric anisotropy liquid crystals.

5.3 Applications of liquid crystals

Liquid crystals with negative dielectric anisotropy have attracted attention recently due to the development of the vertical alignment (VA) LCD technology. Figure 8 shows VA and twisted nematic (TN) display technology.^{5,6.}

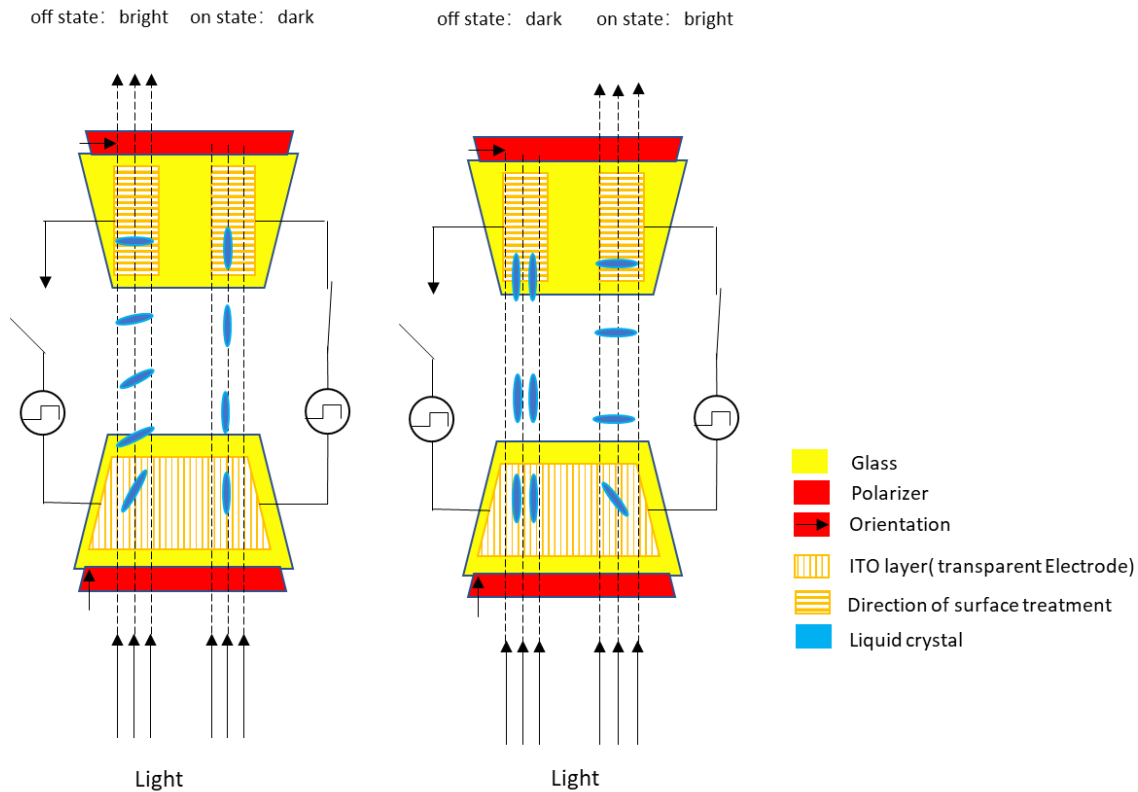


Figure 8. Liquid crystal display. a) TN display technology. b) VA display technology.

As is illustrated in Figure 8, the direction of surface treatment at the top and bottom glass of the device are oriented 90° to each other. In the TN displays, liquid crystal molecules are twisted 90° between the two glass ends. When no voltage is applied, the polarized light from the bottom passes through the liquid crystals, and is twisted by 90° , in order to pass through the top polarizer to create a bright state (this is also called the 'normal white mode'). When an external electric

field is applied, the liquid crystals align themselves parallel to the electric field, therefore light is blocked by the top polarizer, and it shows a black state (black mode).

However, in VA displays, at the beginning, since liquid crystal molecules align perpendicular to the substrates, light passes through the liquid crystalline molecules without a change in polarization and it is blocked by the top polarizer, creating a black mode when no voltage is applied. When a voltage is applied, the liquid crystal molecules rotate vertical to the electric field due to their negative dielectric anisotropy and this allows light to pass through.

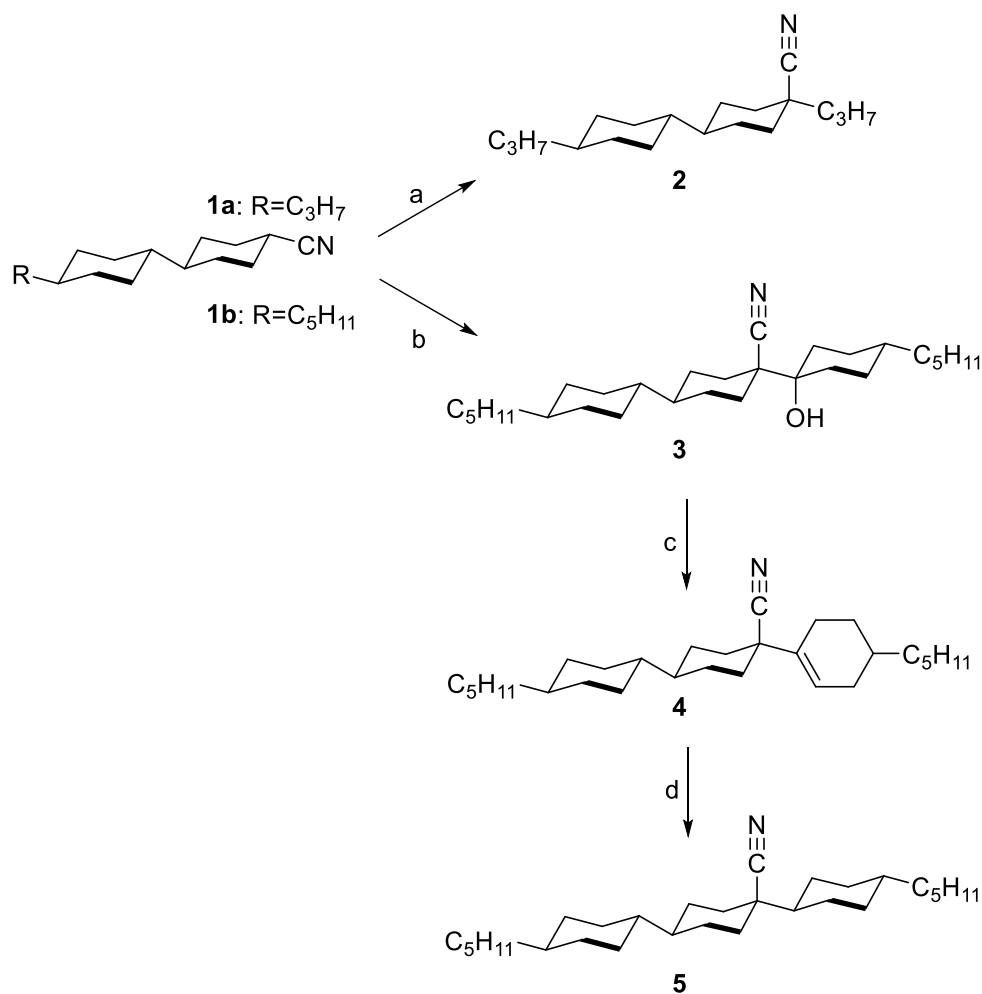
By comparison with the traditional TN displays, VA displays have many advantages. Firstly, light is almost completely blocked by VA displays (1 % leakage, whereas there is 5 % light leakage in a TN display), and VA panels can achieve higher contrast ratios. Secondly, VA panels can also have faster response speeds because the LC molecules are simply switched between the vertical and horizontal alignments. Last but not least, LC molecules are either vertical or horizontal within the VA display. This results in a wider viewing angle than found in a TN display because LC molecules are not completely perpendicular in TN display. Due to these advantages, VA display technology has been widely used in PC monitors, laptops and TV screens, and negative dielectric anisotropy liquid crystals are in demand.

5.4 Negative dielectric anisotropic liquid crystals

In order to prepare a negative dielectric anisotropic liquid crystal, a polar group is required perpendicular to the long axis of the molecule. There are several types of this kind liquid crystal.

5.4.1 Nitrile group in a perpendicular orientation

As the nitrile group has a large dipole moment, it is quite easy to achieve high negative dielectric anisotropy by placing a nitrile perpendicular to the molecule axis. In fact, this type of system is the earliest liquid crystal with negative dielectric anisotropy. The synthesis of some typical structures are shown in Scheme 1.^{7,8}

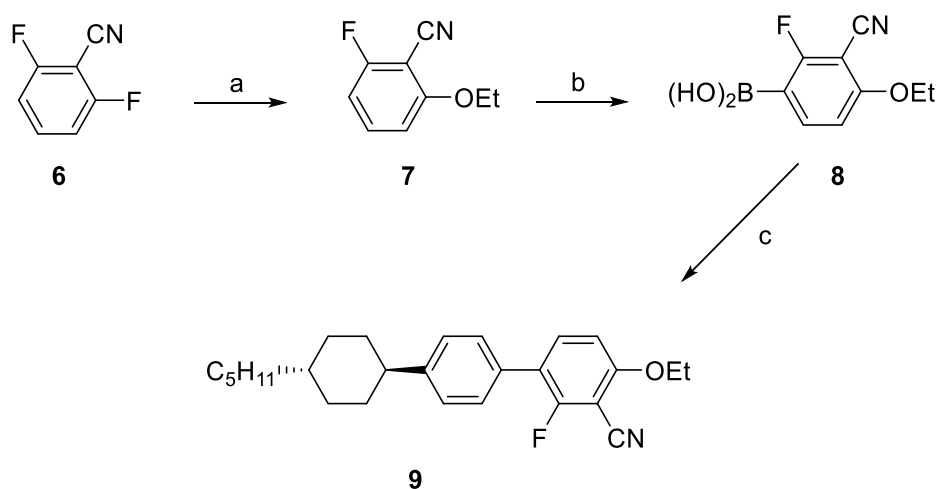


Scheme 1: Synthesis of liquid crystals carrying a perpendicular nitrile group: a) 1. LDA, THF, -25 °C; 2. C₃H₇Br; b) 1. LDA, THF, -25 °C; 2. 4-pentylcyclohexanone, -25 °C; c) H₂SO₄, toluene. d) Pd-C, ethyl acetate.^{7,8}

The resulting materials **2** and **5** have $\Delta\epsilon$ values of -8.2 and -4.7, respectively. However, the cyano group has some bad consequences, such as high viscosity, low solubility and so on. Therefore, alternative structures require to be explored.

5.4.2 2,3-Disubstituted phenyl unit

2,3-Disubstituted phenyl groups are most widely used to generate dielectrically negative liquid crystals. The most obvious is again to incorporate nitrile groups. However, as discussed, this is not optimal. Therefore, refinement of the concept led to the replacement of a cyano group by a fluorine atom. A route to prepare this type of molecule is shown in Scheme 2.⁸

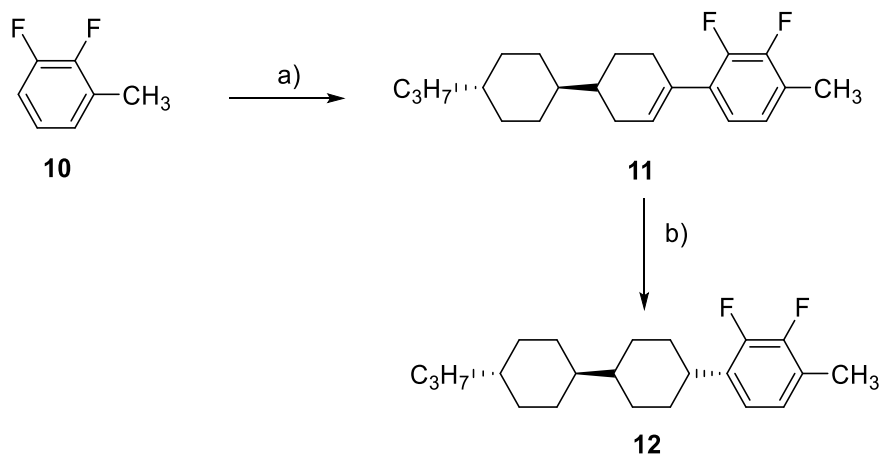


Scheme 2. Synthesis of **9**. a) NaOEt, THF, rt; b) 1. LDA, THF, -70°C; 2. B(OMe)₃, -70°C to rt; 3. HCl; c) (4-Bromophenyl)pentylcyclohexane, Pd(PPh₃)₄, Na₂CO₃, toluene, reflux.⁸

Even though the properties of fluorocyanobenzene derivatives are significantly improved in comparison to the dicyano motif, they still suffer from poor solubility and high viscosity. Therefore, replacement of the second cyano group by fluorine is obvious. Liquid crystals with a

2,3-difluorobenzene unit are the most widely used materials in display applications currently.

The general route to these systems is shown in Scheme 3.⁹



Scheme 3. Synthesis of 2,3-difluorobenzene liquid crystals. a) 1. n-BuLi, -70°C ; 2. *trans*-4-propylbicyclohexane-4'-one, -70°C to rt; 3. TsOH, xylene; b) Pd-C, H_2 , THF, rt.⁹

More recently, the trifluoromethyl group was developed to replace one of the fluorines in order to achieve a higher $\Delta\epsilon$ value,¹⁰ due to an increased dipole moment. An example is shown in Figure 9.

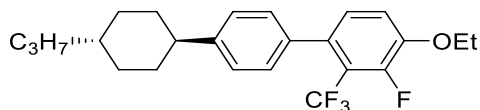
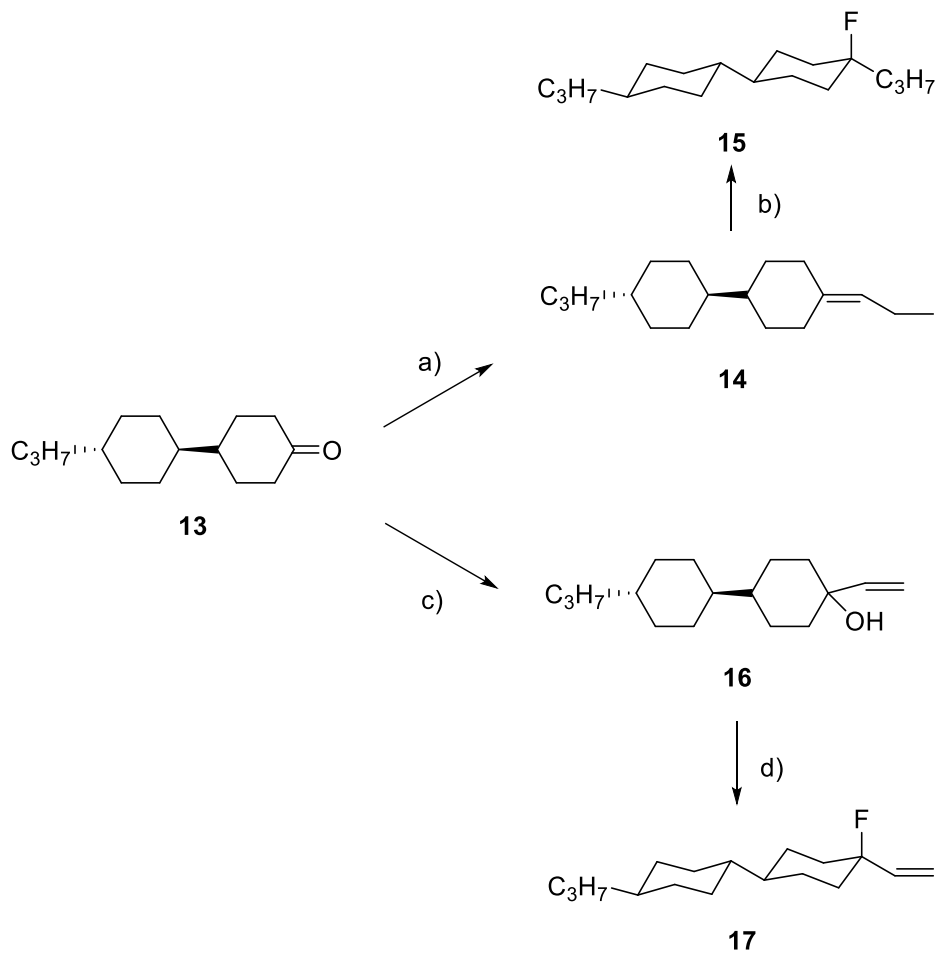


Figure 9. Negative dielectric anisotropic liquid crystal containing a trifluoromethyl group.¹¹

5.4.3 Axially fluorinated cyclohexane unit

Even though difluorobenzene derivatives are the only class of materials used in the market now, there are still two main problems. They have high viscosity and low clearing temperatures. Based on the same concept, the alternative way to explore new structures is to incorporate fluorine

atoms orientated axial on a cyclohexane instead of cyano groups. A synthetic route to this type of molecule is shown in Scheme 4.¹²

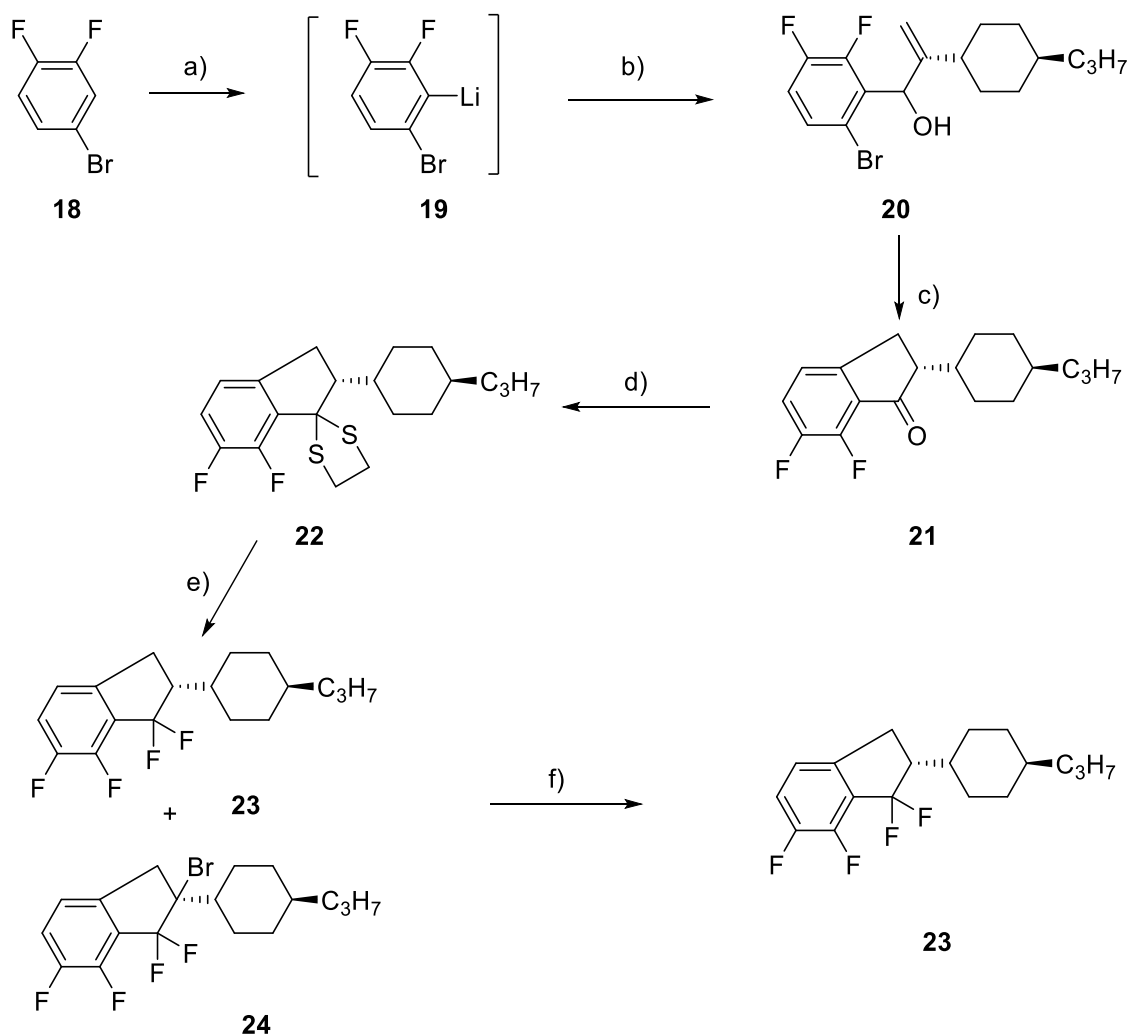


Scheme 4. Synthesis of fluorobicyclohexane **15** and **17**. a) C₂H₅CH₂PPh₃⁺Br⁻, KOtBu, THF, -10°C to rt; b) Hf/Py, CH₂Cl₂; c) CH₂=CHMgBr, THF, rt to 60°C; d) DAST, CH₂Cl₂, rt.¹²

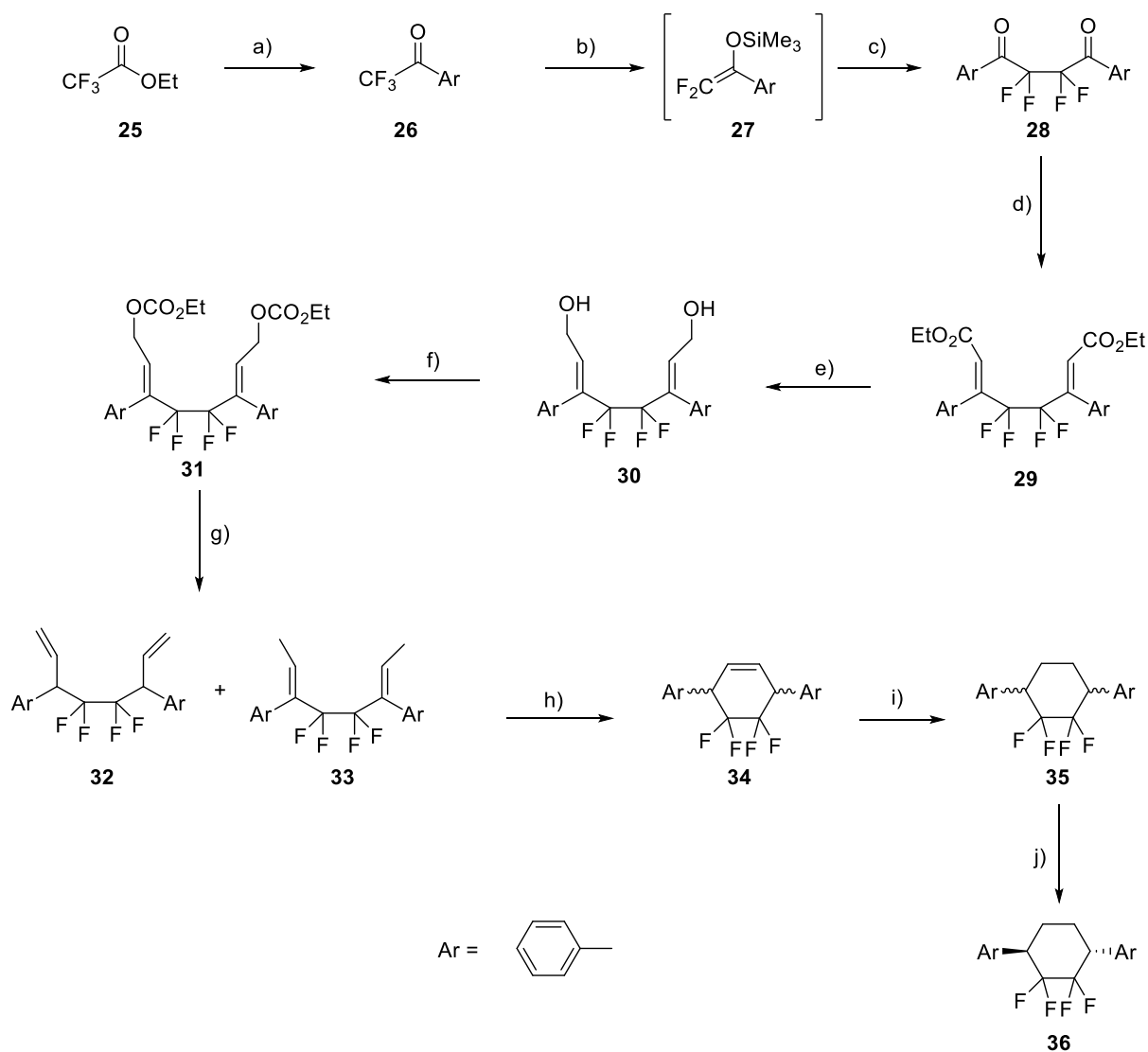
Liquid crystal materials such as **17** are relatively easy to prepare and they show a wide nematic mesophase in combination with low viscosity. However, these materials have never been adopted as commercial liquid crystals because the tertiary fluorine is not stable and can eliminate HF spontaneously.

5.4.4 Tetrafluoroindane and tetrafluorocyclohexane liquid crystals

Two new classes of liquid crystal based on tetrafluoroindane and tetrafluorocyclohexane skeletons have been developed recently to generate negative dielectronic anisotropy. The synthesis of these liquid crystals is shown in Scheme 5 and Scheme 6.^{13,14}



Scheme 5. Synthetic route to tetrafluoroindanes **23**. a) LDA, -70°C ; b) α,β -Unsaturated aldehyde; c) NEt_3 , $[(o\text{-tolyl})_3\text{P}]_2\text{Pd(II)Cl}_2$, 87°C , MeCN; d) BF_3 , $\text{HSCH}_2\text{CH}_2\text{SH}$, CH_2Cl_2 . e) DBH, HF/Py, CH_2Cl_2 . f) 1. DBU; 2. H_2 .¹³



Scheme 6. Synthetic route to tetrafluorocyclohexane **36**. a) ArMgBr, THF, -78°C; b) Mg, Me₃SiCl, THF, 0°C; c) Cu(OTf)₂, MeCN, rt; d) (EtO)₂P(O)CH₂CO₂Et, NaH, THF. e) DiBAL-H, CH₂Cl₂; f) ClCO₂Et, Py, CH₂Cl₂; g) Pd₂(dba)₃·CHCl₃, PPh₃, HCO₂⁻NEt₃H⁺, DMF; h) Grubbs 2nd, CH₂Cl₂; i) H₂, Pd-C; j) Recrystallization.¹⁴

Even though these materials are ideal candidates for negative dielectric liquid crystals, they are rather challenging to prepare.

5.5 Aims and objectives

The aspect of the project aimed to develop new materials for the vertical alignment (VA) display mode. This requires the design of new negative dielectric liquid crystals. To date, there are several types of liquid crystals, which show negative dielectric anisotropy as mentioned above, however, several issues, such as the stability or complexity in synthesis, limits their practical applications. Therefore, it is highly desirable to develop novel easily accessible liquid crystal candidates with negative dielectric anisotropy. Therefore, we designed four liquid crystal candidates containing fluorinated cyclopropanes, as illustrated in Figure 10, anticipating they may show negative dielectric anisotropy.

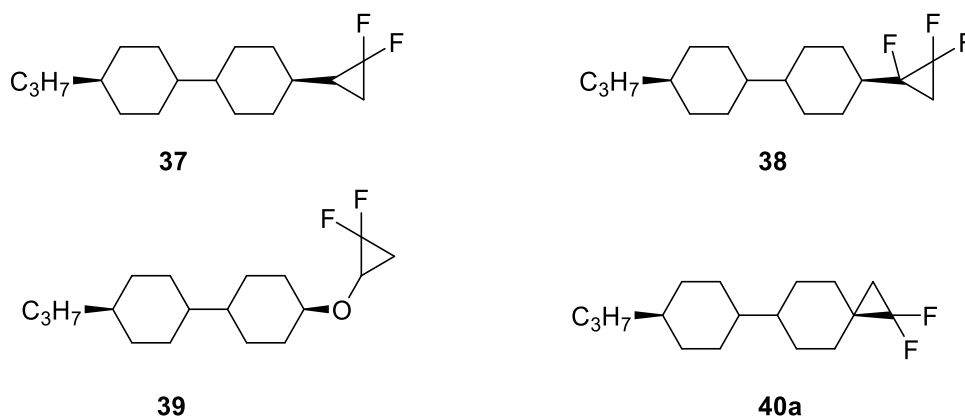
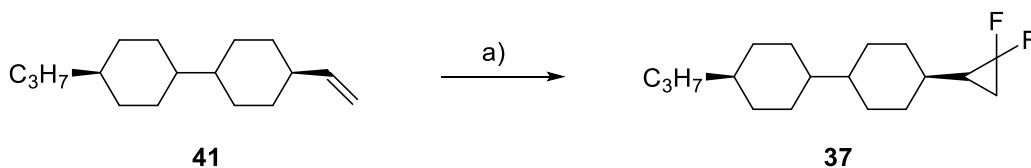


Figure 10. Liquid crystal candidates **37-40a**.

Based on our previous work, the synthesis of difluorinated and trifluorinated cyclopropanes is straightforward. If compounds **37-40a** really show negative dielectric anisotropy, they can be easily prepared. A cyclopropane with geminal fluorines has a large dipole moment, therefore, compound **37** was designed firstly by introducing a geminal difluorocyclopropane motif, anticipating that the polar CF₂ group will point perpendicular to the molecular axis. If this idea

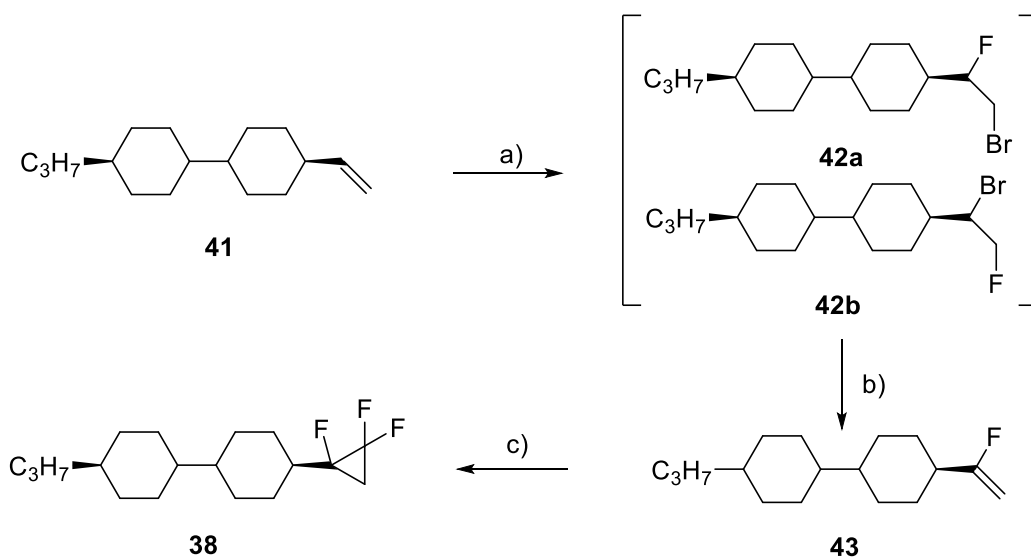
proved to be correct, then adding another fluorine to the equatorial position of cyclohexane ring will continue to increase negative polarity. With this in mind, compound **38** became a target. In addition to fluorine, polarity can also be provided by the alkoxy group and hence compound **39** was envisaged. However, due to the free rotation of the C-C bond, the absolute dielectric anisotropy may be reduced. With this in mind, a fixed spiro compound **40a** was finally designed. Therefore, the aim of Chapter 5 is to synthesise these target liquid crystals and evaluate their physical properties. The analysis of these materials was carried out at Merck LCD, in Darmstadt, Germany.

5.6 Results and discussion



Scheme 6. Synthesis of compound **37**. *Reagents and conditions:* a) TMSCF_3 , NaI, THF, Reflux, 55%.

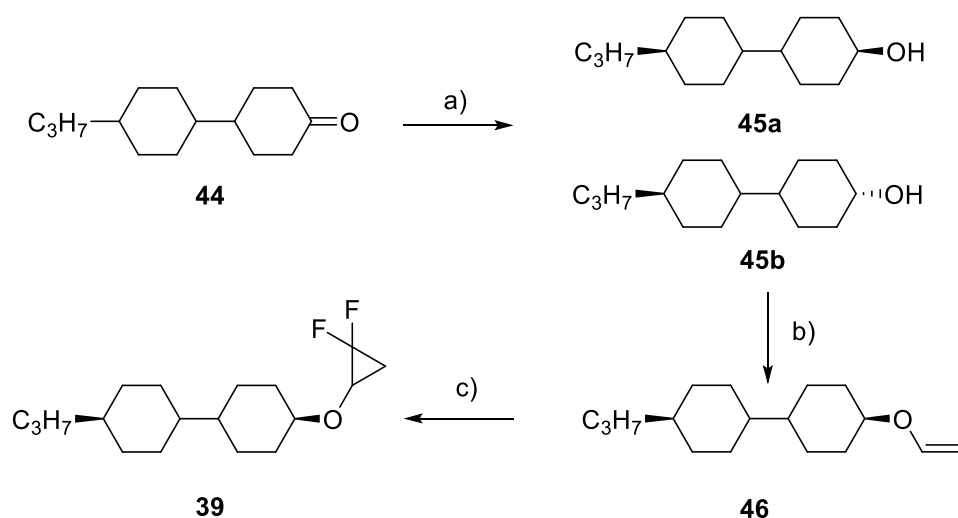
The synthesis of cyclopropane **37** started from olefin **41** (supplied by Merck & Co.), as illustrated in Scheme 6. Difluorocyclopropane **37** can be directly prepared through a [2+1] carbene cycloaddition reaction. Thus, treatment of **41** with the Ruppert-Prakash reagent and sodium iodide under refluxing conditions gave the corresponding product **37** in a 55% yield.¹⁵



Scheme 7. Synthesis of compound **38**. *Reagents and conditions:* a) NBS, HF·Py, DCM; b) *t*-BuOK, DCM, 42% in two steps; c) TMSCF₃, NaI, THF, Reflux, 46%.

The synthesis of trifluorocyclopropane **38** is shown in Scheme 7. Compound **38** was prepared through bromofluorination of **41**, followed by HBr elimination, and then carbene addition to generate **38**. The starting olefin **41** was exposed to an excess of NBS and HF·Py to generate the mixture of regioisomers **42a** and **42b** with a ratio of 4 : 1. After column chromatography, the desired isomer **42a** was isolated. Subsequently addition of potassium *t*-butoxide into a solution of **42a** in DCM efficiently generated the corresponding fluorinated olefin **43** in a 42% yield. Finally, difluorocarbene (:CF₂) addition reaction was repeated to give the final product **38** in a 46 % yield.

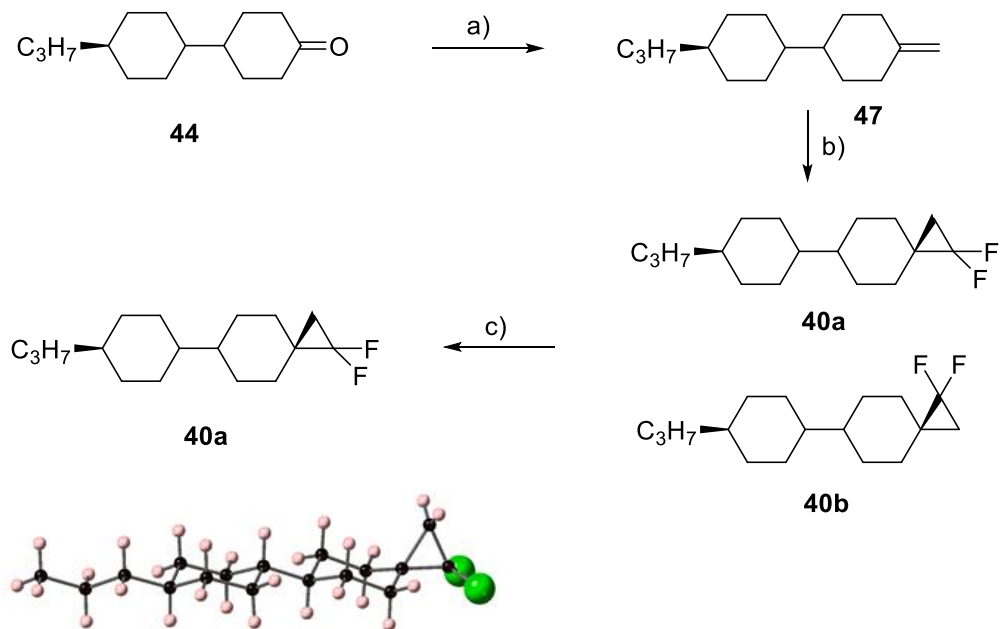
The synthesis of liquid crystal candidates **39** and **40** started from ketone **44** (supplied by Merck & Co.). The synthesis of **39** was carried out as illustrated in Scheme 8.



Scheme 8. Synthesis of compound **39**. *Reagents and conditions:* a) NaBH₄, MeOH, RT, 45%; b) C₄H₉OCH=CH₂, Pd(TFA)₂, BPhen, Et₃N, 75 °C, 62%; c) TMSCF₃, NaI, THF, reflux, 50%.

Reduction of cyclohexanone **44** with NaBH₄, gave cyclohexanol **45** in a ratio of 2 : 1. The major *trans* compound **45a** was purified by column chromatography and was recovered in 45% yield. Vinyl ether **46** was prepared efficiently using the methodology developed by Martin.¹⁶ Thus treatment of **45a** with butyl vinyl ether, BPhen and Et₃N using palladium(II) trifluoroacetate as the catalyst gave **46** in 62% in a single step. Finally, a typical difluorocyclopropanation reaction using the Ruppert Prakash reagent generate compound **39** in 50% yield.¹⁵

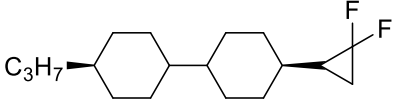
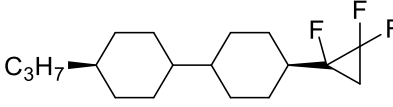
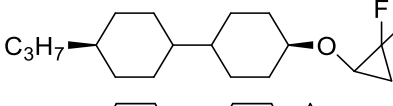
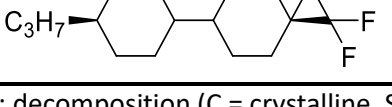
The route to the spiro ring liquid crystal **40** is shown in Scheme 9. Ketone **44** was treated with the appropriate Wittig reagent, which efficiently generated methylene cyclohexane **46** in a 72% yield. This olefin was then subject to a difluorocarbene reaction using TMSCF₃ and NaI¹⁵ and generated the two diastereoisomers, **40a** and **40b**, in a ratio of 5 : 1. After three recrystallizations, the pure diastereoisomer **40a** was recovered. The X-ray structure of compound **40a** confirmed its stereochemistry.



Scheme 9. Synthesis of compound **40a**. *Reagents and conditions:* a) $\text{PPh}_3\text{CH}_3\text{Br}$, $t\text{-BuOK}$, Ether, 0°C -RT, 72%; b) TMSCF_3 , NaI, THF, reflux; c) Recrystallization, 27 %.

With these materials in hand, attention focused on evaluation of their thermodynamic and physical properties, such as birefringence (Δn), dielectric anisotropy ($\Delta\epsilon$) and rotational viscosity (γ). This data was determined by Dr. Matthias Bremer and Peer Kirsch at Merck & Co. By using DSC and POM to measure their thermodynamic behaviour, liquid crystals **37** and **38** were observed to exhibit smectic phases. The smectic phase of LC **37** held over a broad temperature range ($54\text{-}84^\circ\text{C}$), whereas **39** and **40a** only showed a melting point and were not liquid crystalline (Table 1).

Table 1. Phase transfer temperatures of compound **37-40a**.

		Phase transfer temperature/°C
	37	C 54 S _m B 84 I
	38	? S _m B 82 I ^[a]
	39	C35 I ^[a]
	40a	C 42 I

a: decomposition (C = crystalline, S_mB = smectic B, I = isotropic).

The electro-optical properties of LC **37-40a** are summarised in Table 2.

Table 2. Physical properties of compounds **37-40a**.

Compound	Δn	$\Delta \epsilon$	Υ (mPa/s)
37 ^[a]	0.056	-0.5	138
38 ^[b]	0.056	-0.2	228
39 ^[b]	0.063	1.3	178
40a ^[a]	0.036	4.8	-----

[a] Δn , $\Delta \epsilon$ and Υ were extrapolated from a 10 wt% solution in liquid crystal mixture Merck ZLI-4792 + Merck ZLI-2857.

[b] Δn , $\Delta \epsilon$ and Υ were extrapolated from a 10 wt% solution in liquid crystal mixture Merck ZLI-4792 + 10 wt% in Merck ZLI-2857.

Data in Table 1 and 2 was recorded by Merck & Co.

The birefringence Δn for compounds **37-40** was measured using an Abbe refractometer. In all cases the Δn values were low, this is consistent with these liquid crystal core structures, which do not have polar aromatic rings. Comparing **37**, **38** and **39**, the differences in Δn were found to be small, suggesting a substitution pattern within the structures which did not significantly affect Δn , whereas the spiro cyclopropane ring directly connected to the core structure, decreased Δn , in the case of compound **40a**.

Dielectric anisotropy is an important parameter which is related to the driving voltage of LCDs. In order to reduce energy consumption, a large dielectric anisotropy is always required. Compounds **37** and **38** were found to exhibit the expected negative $\Delta\epsilon$ values (**37** = -0.5, **38** = -0.2), however the overall polarity is too low. This low $\Delta\epsilon$ value is presumably due to the C-C bond attached to cyclopropane, which enables rotation. Comparing the $\Delta\epsilon$ for **37** and **38**, it is clear that incorporation of the third fluorine lowers the $\Delta\epsilon$ value. This can be explained by a resultant decreasing the dipole moment (μ_{\perp}) along the minor axis. When an ether was used as the linkage in compound **39**, the liquid crystal became more flexible and overall the $\Delta\epsilon$ became more positive. However, changing the core structure to the more rigid spiro structure, brought about a dramatic enhancement of the molecular dipole moment ($\mu_{//}$), resulting in a more positive and increased $\Delta\epsilon$.

Computational study

Density functional theory (DFT) optimisation at the B3LYP-D3/6-31+G(d,p) level was performed to model the minimum energy structures of candidate LC **37-40a**. These structures are illustrated in Figure 11. From the direction of the dipole moment vector, it is clear that **37** has a negative $\Delta\epsilon$ whereas **40a** has a positive $\Delta\epsilon$. This is consistent with the result obtained from experiment. However, for minimum energy structure of compound **38**, the $\epsilon_{//}$ value is slightly higher than that of ϵ_{\perp} , so it has an almost neutral $\Delta\epsilon$, which is an acceptable result comparing to the actual result (-0.2). whereas for compound **39**, it showed an opposite result with the negative $\Delta\epsilon$. The reason for this result maybe because in reality, in order to get $\Delta\epsilon$ value, liquid crystal will usually mix together with other components which may change its actual conformation in mixture.

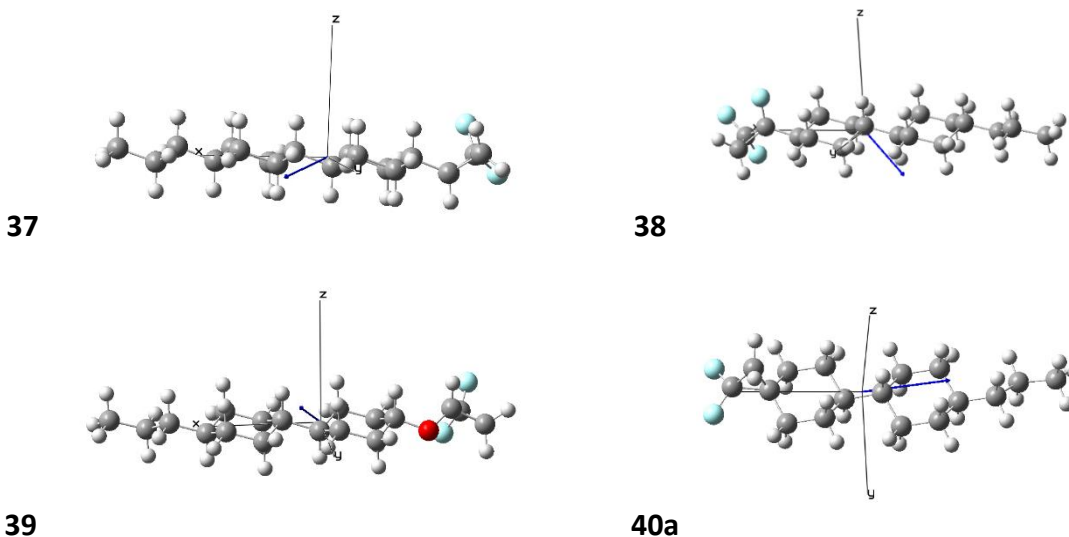


Figure 11. DFT calculation of minimum energy structures of **37-40a**. The blue arrow represents molecular the dipole moment vector.

Another important parameter is the LCD response time. This is related to the rotational viscosity of the liquid crystal. The rotational viscosity values for compounds **37**, **38** were 138 and 228 mPa/s, respectively. The difluorocyclopropane ether LC **39** has a lower rotational viscosity (178 mPa/s) compared to LC **38**. These results clearly indicated that adding fluorine to the terminal group leads to an increase in the viscosity.

5.7 Conclusions

In Chapter 5, a series of novel liquid crystals with fluorinated cyclopropane motifs at their termini were prepared in a straightforward manner. After evaluation of their physical properties, LC **39** and **40a** only showed a melting point. Despite this, these non-LC compounds, can still be viewed as potential candidates for devices, because multiple component mixture systems are widely used in practical application devices to meet specific requirements. Both compounds **37** and **38** exhibited smectic phases and a negative dielectric anisotropy and **37** had the lowest viscosity.

This compound has potential to be used or developed as a material for vertical alignment mode displays. The relatively high positive dielectric anisotropy of compound **40**, also met the key requirement for use in in-plane switching modes, a mode that needs liquid crystals with strong positive dielectronic anisotropy. Although none of the compounds met all the criteria, the study gives an insight into the potential for fluorinated cyclopropane motifs in liquid crystal.

Reference

1. F. Reinitze, *Monatshefte für Chemie (Wien)*., 1888, **9**, 421-44.
2. O. Lehmann, *Zeitschrift für Physikalische Chemie*., 1889, **4**, 462-72.
3. P. Collings, M. Hird, *Introduction to Liquid Crystals: Chemistry and Physics*, Taylor & Francis London, 1997.
4. N. Boden, R. C. Borner, R. J. Bushby, A. N. Cammidge, M. V. Jesudason, *Liquid Crystals*., 1993, **15**, 851.
5. K. Ohmuro, S. Kataoka, T. Sasaki, Y. Koike, *SID Symposium Digest Tech Papers*., 1997, **28**, 845.
6. NXP Semiconductors. <http://www.nxp.com/docs/en/user-guide/UM10764.pdf>. (accessed November 2019).
7. R. Eidenschink, G. Haas, M. Römer, B. S. Scheuble, *Angew. Chem.*, 1984, **23**, 147.
8. P. Kirsch, V. Reiffenrath, M. Bremer, *Synlett*., 1999, **4**, 389-396.
9. *US Pat.*, US2017240809A1, 2017.
10. F. Mongin, R. Maggi, M. Schlosser, *Chimia*., 1996, **50**, 650-652.
11. P. Kirsch, M. Bremer. *Angew. Chem. Int. Ed.*, 2000, **39**, 4216-4235.
12. P. Kirsch, *Liq. Cryst.*, 1999, **3**, 449-452.
13. M. Bremer, L. Lietzau, *New. J. Chem.*, 2005, **29**, 72-74.
14. S. Yamada, S. Hashishita, H. Konishi, Y. Nishi, T. Kubota, T. Asai, T. Ishihara, T. Konno, *J. Fluor. Chem.*, 2017, **200**, 47-58.
15. C. J. Thomson, Q. Zhang. N. Al-Maharik, M. Bühl, D. Cordes, A. Z. Slawin, D. O'Hagan. *Chem. Comm.*, 2018, **54**, 8415-8418.
16. M. Bosch, M. Schlaf, *J. Org. Chem.*, 2003, **68**, 5225-5227.

Chapter 6. Experimental

6.1 General experimental

Air and moisture sensitive reactions were carried out under an atmosphere of argon in flame-dried glassware. Room temperature (RT) refers to 18-25°C. All evaporations and concentrations were performed under reduced pressure (*in vacuo*). All chemicals were purchased from Sigma Aldrich UK, Fluorochem, Apollo, Manchester Organics, Acros, Alfa Aesar, Fisher Scientific, Tokyo Chemical Industry UK Ltd or Merck and were used without further purification, unless stated otherwise. Anhydrous solvents (Et₂O, THF, CH₂Cl₂, Toluene) were obtained from MBraun MB SPS-800 solvent purification system by passage through two drying columns and dispensed under an argon atmosphere. Triethylamine and pyridine were distilled from KOH and stored over KOH. Brine refers to sat. aq. sodium chloride solution. Petroleum ether refers to the fraction with a boiling point between 40-60°C. Acetonitrile HPLC grade was bought from Fisher Scientific.

Thin layer chromatography and column chromatography

Reactions were monitored by thin-layer chromatography (TLC) using aluminium plates coated with silica gel (60 F₂₄₅ Merck). TLC plates were examined under UV light (254 nm and 266 nm) before being stained by alkaline potassium permanganate or ninhydrin solutions and developed by heating. Column chromatography was performed on Merck Geduran silica gel 60 (250-400 mesh) under a positive pressure of compressed air eluting with solvents (reported as v/v) as supplied.

Purification by HPLC

HPLC analysis were performed using a Shimadzu Prominence (SIL-20A HT autosampler, CL-20AT ternary pump, DGU-20A3R solvent degasser, SPD 20A UV detector and CMb-20A controller module) with reverse phase column (Phenomenex Luna C18 (250 × 10.00 mm, 5 μ). All solvents used were HPLC grade and were degassed prior to use by bubbling nitrogen through the solvents. Samples were freeze dried from frozen solutions in H₂O in a Christ Alpha 1-2 LO Plus freeze drier.

NMR

All NMR spectra were recorded on a Bruker Avance III 500, Bruker Avance II 400, Bruker Avance 300 or 500 spectrometers. Deuterated solvent was used as the internal deuterium lock for ¹H and ¹³C NMR spectra. ¹H NMR spectra were recorded at either 300, 400 or 500 MHz. ¹³C NMR chemical shifts were reported to one decimal place and spectra were recorded at either 75 MHz, 100 MHz or 126 MHz. ¹⁹F NMR chemical shifts were reported to one decimal place and spectra were recorded at 282, 376 or 470 MHz. Chemical shifts (δ) are reported in parts per million (ppm) and coupling constants (J) are given in Hertz (Hz). For ¹H and ¹³C NMR spectra, the reference point is tetramethylsilane (TMS). ¹⁹F NMR spectra were referenced to CFCl₃ as an external standard. Data processing was carried out using Bruker Topspin or MestReNova. The abbreviations for the multiplicity of the proton, carbon and fluorine signals are as follows: s singlet, d doublet, dd doublet of doublet, ddd doublet of doublet of doublet, t triplet, dt doublet of triplets, q quartet, br s broad singlet. When necessary, resonances were assigned using two-dimensional experiments (COSY, HSQC, HMBC, TOCSY).

1 D selective ^1H , ^{19}F -HONEY NMR was carried out by Dr Tomas Lebl on a Bruker Avance 500 spectrometer. ^{19}F NMR was recorded at multiple temperatures in CD_2Cl_2 on a Bruker Avance 500 spectrometer.

Melting point

Melting points were measured using a Griffin MPA350 or an Electrothermal IA 9100 melting point apparatus and are uncorrected.

Mass Spectrometry

High resolution mass spectra were obtained by electron impact (EI), electrospray ionisation (ESI), chemical ionisation (CI), atmospheric pressure chemical ionisation (APCI), atmospheric solid analysis probe (ASAP). These spectra were obtained by Caroline Horsburgh (University of St Andrews) and the EPSRC National Mass Spectrometry Service Centre, Swansea.

Infrared Spectrometry

Infrared spectra were measured on a Perkin Elmer Spectrum GX FTIR apparatus spectrometer either as KBr pellets, or as a thin film between NaCl plates, or on a Shimadzu IRAffinity-1S spectrometer with a diamond ATR attachment. Absorption Maxima are reported in units of wavenumbers (cm^{-1}).

Single Crystal X-ray Analysis

Single crystal X-ray analysis was carried out by Prof. Alexandra Slawin and Dr. David Cordes, using either a molybdenum or copper X-ray source. The molybdenum system used a MM-007 high-brilliance generator with VariMax optics and either an AFC8/Saturn 70 or an AFC7/Mercury

detector. The copper system used a MM-007 high brilliance generator with an AFC10/Saturn 92 detector. All the published structures have been deposited in CCDC. Please see **Appendix** for the complete account of the crystallographic data. The *cif*. files are included on the attached CD.

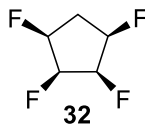
6.2 Compounds preparation for Chapter 2

6.2.1 *cis* 1,2,3,4-Diepoxycyclopentane



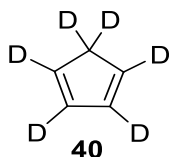
Ozone was bubbled through a solution of triphenylphosphite (14.8 g, 12.5 mL, 47.7 mmol) in dry methylene chloride (150 mL) at -78 °C. When the blue colour of excess of ozone was observed, oxygen was bubbled through the solution until the blue colour has been completely disappeared at maintain temperature. The solution was warmed to -30 °C, stirred for 10 min, then cooled to -78 °C again, and cyclopentadiene (3 g, 3.82 mL, 45.5 mmol) was added and the solution was stirred at the maintained temperature for 1h. Thereafter a solution of RuCl₂(PPh₃)₃ (0.5 g, 0.75 mmol) in methylene chloride (5 mL) was quickly added. The reaction mixture was stirred at -78 °C for 1h, at -40 °C for 0.5h and finally at -25 °C for 1h. Solvent was carefully removed under reduced pressure, and the dark brown residue was subjected to column chromatography (petroleum ether/diethyl ether 1:1) to give the product (1.7 g, 38%) as yellow oil; ¹H NMR (400 MHz, CDCl₃) δ_H 3.74 (2 H, ddd, *J* = 3.0, 1.9, 1.2 Hz, 2CHO), 3.53 (2 H, dd, *J* = 1.9, 1.2 Hz, 2CHO), 2.12 (1 H, d, *J* = 16.3 Hz, CH₂), 1.65 (1 H, dt, *J* = 16.3, 3.0 Hz, CH₂); ¹³C NMR (100 MHz, CDCl₃) δ_c 65.2 (CHO), 52.2 (CHO), 28.4 (CH₂); HRMS (ESI⁺) *m/z* calc. for C₅H₆Na [M+Na]⁺ 121.0259, found 121.0265. Data agreement with the literature.¹

6.2.2 All *cis*-1,2,3,4-tetrafluorocyclopentane



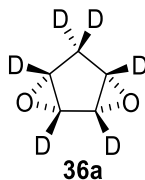
A solution of diepoxide (0.9 g, 9.1 mmol) in $\text{Et}_3\text{N}\cdot 3\text{HF}$ (12 mL, 68.3 mmol) in a Teflon flask was stirred at 120 °C for 24h. The reaction mixture was poured into water (10 mL) and extracted with diethyl ether (20 mL x 3). The combined organic layers were dried over magnesium sulphate, filtered and the solvent was removed under reduced pressure to give a mixture of **37a** and **37b** (2.1 g) in 2:1 ratio. The mixture was dissolved in anhydrous methylene chloride (25 mL), trifluoromethanesulfonic anhydride (15.4 mL, 91.3 mmol) and pyridine (5 mL, 60.9 mmol) were added subsequently under argon atmosphere at 0 °C. After 24h stirring at room temperature, the mixture was extracted with petroleum ether and diethyl ether (150 mL x 3) then filtered. The solvent was removed under reduced pressure to give a mixture of triflates **38a** and **38b** (2.2 g), which was used for reaction without further purification. The triflates and $\text{Et}_3\text{N}\cdot 3\text{HF}$ (8.9 mL, 54 mmol) were placed in a Teflon flask and stirred at 100 °C under argon atmosphere for 48h. The reaction mixture was poured into water (20 mL) and extracted with ether (20 mL x 3). The combined organic extracts were dried over sodium sulfate, filtered, and concentrated under reduced pressure (500 mbar) at room temperature. The residue was purified by silica gel chromatography (petroleum ether/ diethyl ether 3:2) to give the desired tetrafluorocyclopentane (113 mg, 8.7%) as a white solid. **M.p.** = 39-40 °C; $^1\text{H NMR}$ (400 Hz, CDCl_3) δ_{H} 5.12-4.92 (2 H, dm, CHF), 4.93-4.76 (2 H, dm, CHF), 2.74-2.40 (2 H, m, CH_2); $^1\text{H}\{^{19}\text{F}\}$ NMR (400 Hz, CDCl_3) δ_{H} 5.02 (2 H, dddd, $J = 7.4, 4.3, 3.2, 1.8$ Hz, CHF), 4.84 (2 H, dd, $J = 3.2, 1.8$ Hz, CHF), 2.66 (1 H, dt, $J = 16.3, 7.4$ Hz, CH_2), 2.51 (1 H, dt, $J = 16.3, 4.3$ Hz, CH_2); $^{13}\text{C NMR}$ (100 Hz, CDCl_3) δ_{C} 35.9 (t, $J = 23.1$ Hz, CH_2), 87.8 (dm, $J = 195.4$ Hz, CHF), 88.3 (dm, $J = 203.4$ Hz, CHF); $^{19}\text{F}\{^1\text{H}\}$ NMR (376 Hz, CDCl_3) δ_{F} -196.2 (d, $J = 3.2$ Hz, CHF), -219.4 (d, $J = 3.2$ Hz, CHF); $^{19}\text{F NMR}$ (376 Hz, CDCl_3) δ_{F} -196.2 (m, CHF), -219.4 (m, CHF); **HRMS** (ESI⁺) m/z calc. for $\text{C}_5\text{H}_6\text{F}_4\text{Na}$ $[\text{M}+\text{Na}]^+$ 165.0298, found 165.0297.

6.2.3 [²H₆]-Cyclopentadiene



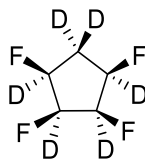
Sodium (15 g, 0.652 mol) was added to D₂O (165 g, 150 mL, 8.25 mol) at a slow rate to keep the temperature below 10 °C. After addition was complete, NaOD/D₂O solution (20 mL) was syringed into a flask containing freshly cracked cyclopentadiene (14 g, 18 mL, 0.214 mol) and Me₂SO (22 g, 20 mL, 0.28 mol) at 0 °C. The mixture was stirred vigorously for 1 h. The resulting layers were separated, and the top layer (cyclopentadiene) was syringed into another flask containing the NaOD/D₂O solution (20 mL) and Me₂SO (22 g, 20 mL, 0.28 mol) at 0 °C. The mixture was again stirred for 1 h, and the layers were separated. This entire procedure was repeated at least for 3 times, at which time the diene was determined by ¹H NMR spectroscopy to be > 99% deuterated. Finally, the [²H₆]-cyclopentadiene (8 mL, 44 %) was obtained. **HRMS** (EI⁺) m/z calcd. for C₅²H₆ [M] 72.0846, found 72.0846. Data agreement with the literature.²

6.2.4 [²H₆]-*cis*-1,2,3,4-diepoxy-cyclopentane



Ozone was bubbled through a solution of triphenylphosphite (6.5 g, 5.5 mL, 20.8 mmol) in dry methylene chloride (150 mL) at -78 °C. When the blue colour of excess of ozone was observed, oxygen was bubbled through the solution until the blue colour has been completely disappeared at maintain temperature. The solution was warmed to -30 °C, stirred for 10 min, then cooled to -78 °C again, and [²H₆]-cyclopentadiene **40** (1 g, 1.2 mL, 13.9 mmol) was added and the solution was stirred at maintain temperature for 1h. Thereafter a solution of RuCl₂(PPh₃)₃ (0.2 g, 0.3 mmol) in methylene chloride (5 mL) was quickly added. The reaction mixture was stirred at -78 °C for 1h, at -40 °C for 0.5h and finally at -25 °C for 1h. Solvent was carefully removed under reduced pressure, and the dark brown residue was subjected to column chromatography (petroleum ether/diethyl ether 1:1) to give the product (0.188 g, 13%) as brown oil. ¹³C NMR (125 MHz, CDCl₃) δ_c 64.9 (t, ¹J_{CD} = 28.6 Hz, CDO), 52.2 (t, ¹J_{CD} = 28.6 Hz, CDO), 27.4 (m, CD₂); HRMS (ESI⁺) m/z calcd for C₅²H₆O₂[M+Na]⁺ 127.0642, found 127.0635.

6.2.5 All *cis*-1,2,3,4-[²H₆]-tetrafluorocyclopentane

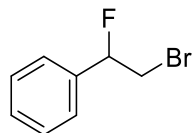


32a

A solution of [²H₆]-diepoxide (0.188 g, 1.8 mmol) in Et₃N·3HF (1 mL, 5.7 mmol) in a Teflon flask was stirred at 120 °C for 24h. The reaction mixture was poured into water (1 mL) and extracted with diethyl ether (10 mL x 3). The combined organic layers were dried over magnesium sulphate, filtered and the solvent was removed under reduced pressure to give a mixture of **37a** and **37b** (0.250 g). The mixture was dissolved in anhydrous methylene chloride (25 mL), trifluoromethanesulfonic anhydride (1.3 mL, 7.6 mmol) and pyridine (0.4 mL, 5.1 mmol) were added subsequently under argon atmosphere at 0 °C. After 24h stirring at room temperature, the mixture was extracted with diethyl ether (10 mL x 3) then filtered. The solvent was removed under reduced pressure to give a mixture of triflates **38a** and **38b** (0.2 g), which was used for reaction without further purification. The triflates and Et₃N·3HF (1 mL, 5.7 mmol) were placed in a Teflon flask and stirred at 100 °C under argon atmosphere for 48h. The reaction mixture was poured into water (20 mL) and extracted with ether (20 mL x 3). The combined organic extracts were dried over sodium sulphate, filtered, and concentrated under reduced pressure (500 mbar) at room temperature. The residue was purified by silica gel chromatography (petroleum ether/diethyl ether 3:2) to give the desired [²H₆]-tetrafluorocyclopentane (18 mg, 6.7%) as a white solid. **M.p.** = 39-40 °C; **²H NMR** (76 MHz, CHCl₃) δ_D 5.01-4.60 (4 D, m), 2.62-2.28 (2 D, m); **¹⁹F {¹H} NMR** (376 Hz, CDCl₃) δ_F -197.7 (br, CHF), -220.5 (br, CHF); **¹³C NMR** (125 MHz, CDCl₃) δ_C 88.2 (m, CDF), 86.7 (m, CDF), 34.9 (m, CD₂); **HRMS** (ESI⁺) *m/z* calcd for C₅²H₆F₄Na [M+Na]⁺ 171.0680, found 171.0672.

6.3 Compounds preparation for Chapter 3

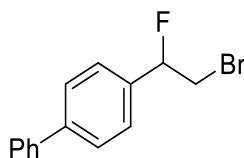
6.3.1 (2-Bromo-1-fluoroethyl)benzene



75

A mixture of NBS (9.56 g, 52.8 mmol), styrene **63** (5.0 g, 48.0 mmol) in DCM (20 mL) was treated with Et₃N·3HF (11.76 mL, 72 mmol) and stirred for 24h at RT. Next, water (10 mL) was added and the resultant mixture was extracted with DCM (3 × 10 mL). The organic layer was dried over Na₂SO₄ and concentrated under reduced pressure. Flash chromatography (hexane) afforded the compound as a colourless oil (7.7 g, 80%). ¹H NMR (500 MHz, CDCl₃) δ_H 7.45-7.36 (5H, m, Ar-CH), 5.64 (1H, ddd, ²J_{HF} = 46.8, ³J_{HH} = 7.9, 4.1 Hz, CHF), 3.74-3.57 (2H, m, CH₂Br); ¹⁹F {¹H} NMR (376 MHz, CDCl₃) δ_F -174.2 (s). Data agreement with the literature.³

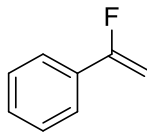
6.3.2 4-(2-Bromo-1-fluoroethyl)-1,1'-biphenyl



76

Following the analogous procedure above (**6.3.1**), the product was obtained by flash column chromatography (petroleum ether) as a colourless solid (72%). ¹H NMR (400 MHz, CDCl₃) δ_H 7.64-7.37 (9H, m, Ar-CH), 5.68 (1H, ddd, ²J_{HF} = 46.5 Hz, ³J_{HH} = 7.9, 4.1 Hz, CHF), 4.77-3.61 (2H, m, CH₂Br); ¹⁹F {¹H} NMR (376 MHz, CDCl₃) δ_F -176.6 (s). Data agreement with the literature.³

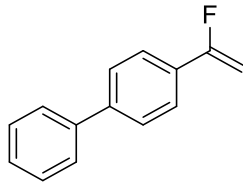
6.3.3 (1-Fluorovinyl)benzene



53

(2-Bromo-1-fluoroethyl)benzene **75** (5.0 g, 24.6 mmol) and potassium *t*-butoxide (4.12 g, 36.2 mmol) were added into the THF (20 mL). The reaction was stirred for the 24h at RT. After reaction, the product was obtained by flash column chromatography (petroleum ether) as a colourless oil (1.92 g, 64 %). $^1\text{H NMR}$ (400 MHz, CDCl_3) δ_{H} 7.61-6.54 (2H, m, Ar-CH), 7.41-7.34 (3H, m, Ar-CH), 5.04 (1H, dd, $^3J_{\text{HFtrans}} = 49.8$ Hz, $^2J_{\text{HH}} = 3.5$ Hz, CH_2), 4.86 (1H, dd, $^3J_{\text{HFcis}} = 17.3$ Hz, $^2J_{\text{HH}} = 3.5$ Hz, CH_2); $^{19}\text{F} \{^1\text{H}\}$ NMR (376 MHz, CDCl_3) δ_{F} -107.9 (s). Data agreement with the literature.³

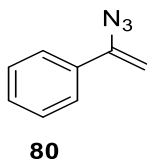
6.3.4 4-(1-Fluorovinyl)-1,1'-biphenyl



77

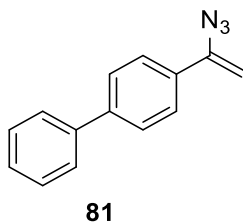
Following the analogous procedure above (**6.3.3**), the product was obtained by flash column chromatography (petroleum ether) as a colourless solid (60 %). $^1\text{H NMR}$ (400 MHz, CDCl_3) δ_{H} 7.67–7.62 (6H, m, Ar-CH), 7.50–7.46 (2H, m, Ar-CH), 7.41–7.38 (1H, m, Ar-CH), 5.08 (1H, dd, $^3J_{\text{HFtrans}} = 49.7$ Hz, $^2J_{\text{HH}} = 3.5$ Hz, CH_2), 4.89 (1H, dd, $^3J_{\text{HFcis}} = 17.9$ Hz, $^2J_{\text{HH}} = 3.5$ Hz, CH_2); $^{19}\text{F} \{^1\text{H}\}$ NMR (376 MHz, CDCl_3) δ_{F} -108.0 (s). Data agreement with the literature.³

6.3.5 (1-Azidovinyl)benzene



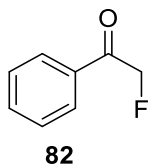
To a solution of phenylacetylene **78** (3 g, 3.22 mL, 29.0 mmol), TMS-N₃ (6.76 g, 7.68 mL, 58.0 mmol) and H₂O (1.05 g, 1.05 mL, 58.0 mmol) in DMSO (20 mL) at 80 °C, Ag₂CO₃ (810 mg, 5.8 mmol) was added. The mixture was then stirred for 2h until substrate starting material consumed as indicated by TLC. The resulting mixture was concentrated and taken up by dichloromethane (3 × 30 mL). The organic layer was washed with brine (3 × 40 mL), dried over MgSO₄ and concentrated. Purification of the crude product with flash column chromatography (petroleum ether) and concentrated *in vacuo* to afford product as an oil (3.07 g, 72 %). ¹H NMR (500 MHz, CDCl₃) δ_H 7.57-7.55 (m, 2H), 7.37-7.35 (m, 3H), 5.43 (d, *J* = 2.0 Hz, 1H), 4.96 (d, *J* = 2.0 Hz, 1H). Data agreement with the literature.⁴

6.3.6 4-(1-Azidovinyl)-1,1'-biphenyl



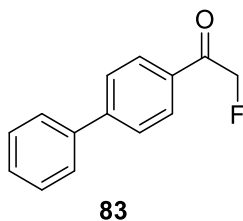
Following the analogous procedure above (6.3.5), the product was obtained by flash column chromatography (petroleum ether) as a colourless solid (70 %). ¹H NMR (500 MHz, CDCl₃) δ_H 7.68-7.65 (m, 2H), 7.63-7.58 (m, 4H), 7.47 (d, *J* = 7.5 Hz, 2H), 7.38 (t, *J* = 7.5 Hz, 1H), 5.51 (d, *J* = 2.0 Hz, 1H), 5.00 (d, *J* = 2.0 Hz, 1H) ; Data agreement with the literature.⁴

6.3.7 2-Fluoroacetophenone



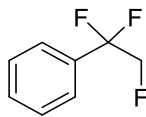
To a suspension of Selectfluor (7.3 g, 20 mmol), NaHCO₃ (2.3 g, 27.0 mmol), and H₂O (0.49 mL, 27.0 mmol) in CH₃CN (20 mL) was added vinyl azide **80** (2.0 g, 13.7 mmol) at RT. The resulting mixture was stirred for 2h. The solvent was then removed under reduced pressure and the residue was purified by flash column chromatography on silica gel to give product as a colourless oil (1.2 g, 65 % yield). ¹H NMR (400 MHz, CDCl₃): δ_H 7.89–7.87 (m, 2H), 7.62–7.59 (m, 1H), 7.50–7.46 (m, 2H), 5.51 (d, 2H, *J* = 47.0 Hz); ¹⁹F {¹H}NMR (376 MHz, CDCl₃) δ_F -230.8 (s, 1F); Data agreement with the literature.⁵

6.3.8 1-(Biphenyl-4-yl)-2-fluoroethanone



Following the analogous procedure above (**6.3.7**), the product was obtained by flash column chromatography (petroleum ether) as a colourless solid (70 %). ¹H NMR (400 MHz, CDCl₃) δ_H 7.98 (d, *J* = 8.1 Hz, 2H), 7.72 (d, *J* = 8.1 Hz, 2H), 7.63 (d, *J* = 7.4 Hz, 2H), 7.49 (t, *J* = 7.3 Hz, 2H), 7.46 – 7.39 (m, 1H), 5.56 (d, *J* = 46.9 Hz, 2H). ¹⁹F {¹H}NMR (376 MHz, CDCl₃) δ_F -230.33 (s, 1F). Data agreement with the literature.⁵

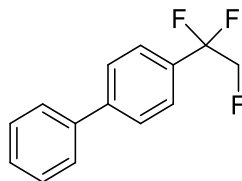
6.3.9 1-Phenyl-1,1,2-trifluoroethane



84

DAST (2.1 g, 1.72 mL, 13.1 mmol) was added to a solution of compound **82** (1.2 g, 8.7 mmol) in anhydrous toluene (10 mL) under N₂ atmosphere. The mixture was stirred for overnight at 50 °C. After the mixture was cooled at 0 °C, 10 mL of water was slowly added (exothermic) and the mixture washed until neutral with a NaHCO₃ solution. After extraction with ether and drying of the extracts, removal of the solvents *in vacuo* then purified by flash column chromatography (pentane) to afford product as a colourless oil (668 mg, 48 %). ¹H NMR (400 MHz, CDCl₃) δ_H 7.54-7.44 (m, 5 H, arom.), 4.63 (dt, 2 H, ²J_{HF} = 46.2 Hz, ³J_{HF} = 12.0 Hz); ¹⁹F {¹H} NMR (376 MHz, CDCl₃) δ_F -107.9 (d, 2 F, J = 18 Hz), -231.7 (t, 1 F, J = 18 Hz). Data agreement with the literature.⁶

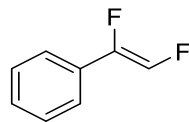
6.3.10 4-(1,1,2-Trifluoroethyl)-1,1'-biphenyl



85

Following the analogous procedure above (**6.3.9**), the product was obtained by flash column chromatography (petroleum ether) as a colourless solid (50 %). **M.p.** = 62 °C; ¹H NMR (400 MHz, CDCl₃) δ_H 7.69 (d, 2 H, J = 8.2 Hz, arom.), 7.60 (m, 4 H, arom.), 7.46 (m, 2 H, arom.), 7.39 (m, 1 H, arom.), 4.67 (dt, 2 H, ²J_{HF} = 46.5 Hz, ³J_{HF} = 12.2 Hz); ¹⁹F {¹H} NMR (376 MHz, CDCl₃) δ_F -107.5 (d, 2 F, J = 18 Hz), -231.6 (t, 1 F, J = 18 Hz); ¹⁹F NMR (376 MHz, CDCl₃) δ_F -107.5 (dt, 2 F, J = 18, 12 Hz), -231.6 (m, 1 F); ¹³C NMR (125 MHz, CDCl₃) δ_C 82.6 (dt, J_{CF} = 186 Hz, ²J_{CF} = 36 Hz, CHF), 118.6 (m, CF₂), 126.0 (t, J = 6.3 Hz), 127.2, 127.4, 127.9, 128.9, 131.9 (t, J = 25 Hz), 140, 143.7; **HRMS** (ASAP⁺) m/z calcd for C₁₄H₁₁F₃ [M] 236.0813, found 236.0816, calcd. C₁₄H₁₂F₃ [M+H] 237.0847, found 237.0849.

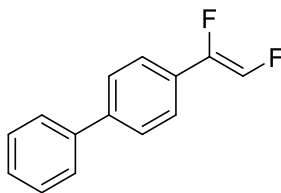
6.3.11 *Cis*- α,β -Difluorstyrene



86

Potassium *tert*-butoxide (2.02 g, 18.1 mmol) was added to a solution of compound **84** (1.0 g, 7 mmol) in 10 mL *tert*-butyl alcohol. The mixture was heated for 4h at 100°C. After cooling, the mixture was poured into water (50 mL) and then extracted with ether. The extract was dried over MgSO₄. After rotary evaporation of the solvents, the compound was purified by flash column chromatography (pentane) as a colourless oil (329 mg, 32 %). ¹H NMR (300 MHz, CDCl₃) δ_{H} 7.41-7.36 (m, 5 H, arom.), 6.95(dd, 1 H, ²J_{HF} = 71 Hz, ³J_{HF} = 17.0 Hz); ¹⁹F {¹H} NMR (282 MHz, CDCl₃) δ_{F} -142.1 (d, 1 F, ³J_{FF} = 11 Hz), -164.4 (d, 1 F, J = 11 Hz); ¹⁹F NMR (282 MHz, CDCl₃) δ_{F} -142.1(dd, 1 F, ³J_{HF} = 17.0 Hz, ³J_{FF} = 11 Hz, PhCF), -164.4 (dd, 1 F, ²J_{HF} = 71 Hz, ³J_{FF} = 11 Hz, CHF). Data agreement with the literature.⁶

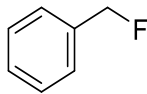
6.3.12 (Z)-4-(1,2-Difluorovinyl)-1,1'-biphenyl



87

Following the analogous procedure above (**6.3.11**), the product was obtained by flash column chromatography (petroleum ether) as a colourless solid (28 %). **M.p.** = 102 °C; **¹H NMR** (400 MHz, CDCl₃) δ_H 7.60 (m, 4 H, arom.), 7.46 (m, 4 H, arom.), 7.37 (m, 1 H, arom.), 7.03 (dd, 1 H, ²J_{HF} = 72 Hz, ³J_{HF} = 17 Hz); **¹⁹F {¹H} NMR** (376 MHz, CDCl₃) δ_F -142.1 (d, 1 F, ³J_{FF} = 11 Hz, PhCF), -164.4 (d, 1 F, J = 11 Hz, CHF); **¹⁹F NMR** (376 MHz, CDCl₃) δ_F -142.1 (dd, 1 F, ³J_{HF} = 17.0 Hz, ³J_{FF} = 11 Hz, PhCF), -164.4 (dd, 1 F, ²J_{HF} = 71 Hz, ³J_{FF} = 11 Hz, CHF); **¹³C NMR** (125 MHz, CDCl₃) δ_c 124.1 (t, J = 5.5 Hz), 127.0, 127.4, 127.8, 128.9, 132.2 (d, J = 3.6 Hz), 134.1 (dd, ¹J_{CF} = 257 Hz, ²J_{CF} = 15.6 Hz, CHF), 140.1, 142.2, 148.3 (dd, ¹J_{CF} = 246 Hz, ²J_{CF} = 10 Hz, CF). **HRMS** (ASAP⁺) m/z calcd for C₁₄H₁₀F₂ [M] 216.0751, found 216.0748, calcd. C₁₄H₁₁F₂ [M+H]⁺ 217.0829, found 217.0813.

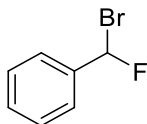
6.3.13 Benzyl fluoride



90

Benzyl bromide **89** (5 g, 29 mmol, 3.5 mL) was added to a solution of TBAF (10.2 g, 32.2 mmol) in acetonitrile at RT. The reaction was reacted at 30 °C for overnight. After reaction, the reaction mixture was poured into water (20 mL) and extracted with pentane (20 mL x 3). The combined organic extracts were dried over sodium sulphate, filtered, and concentrated under reduced pressure to yield the colorless oil (2.3 g, 72 %). $^1\text{H NMR}$ (400 Hz, CDCl_3) δ_{H} 7.4 (s, 5H, arom.), 5.39 (d, 2 H, $^2J_{\text{HF}} = 47.8$ Hz); ^{19}F $\{^1\text{H}\}$ NMR (376 Hz, CDCl_3) δ_{F} -206.6 (s). Data agreement with the literature.⁷

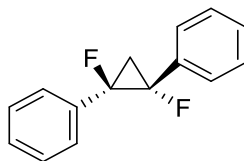
6.3.14 Bromofluoromethylbenzene



42

A solution of benzyl fluoride **90** (1.98 g, 18 mmol) was added into a reactor under an inert atmosphere which contains a suspension of N-bromosuccinimide (3.5 g, 18.9 mmol) in carbon tetrachloride (40 mL), surmounted by a mercury vapour UV lamp. The reaction mixture was irradiated overnight at ambient temperature. The mixture is then filtered, extracted with dichloromethane, washed with water, dried over magnesium sulphate, filtered and then concentrated. The residue is then purified on a chromatography column (petroleum ether) to produce compound as a colourless oil (1.68 g, 50 %). $^1\text{H NMR}$ (400 Hz, CDCl_3) δ_{H} 7.52-7.40 (m, 5H, arom.), 7.40 (d, 1H, $^2J_{\text{HF}} = 49.4$ Hz); ^{19}F $\{^1\text{H}\}$ NMR (376 Hz, CDCl_3) δ_{F} -130.0 (s). Data agreement with the literature.⁸

6.3.15 (1*R**, 2*R**)-1,2-Difluoro-1,2-diphenylcyclopropane



91

(1-Fluorovinyl)benzene **53** (142.7 mg, 1.17 mmol), (bromofluoromethyl)benzene **42** (200 mg, 1.06 mmol) and potassium *t*-butoxide (143 mg, 1.28 mmol) were added into a flask. The reaction was stirred at 100 °C for 24h under nitrogen atmosphere. After reaction, the product was obtained by flash column chromatography (petroleum ether) as a colourless solid (92.6 mg, 38 %). **M.p.** = 82-84°C. **¹H NMR** (400 MHz, CDCl₃) δ_H 7.52-6.54 (4H, m, Ar-CH), 7.42-7.45 (6H, m, Ar-CH), 2.19 (2H, m, CH₂); **¹⁹F {¹H} NMR** (376 MHz, CDCl₃) δ_F -173.2 (s); **¹⁹F NMR** (376 MHz, CDCl₃) δ_F -173.2 (m); **¹³C NMR** (125 MHz, CDCl₃) δ_C 21.9 (t, ²J_{CF} = 11.9 Hz, CH₂) 81.7 (dd, J_{CF} = 225.2 Hz, ²J_{CF} = 14.9 Hz, CFPh) 127.0 (t, ³J_{CF} = 3.4 Hz, Arom-C), 128.4 (s, Arom-C), 128.7 (s, Arom-C), 133.2 (d, ²J_{CF} = 22.2 Hz, Arom-C); **HRMS** (ASAP⁺) *m/z* calcd for C₁₅H₁₃F₂ [M+H]⁺ 231.0985, found 231.0984.

General procedure A for :CHF carbene addition to olefin

To a stirred solution of olefin **63**, **53** or **86** (1 equiv.) in dry PE was added CHF₂ (2 equiv.) at 0 °C under N₂ atmosphere. Et₂Zn (1 M hexane solution, 2 equiv.) was added slowly into the mixture and keep the temperature below 5 °C. The reaction was then reacted at 0 °C and monitored by NMR.

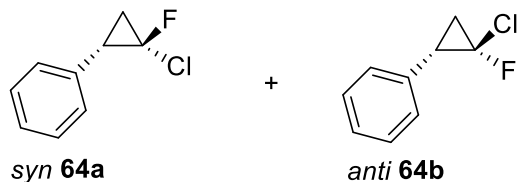
General procedure B for :CFCl carbene addition to olefin

Titanium tetrachloride (3 equiv.) was slowly added to anhydrous THF solution at 0 °C under nitrogen atmosphere. The addition was exothermic and the white vapour was produced along with a yellow precipitate. Lithium aluminium hydride (3 equiv.) in 50 mL anhydrous THF was carefully added to the mixture to remain temperature below 10 °C. The reaction was exothermic and gas was evolved. Upon addition, a brown colour was produced and disappeared again, the reaction mixture became green and finally dark brown. Then the mixture was allowed to stir as it slowly warmed to 20 °C over a period of 30 min. The flask was cooled again in a salt-ice bath. When the temperature had fallen to 0 °C, olefin (1 equiv.) was added. Then, a solution of fluorotrichloromethane (3 equiv.) in 10 mL of dry THF was added over a period of 22 min at such a rate that the temperature remained at or below 0 °C. The mixture was allowed to stir at 0 °C for 1h. The cold mixture was carefully poured into 100 mL of 10 % aqueous hydrochloric acid, containing some ice, in a 600-mL beaker. Rapid stirring was maintained during this hydrolysis. The brown aqueous mixture was extracted with pentane (50 mL x 3), dried over anhydrous sodium sulfate, filtered, and concentrated under reduced pressure (500 mbar) at room temperature. The residue was purified by silica gel chromatography (pentane) to give the desired product.

General procedure C for reduction of chlorofluorocyclopropanes

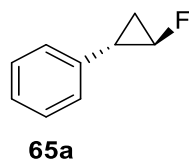
Tri-n-butyltin hydride (1.2 equiv.) and AIBN (0.1 equiv.) were added to the Halofluorocyclopropane (1 equiv.). The reaction was reacted at 88 °C for overnight. After reaction, the mixture was poured into the potassium iodide aqueous solution and extracted with pentane (25 mL x 3). The combined organic extracts were dried over sodium sulphate, filtered, and concentrated under reduced pressure (500 mbar) at room temperature. The residue was purified by silica gel chromatography (pentane) to give the desired product.

6.3.16 2-Chloro-2-fluoro-1-phenylcyclopropane



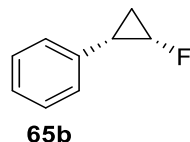
General procedure **B**. The mixture was purified by silica gel chromatography (pentane) to give the desired products (740 mg, 42%, *syn*-/*anti*- = 52 : 48) as a colourless liquid. $^1\text{H NMR}$ (400 Hz, CDCl_3) δ_{H} 7.43-7.20 (5 H, m, arom., *syn* and *anti*), 2.89 (1H, ddd, $J = 17.0, 11.5$ Hz and 8.5 Hz, CHPh, *syn*), 2.71 (1H, m, CHPh, *anti*), 2.03-1.60 (2 H, m, CH_2 , *syn* and *anti*); ^{19}F $\{^1\text{H}\}$ NMR (376 Hz, CDCl_3) δ_{F} -128.4 (s, *syn*), -148.7 (s, *anti*). Data agreement with the literature.⁹

6.3.17 *Trans*-2-Fluorocyclopropylbenzene



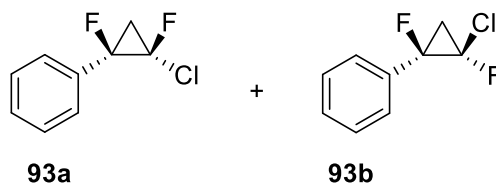
General procedure **C**. The residue was purified by silica gel chromatography (pentane) to give the desired product as a colourless liquid (49 mg, 21%). $^1\text{H NMR}$ (400 Hz, CDCl_3) δ_{H} 7.30-7.28 (2H, m, arom.), 7.21-7.18 (1H, m, arom.), 7.05-7.03 (2H, m, arom.), 4.64 (1H, m, CHF), 2.41 (1H, m, CHPh), 1.51 (1H, m, CH_2), 1.10 (1H, m, CH_2); ^{19}F $\{^1\text{H}\}$ NMR (376 Hz, CDCl_3) δ_{F} -202.5(s); $^{19}\text{F NMR}$ δ_{F} -202.5(m). Data agreement with the literature.¹⁰

6.3.18 *Cis*-2-Fluorocyclopropylbenzene



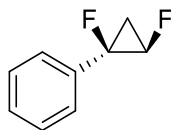
General procedure **C**. *Cis*-2-fluorocyclopropylbenzene was obtained as a colourless liquid (38 mg, 16%). $^1\text{H NMR}$ (400 Hz, CDCl_3) δ_{H} 7.34-7.20 (5 H, m, arom.), 4.76 (1H, m, CHPh), 2.08 (1H, m, CHPh), 1.35-1.16 (2 H, m, CH_2); ^{19}F $\{^1\text{H}\}$ NMR (376 Hz, CDCl_3) δ_{F} -222.5(s); $^{19}\text{F NMR}$ δ_{F} -222.5(m). Data agreement with the literature.¹⁰

6.3.19 2-Chloro-1,2-difluorophenylcyclopropane



General procedure **B**. The mixture was purified by silica gel chromatography (pentane) to give the desired products (495 mg, 30 %, **93a/93b** = 45: 55). $^1\text{H NMR}$ (400 Hz, CDCl_3) δ_{H} 7.45 (5 H, s, arom.), 2.34-2.20 (1H, m, CH_2), 2.11-1.98 (1 H, m, CH_2); ^{19}F $\{^1\text{H}\}$ NMR (376 Hz, CDCl_3) δ_{F} -142.08 (1 F, CFCl, d, J = 3.6 Hz, **93b**), -147.96 (1 F, CFCl, d, J = 6.0 Hz, **93a**), -167.08 (1 F, CFPh, d, J = 3.6 Hz, **93b**), -176.75 (1 F, CFPh, d, J = 6.0 Hz, **93a**), $^{19}\text{F NMR}$ δ_{F} -142.07(1 F, CFCl, ddd, J = 18.6, 8.7, 3.6 Hz, **93b**), -147.95 (1 F, CFCl, ddd, J = 15.6, 9.6, 6.0 Hz, **93a**), -167.08 (1 F, CFPh, ddd, J = 21.1, 11.5, 3.6 Hz, **93b**), 176.75 (1 F, CFPh, ddd, J = 24.7, 13.3, 6.0 Hz, **93a**); $^{13}\text{C NMR}$ (125 MHz, CDCl_3) δ_{C} 25.4 (t, CH_2 , J = 11.7 Hz), 26.6 (t, CH_2 , J = 12.6 Hz), 79.6 (dd, CFPh, J = 234, 12.4 Hz), 80.5 (dd, CFPh, J = 234.4, 9.5 Hz), 91.2 (dd, CFCl, J = 313, 1 Hz), 91.3 (dd, CFCl, J = 307, 14.8 Hz), 127.2 (d, CH-arom., J = 5.2 Hz), 127.6 (d, CH-arom., J = 4.5 Hz), 128.5 (s, CH-arom.), 128.6 (s, CH-arom.), 129.5 (d, CH-arom., J = 1.4 Hz), 129.7 (d, CH-arom., J = 1.9 Hz), 130.9 (d, , CH-arom., J = 20.5 Hz), 131.8 (d, , CH-arom., J = 19.9Hz);

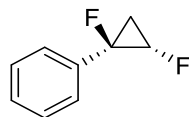
6.3.20 *Cis*-1,2-Difluorocyclopropylbenzene



92a

General procedure **C**. The residue was purified by silica gel chromatography (pentane) to give the desired product as a colourless liquid (60 mg, 26%). **¹H NMR** (400 Hz, CDCl₃) δ_H 7.41-7.34 (m, 3 H, arom.), 7.26-7.23 (m, 2 H, arom.) 4.55 (m, 1 H, CHF, ²J_{CF} = 62.6 Hz), 1.92-1.75 (m, 1 H, CH₂), 1.51-1.62 (m, 1 H, CH₂); **¹⁹F {¹H} NMR** (376 Hz, CDCl₃) δ_F -196.1 (s, 1 F, CFPh), -219.2 (s, CFH); **¹⁹F NMR** δ_F -196.1 (dd, 1 F, CFPh, *J* = 25.6, 13.7 Hz), -219.2 (ddd, 1 F, CFH, *J* = 62.6, 28.3, 14.9 Hz); **¹³C NMR** (125 MHz, CDCl₃) δ_C 18.7 (t, CH₂, *J* = 10 Hz), 73.1 (dd, CFH, *J* = 236, 9.1Hz), 76.6 (dd, CFPh, *J* = 222, 9.1Hz), 124.6 (d, C-arom., *J* = 5.5 Hz), 128.3 (C-arom.), 128.6 (C-arom.), 136.5 (dd, C-arom., *J* = 20.8, 1.8 Hz); **HRMS** (ASAP⁺) *m/z* calcd for C₉H₈F₂ [M] 154.0594, found 154.0591, calcd C₉H₇F₂ [M-H] 153.0516, found 153.0520.

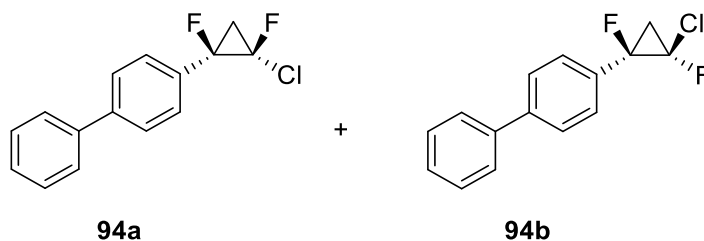
6.3.21 *Trans*-1,2-Difluorocyclopropylbenzene



92b

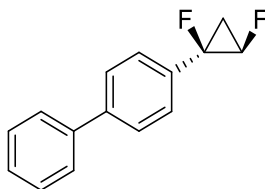
General procedure **B**. The residue was purified by silica gel chromatography (pentane) to give the desired product as a colorless liquid (80 mg, 34%). **¹H NMR** (400 Hz, CDCl₃) δ_H 7.48-7.30 (m, 5 H, arom.), 5.08 (m, 1 H, CHF, ²J_{CF} = 62.6 Hz), 1.80-1.67 (m, 2 H, CH₂); **¹⁹F {¹H} NMR** (376 Hz, CDCl₃) δ_F -172.2 (s, 1 F, CFPh), -215.1 (s, CFH); **¹⁹F NMR** δ_F -172.2 (dt, 1 F, CFPh, *J* = 22.6, 12.5 Hz), -215.1 (ddd, 1 F, CFH, *J* = 62.6, 24.8, 13.2 Hz); **¹³C NMR** (125 MHz, CDCl₃) δ_C 19.5 (t, CH₂, *J* = 12.6 Hz), 73.5 (dd, CFH, *J* = 234, 19.1Hz), 78.7 (dd, CFPh, *J* = 221, 10 Hz), 129.9 (d, C-arom., *J* = 5.5 Hz), 128.4 (C-arom.), 128.7 (dd, C-arom., *J* = 1.7 Hz), 133.1 (d, C-arom., *J* = 19 Hz); **HRMS** (ASAP⁺) *m/z* calcd for C₉H₈F₂ [M] 154.0594, found 154.0591, calcd C₉H₇F₂ [M-H] 153.0516, found 153.0520.

6.3.22 4-(2-Chloro-1,2-difluorocyclopropyl)-1,1'-biphenyl



General procedure **B**. The mixture was purified by silica gel chromatography (PE) to give the desired product as a white solid (70 mg, 50%, **94a/94b** = 44: 56). $^1\text{H NMR}$ (500 Hz, CDCl_3) δ_{H} 7.67-7.65 (2 H, m, arom.), 7.62-7.59 (2 H, m, arom.), 7.53-7.51 (2 H, m, arom.), 7.47-7.44 (2 H, m, arom.), 7.39-7.36 (1 H, m, arom.), 2.36-2.20 (1H, m, CH_2), 2.13-2.02 (1 H, m, CH_2); ^{19}F $\{^1\text{H}\}$ NMR (376 Hz, CDCl_3) δ_{F} -141.9 (1 F, CFCl , d, $J = 3.8$ Hz, **94b**), -147.8 (1 F, CFCl , d, $J = 5.7$ Hz, **94a**), -167.1 (1 F, CFPh , d, $J = 3.8$ Hz, **94b**), -176.7 (1 F, CFPh , d, $J = 5.7$ Hz, **94a**); HRMS (ASAP⁺) m/z calcd for $\text{C}_{15}\text{H}_{11}\text{F}_2\text{Cl}$ [M] 264.0470, found 264.0467, calcd $\text{C}_{15}\text{H}_{10}\text{F}_2^{35}\text{Cl}$ [M-H] 263.0436, found 264.0434.

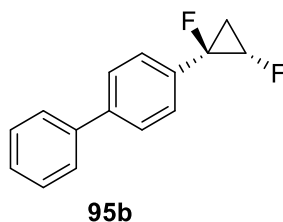
6.3.23 *Cis*-4-(1,2-Difluorocyclopropyl)-1,1'-biphenyl



95a

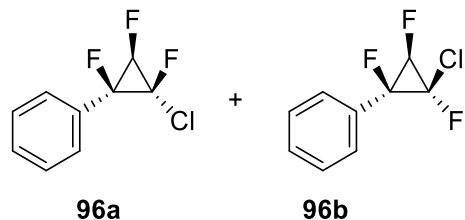
General procedure **C**. The residue was purified by silica gel chromatography (PE) to give the desired product as a solid (17 mg, 28%). **M.p.** = 95-97 °C. **¹H NMR** (500 Hz, CDCl₃) δ_H 7.62-7.57 (m, 4 H, arom.), 7.46-7.43 (m, 2 H, arom.), 7.38-7.35 (m, 1 H, arom.), 7.32(d, 2 H, arom., *J* = 8.9 Hz), 4.58 (m, 1 H, CHF, ²*J*_{CF} = 62.5 Hz), 1.94-1.80 (m, 1 H, CH₂), 1.65-1.55 (m, 1 H, CH₂); **¹⁹F {¹H} NMR** (470 Hz, CDCl₃) δ_F -195.8 (s, 1 F, CFPh), -219.0 (s, CFH); **¹⁹F NMR** δ_F-196.1 (dd, 1 F, CFPh, *J* = 25.6, 13.7 Hz), -219.22 (ddd, 1 F, CFH, *J* = 62.6, 28.3, 15.0 Hz); **¹³C NMR** (125 MHz, CDCl₃) δ_c 18.8 (t, CH₂, *J* = 11 Hz), 73.1 (dd, CFH, *J* = 237, 9.1Hz), 76.6 (dd, CFPh, *J* = 222, 9.1Hz), 125.2 (d, C-arom., *J* = 5.5 Hz), 127.1 (s, C-arom.), 127.4 (s, C-arom.), 127.6 (s, C-arom.), 128.9 (s, C-arom.), 135.4 (dd, C-arom., *J* = 20.1, 1.8 Hz) 140.3 (s, C-arom.), 141.3 (s, C-arom.); **HRMS** (ASAP⁺) *m/z* calcd for C₁₅H₁₂F₂ [M] 230.0907, found 230.0907, calcd C₁₅H₁₃F₂ [M+H] 231.0941, found 231.0957.

6.3.24 *Trans*-4-(1,2-Difluorocyclopropyl)-1,1'-biphenyl



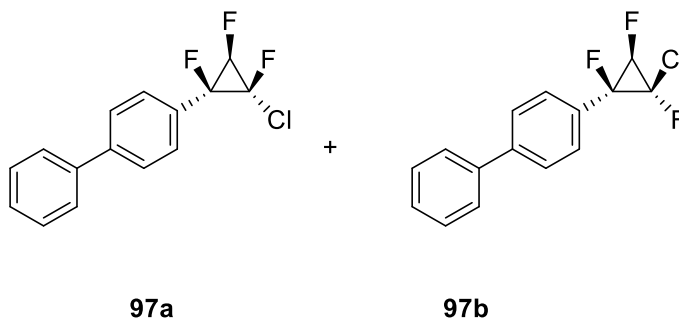
General procedure **C**. The residue was purified by silica gel chromatography (PE) to give the desired product as a solid (22 mg, 35%). **M.p.** = 67-68 °C. **¹H NMR** (500 Hz, CDCl₃) δ_H 7.66-7.60 (m, 4 H, arom.), 7.55-7.54 (m, 2 H, arom.), 7.47-7.44 (m, 2 H, arom.), 7.39-7.36 (m, 1 H, arom.), 5.06 (m, 1 H, CHF, ²J_{CF} = 62.4 Hz), 1.83-1.72 (m, 2 H, CH₂); **¹⁹F {¹H} NMR** (470 Hz, CDCl₃) δ_F -172.3 (s, 1 F, CFPh), -214.9 (s, CFH); **¹⁹F NMR** δ_F -172.2 (dt, 1 F, CFPh, J = 22.0, 12.9 Hz), -214.9 (m, 1 F, CFH, J = 62.6); **¹³C NMR** (125 MHz, CDCl₃) δ_C 19.6 (t, CH₂, J = 12.6 Hz), 73.7 (dd, CFH, J = 234, 19.1 Hz), 78.6 (dd, CFPh, J = 221, 10 Hz), 127.1 (s, C-arom.), 127.2 (s, C-arom.), 127.3 (d, C-arom., J = 5.5 Hz), 127.6 (s, C-arom.), 128.9 (s, C-arom.), 132.1 (d, C-arom., J = 19 Hz), 140.5 (s, C-arom.), 141.6 (s, C-arom.); **HRMS** (ASAP⁺) m/z calcd for C₁₅H₁₂F₂ [M] 230.0907, found 230.0908, calcd C₁₅H₁₃F₂ [M+H] 231.0941, found 231.0968.

6.3.25 2-Chloro-1,2,3-trifluorocyclopropylbenzene



General procedure **B**. The mixture was purified by silica gel chromatography (PE) to give the desired product as the white liquid (200 mg, 25 %, **96a/96b** = 1: 1.2). $^1\text{H NMR}$ (400 Hz, CDCl_3) δ_{H} 7.26 (10 H, s, arom.), 4.84 (1H, dd, $J = 58.1, 14.2$ Hz CHF, **96b**), 4.63 (1 H, d, $J = 57.9$ Hz, CHF, **96a**); ^{19}F $\{^1\text{H}\}$ NMR (376 Hz, CDCl_3) δ_{F} -148.7 (dd, 1 F, $J = 13.6, 7.1$ Hz, CFCl, **96b**), -168.7 (d, $J = 2.0$ Hz, CFCl, **96a**), -180.1 (d, 1F, $J = 7.1$ Hz, CFPh, **96b**), -191.0 (dd, 1F, $J = 9.5, 2.0$ Hz, CFPh, **96a**), -223.8 (d, 1F, $J = 13.6$, CFH, **96b**), -230.2 (d, 1F, $J = 9.5$ Hz, CFH, **96a**); $^{19}\text{F NMR}$ δ_{F} -148.7 (ddd, 1 F, $J = 14.2, 13.6, 7.1$ Hz, CFCl, **96b**), -168.7(d, $J = 2.0$ Hz, CFCl, **96a**), -180.1 (d, 1F, $J = 7.1$ Hz, CFPh, **96b**), 191.0 (dd, 1F, $J = 9.5, 2.0$ Hz, CFPh, **96a**), -223.8 (dd, 1F, $J = 58.1, 13.6$, CFH, **96b**), -230.2 (dd, 1F, $J = 57.9, 9.5$ Hz, CFH, **96a**); HRMS (EI $^+$) m/z calcd for $\text{C}_9\text{H}_6\text{F}_3^{35}\text{Cl}$ [M] 206.0119, found 206.0118.

6.3.26 4-(2-Chloro-1,2,3-trifluorocyclopropyl)-1,1'-biphenyl

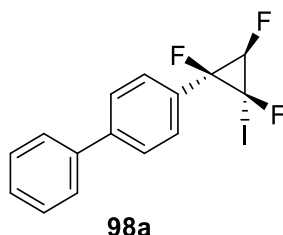


General procedure **B**. The mixture was purified by silica gel chromatography (PE) to give the desired product as the white solid (39 mg, 30 %, **97a/97b** = 1: 1.3). $^1\text{H NMR}$ (400 Hz, CDCl_3) δ_{H} 7.70-7.68 (m, 4H), 7.61-7.55 (m, 8H), 7.48-7.45 (m, 4H), 7.40-7.39 (m, 2H), 5.09 (1H, dd, $J = 58.1, 14.1$ Hz CHF, **97b**), 4.89 (1 H, d, $J = 57.9$ Hz, CHF, **97a**); ^{19}F $\{^1\text{H}\}$ NMR (376 Hz, CDCl_3) δ_{F} -148.4 (dd, 1 F, $J = 13.8, 7.7$ Hz, CFCl, **97b**), -168.7 (s, CFCl, **97a**), -179.9 (d, 1F, $J = 7.7$ Hz, CFPh, **96b**), -190.7 (d, 1F, $J = 9.0$, CFPh, **97a**), -223.5 (d, 1F, $J = 13.7$, CFH, **97b**), -229.9 (d, 1F, $J = 9.0$ Hz, CFH, **97a**); ^{19}F NMR (376 Hz, CDCl_3) δ_{F} -148.5 (ddd, 1 F, $J = 14.1, 13.3, 7.7$ Hz, CFCl, **97b**), -168.5 (br s, CFCl, **97a**), -179.9 (d, 1F, $J = 7.7$ Hz, CFPh, **97b**), -190.7 (d, 1F, $J = 9.0$ Hz, CFPh, **97a**), -223.5 (dd, 1F, $J = 58.1, 13.6$ Hz, CFH, **97b**), -229.9 (d, 1F, $J = 57.9, 9.0$ Hz, CFH, **97a**); **HRMS** (EI^+) m/z calcd for $[\text{M}]$ $\text{C}_{15}\text{H}_{10}\text{F}_3^{35}\text{Cl}$ 248.0423, found 248.0426.

General procedure D for :CFBr (:CFI) carbene addition to olefin¹¹

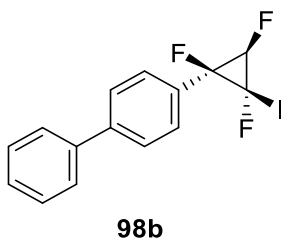
A 50% aqueous solution of NaOH was added dropwise to a stirred mixture of the corresponding alkene (1 equiv.), CHBr₂F (1.5 equiv.) (or CHFI₂), and TEBAC (0.1 equiv.) in dichloromethane at 0 °C. The reaction mixture was warmed to room temperature and stirred for 24 h. The organic phase was separated and the water phase extracted with dichloromethane. The combined organic layers were washed with water and dried over MgSO₄. The solvent was evaporated in *vacuo*; the residue was purified by preparative column chromatography.

6.3.27 4-((1S*,2S*,3R*)-1,2,3-Trifluoro-2-iodocyclopropyl)-1,1'-biphenyl



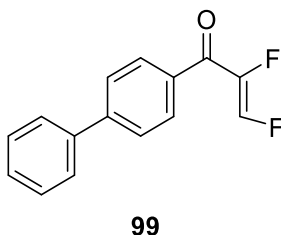
General procedure D. ¹H NMR (400 MHz, CDCl₃) δ_H 7.73-7.66 (m, 2H), 7.65-7.58 (m, 2H), 7.57-7.50 (m, 2H), 7.47 (m, 2H), 7.44-7.35 (m, 1H), 4.91 (d, *J* = 58.7 Hz, 1 H, CHF); ¹⁹F {¹H} NMR (376 MHz, CDCl₃) δ_F -173.0 (d, *J* = 3.4 Hz), -192.2 (dd, *J* = 10.7, 3.1 Hz), -226.8 (d, *J* = 10.2 Hz). HRMS (ASAP⁺) *m/z* calcd for [M-F] C₁₅H₁₀F₂I 354,9795, found 354.9793.

6.3.28 4-((1S*,2R*,3R*)-1,2,3-Trifluoro-2-iodocyclopropyl)-1,1'-biphenyl



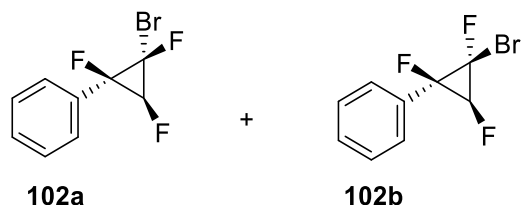
General procedure **D**. $^1\text{H NMR}$ (400 MHz, CDCl_3) δ_{H} 7.68 (2H, d, $J = 8.1$ Hz), 7.62-7.51 (4H, m), 7.49-7.44 (2H, m), 7.42-7.36 (1H, m), 5.01 (1 H, dd, $J = 59.1, 16.2$ Hz, CHF); ^{19}F $\{^1\text{H}\}$ NMR (376 MHz, CDCl_3) δ_{F} -152.7 (dd, $J = 24.9, 19.1$ Hz), -162.12 (dd, $J = 19.6, 5.6$ Hz), -207.5 (dd, $J = 25.1, 5.8$ Hz). **HRMS** (ASAP⁺) m/z calcd for $[\text{M}-\text{F}] \text{C}_{15}\text{H}_{10}\text{F}_2\text{I}$ 354,9795, found 354.9793.

6.3.29 (Z)-1-([1,1'-Biphenyl]-4-yl)-2,3-difluoroprop-2-en-1-one



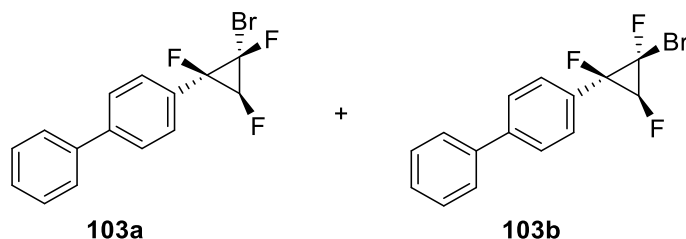
General procedure **C**. **M.p.** = 86-87 °C. $^1\text{H NMR}$ (500 MHz, CDCl_3) δ_{H} 7.96-7.93 (m, 2H), 7.73-7.71 (m, 2H), 7.64-7.63 (m, 2H), 7.51-7.47 (m, 2H), 7.44-7.41(m, 1H), 7.37 (dd, $J = 70.6, 14.6$ Hz, 1H, CHF), $^{19}\text{F NMR}$ (470 MHz, CDCl_3) δ_{F} -142.2 (dd, $J = 70.6, 6.8$ Hz, CHF), -145.2 (ddt, $J = 14.6, 6.8, 1.4$ Hz, CF); $^{13}\text{C NMR}$ (125 MHz, CDCl_3) δ_{C} 185.7 (dd, $J = 22.3, 6.7$ Hz, CO), 146.9 (dd, $J = 265.7, 7.9$ Hz, CF=CHF), 146.5, 145.8 (dd, $J = 280.9, 11.9$ Hz), 139.5, 129.7, 129.7, 129.0, 128.5, 127.38, 127.33.. **HRMS** (ASAP⁺) m/z calcd for $[\text{M}+\text{H}] \text{C}_{15}\text{H}_{11}\text{OF}_2$ 245.0778, found 245.0780.

6.3.30 (2-Bromo-1,2,3-trifluorocyclopropyl)benzene



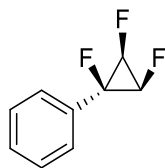
General procedure **D**. The residue was purified by silica gel chromatography (pentane) to give the desired products as a mixture (liquid, 70 mg, 21.6 %). $^1\text{H NMR}$ (500 MHz, CDCl_3) δ_{H} 7.48(5 H, m, arom.), 5.04 (1 H, dd, $J = 58.6, 15.1$ Hz, CHF), 4.91 (1 H, d, $^2J_{\text{HF}} = 58.4$ Hz, CHF); $^{19}\text{F}\{^1\text{H}\}$ NMR (470 MHz, CDCl_3) δ_{F} -148.7(dd, $J = 18.8, 13.0$ Hz), -169.0(d, $J = 2.6$ Hz), -172.9 (d, $J = 13.0$ Hz), -190.7 (dd, $J = 10.5, 2.6$ Hz), -217.3 (d, $J = 18.8$ Hz), -228.7 (d, $J = 10.5$ Hz). HRMS (EI^+) m/z calcd for [M] $\text{C}_9\text{H}_6\text{F}_3^{79}\text{Br}$ 249.9600, found 249.9574.

6.3.31 4-(2-Bromo-1,2,3-trifluorocyclopropyl)-1,1'-biphenyl



General procedure **D**. The residue was purified by silica gel chromatography (pentane) to give the desired products as a mixture (solid, 20 mg, 26.5 %). $^1\text{H NMR}$ (400 MHz, CDCl_3) δ_{H} 7.71-7.68 (4H, m, arom.), 7.62-7.55 (8H, m, arom.), 7.47-7.45 (4 H, m, arom.), 7.41-7.38 (2 H, m, arom.), 5.07 (1 H, dd, $J = 58.5, 15.1$ Hz, CHF), 4.94 (1 H, d, $^2J_{\text{HF}} = 58.0$ Hz, CHF); $^{19}\text{F}\{^1\text{H}\}$ NMR (376 MHz, CDCl_3) δ_{F} -148.6(dd, $J = 19.1, 13.0$ Hz), -168.8(d, $J = 3.4$ Hz), -172.0 (dd, $J = 13.0, 1.9$ Hz), -190.4 (dd, $J = 10.0, 3.4$ Hz), -217.0 (d, $J = 19.1$ Hz), -228.4 (d, $J = 10.0$ Hz). HRMS (EI^+) m/z calcd for [M] $\text{C}_{15}\text{H}_{10}\text{F}_3^{79}\text{Br}$ 325.9918, found 325.9917.

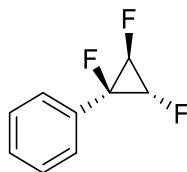
6.3.32 ((1*s*,2*R*,3*S*)-1,2,3-Trifluorocyclopropyl)benzene



72a

General procedure **C**. Purification by flash column chromatography (pentane) gave the desired product as the liquid (volatile, $R_f = 0.2$ in PE, 14 mg, 15.4 %, volatile). $^1\text{H NMR}$ (500 MHz, CDCl_3) δ_{H} 7.44 (m, 3H, arom), 7.31 (m, 2H, arom), 4.55 (m, 2H); $^{19}\text{F}\{^1\text{H}\}$ NMR (470 MHz, CDCl_3) δ_{F} -209.4 (t, 1 F, $J = 4.7$ Hz, PHCF), -242.6 (d, 2 F, $J = 4.7$ Hz, CHF); ^{19}F NMR (470 MHz, CDCl_3) δ_{F} -209.4 (t, 1 F, $J = 4.7$ Hz, PHCF), -242.6 (m, 2 F, CHF); ^{13}C NMR (125 MHz, CDCl_3) δ_{C} 132.6 (tertiary), 129.0, 126.8, 125.9, 70.7, 68.8.; HRMS (EI^+) m/z calcd for [M] $\text{C}_9\text{H}_7\text{F}_3$ 172.0494, found 172.0455.

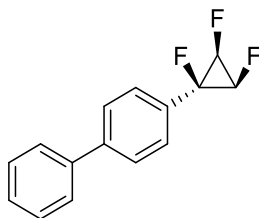
6.3.33 ((2*S**,3*S**)-1,2,3-Trifluorocyclopropyl)benzene



72b

General procedure **C**. Purification by flash column chromatography (pentane) gave the desired product as the liquid (volatile, $R_f = 0.7$ in PE, 20 mg, 22 %, volatile). $^1\text{H NMR}$ (400 MHz, CDCl_3) δ_{H} 7.46 (m, 5H, arom), 5.31 (dddd, $J = 58.0, 19.4, 18.7, 1.9$ Hz, 1H, arom), 5.02 (dddd, $J = 57.7, 16.0, 1.9, 1.2$ Hz, 1H); $^{19}\text{F}\{^1\text{H}\}$ NMR (376 MHz, CDCl_3) δ_{F} -188.2 (dd, $J = 3.2, 12.2$ Hz, 1F, PhCF), -220.7 (dd, $J = 7.7, 3.0$ Hz, 1F, CHF), -228.3 (dd, $J = 12.2, 7.6$ Hz, CHF); ^{19}F NMR (376 MHz, CDCl_3) δ_{F} -188.2 (m, 1F, PhCF), -220.7 (m, 1F, CHF), -228.3 (m, 1F, CHF); HRMS (EI^+) m/z calcd for [M] $\text{C}_9\text{H}_7\text{F}_3$ 172.0494, found 172.0475.

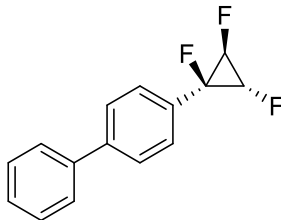
6.3.34 4-((1*S*,2*R*,3*S*)-1,2,3-Trifluorocyclopropyl)-1,1'-biphenyl



73a

General procedure **C**. The final product was obtained as the solid (2.7 mg, 17.7 %). **M.p.** = 84-85 °C. **¹H NMR** (500 MHz, CDCl₃) δ_H 7.69–7.63 (m, 2H), 7.59-7.55 (m, 2H), 7.49-7.43 (m, 2H), 7.41-7.35 (m, 3H), 4.77-4.37 (m, 2H); **¹⁹F {¹H}NMR** (470 MHz, CDCl₃) δ_F -208.8 (t, *J* = 4.7 Hz, 1F, PhCF), -242.4 (d, *J* = 4.7 Hz, 2F, CHF); **¹⁹F NMR** (376 MHz, CDCl₃) δ_F -208.8 (m, 1F, PhCF), -242.4 (m, 2F, CHF); **¹³C NMR** (176 MHz, CDCl₃) δ_C 142.7, 140.0, 132.1, 128.9, 127.8, 127.7, 127.2, 126.6, 71.8, 67.8; **HRMS** (EI⁺) *m/z* calcd for [M] C₁₅H₁₁F₃ 248.0807, found 248.0803.

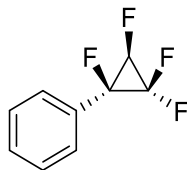
6.3.35 4-((2*S*^{*}, 3*S*^{*})-1,2,3-Trifluorocyclopropyl)-1,1'-biphenyl



73b

General procedure **C**. The final product was obtained as the solid (3.7 mg, 24.3 %). **M.p.** = 76-77 °C. **¹H NMR** (500 MHz, CDCl₃) δ 7.70-7.64 (m, 2H), 7.62-7.58 (m, 2H), 7.54 (dd, *J* = 8.3, 1.6 Hz, 2H), 7.50-7.44 (m, 2H), 7.41-7.36 (m, 1H), 5.33 (m, *J* = 58.0, 18.9, 1.9 Hz, 1H), 5.05 (m, *J* = 57.7, 16.0, 1.6 Hz, 1H).; **¹⁹F {¹H} NMR** (470 MHz, CDCl₃) δ_F -187.7 (dd, *J* = 11.5, 3.8 Hz, 1F, PhCF), -220.4 (dd, *J* = 8.6, 3.8 Hz, 1F, CHF), -227.9 (dd, *J* = 11.5, 8.6 Hz, CHF); **¹⁹F NMR** (376 MHz, CDCl₃) δ_F -188.7 (m, 1F, PhCF), -220.4 (m, 1F, CHF), -227.9 (m, 1F, CHF); **¹³C NMR** (126 MHz, CDCl₃) δ_C 142.9, 140.2, 132.1, 128.9, 128.2, 127.9, 127.6, 127.2, 80.8, 75.8, 75.5; **HRMS** (EI⁺) *m/z* calcd for [M] C₁₅H₁₁F₃ 248.0807, found 248.0800.

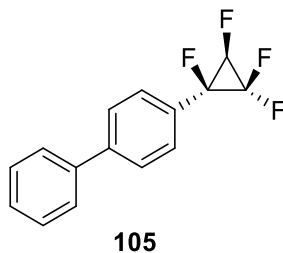
6.3.36 1,2,2,3-Tetrafluorocyclopropylbenzene



104

To a solution of *cis*- α,β -Difluorostyrene **86** (40 mg, 0.28 mmol, 1 equiv) and TMSCF_3 (101.4 mg, 0.71 mmol, 2.5 equiv) in anhydrous THF, NaI (106 mg, 0.71 mmol, 2.5 equiv) was added. The resulting suspension was stirred at 75 °C for 20 h under N_2 atmosphere. After completion, the reaction mixture was allowed to cool to RT and solvent was removed *in vacuo*. The crude residue was diluted with diethyl ether (50 mL) and washed with distilled water (50 mL). The phases were separated and the aqueous layer was extracted with diethyl ether (2 x 50 mL). The combined organic phases were washed sequentially with saturated aqueous solutions of Na_2SO_3 and NaHCO_3 , followed by drying over Na_2SO_4 , filtration and evaporation of *solvent in vacuo*. Purification by flash column chromatography (petroleum ether) gave the desired product as the white oil (21.4 mg, 40 %). $^1\text{H NMR}$ (400 MHz, CDCl_3) δ_{H} 7.48 (s, 5 H, arom), 4.94 (ddd, $J = 57.0, 11.0, 1.3$ Hz, 1 H), $^{19}\text{F}\{^1\text{H}\}$ NMR (376 MHz, CDCl_3) δ_{F} -139.9 (dd, 1 F, $J = 193.1, 6.9$ Hz, CF_2), -155.7 (dd, 1 F, $J = 193.1, 3.6$ Hz, CF_2), -195.6 (d, 1 F, $J = 10.2$ Hz, PhCF), -236.9 (ddd, 1 F, $J = 10.5, 6.8, 3.3$ Hz, CHF), $^{19}\text{F NMR}$ (376 MHz, CDCl_3), -139.9 (ddd, 1 F, $J = 193.1, 11.0, 6.9$ Hz, CF_2), -155.7 (ddd, 1 F, $J = 193.1, 3.2, 1.3$ Hz, CF_2), -195.6 (d, 1 F, $J = 10.2$ Hz, PhCF), -236.9 (m, 1 F, CHF). $^{13}\text{C NMR}$ (125 MHz, CDCl_3) δ_{C} 130.7, 129.1, 128.16, 128.13, 103.9 (m), 76.9 (m), 71.3 (m); HRMS (ASAP⁺) m/z calcd. for $\text{C}_9\text{H}_6\text{F}_4$ 190.0400, found 190.0398.

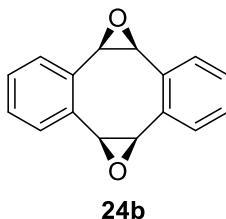
6.3.37 4-(1,2,2,3-Tetrafluorocyclopropyl)-1,1'-biphenyl



Following the analogous procedure above (**6.3.25**), the product was obtained by flash column chromatography (petroleum ether) as a colourless solid (30 mg, 48.1 %). **M.p.** = 102-103°C; **¹H NMR** (400 MHz, CDCl₃) δ_H 7.74-7.66 (m, 2 H, arom), 7.57 (m, 4 H, arom), 7.52-7.44 (m, 2 H, arom), 7.43-7.39 (m, 1 H, arom), 4.97 (ddd, *J* = 57.1, 10.9, 1.3 Hz, 1 H). **¹⁹F {¹H} NMR** (376 MHz, CDCl₃) δ_F -139.6 (dd, 1 F, *J* = 193.1, 6.9 Hz, CF₂), -155.7 (dd, 1 F, *J* = 193.1, 3.3 Hz, CF₂), -195.2 (d, 1 F, *J* = 9.6 Hz, PhCF), -236.9 (ddd, 1 F, *J* = 9.9, 6.9, 3.1 Hz, CHF), **¹⁹F NMR** (376 MHz, CDCl₃), -139.6 (ddd, 1 F, *J* = 193.1, 10.8, 6.9 Hz, CF₂), -155.7 (dd, 1 F, *J* = 193.1, 3.4 Hz, CF₂), -195.6 (d, 1 F, *J* = 10.0 Hz, PhCF), -236.9 (m, 1 F, CHF); **¹³C NMR** (125 MHz, CDCl₃) δ_C 143.7(2 x C), 139.8, 129, 128.7 (d, *J* = 3.7 Hz), 128.1, 127.8, 127.2, 104.5 (m), 76.9 (m), 71.3 (m); **HRMS** (ASAP⁺) *m/z* calcd for C₁₅H₁₀F₄ 260.0719, found 260.0719.

6.4 Compounds preparation for Chapter 4

6.4.1 (1aR*,5bS*,6aR*,10bS*)-1a,5b,6a,10b-Tetrahydrodibenzo[3,4:7,8]cycloocta[1,2-b:5,6-b']bis(oxirene)

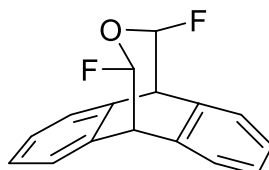


mCPBA (338 mg, 1.96 mmol, 4 equiv.) was added to a solution of dibenzo[a,e]cyclooctene **5** (100 mg, 0.49 mmol, 1 equiv.) in DCM (5 mL). The reaction was left at RT for overnight. After reaction, the mixture was then extracted into DCM (5 ml x 2) and the organic layer was washed with water (5 ml x 3), dried over anhydrous sodium sulfate and the solvent was removed under reduced pressure. The solid was purified by column chromatography (PE/Ether acetate = 15 : 1) to afford a colourless solid (29 mg, 25 %). **M.p.** = 178.5-179.1 °C; **¹H NMR** (400 MHz, CDCl₃) δ_H 7.32-7.27 (m, 4H), 7.19-7.14 (m, 4H), 4.38 (s, 4H); **¹³C NMR** (126 MHz, CDCl₃) δ_C 133.2, 128.1, 127.3, 55.1.

General procedure E for fluorination of dibenzo[a,e]cyclooctene **5** ^{12,13}

NBS (2 equiv.) was added to a solution of dibenzo[a,e]cyclooctene **5** (1 equiv.) and dry solvent (DCM, Et₂O, THF, Toluene, Acetonitrile) in an oven-dried PTFE flask. The flask was then sealed, evacuated and backfilled with argon, followed by addition of HF·Py (70 %) *via* syringe. The mixture was stirred for 2 hours at RT, then AgF (2 equiv.) was added and reaction left to stir for overnight. After completion, the reaction mixture was quenched with sodium hydrogen carbonate. The resulting mixture was extracted with dichloromethane and the combined organic phases were washed with water, followed by drying over Na₂SO₄. After filtration, solvent was removed in *vacuo*. Purification by flash column chromatography afforded the compound.

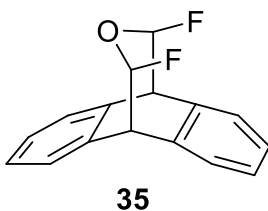
6.4.2 *trans*-11,13-Difluoro-9,10-dihydro-9,10-(methanooxymethano)anthracene



34

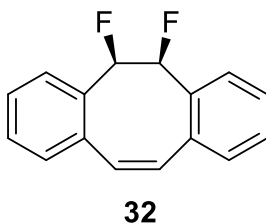
General procedure **E**, using DCM as the solvent. The product was purified by column chromatography (PE : Ether = 10 : 1) and obtained as a white solid (*R*_f = 0.3, 34 %). **M.p.** = 159-160 °C; **¹H NMR** (400 MHz, CDCl₃) δ_H 7.41-7.36 (m, 4H), 7.31-7.28 (m, 4H), 5.85-5.68 (m, 2H), 4.34-4.28 (m, 2H); **¹⁹F {¹H}NMR** (376 MHz, CDCl₃) δ_F -123.2 (s, CHF); **¹⁹F NMR** (376 MHz, CDCl₃) δ_F -123.2 (m, CHF); **¹³C NMR** (126 MHz, CDCl₃) δ_C 136.6 (x2), 136.3 (x2), 128.4 (x2), 127.8 (x2), 127.7 (x2), 126.5 (x2), 104.7(d, ¹J_{CF} = 223.6 Hz), 104.3 (d, ¹J_{CF} = 223.9 Hz), 52.3 (d, ²J_{CF} = 26.2 Hz, (x2)). **HRMS** (ESI⁺) *m/z* calcd for C₁₆H₁₂F₂ONa [M+Na]⁺ 281.0748, found 281.0741.

6.4.3 *cis*-11,13-Difluoro-9,10-dihydro-9,10-(methanooxymethano)anthracene



General procedure **E**, using DCM as the solvent. The product was purified by column chromatography (PE : Ether = 10 : 1) and obtained as a white solid ($R_f = 0.2$, 38 %). **M.p.** = 177-179 °C; $^1\text{H NMR}$ (500 MHz, CDCl_3) δ_{H} 7.41 (dd, $J = 5.4, 3.3$ Hz, 2H), 7.37 (dd, $J = 5.4, 3.2$ Hz, 2H), 7.30 (dd, $J = 5.5, 3.2$ Hz, 2H), 7.27-7.25 (m, 2H), 5.91-5.43 (m, 2H), 4.38 (d, $J = 5.1$ Hz, 2H); ^{19}F $\{^1\text{H}\}$ NMR (470 MHz, CDCl_3) δ_{F} -117.3 (s, CHF); $^{19}\text{F NMR}$ (470 MHz, CDCl_3) δ_{F} -117.3 (m, CHF); $^{13}\text{C NMR}$ (126 MHz, CDCl_3) δ_{C} 137.2 (t, $^3J_{\text{CF}} = 3.4$ Hz), 136.6, 127.9, 127.7, 127.3, 127.1, 103.9 (d, $^1J_{\text{CF}} = 223.9$ Hz), 51.8 (dt, $J_{\text{CF}} = 24.3, 7.2$ Hz). **HRMS** (ESI $^+$) m/z calcd for $\text{C}_{16}\text{H}_{12}\text{F}_2\text{ONa}$ $[\text{M}+\text{Na}]^+$ 281.0748, found 281.0746.

6.4.4 (*meso*)-5,6-Difluoro-5,6-dihydrodibenzo[a,e]cyclooctatetraene

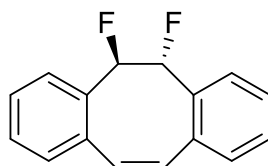


General procedure **E**, using ether as the solvent. The product was purified by column chromatography (PE) and obtained as a white solid ($R_f = 0.15$, 14 %). **M.p.** = 145-146 °C; $^1\text{H NMR}$ (400 MHz, CDCl_3) δ_{H} 7.66 (m, 2H), 7.30 (m, 4H), 7.17 (m, 2H), 6.86 (s, 2H, CH=CH), 6.29 (m, 2H, CHF); ^{19}F $\{^1\text{H}\}$ NMR (376 MHz, CDCl_3) δ_{F} -182.0 (s, CHF); $^{19}\text{F NMR}$ (376 MHz, CDCl_3) δ_{F} -182.0 (m, CHF); $^{13}\text{C NMR}$ (126 MHz, CDCl_3) δ_{C} 133.4, 132.9 (m), 131.8, 129.5, 128.6 (t, $J = 5.6$ Hz), 128.1, 127.5, 91.5 (dd, $^1J_{\text{CF}} = 178.0$ Hz, $^2J_{\text{CF}} = 21.4$ Hz). **HRMS** (ASAP $^+$) m/z calcd for $\text{C}_{16}\text{H}_{12}\text{F}_2$ $[\text{M}]^+$ 242.0907, found 242.0909.

6.4.5

(5R*,6R*,Z)-5,6-difluoro-5,6-

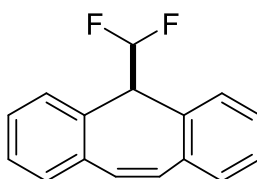
dihydrodibenzo[a,e]cyclooctatetraene



33

The product was prepared by following the general procedure, using ether as the solvent. The product was purified by column chromatography (PE) and obtained as a white solid ($R_f = 0.1$, 55 %). **M.p.** = 137-138 °C; $^1\text{H NMR}$ (400 MHz, CDCl_3) δ_{H} 7.46 (m, 2H), 7.27 (m, 4H), 7.16 (m, 2H), 7.05 (s, 2H, CH=CH), 6.01 (m, 2 H, CHF); $^{19}\text{F}\{^1\text{H}\}\text{NMR}$ (376 MHz, CDCl_3) δ_{F} -182.0 (s, CHF); $^{19}\text{F NMR}$ (376 MHz, CDCl_3) δ_{F} -182.0 (m, CHF); $^{13}\text{C NMR}$ (126 MHz, CDCl_3) δ_{C} 134.5 (d, $^3J_{\text{CF}} = 4.4$ Hz), 133.4 (dd, $^2J_{\text{CF}} = 19.4$, $^3J_{\text{CF}} = 8.5$ Hz), 132.2, 128.9, 128.8 (d, $J = 6.2$ Hz), 128.5 (d, $J = 2.5$ Hz), 127.8, 95.3 (dd, $^1J_{\text{CF}} = 176.5$ Hz, $^2J_{\text{CF}} = 27.3$ Hz). **HRMS** (ASAP⁺) m/z calcd for $\text{C}_{16}\text{H}_{12}\text{F}_2$ $[\text{M}]^+$ 242.0907, found 242.0911.

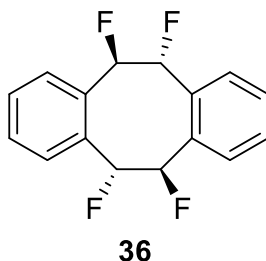
6.4.6 5-(Difluoromethyl)-5H-dibenzo[a,d]cycloheptatriene



37

General procedure E, using toluene as the solvent. The product was purified by preparative thin-layer chromatography (PE) and obtained as a yellow solid ($R_f = 0.25$, 10 %). **M.p.** = 84-86 °C. $^1\text{H NMR}$ (500 MHz, CDCl_3) δ_{H} 7.35 (m, 8H), 6.95 (s, 2H, CH=CH), 6.13 (td, $J = 57.5$, 7.8, 1 Hz, 1H, CHF_2), 4.30 (m, 1H, CH); $^{19}\text{F}\{^1\text{H}\}\text{NMR}$ (470 MHz, CDCl_3) δ_{F} -116.2 (s, CHF_2); $^{19}\text{F NMR}$ (470 MHz, CDCl_3) δ_{F} -116.2 (dd, $^2J_{\text{HF}} = 57.5$ Hz, $^3J_{\text{HF}} = 11.9$ Hz, CHF_2); $^{13}\text{C NMR}$ (126 MHz, CDCl_3) δ_{C} 134.1, 133.9 (t, $^3J = 4.0$ Hz), 131.0, 130.9, 129.6, 129.3, 127.8, 113.1 (t, $^1J_{\text{CF}} = 242.8$ Hz), 58.9 (t, $^2J_{\text{CF}} = 23.7$ Hz). **HRMS** (EI⁺) m/z calcd for $\text{C}_{16}\text{H}_{12}\text{F}_2$ 242.0901, found 242.0891.

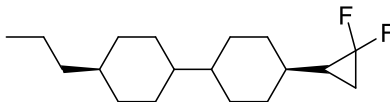
6.4.7 (5R*,6R*,11R*,12R*)-5,6,11,12-Tetrafluoro-5,6,11,12-tetrahydrodibenzo[a,e]cyclooctatetraene



General procedure E, using DCM as the solvent. The product was purified by preparative thin-layer chromatography (PE : Ether = 10 : 1) and obtained as a white solid ($R_f = 0.35$, 4 %). **M.p.** = 154-156 °C. **$^1\text{H NMR}$** (500 MHz, CDCl_3) δ_{H} 7.52 (d, $J = 7.8$ Hz, 2H), 7.33 (t, $J = 7.8$ Hz, 2H), 7.18 (t, $J = 7.6$ Hz, 2H), 7.06 (d, $J = 7.6$ Hz, 2H), 6.43 (ddd, $J = 47.0, 18.7, 6.4$ Hz, 2H), 5.58 (ddd, $J = 48.4, 25.4, 6.4$ Hz, 2H); **$^{19}\text{F}\{^1\text{H}\}$ NMR** (470 MHz, CDCl_3) δ_{F} -164.1 (d, $J = 9.8$ Hz, CHF), -180.4 (d, $J = 9.8$ Hz, CHF) ; **^{19}F NMR** (470 MHz, CDCl_3) δ_{F} -164.1 (ddd, $J = 48.4, 18.7, 9.8$ Hz, CHF), -180.4 (ddd, $J = 47.0, 25.4, 9.8$ Hz, CHF); **^{13}C NMR** (126 MHz, CDCl_3) δ_{C} 134.2, 132.1, 131.0, 130.4, 129.3, 124.8, 99.5, 93.4. **HRMS** (ESI⁺) m/z calcd for $\text{C}_{16}\text{H}_{12}\text{F}_4\text{Na}$ [$\text{M}+\text{Na}$]⁺ 303.0767, found 303.0766.

6.5 Compound preparation for Chapter 5

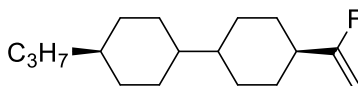
6.5.1 4-(2,2-Difluorocyclopropyl)-4'-propyl-1,1'-bicyclohexyl



37

To a solution 1'-propyl-4-vinyl-1,4'-bicyclohexane **41** (100 mg, 0.43 mmol, 1 equiv) and TMSCF_3 (151.7 mg, 1.07 mmol, 2.5 equiv) in anhydrous THF, NaI (159 mg, 1.07 mmol, 2.5 equiv) was added. The resulting suspension was stirred at 75 °C for 20 h under N_2 atmosphere. After completion, the reaction mixture was allowed to cool to RT and solvent was removed *in vacuo*. The crude residue was diluted with diethyl ether (50 mL) and washed with distilled water (50 mL). The phases were separated and the aqueous layer was extracted with diethyl ether (2 x 50 mL). The combined organic phases were washed sequentially with saturated aqueous solutions of Na_2SO_3 and NaHCO_3 , followed by drying over Na_2SO_4 , filtration and evaporation of *solvent in vacuo*. Purification by flash column chromatography (petroleum ether) gave the desired product as a white solid (66.7 mg, 55 %); $^1\text{H NMR}$ (400 MHz, CDCl_3) δ_{H} 2.02-1.60 (m, 8H), 1.42-0.62 (m, 22H); ^{19}F $\{^1\text{H}\}$ NMR (376 MHz, CDCl_3) δ_{F} -126.6 (d, $J = 155.6$ Hz, 1F, CF_2), -145.0 (d, $J = 155.6$ Hz, 1F, CF_2); ^{19}F NMR (376 MHz, CDCl_3) δ_{F} -126.6 (m, 1F, CF_2), -145.0 (m, 1F, CF_2); $^{13}\text{C NMR}$ (125 MHz, CDCl_3) δ_{C} 114 (t, $J = 284.0$ Hz), 43.4, 42.9, 39.8, 37.6, 37.0, 33.6, 33.4, 32.1, 30.1, 29.7, 29.5, 28.7 (t, $J = 10.4$ Hz), 20.0, 15.2 (t, $J = 10.7$ Hz), 14.5; **HRMS** (ASAP⁺) m/z calcd for $\text{C}_{18}\text{H}_{30}\text{F}_2$ 284.2316, found 284.2313.

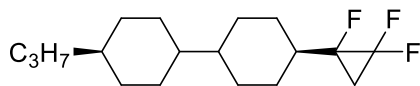
6.5.2 4-(1-Fluorovinyl)-4'-propyl-1,1'-bi(cyclohexane)



43

To a solution 1'-propyl-4-vinyl-1,4'-bicyclohexane **41** (2.1 g, 8.97 mmol, 1 equiv) in anhydrous DCM, NBS (3.24 g, 17.9 mmol, 2 equiv) and HF·Py (0.48 g, 17.9 mmol, 2 equiv) were added under N₂ atmosphere at 0 °C. The reaction mixture was warmed to RT, and then stirred for overnight. After completion, *t*-BuOK (4.03 g, 35.88 mmol, 4 equiv) was added to the mixture and the colour of mixture became brown. The reaction mixture was monitored by NMR. After the completion, the reaction mixture was slowly poured into dilute HCl solution at 0 °C and stirred for 10 minutes. The resulting solution was extracted with CH₂Cl₂ (3 x 50 mL) and the combined organic phases were washed sequentially with aqueous dilute HCl (0.1 M, 50 mL) and a saturated aqueous solution of NaHCO₃ (50 mL), followed by drying over Na₂SO₄. After filtration, solvent was removed in vacuo. Purification by flash column chromatography (petroleum ether) afforded the product as an oil (0.949 g, 42 %). ¹H NMR (400 MHz, CDCl₃) δ_H 4.42 (dd, *J* = 18.6, 2.8 Hz, CFCH₂, 1H), 4.16 (ddd, *J* = 51.6, 2.8, 0.9 Hz, CFCH₂, 1H), 2.08-1.89 (m, 3H), 1.81-1.66 (m, 6H), 1.36-1.09 (m, 7H), 1.07-0.90 (m, 6H), 0.90-0.79 (m, 5H); ¹⁹F {¹H} NMR (376 MHz, CDCl₃) δ_F -99.0 (s, 1F, CHF); ¹⁹F NMR (376 MHz, CDCl₃) δ_F -99.0 (ddd, *J* = 51.6, 18.6, 12.5 Hz, 1F, CHF); ¹³C NMR (125 MHz, CDCl₃) δ_C 171.1 (d, *J* = 257.9 Hz), 87.1 (d, *J* = 20.8 Hz), 43.3, 42.8, 40.6 (d, *J* = 25.1 Hz), 39.8, 37.6, 33.5, 30.1 (d, *J* = 2.5 Hz), 30.0, 29.4, 20.0, 14.5; HRMS (EI⁺) *m/z* calcd for C₁₇H₂₉F 252.2247, found 252.2235.

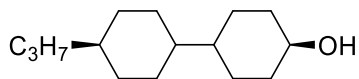
6.5.3 4-Propyl-4'-(1,2,2-trifluorocyclopropyl)-1,1'-bi(cyclohexane)



38

To a solution of **43** (0.9 g, 3.57 mmol, 1 equiv) and TMSCF_3 (1.26 g, 8.93 mmol, 2.5 equiv) in anhydrous THF, NaI (1.33 g, 8.93 mmol, 2.5 equiv) was added. The resulting suspension was stirred at 75 °C for 20 h under N_2 atmosphere. After completion, the reaction mixture was allowed to cool to RT and solvent was removed *in vacuo*. The crude residue was diluted with diethyl ether (50 mL) and washed with distilled water (50 mL). The phases were separated and the aqueous layer was extracted with diethyl ether (2 x 50 mL). The combined organic phases were washed sequentially with saturated aqueous solutions of Na_2SO_3 and NaHCO_3 , followed by drying over Na_2SO_4 , filtration and evaporation of *solvent in vacuo*. Purification by flash column chromatography (petroleum ether) gave the desired product as a white solid (496 mg, 46 %). **^1H NMR** (400 MHz, CDCl_3) δ_{H} 1.85-1.67 (m, 9H), 1.47-1.26 (m, 6H), 1.17-0.93 (m, 9H), 0.88-0.80 (m, 5H); **^{19}F { $^1\text{H}}$ NMR** (376 MHz, CDCl_3) δ_{F} -140.2 (dd, $J = 169.5, 13.6$ Hz, 1F, CF_2), -140.8 (d, $J = 169.5$, Hz, 1F, CF_2), -202.6 (d, $J = 13.6$ Hz, CHF); **^{19}F NMR** (376 MHz, CDCl_3) δ_{F} -140.2 (m, 1F, CF_2), -140.8 (ddd, $J = 169.5$ Hz, 17.6, 6.7 Hz, 1F, CF_2), -202.6 (m, CHF); **^{13}C NMR** δ_{C} 110.6 (dt, $J = 294.8, 10.0$ Hz, CF_2), 81.2 (ddd, $J = 238.5, 12.7, 8.8$ Hz, CHF), 43.2, 42.6, 39.8, 38.7 (d, $J = 19.2$ Hz), 37.6, 33.6, 30.0, 29.5, 29.4, 28.1, 27.0, 21.2 (m), 20.0, 14.4; HRMS (ASAP⁺) m/z calcd for $\text{C}_{18}\text{H}_{29}\text{F}_3$ 302.2221, found 302.2217.

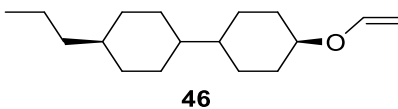
6.5.4 4'-Propyl-[1,1'-bi(cyclohexane)]-4-ol



45a

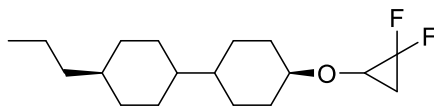
To a solution of **44** (5.0 g, 22.4 mmol, 1 equiv) in MeOH (200 mL), NaBH₄ (420 mg, 11.2 mmol, 0.5 equiv) was added. The resulting suspension was stirred at RT for overnight under N₂ atmosphere. After completion, the reaction mixture was added water (50 mL) and extracted with DCM (50 mL x 3). The combined organic phases were washed with water, followed by drying over Na₂SO₄, filtration and evaporation of *solvent in vacuo*. Purification by flash column chromatography (petroleum ether : ether = 2 : 1) gave the desired product as a white solid (2.3 g, 45 %). ¹H NMR (400 MHz, CDCl₃) δ_H 3.51 (m, 1 H), 0.79-1.38 (m, 18 H), 2.08-1.91 (m, 2 H), 1.84-1.61 (m, 7 H). Data is in agreement with the literature data.¹⁴

6.5.5 4-Propyl-4'-(vinyloxy)-1,1'-bi(cyclohexane)



Palladium trifluoro acetate (96 mg, 0.29 mmol, 0.05 equiv) and 4,7-diphenyl-phenanthroline (96 mg, 0.29 mmol, 0.05 equiv) were dissolved in butyl vinyl ether (11.6 g, 116 mmol, 20 equiv). Alcohol **45a** (1.3 g, 5.8 mmol, 1 equiv) and triethyl amine (0.058 mg, 0.029 mmol, 0.1 equiv) were added to the yellow solution, the flask sealed and stirred at 75 °C for 13 h. After completion, the resulting solution was extracted with CH₂Cl₂ (3 x 50 mL) and the combined organic phases were washed sequentially with water (2 x 50 mL), followed by drying over Na₂SO₄. After filtration, solvent was removed in vacuo. Purification by flash column chromatography (petroleum ether) afforded the product as a colourless liquid (900 mg, 62 %). ¹H NMR (400 MHz, CDCl₃) δ_H 6.33 (dd, *J* = 14.1, 6.6 Hz, 1H), 4.28 (dd, *J* = 14.1, 1.4 Hz, 1H), 3.97 (dd, *J* = 6.6, 1.4 Hz, 1H), 3.67-3.57 (m, 1H), 2.11-2.01 (m, 2H), 1.80 - 1.69 (m, 6H), 1.35-1.21 (m, 5H), 1.18 - 1.08 (m, 3H), 1.08 - 0.76 (m, 10H); ¹³C NMR (125 MHz, CDCl₃) δ_C 150.7, 88.0, 78.8, 42.8, 42.3, 39.8, 37.5, 33.5, 32.3, 30.2, 27.8, 20.0, 14.4; HRMS (ES) *m/z* calcd for [M+H]⁺ C₁₇H₃₁O 251.2366, found 251.2369.

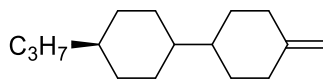
6.5.6 4-(2,2-Difluorocyclopropoxy)-4'-propyl-1,1'-bi(cyclohexane)



39

To a solution alkene **46** (490 mg, 1.96 mmol, 1 equiv) and TMSCF_3 (556.6 mg, 3.92 mmol, 2.0 equiv) in anhydrous THF, NaI (584 mg, 3.92 mmol, 2.0 equiv) was added. The resulting suspension was stirred at 75 °C for 20 h under N_2 atmosphere. After completion, the reaction mixture was allowed to cool to RT and solvent was removed *in vacuo*. The crude residue was diluted with diethyl ether (50 mL) and washed with distilled water (50 mL). The phases were separated and the aqueous layer was extracted with diethyl ether (2 x 50 mL). The combined organic phases were washed sequentially with saturated aqueous solutions of Na_2SO_3 and NaHCO_3 , followed by drying over Na_2SO_4 , filtration and evaporation of *solvent in vacuo*. Purification by flash column chromatography (petroleum ether) gave the desired product as a white solid (294 mg, 50 %). **^1H NMR** (400 MHz, CDCl_3) δ_{H} 3.63 (m, 1H), 3.37 (m, 1H), 2.08 (m, 2H), 1.82-1.65 (m, 6H), 1.54-0.77 (m, 20H); **^{19}F { $^1\text{H}}$ NMR** (376 MHz, CDCl_3) δ_{F} -130.7 (d, $J = 164.4$ Hz, 1F, CF_2), -147.4 (d, $J = 164.4$ Hz, 1F, CF_2); **^{19}F NMR** (376 MHz, CDCl_3) δ_{F} -130.7 (m, 1F, CF_2), -147.4 (m, 1F, CF_2); **^{13}C NMR** (125 MHz, CDCl_3) δ_{C} 111.5 (t, $J = 289.5$ Hz), 79.9, 54.9 (dd, $J = 13.6, 9.3$ Hz), 42.8, 42.4, 39.7, 37.5, 33.5, 32.3, 32.0, 30.1, 28.0, 27.9, 20.0, 18.1 (t, $J = 10.3$ Hz), 14.4; **HRMS** (ASAP) m/z calcd [M-H] $\text{C}_{18}\text{H}_{29}\text{F}_2\text{O}$ 299.2187, found 299.2183, calcd. [M] 300.2220, found 300.2230.

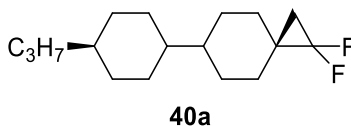
6.5.7 4-Methylene-4'-propyl-1,1'-bi(cyclohexane)



47

To a flame-dried flask were added ketone **44** (1.0 g, 4.5 mmol, 1.0 equiv), methyltriphenylphosphonium bromide (1.74 g, 5.4 mmol, 1.2 equiv) and diethyl ether (50 mL). Potassium *tert*-butylate (0.6 g, 5.4 mmol, 1.2 equiv) was added down the walls of the flask. The reaction mixture was allowed to stir at room temperature for 6 h. After completion, the crude residue was diluted with diethyl ether (50 mL) and washed with distilled water (50 mL). The phases were separated and the aqueous layer was extracted with diethyl ether (2 x 50 mL). The combined organic phases were washed sequentially with saturated aqueous solutions of Na₂SO₃ and NaHCO₃, followed by drying over Na₂SO₄, filtration and evaporation of *solvent in vacuo*. Purification by flash column chromatography (petroleum ether) gave the desired product as a liquid (732 mg, 73.8 %). **¹H NMR** (400 MHz, CDCl₃) δ_H 4.57 (t, *J* = 1.7 Hz, 2H), 2.45-2.19 (m, 2H), 2.08-1.88(m, 2H), 1.83-1.61 (m, 7H), 1.37-0.76 (m, 15H); **¹³C NMR** (101 MHz, CDCl₃) δ_C 150.5, 106.2, 42.94, 42.91, 39.8, 37.6, 35.0, 33.6, 31.5, 30.1, 20.0, 14.4; **HRMS** (EI⁺) *m/z* calcd [M] C₁₆H₂₈ 220.2191, found 220.2193.

6.5.8 1,1-Difluoro-6-(4-propylcyclohexyl)spiro[5.2]octane



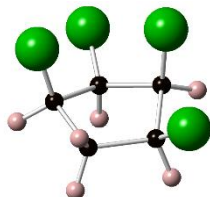
To a solution alkene **47** (730 mg, 3.31 mmol, 1 equiv) and TMSCF_3 (1.18 g, 8.29 mmol, 2.5 equiv) in anhydrous THF, NaI (1.24 g, 8.29 mmol, 2.5 equiv) was added. The resulting suspension was stirred at 75 °C for 20 h under N_2 atmosphere. After completion, the reaction mixture was allowed to cool to RT and solvent was removed *in vacuo*. The crude residue was diluted with diethyl ether (50 mL) and washed with distilled water (50 mL). The phases were separated and the aqueous layer was extracted with diethyl ether (2 x 50 mL). The combined organic phases were washed sequentially with saturated aqueous solutions of Na_2SO_3 and NaHCO_3 , followed by drying over Na_2SO_4 , filtration and evaporation of *solvent in vacuo*. Purification by flash column chromatography (petroleum ether) afforded the stereoisomers. After recrystallisation (Petroleum ether/ Ethyl acetate = 5: 1) for three times, the desired product was obtained as a white solid (241 mg, 27 %). $^1\text{H NMR}$ (400 MHz, CDCl_3) δ_{H} 1.80-1.56 (m, 8H), 1.40-1.24 (m, 4H), 1.19-0.87 (m, 16H); ^{19}F $\{^1\text{H}\}$ NMR (376 MHz, CDCl_3) δ_{F} -139.1 (s, 2F, CF_2); $^{19}\text{F NMR}$ (376 MHz, CDCl_3) δ_{F} -139.1 (t, $J = 8.3$ Hz, 2F, CF_2); $^{13}\text{C NMR}$ δ_{C} 116.9 (t, $J = 287.7$ Hz), 43.0, 42.9, 39.8, 37.6, 33.5, 30.1, 29.5 (t, $J = 10.7$ Hz), 28.8, 27.5, 21.7 (t, $J = 10.0$ Hz), 20.1, 14.5; **HRMS** (EI^+) m/z calcd. $[\text{M}]$ $\text{C}_{17}\text{H}_{28}\text{F}_2$ 270.2159, found 270. 2157.

References

1. M. Suzuki, H. Ohtake, Y. Kameya, N. Hamanaka, R. Noyori, *J. Org. Chem.*, 1989, **54**, 5292.
2. J. B. Lambert, R. B. Finzel, *J. Am. Chem. Soc.*, 1983, **105**, 1954-1958.
3. C. J. Thomson, Q. Zhang, N. Al-Maharik, M. Buhl, D. B. Cordes, A. M. Z. Slawin, D. O'Hagan, *Chem. Comm.*, 2018, **54**, 8415-8418.
4. Z. Liu, P. Liao, X. Bi, *Org. Lett.*, 2014, **16**, 3668-3671.
5. S. Wu, F. Liu, *Org. Lett.*, 2016, **18**, 3642-3645.
6. J. Leroy, *J. Org. Chem.*, 1981, **46**, 206-209.
7. G. S. Lal, G. P. Pez, R. J. Pesaresi, F. M. Prozonic, H. Cheng, *J. Org. Chem.*, 1999, **64**, 7048-7054.
8. R. A. Moss, H. Fan, R. Gurumuthy, G. Ho, *J. Am. Chem. Soc.*, 1991, **113**, 1435-1437.
9. W. R. Dolbier, C. R. Burkholder, *J. Org. Chem.*, 1990, **55**, 589.
10. T. Ando, H. Yamanaka, F. Namigata, W. Funasaka, *J. Org. Chem.*, 1970, **35**, 33-38.
11. P. Weyerstahl, G. Blume, C. Müller, *Tetrahedron Lett.*, 1971, **42**, 3869-3872.
12. G. A. Olah, J. T. Welch, Y. D. Vankar, M. Nojima, I. Kerekes, J. A. Olah, *J. Org. Chem.*, 1979, **44**, 3872-3881.
13. M. Schüler, D. O'Hagan, A. M. Z. Slawin, *Chem. Comm.*, 2005, 4324-4326.
14. K. Kiyoshi, T. Sadao, H. Tamejiro. *Bull. Chem. Soc. Jpn.*, 2000, **73**, 1875-1892.

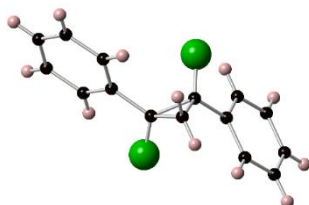
Appendix-Crystallographic Data

All cis-1,2,3,4-Tetrafluorocyclopentane



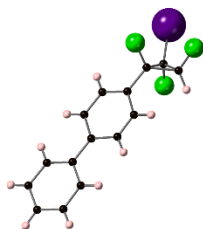
Chemical Formula: $C_5H_6F_4$, $M = 142.10$, colourless prism, crystal dimensions $0.150 \times 0.030 \times 0.030$ mm, monoclinic, space group $P 2_1/c$, $a = 10.1150(19)$, $b = 4.5875(11)$, $c = 11.876(3)$ Å, $\beta = 90.026(18)^\circ$, $V = 551.1(2)$ Å³, $Z = 4$, $D_c = 1.713$ g/cm⁻³, $T = 93$ K, $R = 0.0638$, $R_w = 0.1610$, for 987 reflections with $I > 2\sigma(I)$ and 83 variables. Data were collected using multi-layer mirror monochromated Mo-K α radiation, $\lambda = 0.71075$ Å.

(1*R, 2*R**)-1,2-Difluoro-1,2-diphenylcyclopropane**



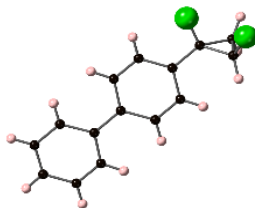
Chemical Formula: C₁₅H₁₁F₂, *M* = 230.26, crystal dimensions 0.110 × 0.030 × 0.010 mm, orthorhombic, space group *P*2₁2₁2₁, *a* = 7.9419(16), *b* = 12.467(2), *c* = 5.6819(14) Å, *V* = 562.6(2) Å³, *Z* = 2, *D*_c = 1.359 g/cm⁻³, *T* = 173 K, *R*₁ = 0.0923, *wR*₂ = 0.2126, for 664 reflections with *I* > 2σ(*I*) and 78 variables. Data were collected using multi-layer mirror monochromated Cu-Kα radiation, λ = 1.54187 Å.

4-(1,2,3-Trifluoro-2-iodocyclopropyl)-1,1'-biphenyl



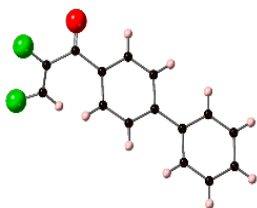
Chemical Formula: $C_{15}H_{10}F_3I$, $M = 374.14$, colourless platelet, crystal dimensions $0.100 \times 0.100 \times 0.010$ mm, monoclinic, space group $P2_1$, $a = 5.9337(5)$, $b = 7.5484(8)$, $c = 15.1871(13)$ Å, $\beta = 96.119(9)^\circ$, $V = 676.35(11)$ Å³, $Z = 2$, $D_c = 1.837$ g/cm⁻³, $T = 93$ K, $R_1 = 0.1217$, $wR_2 = 0.3049$, for 2510 reflections with $I > 2\sigma(I)$ and 172 variables. Data were collected using multi-layer mirror monochromated Cu-K α radiation, $\lambda = 1.54187$ Å.

***Cis*-4-(1,2-Difluorocyclopropyl)-1,1'-biphenyl**



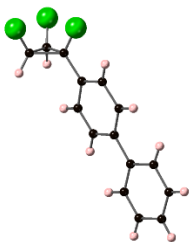
Chemical Formula: $C_{15}H_{12}F_2$, $M = 230.26$, colourless platelet, crystal dimensions $0.380 \times 0.080 \times 0.010$ mm, monoclinic, space group $P2_1/c$, $a = 15.873(2)$, $b = 5.6329(5)$, $c = 25.223(3)$ Å, $\beta = 95.875(11)^\circ$, $V = 2243.4(4)$ Å³, $Z = 8$, $D_c = 1.363$ g/cm³, $T = 173$ K, $R_1 = 0.1169$, $wR_2 = 0.3267$, for 2504 reflections with $I > 2\sigma(I)$ and 327 variables. Data were collected using multi-layer mirror monochromated Cu-K α radiation, $\lambda = 1.54187$ Å.

(Z)-1-([1,1'-Biphenyl]-4-yl)-2,3-difluoroprop-2-en-1-one



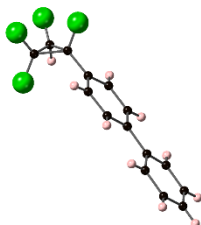
Chemical Formula: $C_{15}H_{10}F_2O$, $M = 244.24$, colourless platelet, crystal dimensions $0.190 \times 0.080 \times 0.010$ mm, monoclinic, space group $P2_1/c$, $a = 5.9713(5)$, $b = 7.3226(6)$, $c = 26.183(3)$ Å, $\beta = 94.546(9)^\circ$, $V = 1141.26(19)$ Å³, $Z = 4$, $D_c = 1.421$ g/cm⁻³, $T = 173$ K, $R_1 = 0.0684$, $wR_2 = 0.1993$, for 1552 reflections with $I > 2\sigma(I)$ and 163 variables. Data were collected using multi-layer mirror monochromated Cu-K α radiation, $\lambda = 1.54187$ Å.

4-(1,2,2,3-Tetrafluorocyclopropyl)-1,1'-biphenyl



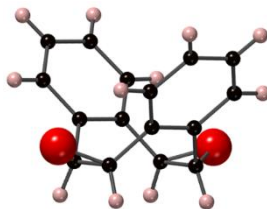
Chemical Formula: $C_{15}H_{11}F_3$, $M = 248.25$, colourless platelet, crystal dimensions $0.060 \times 0.020 \times 0.010$ mm, triclinic, space group $P1$, $a = 8.3714(7)$, $b = 13.6749(7)$, $c = 16.1180(8)$ Å, $\alpha = 82.280(4)$, $\beta = 87.767(5)$, $\gamma = 73.097(6)^\circ$, $V = 1749.4(2)$ Å³, $Z = 6$, $D_c = 1.414$ g/cm⁻³, $T = 173$ K, $R_1 = 0.0948$, $wR_2 = 0.2188$, for 3548 reflections with $I > 2\sigma(I)$ and 973 variables. Data were collected using multi-layer mirror monochromated Cu-K α radiation, $\lambda = 1.54187$ Å.

4-(1,2,2,3-Tetrafluorocyclopropyl)-1,1'-biphenyl



Chemical Formula: $C_{15}H_{10}F_4$, $M = 266.24$, colourless platelet, crystal dimensions $0.100 \times 0.100 \times 0.010$ mm, monoclinic, space group $P2_1/c$, $a = 5.7483(14)$, $b = 7.9388(15)$, $c = 26.104(11)$ Å, $\beta = 95.14(3)^\circ$, $V = 1186.5(6)$ Å³, $Z = 4$, $D_c = 1.490$ g/cm³, $T = 125$ K, $R_1 = 0.2229$, $wR_2 = 0.5760$, for 1449 reflections with $I > 2\sigma(I)$ and 172 variables. Data were collected using multi-layer mirror monochromated Cu-K α radiation, $\lambda = 1.54187$ Å.

(1aR*,5bS*,6aR*,10bS*)-1a,5b,6a,10b-Tetrahydrodibenzo[3,4:7,8]cycloocta[1,2-b:5,6-b']bis(oxirene)



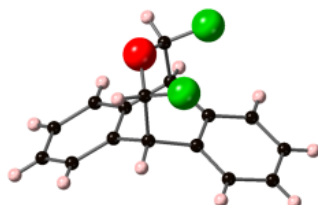
Chemical Formula: $C_{16}H_{12}O_2$, $M = 236.27$, crystal dimensions $0.210 \times 0.110 \times 0.030$ mm, monoclinic, space group $I2/a$, $a = 13.575(4)$, $b = 5.7938(15)$, $c = 15.586(4)$ Å, $\beta = 109.94(2)^\circ$, $V = 1152.4(6)$ Å³, $Z = 4$, $D_c = 1.362$ g/cm⁻³, $T = 173$ K, $R_1 = 0.0336$, $wR_2 = 0.0872$, for 938 reflections with $I > 2\sigma(I)$ and 82 variables. Data were collected using multi-layer mirror monochromated Mo-K α radiation, $\lambda = 0.71075$ Å.

(9*R,10*R**,11*S**,13*S**)-11,13-Difluoro-9,10-dihydro-9,10-(methanooxymethano)anthracene**



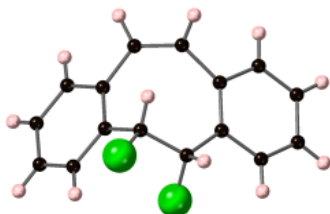
Chemical Formula: $C_{16}H_{12}F_2O$, $M = 258.27$, colourless plate, crystal dimensions $0.090 \times 0.030 \times 0.010$ mm, orthorhombic, space group $Iba\ 2$, $a = 14.2552(3)$, $b = 22.1202(7)$, $c = 7.4973(2)$ Å, $V = 2364.11(11)$ Å³, $Z = 8$, $D_c = 1.451$ g/cm⁻³, $T = 173$ K, $R = 0.0531$, $R_w = 0.1362$, for 2383 reflections with $I > 2\sigma(I)$ and 185 variables. Data were collected using graphite monochromated Cu-K α radiation, $\lambda = 1.54187$ Å.

(*meso*)-11,13-Difluoro-9,10-dihydro-9,10-(methanooxymethano)anthracene



Chemical Formula: $C_{16}H_{12}F_2O$, $M = 258.27$, colourless prism, crystal dimensions $0.30 \times 0.060 \times 0.030$ mm, trigonal, space group $P3_1$, $a = 8.8519(6)$, $b = 8.8519(6)$, $c = 13.9613(10)$ Å, $V = 947.39(15)$ Å³, $Z = 3$, $D_c = 1.358$ g/cm⁻³, $T = 177.2$ K, $R = 0.0695$, $R_w = 0.2084$, for 2225 reflections with $I > 2\sigma(I)$ and 172 variables. Data were collected using graphite monochromated Cu-K α radiation, $\lambda = 1.54187$ Å.

(meso)-5,6-Difluoro-5,6-dihydrodibenzo[a,e] cyclooctatetraene



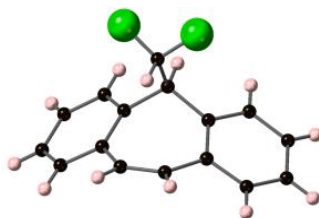
Chemical Formula: $C_{16}H_{12}F_2$, $M = 242.27$, colourless needle, crystal dimensions $0.020 \times 0.010 \times 0.010$ mm, monoclinic, space group $P 2_1/c$, $a = 10.4484(5)$, $b = 12.8848(4)$, $c = 8.6234(4)$ Å, $\beta = 100.333^\circ$, $V = 1142.10(9)$ Å³, $Z = 4$, $D_c = 1.409$ g/cm⁻³, $T = 125$ K, $R = 0.0578$, $R_w = 0.1645$, for 2325 reflections with $I > 2\sigma(I)$ and 164 variables. Data were collected using graphite monochromated Cu-K α radiation, $\lambda = 1.54187$ Å.

(5*R,6*R**,*Z*)-5,6-Difluoro-5,6-dihydrodibenzo[*a,e*] cyclooctatetraene**



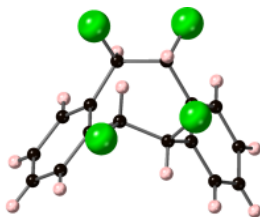
Chemical Formula: $C_{16}H_{12}F_2$, $M = 242.27$, crystal dimensions $0.160 \times 0.020 \times 0.020$ mm, trigonal, space group $R\bar{3}$, $a = 35.747(2)$, $b = 35.747(2)$, $c = 4.9640(4)$ Å, $\beta = 90^\circ$, $V = 5473.5(8)$ Å³, $Z = 18$, $D_c = 1.323$ g/cm⁻³, $T = 173$ K, $R = 0.0527$, $R_w = 0.1392$, for 2212 reflections with $I > 2\sigma(I)$ and 163 variables. Data were collected using graphite monochromated Cu-K α radiation, $\lambda = 1.54187$ Å.

5-(Difluoromethyl)-5*H*-ibenzo[*a,d*]cycloheptatriene



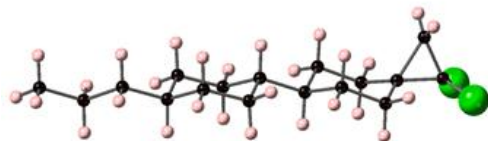
Chemical Formula: $C_{16}H_{12}F_2$, $M = 242.26$, crystal dimensions $0.140 \times 0.030 \times 0.010$ mm, trigonal, space group $R\bar{3}$, $a = 34.4377(4)$, $b = 34.4377(4)$, $c = 5.42477(7)$ Å, $\beta = 90^\circ$, $V = 5571.60(15)$ Å³, $Z = 18$, $D_c = 1.300$ g/cm⁻³, $T = 125$ K, $R = 0.0445$, $R_w = 0.1235$, for 2550 reflections with $I > 2\sigma(I)$ and 163 variables. Data were collected using graphite monochromated Cu-K α radiation, $\lambda = 1.54187$ Å.

(5R*,6R*,11R*,12R*)-5,6,11,12-Tetrafluoro-5,6,11,12-tetrahydrodibenzo[a,e]cyclooctatetraene



Chemical Formula: $C_{16}H_{12}F_4$, $M = 280.26$, crystal dimensions $0.140 \times 0.030 \times 0.010$ mm, monoclinic, space group $P 2_1/c$, $a = 12.7703(4)$, $b = 7.4822(2)$, $c = 13.8047(5)$ Å, $\beta = 110.433^\circ$, $V = 1236.05(7)$ Å³, $Z = 4$, $D_c = 1.506$ g/cm⁻³, $T = 125$ K, $R = 0.0625$, $R_w = 0.1869$, for 2524 reflections with $I > 2\sigma(I)$ and 181 variables. Data were collected using graphite monochromated Cu-K α radiation, $\lambda = 1.54187$ Å.

1,1-Difluoro-6-(4-propylcyclohexyl)spiro[5.2]octane



Chemical Formula: $C_{17}H_{28}F_2$, $M = 270.40$, colourless prism, crystal dimensions $0.100 \times 0.100 \times 0.030$ mm, triclinic, space group $P\bar{1}$, $a = 5.95332(14)$, $b = 10.8810(2)$, $c = 13.1778(3)$ Å, $\alpha = 113.800^\circ$, $\beta = 90.4964^\circ$, $\gamma = 98.6123^\circ$, $V = 769.98(3)$ Å³, $Z = 2$, $D_c = 1.166$ g/cm⁻³, $T = 125$ K, $R = 0.0488$, $R_w = 0.2293$, for 3050 reflections with $I > 2\sigma(I)$ and 172 variables. Data were collected using graphite monochromated Cu-K α radiation, $\lambda = 1.54187$ Å

Appendix-Publications

1. **Polar alicyclic rings: Synthesis and structure of all cis-1,2,3,4-tetrafluorocyclopentane**
Z. Fang, N. Al-Maharik, A. M. Z. Slawin, D. O'Hagan, *Chem. Commun.*, 2016, **52**, 5116-5119.
2. **Fluorine containing cyclopropanes: Synthesis of aryl substituted all-cis 1,2,3-trifluorocyclopropanes, a facially polar motif**
Z. Fang, D. Cordes, A. M. Z. Slawin, D. O'Hagan, *Chem. Commun.*, 2019, **55**, 10539-10542.
3. **Unexpected α,α' -difluoroethers from Ag(I)F and N-bromsuccinimide reactions of dibenzo[a,e]cyclooctatetraene.**
Z. Fang, R. Z. Gillatt, D. Cordes, A. M. Z. Slawin, C. L. Carpenter-Warren, David O'Hagan, *Chem. Commun.* 2019, **55**, 14295-14298.